Functional and Structural Characterisation of Staphylococcal Superantigen-Like Protein 10 (SSL10)

Deepa Patel

A thesis submitted in fulfilment of the requirements for the degree of Doctor of Philosophy

Department of Molecular Medicine and Pathology
The University of Auckland
2011

Abstract

Staphylococcus aureus is a highly versatile gram-positive bacterium that owes its success to the remarkable range of pathogenic factors that it has at its disposal. Staphylococcal superantigen-like protein 10 (SSL10) is a tightly regulated, highly conserved protein exclusive to the arsenal of *S.aureus.* It is located on the genomic island *vSaα* alongside ten other related *ssl* genes. The 2.75 Å crystal structure of SSL10 displays strong structural homology to the superantigen toxins with an N-terminal OB-fold domain linked to a C-terminal β-grasp domain; however they are functionally distinct.

SSL10 binds to human IgG and displays striking specificity for the Fc domain of the γ1 subclass. Its strong affinity for IgG only extends to primate species. Kinetic analysis of SSL10 binding to human IgG1 suggests a dissociation constant in the high nanomolar range through a single site 1:1 stoichiometry interaction. Truncation of SSL10 into its C-terminal β-grasp domain abolished its ability to bind IgG1 suggesting the presence of key residues in the N-terminal OB-fold domain. SSL10 competes for binding to IgG1 with cell surface FcγRs on monocytes, and consequently interferes with the phagocytosis of IgG1-opsonised bacteria by neutrophils. This is a key survival strategy for *S.aureus* given that phagocytic cells play a crucial role in the immune clearance of gram positive bacteria.

This small 24 kDa protein displays strong functional diversity through its C-terminal β-grasp domain, disrupting the proteolytic cascades of complement and coagulation. It targets complement C4 and inhibits the classical and mannan-binding lectin pathways of complement. SSL10 also affinity purifies prothrombin, fibrinogen, fibronectin and plasminogen from plasma; key factors involved in the clotting process. It potently delays coagulation prior to thrombin activation suggesting an alternative role for fibrinogen and fibronectin in anchoring SSL10 at the site of infection where it would be most effective. It is clear these bacterial proteins are strategically designed to accommodate a number of circumstances. This study illustrates the incredible complexity of host-pathogen interactions and highlights the need for a comprehensive understanding of this bacterium if we are to successfully develop alternative therapeutics in the future.

Acknowledgements

I owe my deepest gratitude to so many people who have supported me throughout my PhD and made it an enjoyable and rewarding experience.

Thank you to my supervisor, Professor John Fraser for giving me the opportunity to work on a challenging and exciting project and also for his continued enthusiasm, guidance and encouragement across all aspects of my PhD. Thank you to my co-supervisor Dr Ries Langley for all the valuable technical advice and for encouraging me to think outside the box. And thank you to Dr Bruce Wines for his expertise and continued enthusiasm and support that assisted in publication of this work.

I would also like to acknowledge Professor Ted Baker, Heather Baker and Dr Paul Young for their guidance with the structural aspect of my project and Ivan Ivonovic for setting up the crystallisation screens on the robot. A sincere thank you to Richard Bunker, Christian Linke and members of the SBS structural biology lab for their continued advice and support.

Thank you to Stephen Edgar and Vicki Scott for assistance with the flow cytometer, Hillary Holloway for assistance with confocal microscopy, and Dr Mark Oliver, Dr Mark Green, Dr Ellen Knapp and Auckland Zoo for generously providing animal sera. I am also very grateful to all the volunteers who kindly donated blood and to Laura Young, Vicki Scott, Maria Rowe, Stephen Richie, Andrew Wood, Richard Sequeira and Natalie Lorenz for assistance with phlebotomy. Thank you to all the past and present members of the Fraser lab for all the memorable times. It has been a pleasure working with you. And a warm thank you to my friends who have always believed in me and stood behind me throughout my PhD.

I would also like to thank Professor Roger Booth for his words of wisdom that encouraged me to undertake this PhD and acknowledge the generous financial support from the University of Auckland Doctoral scholarship and Maurice Wilkins Centre for Molecular Biodiscovery that has made this work possible.

To my brother, Kevin, thank you for all your encouragement and patience and for always keeping the humour alive. And to my parents, Rajesh and Kundan, thank you for your unconditional support and all the sacrifices that you have made so I could have this opportunity.

Table of Contents

List of Figures

List of Tables

Abbreviations

°C	Degrees celsius
amp	Ampicillin
ATCC	American type cell culture collection
BaCl	Barium chloride
bp	Base pair
BSA	Bovine serum albumin
CH	Heavy chain constant region
CHIPS	Chemotaxis inhibitory protein of *Staphylococcus aureus*
C-terminal	Carboxy terminus
DNA	Deoxyribonucleic acid
dNTP	Deoxynucleotide triphosphate
DTT	Dithiothreitol
Eap	Extracellular adherence protein
ECM	Extracellular matrix
Ecb	Extracellular complement binding protein
Efb	Extracellular fibrinogen binding protein
Fab	Immunoglobulin antigen binding fragment
FACS	Fluorescence activated cell sorter
Fc	Immunoglobulin crystallisable fragment
FcγR	Immunoglobulin G Fc receptor
FCS	Fetal calf serum
Fig	Figure
fMLP	N-formyl-methionyl-leucyl-phenylalanine
FPLC	Fast performance liquid chromatography
FSC	Forward scatter
g	Gram
GlcNAc	N-acetylglucosamine
hr	Hour
HrtA	Heme transporter A
IDA	Iminodiacetic acid
IEC	Immune evasion cluster
Ig	Immunoglobulin
IPTG	Isopropyl β-D-thiogalactopyranoside
ITC	Isothermal titration calorimetry
kDa	Kilodalton
L	Litre

LB	Luria-Bertani broth
LPS	Lipopolysaccharide
M	Molar
mA	Milliampere
MFI	Mean fluorescence intensity
mg	Milligram
MHC	Major histocompatablity complex
min	Minute(s)
µL	Microlitre
mL	Milliliter
µM	Micromolar
mM	Millimolar
Mr	Molecular weight
ng	Nanogram
NMS	Normal mouse serum
NRS	Normal rabbit serum
NTA	Nitrilotriacetic acid
N-terminus	Amino-terminus
OB-fold	Oligosaccharide/oligonucleotide binding fold
O/N	Overnight
PBL	Peripheral blood lymphocyte
PBMC	Peripheral blood mononuclear cell
PBS	Phosphate buffered saline
PCR	Polymerase chain reaction
PE	Phycoerythrin
pg	Picogram
PHA	Phytohemagglutinin
pI	Isoelectric point
PMSF	Phenylmethylsulfonyl fluoride
PNGase F	Peptide-N-glycosidase F
RBC	Red blood cell
rpm	Revolutions per minute
RPMI	Roswell Park Memorial Institute Medium - 1640
RT	Room temperature
s	Second(s)
Sag	Superantigen
Sbi	*S. aureus* IgG-binding protein
SCIN	Staphylococcal complement inhibitor protein
SDS	Sodium dodecyl sulphate
SDS-PAGE	Sodium dodecyl sulphate-polyacrylamide gel electrophoresis
SET	Staphylococcal exotoxin-like
SpA	Staphylococcal Protein A

SPR	Surface plasmon resonance
SSC	Side scatter
TBS	Tris buffered saline
TCA	Trichloroacetic acid
TCR	T-cell receptor
TEMED	N,N,N,N – teramethylethylenediamine
TNFα	Tumor necrosis factor alpha
Trx	Thioredoxin
TSST-1	Toxic shock syndrome toxin-1
V	Volts
VH	Heavy chain variable region
VL	Light chain variable region
w/w	Weight per weight
w/v	Weight per volume
v/v	Volume per volume

Chapter 1
Introduction

1.1 *Staphylococcus aureus*: rise of the superbug

Staphylococcus aureus is an opportunistic gram-positive bacterium that can cause extensive morbidity and mortality in humans. This versatile pathogen exists as golden clusters that can be differentiated based on its catalase, coagulase and mannitol fermentation properties (Lowy, 1998). It is primarily found in the anterior nare but it is also a local resident of the skin, gut and throat microflora (Peacock, de Silva, & Lowry, 2001; Sibbald et al., 2006). Approximately 20% of the human population are persistently colonised with *S.aureus* while another 60% are transient carriers; in both cases causing no ill effects (Fournier & Philpott, 2005; von Eiff, Becker, Machka, Stammer, & Peters, 2001). However under certain conditions that are poorly understood, *S.aureus* can overwhelm the host immune system and cause severe detrimental effects; a risk that is increased in individuals colonised with the bacterium (Lowy, 1998; von Eiff et al., 2001). *S.aureus* infections range from superficial skin infections such as abscesses and impetigo, to more serious life-threatening conditions such as septicemia, endocarditis and toxic-shock syndrome (Lowy, 1998). These infections were predominantly observed in immuno-compromised patients, but are now also increasingly observed worldwide in the general community, causing serious infections in otherwise healthy individuals (Tadashi Baba et al., 2002; Foster, 2005).

1.1.1 Antibiotic resistance

Over the last five decades the treatment of *S.aureus* infections has become progressively difficult due to the rapid spread of multi-drug resistant strains. The most widely spread is penicillin resistance. *S.aureus* strains have also gained methicillin resistance (MRSA) through acquisition of the *mecA* gene, which encodes an altered penicillin binding protein (PBP-2a) (Ubukata, Nonoguchi, Matsuhashi, & Konno, 1989). PBP-2a is less susceptible to most β-lactam antibiotics thus retains its ability to carry out its role in the transpeptidation reaction of cell wall peptidoglycans (Navarre & Schneewind, 1999; Ubukata et al., 1989). The *mecA* gene resides on the staphylococcal cassette chromosome mec element (SCCmec) that is commonly shared among staphylococcal species (Hanssen & Sollid, 2006). More recently, some MRSA strains have also acquired resistance to vancomycin, a formally consistent therapeutic against MRSA infections (Sieradzki, Roberts, Haber, & Tomasz, 1999). Vancomycin-intermediate *S.aureus* strains (VISA) have a thickened cell wall that allows the bacterium to capture more vancomycin and weaken its

detrimental effects (Cui et al., 2003), while Vancomycin-resistant strains (VRSA) have emerged through acquisition of the *vanA* gene from *Enterococcus faecalis* (S. Chang et al., 2003) that encodes an altered peptidoglycan precursor to which vancomycin is no longer able to bind (Bugg, Dutka-Malen, Arthur, Courvalin, & Walsh, 1991). Given the direct threat posed by antibiotics to bacterial survival it wouldn't be surprising if these rapidly evolving strains gain advanced means of resistance against antibiotics over the next few decades.

1.1.2 The *S.aureus* genome

Our knowledge of staphylococcal pathogenesis has rapidly expanded since the sequencing of multiple *S.aureus* genomes (Appendix A). The core genome is comprised of housekeeping genes, which are involved in cell growth and survival, and are generally conserved among various isolates. The remaining genes form the accessory genome or 'flexible gene pool'. It consists of genomic islands, pathogenicity islands, prophages, plasmids and transposons, which provide the main source of variation between strains (Gak-Mor & Finlay, 2006; Lindsay & Holden, 2004). Interestingly these elements contain majority of the genes involved in immune evasion and virulence and thus determine the pathogenic potential of the organism and also the individual strains (Gak-Mor & Finlay, 2006; Novick, 2003; Zakour, Guinane, & Fitzgerald, 2008). Many of these distinct genomic regions also have the capacity to form infectious phage-like particles for the transmission of genes between strains, and occasionally bacterial species (Chen & Novick, 2009; Novick, Schlievert, & Ruzin, 2001).

1.1.3 The expression of virulence factors

The expression of pathogenic determinants is a dynamic process that responds to cell density and environmental signals. Two major global regulator families exist for virulence factor genes: the two component regulatory systems and the SarA protein family (Cheung, Bayer, Zhang, Gresham, & Xiong, 2004; Cheung & Zhang, 2002). Their combined activity directs the expression of cell-wall associated proteins that are important for colonisation during the exponential phase of growth, and the expression of secreted proteins that are important for bacterial evasion during the post-exponential and stationary phase of growth (Sibbald et al., 2006). Furthermore *S.aureus* has adapted control mechanisms to respond to the varying circumstances that it encounters during the infection process (Torres et al., 2007). Indeed, any strain specific variations in the regulatory responses to a certain stimuli could influence the specific virulence factors produced and in turn also have a substantial impact on the pathogenic potential of different strains (Sibbald et al., 2006).

1.2 Defence mechanisms of the human immune system

The human immune system is a complex network of defence mechanisms specifically designed to recognise and destroy invading pathogens. Bacteria are generally restricted by physical barriers comprising of the skin and mucous membrane. If this barrier is breached the immune system employs a series of rapid inflammatory responses. In parallel, the coagulation cascade is activated to seal the breach and limit further bacterial spread and tissue damage. Bacterial clearance is mediated by phagocytic cells such as neutrophils and macrophages that are activated and recruited to the site of infection along a chemotactic concentration gradient (L. Patel, Charlton, Chambers, & Macphee, 2001). With the aid of antibodies and complement these phagocytic cells recognize and kill the pathogen (Fallman, Andersson, & Andersson, 1993; Shields et al., 2001). Neutrophils also have the capacity to release extracellular traps containing high concentrations of antimicrobial agents that degrade virulence factors and kill bacteria to prevent dissemination (Mendina, 2009).

1.2.1 Antimicrobial factors

The skin and mucous membrane are protected by a number of innate immune defences. Properties, such as the acidic environment of the stomach and ciliary movement in the respiratory tract, physically inhibit bacterial attachment (Hornef, Wick, Rhen, & Normark, 2002). These mechanisms are further supported by a host of antimicrobial factors such as cationic antimicrobial molecules (CAMs) (Friedrich, Moyles, Beveridge, & Hancock, 2000), defensins (Ganz et al., 1985), cathelicidins (Travis et al., 2000) and lysozymes (Morse, 1962) that mediate rapid lysis of bacteria by disrupting the integrity of the bacterial membrane. Bacterial cell wall components such as teichoic acids and peptidoglycans have a net negative charge whereas majority of all host antimicrobial factors are positively charged allowing specific and effective targeting of their activity (Dmitriev, Toukach, & Ehlers, 2005).

1.2.2 Nutrient availability

Bacterial success is largely determined by its ability to acquire essential nutrients from its surrounding environment. Iron in its reduced Fe^{2+} ferrous form or oxidized Fe^{3+} ferric form is a crucial component for many organisms including bacteria (Andrews, Robinson, & Rodriguez-Quinones, 2003). Iron binding proteins transferrin and lactoferrin are utilised by the host to reduce the free extracellullar iron levels to 10^{-18} M; levels insufficient for bacterial growth (Bullen, 1981). Similarly calprotectin, a well known mammalian calcium binding protein, chelates the nutrient Zn^{2+} to inhibit bacterial growth and prevent the spread of infection. This prominent cytosolic neutrophil protein also indirectly inhibits bacterial growth by chelating manganese (Mn2+) (Corbin et al., 2008), an essential component of bacterial superoxide dismutase A

activity, which enzymatically inactivates reactive oxygen species (ROS) that are directly involved in bacterial killing (Yasui & Baba, 2006).

1.2.3 The complement system

The complement system is comprised of a family of elegantly coordinated proteins that produce acute inflammatory responses to directly and indirectly kill foreign invaders. It acts through three distinct pathways: the alternative, lectin and classical pathways; all of which have a role in the host defence against *S.aureus* (Lambris, Ricklin, & Geibrecht, 2008; S. H. M. Rooijakkers & van Strijp, 2007; P F Zipfel, Wurzner, & Skerka, 2007). Sequential activation of these secreted and cell-surface bound proteins can directly lyse bacterial cells through the formation of hydrophobic membrane attack complexes (MAC) (Walport, 2001). This defence is most effective against gram-negative bacteria that have a thin cell wall, whereas gram-positive bacteria such as *S.aureus* are not susceptible due to their thicker peptidoglycan cell wall layer. However, the complement system can also indirectly kill foreign invaders by marking cells for destruction by phagocytic cells (Fallman et al., 1993). This process of complement fixation or opsonisation is the most effective defence against *S.aureus.* Deficiencies in complement can lead to recurrent staphylococcal infections (P. Morgan & Walport, 1991); an effect also observed in mice given cobra venom factor, which transiently depletes complement C3, the central component of all three complement pathways (Kock, Hew, Bammert, Fritzinger, & Vogel, 2004; Sakiniene, Bremell, & Tarkowski, 1999).

1.2.3.1 Activation of complement

The alternative and lectin pathways recognise distinguishing characteristics of the bacterial surface. The alternative pathway forms an amplification loop where complement factor C3b is slowly but continuously produced in fluid phase; primed for immediate activation in response to foreign attack (Fishelson, Pangburn, & Muller-Eberhard, 1983). Host cells are protected by host regulatory proteins such as Factor H and C4-binding protein that promptly inactivate complement-derived opsonins (Anna M Blom, Kask, Ramesh, & Hillarp, 2003; Pickering et al., 2002). In contrast the lectin pathway utilises mannan binding lectin (MBL) proteins or ficolins. In complex with the MBL associated serine protease MASP-2, these factors recognise specific carbohydrates on foreign surfaces (Theil et al., 2000; Thiel et al., 1997) and activate MASP-2 to cleave C4 followed by C2 (Wallis et al., 2007). These calcium dependent complexes specifically recognise D-mannose, N-acetylglucosamine (GlcNAc) and fucose, whereas common features of mammalian glycoproteins such as D-galactose and sialic acid are not targeted. Although these recognition complexes display weak affinity for single carbohydrate domains its avidity dramatically increases when it binds to multiple domains (Petersen, Thiel, & Jensenius, 2001; Walport, 2001).

The classical pathway recognises specific antibody-antigen complexes through complement C1. The C1 complex is formed through the Ca2+ dependent association of two molecules of C1r and C1s (C1s-C1r-C1r-C1s), which subsequently interact with the collagen domain of C1q (Gaboriaud et al., 2004). Cell surface aggregation of IgG dramatically increases the binding affinity of the globular heads of C1q for IgG up to 1000-fold and initiates a conformational change that autoactivates C1r, which in turn activates C1s to produce an activated C1 complex (Budayova-Spano et al., 2002). IgM is a multivalent molecule thus does not require aggregation to efficiently activate C1q; however it does require antigen binding to structurally expose the C1 binding site (Feinstein, Richardson, & Taussig, 1986). Interestingly, C1q also interacts with a number of different ligands through its collagen domain, including DNA, C-reactive protein, serum amyloid protein and decorin, suggesting these complement proteins have links with the wider host response (Lu et al., 2008; Lu, Wu, & Teh, 2007).

1.2.3.2 The terminal complement pathway

All three pathways differ in their method of recognition but converge in the generation of short-lived surface-bound enzyme complexes called C3 convertases. The C3 convertase of the classical and lectin pathways is C4b2a. It is formed through the cleavage of complement factors C4 and C2 by the activated C1 complex or MBL associated serine proteases of the classical and lectin pathways respectively. For the alternative pathway the C3 convertase is C3bBb, which is formed through the binding of Factor B to C3b. It is activated by Factor D to cleave the central component C3 into C3a and C3b (Fishelson et al., 1983). C3b binds to the C3 convertase to form the C5 convertase (C4b2a3b or $(C3b)_2Bb$), which subsequently cleaves C5 to release C5a. C5b proceeds to bind C6, C7, C8 and C9 to form the membrane attack complex, C5b-9, that is involved in end-point cell lysis (Kolb & Muller-Eberhard, 1975). These pathways are also involved in opsonisation and the release of the powerful anaphylotoxins C3a, C4a and C5a, which in addition to formylated peptides, stimulate a potent proinflammatory and chemotatic response from phagocytic cells (Hammel et al., 2007b; Moon, Gorski, & Hughli, 1981). Specific complement receptors (CR1 and CR3) on the membrane of phagocytic cells recognize complement derived proteins C1q, C3b, iC3b and C4b, and promote phagocytosis and immune clearance (Fallman et al., 1993).

1.2.4 Immunoglobulins

Immunoglobulins are a group of five structurally-related heterodimeric glycoproteins that have each been adapted to respond to various environmental and immunological conditions of the host (Table 1.1). Their unique structure encompasses a range of abilities including neutralization of secreted proteins, phagocytosis and communication between the innate and adaptive immune responses (Gessner, Heiken, Tamm, & Schmidt, 1998). IgG, IgA, IgD and IgE comprise of two identical light chains and two identical heavy chains linked by disulfide bonds; IgM forms a larger hexameric or J chain-associated pentameric

structure containing the same basic units (Randall, King, & Corley, 1990). The kappa or lambda light chain (23 kDa) contains a variable and constant domain whereas the heavy chain (50-60 kDa) has a variable domain and up to four to five constant domains depending on the Ig isotype. In general the Fab portion, consisting of the light chain and first domain of the heavy chain (CH1), functions to recognize foreign epitopes, whereas the Fc (fragment crystalline) portion consisting of two to three constant domains triggers numerous effector functions. It is the highly flexible hinge region linking these two domains that allows the immunoglobulin molecule to adapt to different antigenic conformations and in turn influence receptor binding (Gaboriaud et al., 2003; Tan, Shopes, Oi, & Morrison, 1990).

Table 1.1: Physiochemical and biological properties of the five immunoglobulin isotypes.
(Adapted from Harlow & Lane, 1988)

	IgG	IgA	IgM	IgD	IgE
Subclasses	γ1-4	α1-2	-	-	-
Molecular weight (kDa)	150	160	950	180	190
Serum levels (mg/mL)	10	2	1.2	0.04	0.003
Complement fixation	+	-	+	-	-
Transplacental transfer	+	-	-	-	-
Host protection	Serum	Mucosal	B cell surface	B cell surface	Allergy

1.2.4.1 Fc receptors

The Ig Fc domain is recognised by FcRs present on the cell surface of nearly all leukocytes (Nimmerjahn & Ravetch, 2006). Once an Ig molecule binds an immunogenic surface through its Fab portion, it crosslinks the host FcRs and triggers an immune responses dependent on the cell type and FcR subtype. These functions range from phagocytosis, antibody dependent cellular cytotoxicity, secretion of inflammatory mediators and regulation of antibody production (Gessner et al., 1998). The neonatal Fc receptor, FcnR, binds to the Cγ2/Cγ3 domain of IgG to transfer maternal IgG to the fetus and also prevent its catabolism (Burmeister, Huber, & Bojorkman, 1994). The crystal structure of FcγRIII in complex with Fcγ1 clearly demonstrates a single valency, with structural rearrangement of the Cγ2 domain upon binding (Sondermann, Huber, Ooshuizen, & Jacob, 2000). A number of mutagenesis studies have implicated residues in the N-terminal Cγ2 domain and lower hinge region to be important in the interaction with FcγRs, including Leu^{234}, Leu^{235} and Pro^{331} (Canfield & Morrison, 1991; Oganesyan, Gao, Shirinian, Wu, & Dall'Acqua, 2008). Furthermore, the binding of all three FcγR subtypes is highly dependent on the presence

of N-linked carbohydrates that line the central cavity between the Fc heavy chain constant domains (Roy Jefferis, Lund, & Pound, 1998; Krapp, Mimura, Jefferis, Huber, & Sondermann, 2003).

1.2.4.2 Antibodies and complement

The Fc domains of IgG and IgM are ligands for the globular heads of C1q in the activation of the classical complement pathway (Kishore et al., 1998). IgG1 and IgG3 are the most efficient complement activators (Bindon, Hale, Bruggemann, & Waldmann, 1988). The C1q binding site has been localised to the upper Cγ2 domain of human IgG with key residues Asp^{270}, Lys^{322}, Pro^{329} and Pro^{331} forming the core binding site (Idusogie et al., 2000; A. Morgan et al., 1995; Tan et al., 1990; Thommesen, Michaelsen, Loset, Sandlie, & Brekke, 2000). However these residues are also conserved across the IgG subclasses IgG2 and IgG4 that do not activate complement suggesting that additional factors are important for C1q binding and/or complement activation. It has been proposed that the orientation of the Fc region with respect to the Fab domain is a critical determinant of C1q binding. Indeed without the hinge region to mediate this flexibility C1q binding is abolished (Gaboriaud et al., 2003). Interestingly, the C1q binding site on IgM is unique to the IgG site, concentrating on the Cμ3 domain residues Asp^{432}-X-Pro^{434}-X-Pro^{436} and Asp^{417}-Glu^{418}-X-His^{420} (Kojouharova, Reid, & Gadjeva, 2010).

Table 1.2: Physiochemical and biological properties of the four subclasses of human IgG
(Adapted from Gessner et al., 1998; Harlow & Lane, 1988)

	IgG1	IgG2	IgG3	IgG4
% in serum	66	23	7	4
Hinge amino acids	15	12	62	12
Segmental flexibility	Good	Very restricted	Excellent	Restricted
Allotypes	4	1	13	0
Complement fixation	++	+	++	-
Transfer to fetus	+	+	+	+
Protein A binding	+	+	-	+
Protein G binding	+	+	+	+
FcγRI (CD64)	+++	-	+++	+
FcγRII (CD32)	+++	-	+++	-
FcγRIII (CD16)	+++	-	+++	-

1.2.5 The coagulation cascade

The coagulation system, although not a traditional immune response, is crucial for maintaining homeostasis and supporting the inflammatory response (Esmon, 2004). It consists of a family of proteins that proceed along the extrinsic or intrinsic pathway to converge in the activation of Factor X and subsequent cleavage of prothrombin into thrombin (Warn-Cramer & Bajaj, 1986). Thrombin is the central enzyme of the coagulation system that is involved in the activation of platelets and cleavage of soluble fibrinogen into insoluble fibrin (Sambrano, Weiss, Zheng, Huang, & Coughlin, 2001). In the events of tissue injury the cascade is triggered to seal the breach and confine the inflammatory response to the site of injury thereby minimising further tissue damage. In doing so it also limits bacterial invasion and dissemination.

The intrinsic and extrinsic coagulation pathways are interdependent. The extrinsic pathway is activated by tissue factor (TF), a 45 kDa cellular lipoprotein expressed on a number of cells throughout the body that under normal conditions do not come into contact with blood (Drake, Morrissey, & Edgington, 1989). TF binds to and activates Factor VII, which is exclusive to the extrinsic pathway (Banner et al., 1996). Factor VIIa proceeds to cleave Factor X (Warn-Cramer & Bajaj, 1986). Activated Factor X can directly cleave prothrombin to thrombin however it is more efficient as a prothrombinase complex with Factor V, calcium and prothrombin (Krishanswamy, 1990). In contrast, the intrinsic pathway is initiated by the activation of Factor XII (Hageman factor) on a negatively charged activating-surface. Upon contact, a conformational change is induced in Factor XII allowing it to activate Factor XI, which in turn activates Factor IX (Griffin, 1978). Factor IXa and Factor VIIIa are involved in Factor X activation. Both pathways merge at this stage although several feedback loops and accelerating steps exist throughout the cascade. Overall, thrombin activation through the extrinsic pathway is ten-fold higher than the ‘contact-activated’ intrinsic pathway (Markiewski, Nilsson, Ekdahl, Mollnes, & Lambris, 2007).

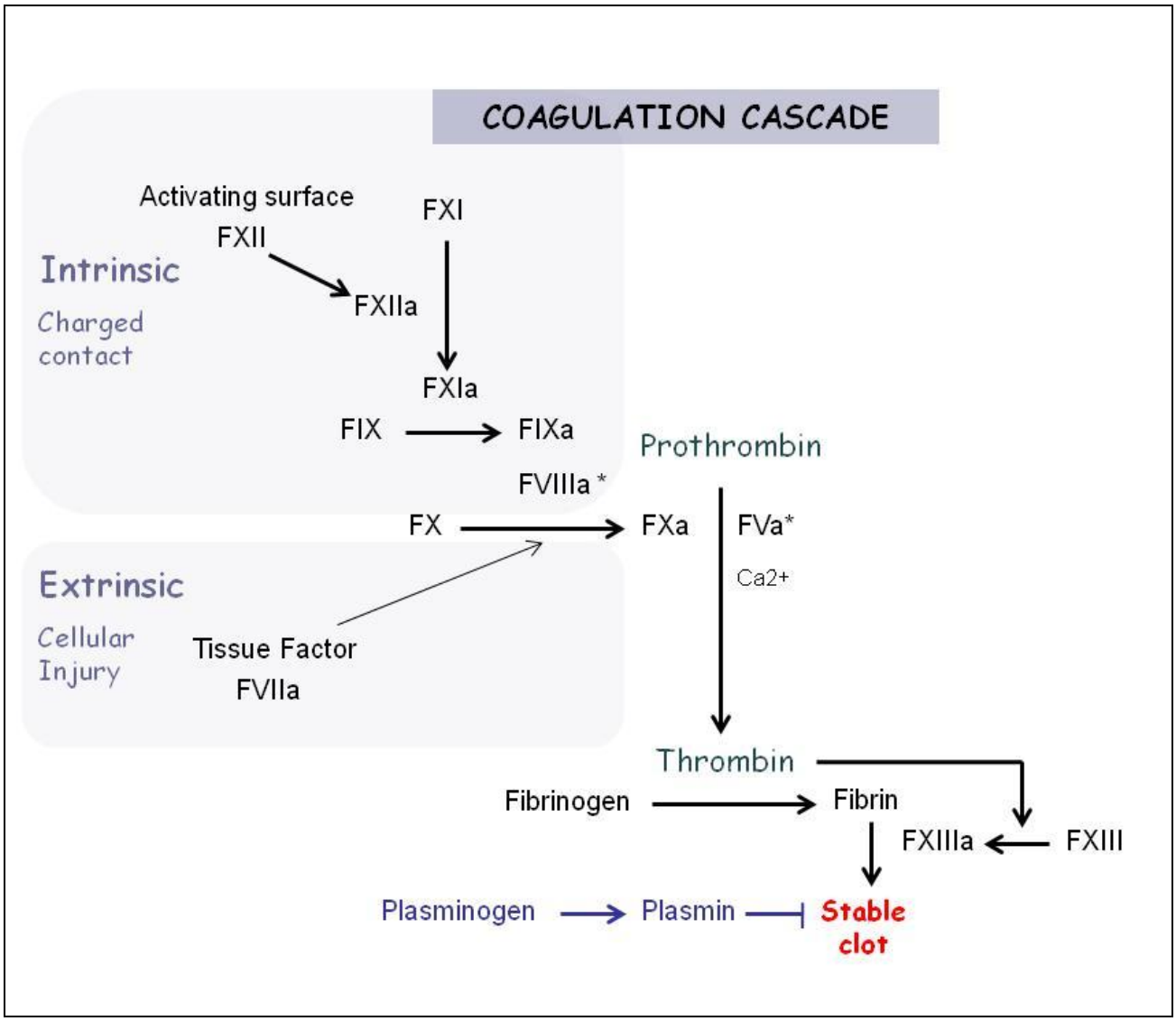

Figure 1.1: The intrinsic and extrinsic pathways of the coagulation cascade

The coagulation pathway consists of a cascade of serine proteases. The intrinsic pathway is activated by Factor XII recognition of negatively charged surfaces and subsequent activation of Factor XI, Factor IX and Factor X. The extrinsic pathway is triggered by release of tissue factor following cellular damage, which together with activated Factor VII cleaves Factor X. Both pathways converge at the cleavage of Factor X and formation of prothrombinase complex (Factor Xa, Factor Va, Prothrombin and calcium) involved in prothrombin cleavage. Thrombin converts fibrinogen into fibrin and activates Factor XIII to cross link the fibrin fibres into a stable clot. *Thrombin also regulates the activation of Factor V and Factor VIII to amplify the coagulation cascade (Markiewski et al., 2007). Plasminogen forms part of the fibrinolytic pathway dissolving clots in its activated plasmin form (Lucas, Fretto, & McKee, 1983). Activated products are denoted by ‘a’.

1.3 Virulence factors of *S.aureus*: pathway to pathogenesis

S.aureus employs sophisticated strategies involving a vast number of molecules that determine its severity and persistence (Fig 1.4). Key features of its attack include the colonisation of host cells and damaged tissues, inhibition of phagocytosis, resistance to antimicrobial agents, immunomodulation and immunological disguise (Foster, 2005; S. H. M. Rooijakkers & van Strijp, 2007). These strategies severely impact the function of phagocytic cells and the complement cascade, two key components of the immune defence against *S.aureus*.

1.3.1 The bacterial cell surface

Adhesion factors are important for breaking the initial barrier of defence to allow colonisation. *S.aureus* produces a collection of adhesion factors such as Protein A, fibronectin-binding protein (Ingham, Brew, Vaz, Sauder, & McGavin, 2004), collagen-binding protein and clumping factor A and B (Foster & Hook, 1998). These proteins are covalently anchored to bacterial cell wall peptidoglycans through the activity of a membrane-associated sortase enzyme that recognises a unique LPXTG motif on their C-terminal domain, prior to the hydrophobic membrane spanning region (Mazmanian, Liu, Ton-That, & Schneewind, 1999). The N-terminus generally contains the extracellular ligand binding domain that allows these molecules to seize ECM proteins, such as fibrinogen and fibronectin, for more effective delivery of direct virulence factors. By covering the bacterial surface with host proteins *S.aureus* is also able to strategically evade recognition by the host immune system (Foster, 2005; Foster & Hook, 1998). Increasing evidence suggests Fibronectin-binding protein also allows *S.aureus* to internalise and survive within host cells thereby concurrently evading the host immune system and antibiotic attack (Dziewanowska et al., 1999). Over recent years a number of unrelated proteins have also been noted to act as adhesions by binding back to the cell surface through ionic interactions and creating a bridge with host components. This includes coagulase, extracellular fibrinogen-binding protein (Efb), the ECM-binding protein, the extracellular adherence protein (Eap) and IsdA (Chavakis, Preissner, & Herrmann, 2007). The precise advantage of these secreted adhesins for the bacterium is still to be investigated.

1.3.2 Inhibition of complement

The complement system acts as a first line of defence against *S.aureus* infection thus it is the particular focus of several evasion strategies (Lambris et al., 2008; S. H. M. Rooijakkers & van Strijp, 2007). The cascade offers several key sites for interference, in particular the cleavage of complement factor C3 that unites all three pathways.

The complement pathways converge in the formation of the C3 convertases C4b2a and C3bBb. By specifically targeting these complexes in humans, Staphylococcal complement inhibitor (SCIN) acts as a potent modulator of all three complement pathways. This 9.8 kDa secreted protein is produced early during growth, presumably to modulate the early immune response (S. H. M. Rooijakkers et al., 2006). It stabilises the C3 convertases to prevent intrinsic decay, which normally results in the cleavage of C3 into C3a and C3b (S. H. Rooijakkers et al., 2009). This interferes with subsequent convertase assembly, C3b deposition and downstream activity of all three complement pathways, in particular the amplification loop of the alternative pathway (Susan H M Rooijakkers et al., 2005). Dimerisation of the convertases by SCIN also prevents their recognition by phagocytic receptors (Ilse Jongerius et al., 2010; S. H. Rooijakkers et al., 2009). Two additional SCIN homologues located on IEC-2, SCIN-B and SCIN-C, display similar complement inhibitory capacities as SCIN (I Jongerius et al., 2007).

Direct interference of C3 itself can disrupt all three complement pathways. The constitutively secreted Extracellular fibrinogen-binding protein (Efb) binds with high affinity to C3 through its C-terminal domain and imposes structural constraints that prevent further processing into C3b (Hammel et al., 2007a). This inhibits the formation of the C3 convertase of the alternative pathway and the C5 convertases of all three complement pathways. Its homologue, the Extracellular complement-binding protein (Ecb) displays similar properties to Efb across several species (I Jongerius et al., 2007). These proteins mimic the activity of the host regulators of complement (RCA), such as Factor H, Factor H-like proteins and C4b-binding protein, which strictly control complement activity (L. Lee et al., 2004). Additionally, the secreted protein Sbi specifically interacts with the C3dg and C3a segments of complement C3 (Burman et al., 2008; Upadhyay et al., 2008) and forms a supercomplex with Factor H or Factor H related protein-1 thereby avoiding further complement deposition (Haupt et al., 2008). Interestingly, the three helix buddle motif of the fourth Sbi domain that mediates C3 binding resembles the structure of Efb, Ecb and SCIN (Upadhyay et al., 2008). Sbi interaction with C3dg is abolished through alanine mutation of Arg^{231} and Asn^{238}. The orthologous residues on Efb are also critical for its interaction with C3d while Ecb activity is abolished with alanine mutation of Asn^{238} (Upadhyay et al., 2008).

1.3.3 Interference of leukocyte recruitment

Phagocytes that are recruited from the blood to the site of infection pose a major threat for *S.aureus*. In patients with leukocyte adhesion deficiency a mutation in the β-subunit shared by the leukocyte adhesive proteins β2 integrin lymphocyte functional associated antigen (LFA-1), macrophage-1 antigen (Mac1) and p150,95, breaks down the leukocyte recruitment process and increases susceptibility to recurrent *S.aureus* infections (A. Fischer & Lisowska-Grospierre, 1988). A similar survival advantage is attained by several secreted *S.aureus* proteins. The 60 kDa extracellular adherence protein (Eap), previously also referred to as the major histocompatibility class II analogue protein (Map), binds to the intercellular adhesion molecule-1 (ICAM-1) on the endothelial surface (Chavakis et al., 2002; Kreikemeyer, McDevitt, & Podbielski, 2002). This prevents the tethering of phagocytic cells through LFA-1 and Mac1, which is required for subsequent leukocyte extravasation (Chavakis et al., 2002).

S.aureus also directly hinders the mobilisation of phagocytic cells in response to chemoattractants. The chemotaxis inhibitory protein (CHIPS) blocks the detection of C5a and formylated peptides that are involved in stimulating a strong chemotactic response from phagocytic cells (Haas et al., 2005). CHIPS binds with high affinity to the C5a receptor, overlapping with several residues involved in C5a binding (Postma et al., 2005). Through a distinctly separate site, CHIPS also binds with lower affinity to the formylated peptide receptor (FPR) to prevent the detection of formylated peptides such as fMLP that are produced during bacterial growth (Wright et al., 2007). Similarly, FPRL1 inhibitory protein (FLIPr) impairs the neutrophil response to FPRL1 agonists by specifically inhibiting FPRL1-mediated calcium mobilization (Prat, Bestebroer, de Haas, van Strijp, & van Kessel, 2006). More recently, a FLIPr-like protein was discovered that inhibits both FPR and FPRL1-mediated calcium mobilisation (Prat et al., 2009).

1.3.4 Evasion of phagocytic cells

The key to avoiding confrontation with phagocytic cells lies in the ability of *S.aureus* to avoid opsonisation and thereby detection. Most individuals establish antibody responses against *S.aureus* however these are inadequate in preventing recurrent infections (Dryla et al., 2005; Holtfreter et al., 2009) This suggests *S.aureus* has established strategies to circumvent antibody function. Staphylococcal Protein A forms hydrophobic interactions with the Cγ2-Cγ3 elbow region of IgG (Cedergren, Andersson, Jansson, Uhlen, & Nilsson, 1993) through its five IgG binding domains in its N-terminal domain (Atkins et al., 2008). It coats the bacterial cell surface with IgG molecules in an unfavourable orientation for recognition by FcγRs on phagocytic cells (Ades et al., 1976). Protein A-deficient *S.aureus* strains are more efficiently phagocytosed by neutrophils *in vitro* and form smaller lesions *in vivo*, highlighting its pathogenic potential in *S.aureus* infections (A. H. Patel, Nowlan, Weavers, & Foster, 1987; Peterson, Verhoef, Sabath, & Quie, 1977). Additional support is provided by the secreted staphylococcal protein Sbi, which binds to the IgG Fc domain

at a site overlapping with that of Protein A (Atkins et al., 2008). Sbi extracellular domains I and II display affinity for IgG from a range of species. *S.aureus* also secretes staphylokinase, which hijacks and activates surface bound plasminogen to cleave the opsonins IgG and C3b (Shibata et al., 1994). Its cleavage of IgG in the hinge region at Lys^{222} removes the IgG Fc domain that is recognized by FcγRs. Similarly it cleaves the α- and β-chains of C3b and C3bi to prevent their detection by complement receptors on phagocytic cells (S. H. M. Rooijakkers, van Kessel, & van Strijp, 2005). Depending on the growth stage and surrounding medium, the deposition and recognition of opsonins by phagocytic cells is further hindered by extracellular polysaccharide capsules (Verburgh, Peterson, Nguyen, Sisson, & Kim, 1982).

1.3.5 Interference of phagocytic killing

Interference of phagocytic killing provides *S.aureus* with a significant survival advantage. Patients with chronic granulomatous disease have recurrent *S.aureus* infections due to a faulty NADPH oxidase that impairs oxidative killing (Quie, White, Holmes, & Good, 1967). Chediak Higashi patients who are defective in phagolysosome maturation also exhibit recurrent *S.aureus* infections (Root, Rosenthal, & Balestra, 1972). *S.aureus* has devised strategies to actively protect itself from phagocytic killing by reducing the lethal effects of singlet oxygen species (O^-). It produces two superoxide dismutase enzymes that actively remove O^- (Clements, Watson, & Foster, 1999). To enhance its protection *S.aureus* also utilises the antioxidant properties of carotenoid pigments that give rise to its characteristic golden colour. Carotenoids are potent free radical scavengers that can efficiently quench singlet oxygen and neutralise their lethal effects. The more virulent strains of *S.aureus* were frequently observed to have enhanced pigmentation and a breakdown in carotenoid synthesis produced non-pigmented staphylococci that were more susceptible to hydrogen peroxide and singlet oxygen. Indeed increased carotenoid production was associated with a dose dependent decrease in susceptibility to singlet oxygen killing (G. Y. Liu et al., 2005). In a separate study several cholesterol lowering drugs were also discovered to harbour anti-staphylococcal activity by blocking the synthesis of staphyloxanthin, an enzyme involved in carotenoid production (C. Liu et al., 2008).

1.3.6 Resistance to antimicrobial proteins

S.aureus enforces a range of mechanisms to neutralise antimicrobial proteins. It releases aureolysin and V8 proteases that inactivate LL37, a structurally simple linear CAM that proves to be an easy target for proteolytic cleavage (Sieprawska-Lupa et al., 2004). It also interferes with the activity of α-defensins using staphylokinase, which captures and actively removes the peptide from its target surface (Jin et al., 2004). *S.aureus* supports these strategies by indirectly circumventing the ability of antimicrobial proteins to interact with the bacterial membrane. By introducing positively charged residues to at least partly neutralise the negative charge of cell surface molecules as peptidoglycans, teichoic acids or phospholipids, the affinity of most positively charged antimicrobial proteins is reduced. D-alanine is commonly incorporated along the

highly negative glycerolphosphate repeating units of teichoic acid (Collins et al., 2002). Likewise, modification of the major membrane lipid phosphatidylglycerol with L-lysine by MprF produces a net positive charge (Peschel et al., 2001). Bacterial mutants that lack the ability to modify the net surface charge are highly susceptible to the activity of CAMs and other cationic host defence factors such as lysozymes, phospholipase A2 and lactoferrin (Collins et al., 2002; Friedrich et al., 2000; Peschel et al., 2001). *S.aureus* also produces a membrane-bound O-acetyltransferase that modifies muramic acid. This enhances their resistance against lysosymes that normally lyse cell by cleaving the central linkage between N-acetylglucosamine and N-acetyl muramic acid of cell wall peptidoglycans (Bera, Herbert, Jakob, Vollmer, & Gotz, 2005).

1.3.7 Leukocyte toxicity

S.aureus produces several toxins that have the ability to damage the membrane of host cells. The β-toxin hydrolyses sphingomyelin and causes large depressions in the membrane of a wide range of leukocytes (Huseby et al., 2007). A number of cytolytic toxins are also secreted as individual components that assemble into β-barrel pores in the host cell membrane to cause lysis. A prime example is the α-toxin, which is secreted as a monomer but combines to form a heptamer in the cell membrane (Gouaux, 1998). Another group of leukotoxins, including the γ-toxin or γ-haemolysin, the panton valentine leukocidin (PVL), leukocidin E/D and leukocidin M/F-PV are secreted as two subcomponents that combine to form hexameric or heptameric structures (Pedelacq et al., 1999). The γ-toxins have been implicated in the lysis of both erythrocytes and leukocytes whereas PVLs are specifically damaging to leukocytes (Prevost et al., 1995).

1.3.8 Avoiding immune recognition

S.aureus infections are the most common cause of infective endocarditis in the developing world (Fitzgerald, Foster, & Cox, 2006). Staphylococcal cells can cause rapid activation of platelets and subsequent thrombus formation by interacting with cell surface receptors directly or indirectly through secreted bacterial proteins or plasma bridging factors. This is demonstrated by fibronectin-binding protein and clumping factor A, which binds to fibronectin and fibrinogen respectively, to makes contact with the integrin GPIIb/IIIa on resting platelets. However, for complete activation, IgG-mediated activation of FcγRIIa or complement-mediated activation of complement receptors is required (Fitzgerald, Loughman et al., 2006; Loughman et al., 2005). Staphylocoagulase exhibits a similar role by interacting with prothrombin and inducing a conformational change that exposes its catalytic site and allows it to cleave soluble fibrinogen into insoluble fibrin fibres (Hendrix, Lindhout, Mertens, Engels, & Hemker, 1983). Staphylococcal cells can ultimately seek refuge to proliferate within the safety of the thrombus (Fitzgerald, Foster et al., 2006).

1.3.9 Superantigens

Superantigens are potent human toxins that target the communication link between the T cell receptor (TCR) and Major histocompatibility complex class II (MHCII) molecule (Proft & Fraser, 2003). They stimulate massive T cell activation, proinflammatory cytokine release and systemic shock by simultaneously binding to the MHCII and variable region of the TCR receptor β-chain (Vβ) (Fraser, Arcus, Kong, Baker, & Proft, 2000; Moza et al., 2007). This prevents contact of the MHCII-bound antigen with specific TCR residues and the normal antigen-stimulated response. Instead the Sag stimulated T cell response is dramatically greater than that of typical antigens with femtograms quantities of Sags activating up to 20% of T cells compared to the 0.001-0.0001% of T cells activated with conventional peptides (Bhardwaj, Friedman, Cole, & Nisanian, 1992). This response mimics a high antigen dose and affinity causing the cells to become unresponsive and undergo apoptosis. The group of T cells stimulated is determined by the affinity of the Sags for distinct Vβ TCR subsets and has been considered the footprint of each toxin (Bernal, Proft, Fraser, & Posnett, 1999). However human *in vitro* studies have produced inconsistent results to *in vivo* studies; possibly due to the site of infection and differential immune responses to varying Sag concentrations. Notably, different Vβ subtypes respond at different Sag concentrations but are all classed as Sag responsive (Fraser et al., 2000; Ulrich, 2000).

The Sags from gram-positive bacteria include Toxic shock syndrome-1 (TSST-1), the staphylococcal enterotoxins (SE), the streptococcal pyrogenic exotoxins (Spe), and the streptococcal mitogenic exotoxins (SMEZ). They share a common structural motif comprising of an N-terminus OB-fold domain and C-terminus β-grasp domain, which can remarkably sustain high levels of variation. Interestingly the expression of these Sags is also linked. TSST positive strains do not show signs of inflammation or tissue destruction in subcutaneous infection models in mice that are normally characteristic of staphylococcal lesions (Vojtov, Ross, & Novick, 2002). This was linked to suppression of majority of the exoproteins at the level of transcription by the cytoplasmic TSST precursor, which also acts as an autorepressor (Vojtov et al., 2002).

A number of B cell Sags have also been isolated from *S.aureus*. Unlike conventional antigens, B cell Sags bind to the Fab regions outside the complementarity determining regions of B cell receptors to cause large scale B cell activation and clonal deletion (Anderson, Sporici, Lambris, LaRosa, & Levinson, 2006; Gregg J Silverman & Goodyear, 2006). Protein A is the best characterized B cell Sag. It binds to the Fab region outside the CDR of VH3+ Igs that are expressed on up to 60% of human B cells (Starovasnik, O'Connell, Fairbrother, & Kelly, 1999). Numerous other B cell Sags also exist including HIV protein gp120 (Karray & Zouali, 1997), endogenous gut-associated sialoprotein Protein Fv (G J Silverman, Pires, & Bouvet, 1996), Protein L (Genovese et al., 2003) and staphylococcal enterotoxin D (Domiati-Saad et al., 1996).

1.4 Staphylococcal superantigen-like proteins (SSLs)

The staphylococcal superantigen-like proteins (SSLs), previously known as staphylococcal exotoxin-like proteins (SET), are a family of fourteen pathogenicity factors that interact with different aspects of the human immune response. These proteins are exclusive to *S.aureus* and were first identified during homology searches for conserved amino acid motifs from superantigens (V. L. Arcus, Langley, Proft, Fraser, & Baker, 2002; Williams et al., 2000). The staphylococcal superantigen TSST-1 shares up to 30% sequence homology with the SSLs (V. L. Arcus et al., 2002). More recently, two homologues, Sca0436 and Sca0905, have been discovered in *Staphylococcus carnosus*, a non-pathogenic bacterium isolated from meat fermentation products (Rosenstein et al., 2009). Interestingly Sca0905 displays close homology to the main cluster of SSL proteins SSL1-SSL11, while Sca0436 is more closely related to the SSL12-SSL14 (Fig. 1.2).

Crystallisation of SSL4 (S Hermans, Personal communications), SSL5 (V. L. Arcus et al., 2002), SSL7 (Al-Shangiti et al., 2004), SSL9 (Dr N Jackson, Personal communication) and SSL11 (Chung et al., 2007) has revealed strong structural homology to superantigens. The classic superantigen fold is composed of a C-terminal β-grasp domain consisting of four to five anti-parallel β-strands that cradle a highly conserved amphiphatic central α helix. This domain is linked to a smaller N-terminal OB-fold domain consisting of a five-stranded closed β-barrel that is capped by an N-terminal α helix (Proft & Fraser, 2003). The OB-fold is an ancient fold capable of binding to oligosaccharides, oligonucleotides and proteins (V. Arcus, 2002). Interestingly, the β-grasp fold is also a common structural feature of a number of unrelated immune evasion factors including staphylokinase, CHIPS and Eap (Haas et al., 2005). This demonstrates the enormous capacity of these structural folds to maintain a diverse range of functions. The SSLs have also diverged to an extent that they do not share the functional properties of superantigens with respect to their ability to bind MHC II and TCR simultaneously and hyperstimuate a T cell-mediated cytokine response (V. L. Arcus et al., 2002). Instead these proteins appear to have distinct roles in the evasion of the immune response.

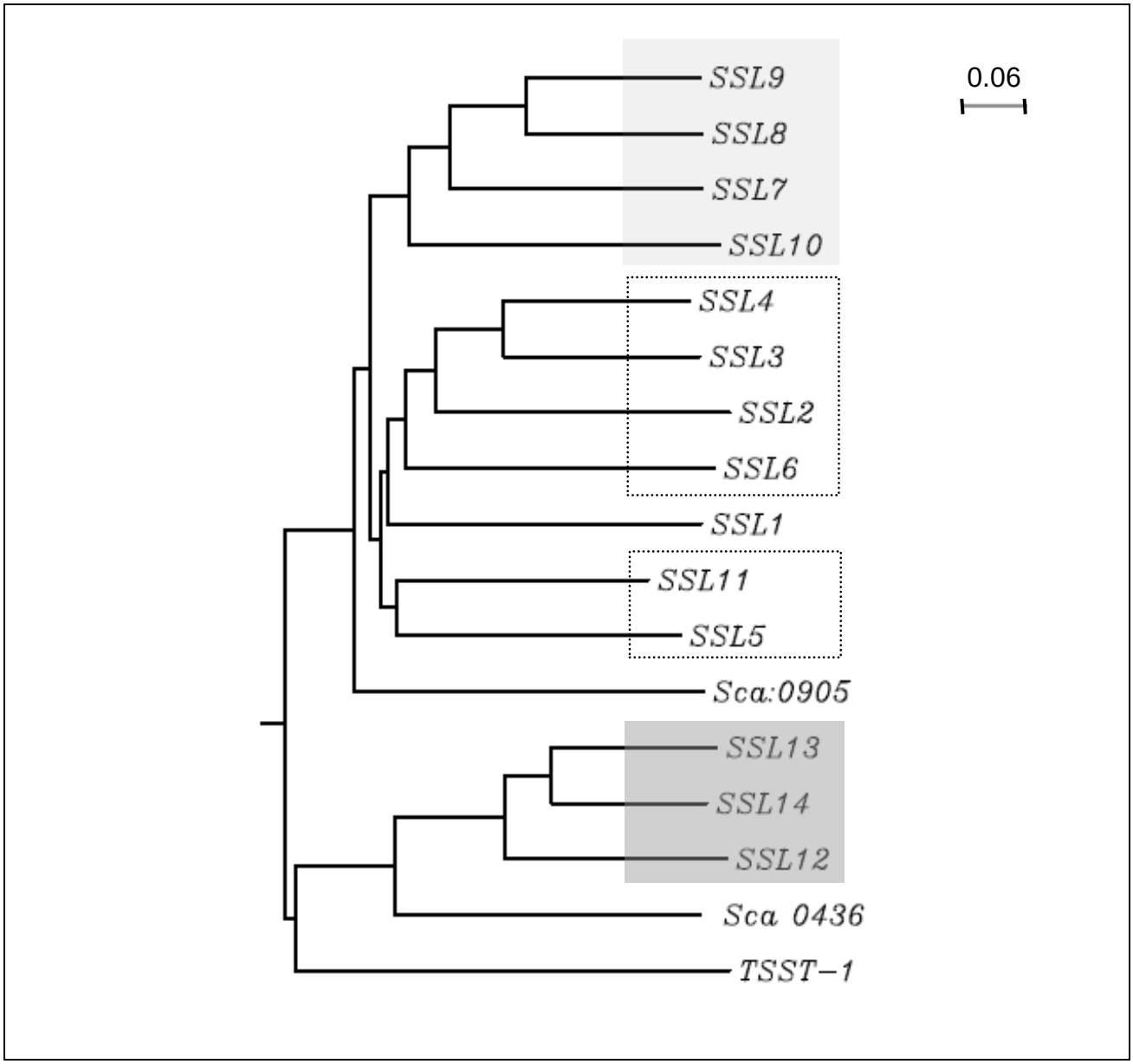

Figure 1.2: Comparison of the Staphylococcal superantigen-like protein family and TSST-1 from *S.aureus* MW2, and homologous proteins from *S.cereveia* using a neighbour-joining tree.

The amino acid sequences of SSL1-SSL14 and TSST-1 from *S.aureus* and two homologous proteins, Sca 0436 and Sca 0905 from *Staphylococcus carnosus*, were aligned using ClustalW and a neighbour-joining tree was constructed (Thompson, Higgins, & Gibson, 1994). SSL10 has strongest amino acid homology to SSL7, SSL8 and SSL9 (light gray) and falls into a distinct group of proteins separate from the carbohydrate binding family (box). A third group of SSLs exists on a separate gene cluster downstream from the main family and shows the greatest sequence divergence (dark gray).

1.4.1 The SSL gene locus

The SSL genes are present on the genomic island *v*Saα (T Baba, Bae, Schneewind, Takeuchi, & Hiramatsu, 2008; Lindsay & Holden, 2004). The main cluster (SSL1 to SSL11) is located in between the *hsdM* and *hsdS* genes that are part of a three component restriction modification system involved in maintaining and stabilising the gene cluster in the genome (Tadashi Baba et al., 2002; Feng et al., 2008). Three other more distantly related SSLs, SSL12-14, are located further downstream from the main cluster on an immune evasion cluster with extracellular fibrinogen-binding protein (Efb), extracellular complement-binding protein (Ecb), SCIN homologues and FLIPr (I Jongerius et al., 2007). The genes contain individual ribosome binding sites immediately upstream of the start codon and putative N-terminal signal peptide sequences suggesting they are individually regulated secreted proteins (Williams et al., 2000).

A total of sixty-three *S.aureus* isolates analysed from human, sheep, bovine and poultry origin were all shown by microarray to harbour the *ssl* locus (Smyth, Meaney, Hartigan, & Smyth, 2007). Given their conservation among the vast number of proteins in the *S.aureus* genome, this suggests there is a strong link between the SSL protein family and host immunity. The 12-17 kb region of sequence itself contains high levels of sequence diversification most likely due to horizontal gene transfer, recombination events and loss of *ssl* genes (Fitzgerald et al., 2003). The prevalence and diversity of the locus makes it an ideal candidate for the genotyping of *S.aureus* strains (Aguiar-Alves et al., 2006).

1.4.2 Sialic acid-binding proteins

A subgroup of the SSL family, SSL2 - SSL6 and SSL11, target glycoproteins expressing the common trisaccharide sialyllactosamine (sLe^x). From this family SSL11 (Chung et al., 2007) and SSL5 (Baker et al., 2007) have been co-crystalised with sLe^x . The specific targeting of sialyated proteins by SSL11 hinders the leukocyte adhesion process supporting neutrophil recruitment (Chung et al., 2007). Mutational analysis of SSL11 identified Thr^{168} in the β-grasp domain to be crucial in mediating this interaction. Interestingly, loss of SSL11 also coincides with a reduction in the adherence of *S.aureus* to the surface of surgical implants in a rat surgical infection model (Laughton, Devillard, Heinrichs, Reid, & McCormick, 2006).

1.4.3 IgA binding protein

IgA is the main immunoglobulin that defends mucosal surfaces thus hindering its activity provides microbial pathogens a strong survival advantage. SSL7 (formally known as SET1) binds to the Fc domain of human IgA1 and IgA2 through its OB-fold domain. It also binds to IgA from primate, pig, rat and horse, and secretory IgA from human, cow and sheep milk (Langley et al., 2005). Two SSL7 molecules bind to one Fcα homodimer in approximately the same plane, thereby making discontinuous but extensive contacts.

Loop regions L1 and L4 of the OB-fold bind to the lower Cα2-Cα3 junction of IgA, shielding majority of the lateral surface of Cα3 domain and competitively inhibiting FcαRI (B. D. Wines, Willoughby, Fraser, & Hogarth, 2006).

1.4.4 Complement inhibitors

SSL7 also interacts with complement factor C5 from human, primate, sheep, pig, and rabbit serum thereby inhibiting complement-mediated hemolysis and serum killing of gram-negative bacteria. This interaction is mediated through the β-grasp domain of SSL7, allowing simultaneous binding of IgA through its OB-fold domain (Langley et al., 2005). Dual interaction of SSL7 with IgA and C5 impedes the cleavage of C5 by the C5 convertase, protecting *S.aureus* from subsequent clearance by phagocytic cells; a priority for gram-positive bacteria than inhibition of end-point complement-mediated lysis (Laursen et al., 2010). A number of other SSLs have been implicated in complement inhibition including the close homolog SSL9 (Dr N Jackson, Personal communications), although their precise mechanisms of action are still to be defined.

1.4.5 Cellular interference

A number of SSL proteins have been reported to directly interact with myeloid cells. SSL11 is rapidly internalised by neutrophils and has been implicated in interfering with actin polymerisation (Chung et al., 2007). SSL7 and SSL9 interact specifically with dendritic cells and monocytes without causing adverse effects to their endocytic, antigen presentation or T cell stimulation capabilities (Al-Shangiti et al., 2004). SSL7 has also been reported to stimulate IL-1, IL-6 and TNFα secretion by peripheral blood mononuclear cells (Williams et al., 2000). The implications of these interactions, in particular with regards to their additional targets in immunity, still require further investigation.

1.4.6 SSL regulation

Numerous studies have noted differential regulation of the *ssl* genes in response to conditions that could mimic physiologically relevant circumstances. The surrounding microflora itself can impact largely on *S.aureus* virulence. This is evident in the expression of SSL11, which is repressed in the presence of *Lactobacillus reuteri* RC14, a gram-positive organism that commonly inhabits the mammalian gut (Laughton et al., 2006). Corbin and colleagues also noted a significant increases in the transcript levels of *ssl12*, *ssl13* and *ssl14* (SACOL1178-80) in the absence of Zn^{2+} (Corbin et al., 2008). More recently, under conditions of stress induced by heme toxicity a number of the *ssl* genes, including *ssl1*, *ssl2* and *ssl5*-*ssl10*, were upregulated to varying degrees along with a host of other virulence factors, transcriptional regulators and stress response systems (Stauff et al., 2008).

1.4.7 Staphylococcal superantigen-like protein 10

Studies investigating specific physiological conditions have noted some intriguing effects on *ssl10* expression. Internalisation of *S.aureus* into epithelial cells increases *ssl10* expression 3.7-fold, 2 and 6 hrs following internalisation, along with iron scavenging and virulence factor genes (Garzoni et al., 2007). Similarly, a 2- to 3-fold increase in both alleles of *ssl10* was observed 180 min following phagocytosis into neutrophils (Voyich et al., 2005). Interestingly, this observation was limited to certain *S.aureus* strains from both hospital and community-acquired infections, displaying differential regulatory capacities (Voyich et al., 2005). Furthermore, exposure of *S.aureus* to hypochloride, which is commonly utilised by phagocytes for microbial assault, also increased *ssl10* expression after 10 min of exposure, along with a number of other major virulence factor genes (M. W. Chang, Toghrol, & Bentley, 2007). In a separate study on *S.aureus* MW2, *ssl10* expression was reduced up to 1.5- to 2-fold in response to hypochloride and hydrogen peroxide exposure after 1 hr while it progressively increased by 3- to 5-fold after 2 h in response to azurophilic granules (Palazzolo-Ballance et al., 2008). Under standard growth conditions, there is a 3.2-fold higher expression of *ssl10* during the early stationary phase of wildtype *S.aureus* compared to the *S.aureus* mutant deficient in the *mgrA* small transcriptional regulator, suggesting that *mgrA* is an important regulator of the *ssl10* response (Luong, Dunman, Murphy, Projan, & Lee, 2006).

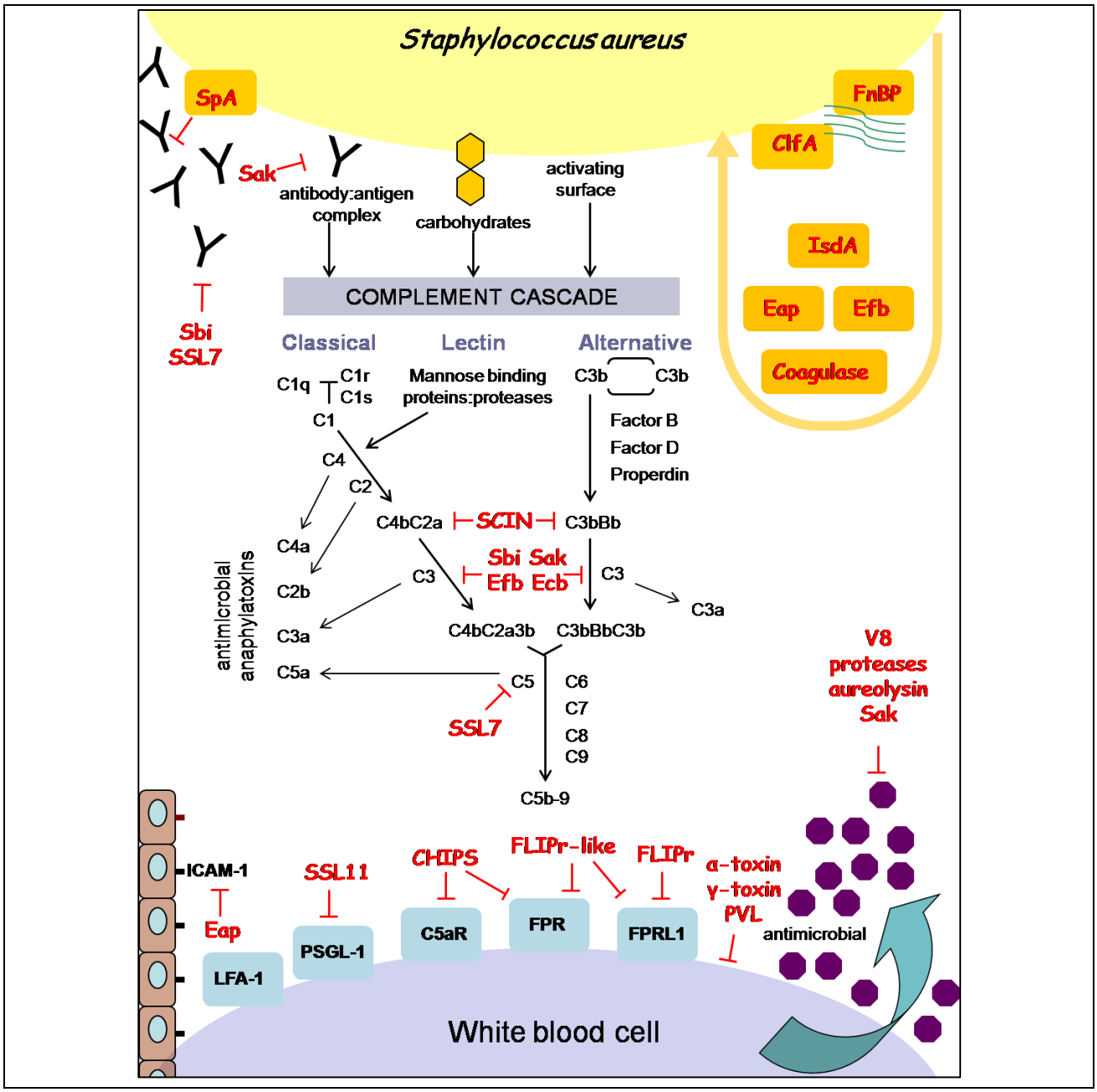

Figure 1.3: Summary of proteins produced by *S.aureus* to evade the host immune response.

S.aureus produces numerous proteins to promote colonisation and ensure its survival against the host responses of complement and phagocytic cells. Spa, staphylococcal protein A; Sak, staphylokinase; Sbi, staphylococcal immunoglobulin binding protein; SSL7, staphylococcal superantigen-like protein 7; ClfA, clumping factor A; FnBP, fibronectin binding protein; IsdA, iron regulated surface determinant protein A; Eap, extracellular adherence protein; Efb, extracellular fibrinogen binding protein; SCIN, staphylococcal complement inhibitory protein; Ecb, extracellular complement binding protein; SSL11, staphylococcal superantigen-like protein 11; CHIPS, chemotaxis inhibitory protein; FLIPr, FPRL1 inhibitory protein; PVL, panton valentine leukocidin; LFA-1, lymphocyte function associated antigen 1; P-selectin glycoprotein 1 PSGL-1 ; C5aR, C5a receptor; FPR, formyl peptide receptor; FRPL1, formyl peptide receptor-like 1.

1.5 Aim

S.aureus is a highly versatile organism that owes it success to the remarkable range of pathogenic factors that it has at its disposal. Advancing our understanding of these factors has become a key focus for developing therapeutics; especially since the emergence of antibiotic resistant strains that have made the treatment of *S.aureus* infections progressively difficult. Given the exclusive nature of the *ssl* genes in the *S.aureus* genome and their widespread distribution across all the isolates analysed to date, the SSLs are likely to play an important role in *S.aureus* pathogenesis. The aim of this research project is to investigate the functional and structural properties of SSL10 (formerly named SET4, SET14 and SET25) and enhance our understanding of its targets in host immunity and mechanisms of action.

Chapter 2
Materials and Methods

2.1 Materials

All reagents are purchased from BDH (UK) unless otherwise stated. Buffers were prepared in ddH_20 and filter sterilised through a 0.22 µm filter (Millipore, USA) or autoclaved at 121 °C, 15 psi.

2.1.1 Molecular biology

2.1.1.1 Reagents

DNA loading dye (10x)	0.25 % (w/v) bromophenol blue, 0.25 % (w/v) xylene cyanol (Serva, Germany), 60 % glycerol, 50 mM Tris pH 7.6
PCR buffer (10x)	0.1 % (v/v) Triton X-100, 500 mM KCl, 100 mM Tris HCl pH 9.0
Solution I	50 mM glucose, 10 mM EDTA, 25 mM Tris HCl pH 8.0
Solution II	1 % (w/v) SDS, 200 mM NaOH
Solution III	3 M potassium acetate, 11.5 % (v/v) glacial acetic acid
S.aureus lysis buffer	5 µg/mL lysostaphin (Sigma Aldrich, USA), 50 µg/mL DNAase-free RNAse A (Roche, Germany), 0.5 % (w/v) SDS, 150mM NaCl, 20mM EDTA, 50 mM Tris HCl pH 7.4
TAE	0.1 % glacial acetic acid, 2 mM EDTA, 40 mM Tris pH 8.0
TFBI	100 mM RbCl, 10 mM $CaCl_2$, 50mM $MgCl_2$, 30 mM potassium acetate, 15 % glycerol. Adjust to pH 5.8 with 0.3 M glacial acetic acid
TFBII	10 mM RbCl, 75 mM $CaCl_2$, 15 % glycerol, 10 mM MOPS pH 7.0

2.1.1.2 Plasmids

pET32a.3C was modified by Dr Ries Langely from pET32a (Novagen, USA) to include a 3C protease cleavage site (Appendix B). This plasmid encodes an ampicillin resistance gene thus can be selected for using 50 µg/mL ampicillin (Sigma Aldrich, USA). Oligonucleotide primers used for sequencing of the cloned gene are Stag forward (gaacgccagcacatggac) and T7 reverse (gctagttattgctcagcgg).

2.1.1.3 Bacterial strains and isolates

Table 2.1: Summary of bacterial strains and isolates

	Source	Details
Escherichia coli		
DH5α	ATCC, USA	Strain used for cloning
AD494(DE3)pLysS	Novagen, USA	Thioredoxin-reductase deficient strain. Resistant to kanamycin and chloramphenicol. Selected using 15 µg/mL kanamycin and 34 µg/mL chloramphenicol (Sigma Aldrich, USA)
Staphylococcus aureus		
ATCC25923 MRSA33938 MRSA13773	Germany	Clinical isolate
US0440 US9487 ATCC33539	Auckland Hospital, Auckland, NZ	Clinical isolate
NU9325 NU9485	Greenlane Hospital, Auckland, NZ	Clinical isolate
SAPRI RC31187 SA1137 SA196	Unknown	Clinical isolate
RN4220	Prof. Friedrich Goetz, University of Tuebingen, Germany	Restriction-deficient derivative of NCTC8325
Newman Newman ΔhrtA	Prof. Erick Skaar, USA	Laboratory strain Mutation of the heme-transporter A
Wood 46	NZ Culture Collection, ESR, NZ	Protein A- deficient strain
Streptococcus pyogenes		
ATCC700294	ATCC, USA	M1 Group A Streptococci from infected wound

2.1.1.4 Oligonucleotides

Table 2.2: Oligonucleotide primer sequence

Primers used for amplification of *ssl10* (Sigma Genosys, Australia). The restriction enzyme recognition sequence is underlined. *Primers designed by Dr RJ Langley, University of Auckland, NZ.

Name	Sequence 5'-3'	Restriction site
SSL10 Fwd*	cgggatccggtcatgcaaaacaaaatcaaag	BamHI
SSL10 Fwd2*	cgggatccaaacaaaatcaaaagtcagtaaataaac	BamHI
SSL10 Fwd3	cgggatccgacaaggaggcactataccgatac	BamHI
SSL10 Cterm Fwd	cgggatccggaacatctggagttgtcagtg	BamHI
SSL10 Rev*	ggaattcttactttaagttaacttcaatatctttaa	EcoRI
SSL10 Nterm Rev	ggaattcattacaccaccaacag	EcoRI

Table 2.3: Mutagenesis primers

Primers used for site-directed mutagenesis of *ssl10* (Sigma Genosys, Australia). The mutation sites are in bold.

Name	Foward primer 5'-3'	Reverse primer 5'-3'
R17A	cactatac**gca**tactacactggaaag	gtgtagtatgcgtatag**tgc**ctccttg
L32K33A	tgct**gcggca**catggtaaaaataac	gttatttttaccatg**tgccgc**agca
H34A	tgaaa**gct**ggtaaaaataacttg	gttatttttacc**agc**tttcaaa
G35K36A	ttgaaacat**gctgca**aataac	caagttatt**tgcagc**atgtttc
K36A	ttgaaacatggt**gca**aataac	caagttatt**tgc**accatgtttc
N37N38A	ggtaaa**gctgcc**ttgcgttttaag	cttaaaacgcaa**ggcagc**tttacc
Q61Q62A	gtaaattt**gcagcg**cgtagttatg	cataactacg**cgctgc**aaatttac
R63A	tttcaacag**gct**agttatgagg	acccctcataact**agc**ctgttg
K76A	ttgttcaagaa**gcc**agagataagcac	cttatctct**ggc**ttcttgaacaaaaaac
D78A	aagaaaaaaga**gct**aagcacg	atcgtgctt**agc**tctttttc
K79A	gagat**gcg**cacgatatattttatac	atatatcgtg**cgc**atctctttttc
H80A	ataag**gcc**gatatattttatac	atatatc**ggc**cttatctc
D81A	gataagcac**gct**atattttatac	aatat**atc**gtgcttatctc

2.1.1.5 Media for bacterial growth

Luria-Bertani broth	1 % (w/v) bacto tryptone (Oxoid, UK), 0.5 % (w/v) bacto yeast extract (Oxoid, UK), 1 % (w/v) NaCl
Todd Hewitt broth	as per manufacturer's instructions (Becton Dickinson, USA)
Tryptic soy broth	as per manufacturer's instructions (Becton Dickinson, USA)
Agar plates	Growth media including 1.5 % bacto agar (Becton Dickinson, USA)

2.1.2 Protein expression and analysis

2.1.2.1 Reagents

Coomassie stain	0.06 % (w/v) Brilliant Blue R-250 (Sigma Aldrich, USA), 50 % (v/v) ethanol, 7.5 % (v/v) acetic acid
Coomassie destain	25 % (v/v) ethanol, 8 % (v/v) acetic acid
IEF sample buffer	30 % (v/v) glycerol, 15 % (v/v) Bio-Lyte ampholines pH 3-10 (Biorad, USA)
IEF staining solution	1.5 % (v/v) perchloric acid, 0.01 % (w/v) brilliant blue G (Sigma Aldrich, USA)
Solvent A	0.1 % v/v acetic acid, 0.005 (v/v) % heptaflurobutyric acid
Solvent B	0.1 % v/v acetic acid, 0.005 % (v/v) heptaflurobutyric acid (Riedel de Haen), 80 % (v/v) acetonitrile
NTA I	10 mM imidazole, 10 % (v/v) glycerol, 300 mM NaCl, 50 mM sodium phosphate pH 8.0
NTA II	100 mM imidazole, 300 mM NaCl, 50 mM sodium phosphate pH 8.0
NTA III	300 mM NaCl, 50 mM sodium phosphate pH 8.0
PBS	2.7 mM KCl, 150 mM NaCl, 10 mM phosphate salts pH 7.4
SDS-PAGE loading dye (2x)	1.2 % SDS, 30 % glycerol, 15 % β-mercaptoethanol (Sigma Aldrich, USA), 1.8 % bromophenol blue, 150 mM Tris HCl pH 6.8
SDS-PAGE running buffer	0.1 % (w/v) SDS, 250 mM glycine, 25 mM Tris HCl
Solution A	30 % (w/v) acrylamide, 0.8 % (v/v) bisacrylamide
Solution B	0.4 % (w/v) SDS, 1.5 M Tris HCl pH 8.8
Solution C	0.4 % (w/v) SDS, 0.5 M Tris HCl pH 6.8

2.1.3 Functional analysis

2.1.3.1 Reagents

Coating buffer	15 mM $NaCO_3$, 35 mM $NaHCO_3$ pH 9.6
Erythrocyte lysis buffer (10x)	9 % (w/v) NH_4Cl, 1 mM tetrasodium EDTA, 100 mM $KHCO_3$ pH 7.4
FACS buffer	0.5 % (w/v) BSA (Gibco, Invitrogen, USA), PBS pH 7.4
GHB^{++} (5x)	0.75 M NaCl, 0.5 % (w/v) Bovine Skin Type B gelatin (Sigma Aldrich, USA), 0.3 mM $CaCl_2$, 2 mM $MgCl_2$, 0.3 M Hepes pH 7.35
GHB/MgEGTA (5x)	0.75 M NaCl, 0.5 % (w/v) Bovine Skin Type B gelatin (Sigma Aldrich, USA), 10 mM EGTA, 10 mM $MgCl_2$, 0.3 M Hepes pH 7.35
$HBS\text{-}EP^{+}$	3.4 mM EDTA, 0.3 M NaCl, 10 mM Hepes pH 7.4, 0.05 % (v/v) P20 surfactant (BIAcore Biosystems, Sweden)
Membrane stripping solution	100 mM β-mercaptoethanol (Sigma Aldrich, USA), 2 % SDS, 62.5 mM Tris HCl pH 6.7
OPD developing solution	50 mM citric acid, 100 mM Na_2HPO_4 pH 9.2. In 12 mL buffer add 0.012% H_2O_2 and 1 tablet O-phenylenediamine (Sigma Aldrich, USA)
Phagocytosis assay buffer	1 mM $MgCl_2$, 0.5 mM $CaCl_2$, 0.5 % (v/v) BSA, PBS pH 7.2
PBL lysis buffer	0.5 % Triton X-100, 300 mM NaCl, 50 mM Tris HCl pH 7.4, 1 tablet EDTA-free mini protease inhibitors per 10 mL (Roche, Germany)
Silver nitrate Developing Sol A	6 % Na_2CO_3, 0.0008 % $Na_2S_2O_3$
Silver nitrate Developing Sol B	0.1 % formaldehyde
TBS	140 mM NaCl, 10 mM Tris HCl pH 8.0
TBS-T	0.05 % (v/v) Tween-20, 140 mM NaCl, 10 mM Tris HCl pH 8.0
Towbin transfer buffer	192 mM glycine, 0.37 % (w/v) SDS, 20 % (v/v) methanol, 25 mM Tris HCl pH 8.3
TSA	0.5 % Triton X-100, 140 mM NaCl, 10 mM Tris HCl pH 8.0
Wash buffer	1 % Triton X-100, 0.1 % SDS, 500 mM NaCl, 10mM Tris HCl pH 8.0

2.1.3.2 Antibodies

Table 2.4: Summary of commercial antibody products

All antibodies are polyclonal unless stated otherwise.

	Species	Source[1]	Dilution	Details
Unconjugated antibodies				
Anti-Human C2	Goat	Calbiochem	1:10000	Detects complement C2
Anti-Human C3c	Rabbit	Sigma	1:4000	Detects activation product of complement C3
Anti-Human C4	Goat	Calbiochem	1:10000	Detects complement C4
Anti-Human C5b-9	Mouse	AbCam	1:4000	Monoclonal against neopeptide on the terminal complex of complement
Anti-Human Fibrinogen	Sheep	Sigma	1:10000	Detects fibrinogen
Anti-Sheep RBC	Rabbit	Virion/Serion	1:3000	Detects surface antigens on sheep erythrocytes
Horseradish peroxidise conjugated antibodies				
Anti-Human IgG	Goat	Serotec	1:10000	Secondary antibody
Anti-Goat IgG	Rabbit	Dako	1:15000	Secondary antibody
Anti-Rabbit IgG	Goat	Dako	1:2000	Secondary antibody
Anti-Mouse IgG	Goat	Dako	1:1000	Secondary antibody
Streptavidin	n/a	BD Pharmingen	1:1000	Binds avidly to biotin
Biotin conjugated antibodies				
Anti-Human IgG1	Mouse	Sigma	1:1000	Purified monoclonal IgG
Anti-Human IgG2	Mouse	Sigma	1:1000	Purified monoclonal IgG
Anti-Human IgG3	Mouse	Sigma	1:1000	Purified monoclonal IgG
Anti-Human IgG4	Mouse	Sigma	1:1000	Purified monoclonal IgG
Anti-SSL10	Mouse	[2]	1:10000	Purified monoclonal IgG1
Phycoerythrin-conjugated antibodies				
Anti-Human CD3	Mouse	Serotec	[3]	Detects T-cell specific marker
Anti-Human CD10	Mouse	Serotec	[3]	Detects Granulocyte specific marker
Anti-Human CD14	Mouse	BD Pharmingen	[3]	Detects Monocyte specific marker
Anti-Human CD19	Mouse	Serotec	[3]	Detects B-cell specific marker

[1] Calbiochem, Sweden; Sigma Aldrich, USA; Dako, Germany; Serotec, UK; AbCam, UK; BD Pharmingen, UK; Virion/Serion, Germany.
[2] Produced by Ms Rosica Petrova and Dr Fiona Radcliff (University of Auckland, NZ)
[3] 5 µL per 10^6 cells/mL as specified by manufacturer

2.1.4 Cell culture

2.1.4.1 Media

Complete RPMI 1640	Roswell Park Memorial Institute media 1640 pH 7.4 (Invitrogen, USA) supplemented with 1.5 mg/mL sodium bicarbonate , 50 U/mL penicillin (Gibco, Invitrogen, USA), 50 µg/mL streptomycin (Gibco, Invitrogen USA), 2 mM L-glutamine (Gibco, Invitrogen, USA), 110 µg/mL sodium pyruvate (Gibco, Invitrogen, USA) and 10 % FCS.
Fetal calf serum	heat inactivated for 30 min at 56°C and filtered (Invitrogen, USA)

2.1.4.2 Cell lines

Table 2.5: Summary of human cell lines and optimal growth conditions

Name	Cell type	Details	Culture conditions
U937 ATCC:CRL-2367	Monocyte	Isolated from adult male with histiocytic lymphoma	Complete RPMI 1640
THP-1 ATCC:TIB-202	Monocyte	Isolated from the peripheral blood of a 1 year old infant with acute monocytic leukemia	Complete RPMI 1640
ARH-77 ATCC:CRL-1621	B-lymphoblastoid	Isolated from peripheral blood of IgG plasma cell leukemia patient. EBV transformed	Complete RPMI 1640, 15 mM glucose, 10 mM HEPES pH 7.4

2.2 Methods

2.2.1 DNA purification

2.2.1.1 Purification of genomic DNA from *S.aureus*

S.aureus was grown in 10 mL LB O/N at 37 °C with shaking at 200 rpm. The bacterial culture was spun at 4,000 g for 5 min, and the pellet was resuspended in 0.5 mL *S.aureus* lysis buffer and incubated at 37°C for 30 min. The lysate was recovered, mixed with an equal volume of phenol and spun at 16,000 g for 10 min at 4°C. The upper aqueous phase containing the genomic DNA was collected and mixed with 1:1 phenol:chloroform before being spun at 16,000 g for 10 min at 4 °C. The upper phase was transferred to a clean tube and the DNA was precipitated with 0.1 volumes of 3 M sodium acetate pH 5.2 and 2 volumes of 100 % ethanol. The plasmid DNA was pelleted by spinning at 16,000 g for 10 min. The DNA pellet was washed with 70 % ethanol, air dried and resuspended in 50 µL sterile H_2O.

2.2.1.2 Extraction of plasmid DNA using alkaline lysis

Bacterial cells containing the plasmid of interest were grown from a single colony or glycerol stock in 3-5 mL LB containing the appropriate antibiotics. The culture was incubated O/N at 37 ^oC with shaking at 200 rpm. The following day, the bacterial cells were collected by spinning the culture at 16,000 g for 1 min. The supernatant was discarded and the pellet was resuspended in 200 µL Solution I. Solution II (200 µL) was added and gently mixed to lyse the cells. Solution III (200 µL) was immediately added and gently mixed by inverting several times to precipitate the chromosomal DNA. The cellular debris and chromosomal DNA were pelleted by spinning at 16,000 g for 10 min. The supernatant containing the plasmid DNA was transferred to a clean tube and precipitated with 2 volumes of 100 % ethanol. The precipitated DNA was pelleted by spinning at 16,000 g for 10 min. The pellet was washed in 70 % ethanol, air dried and resuspended in 50 µL H_2O. Contaminating RNA in the DNA preparation was digested with 10 µg/mL RNAseA (Roche, Germany) for 30 min at 37 ^oC. The plasmid DNA was further purified using 1:1 phenol:chloroform as described in Section 2.2.1.1.

2.2.1.3 Plasmid purification for sequencing

Plasmid DNA (45 µL) was mixed with 2 M NaOH/2 mM EDTA (5 µL) and incubated at 37 ^oC for 30 min. Ethidium bromide (7 µL of 10 mg/mL stock), ammonium acetate (70 µL of 7.5 M stock) and H_2O (75 µL) were added and mixed well. The plasmid preparation was extracted with an equal volume of 1:1 phenol:chloroform as described in Section 2.2.1.1 and resuspended in a final volume of 20 µL. Plasmid

DNA was sent for sequencing to the Allan Wilson Sequencing Facility (Palmerston North, NZ) or School of Biological Science Sequencing Facility (University of Auckland, NZ).

2.2.1.4 Agarose gel electrophoresis

DNA was mixed with 0.1 volumes of 10 x DNA loading dye and run at 90 V through a 1% (w/v) TAE agarose gel. After electrophoresis, the gel was stained in ethidium bromide (Sigma Aldrich, USA) in TAE buffer for 10-15 min. The gel was rinsed with H_2O and visualized using a Gel Doc 2000 (Biorad, UK).

2.2.1.5 Gel extraction

DNA was purified from TAE agarose gel using Promega gel purification kit (Promega, USA) or Zymoclean gel DNA recovery kit (ZymoResearch, USA). The DNA band of interest was excised from the gel over a UV light source, weighed and processed using the method specified by the manufacturer.

2.2.2 Amplification of DNA

2.2.2.1 Polymerase Chain Reaction (PCR)

PCR was performed in a DNA Thermal Cycler (Eppendorf, Germany) using Taq polymerase (produced in *E.coli* by Prof. J D Fraser, University of Auckland, NZ) to amplify DNA from either a bacterial colony (for screening purposes) or purified template DNA. PCR reactions were performed in a total volume of 50 µL containing: ~1 µg template DNA, 100 mM of each dNTP (Bioline, UK), 0.5 µM of each forward and reverse primer, 1x PCR buffer, 2.5 mM $MgCl_2$ and 1 U Taq DNA polymerase. An initial denaturation step was performed at 95 ^{o}C for 2 min, followed by 15-20 cycles of a denaturation step at 95 ^{o}C for 30 secs, annealing step at 55 ^{o}C for 30 secs and an extension step at 72 ^{o}C for 30 secs. A final extension step was performed at 72 ^{o}C for 5 min. For colony PCR, reaction volumes were reduced to 25 µL.

2.2.2.2 Site directed mutagenesis by overlap PCR

A two-step overlap PCR was utilised to introduce specific mutations in the *ssl10* gene sequence (Ho, Hunt, Horton, Pullen, & Pease, 1989). These mutations were incorporated in the design of overlapping primer sets in the forward and reverse orientation by typically altering the first two bases in the amino acid codon to produce an alanine, a structurally simple amino acid. In the first round of PCR, the upstream and downstream fragments of the *ssl10* sequence were separately amplified using each mutant primer together

with the appropriate outer primer. The amplified fragments were gel purified to remove any contaminating plasmid DNA or primers. The excised fragments were combined and frozen at -80 ^{o}C. The frozen fragments were passed through a 1 mL filter tip to separate the agarose from the DNA that is released into the liquid phase. Approximately 5-10 µL of this suspension was used for the second round of PCR. When added together the complimentary regions of these fragments overlap and can be used as the template. As a result, the outer primers of the gene amplify a single fragment containing the introduced mutation.

2.2.3 DNA ligation and transformation

2.2.3.1 Restriction endonuclease digestion of DNA

Typically, digests were performed in a total volume of 50 µL containing 1 volume of 10 x reaction buffer and 0.5-1 µL of restriction enzyme(s) (Roche, Germany); maintaining the total enzyme volume below 10 % to avoid interference from glycerol. Digests were incubated at 37 ^{o}C for 1-2 h.

2.2.3.2 Ligation

Vector and insert DNA was digested with restriction enzymes to produce compatible ends and purified by gel extraction. In a total volume of 10 µL, 1 part vector and 3 parts insert were incubated with 1 µL T4 DNA ligase (Roche, Germany) and 1 µL 10x ligation buffer for O/N at 4 ^{o}C.

2.2.3.3 Production of chemically competent *E.coli*

LB broth (5 mL) supplemented with 20 mM MgCl and 10 mM KCl was inoculated with *E.coli* DH5α or AD494(DE3)pLysS from a glycerol stock and incubated overnight at 37 ˚C with shaking at 200 rpm. For AD494(DE3)pLysS cells the LB broth was supplemented with 15 µg/mL kanamycin and 34 µg/mL chloromphenicol (Sigma Aldrich, USA). The following day, 1 mL of the overnight culture was added to 100 mL LB broth (supplemented as above). The culture was incubated at 37 °C for 2 h or until an absorbance of OD_{600nm} = 0.3-0.4 was reached. The culture was split into 50 mL aliquots and spun at 4,000 g for 10 min at 4 °C. The bacterial cells were resuspended in ice cold TFBI and incubated on ice for 10 min. The bacteria were pelleted at 4,000 g for 10 min at 4 °C and gently resuspended in 4 mL ice cold TFBII. The cells were transferred to sterile tubes and rapidly frozen in an ethanol-dry ice bath before storing at -80 °C. Sterile conditions were maintained throughout the procedure.

2.2.3.4 Transformation of chemically competent *E.coli*

Ligation mix (5 µL) was added to 50 µL chemically competent *E. coli* cells (DH5α or AD494(DE3)pLysS) and incubated on ice for 5 min. The bacterial cells were heat shocked at 42 ^{o}C for 30 sec and placed back on ice immediately for a further 5 min. The cells were spread on prewarmed LB agar plates containing the appropriate antibiotics. The plates were incubated at 37 ^{o}C O/N.

2.2.4 Protein expression and purification

2.2.4.1 Protein expression using pET32a.3c

The expression vector pET32a.3c containing the gene of interest was transformed into *E. coli* AD494(DE3)pLysS and a colony or glycerol stock was used to inoculate 100 mL LB broth supplemented with 50 µg/mL ampicillin, 34 µg/mL chloramphenicol and 15 µg/mL kanamycin. The culture was incubated overnight at 37 ^{o}C with shaking at 200 rpm. The following day, the culture was diluted in 1 L LB containing the appropriate antibiotics (as stated above) and incubated at 37 ^{o}C with shaking at 200 rpm for 1 h or until the cells reach log phase with an OD_{600nm} = 0.6-0.8. The culture was cooled to 30 ^{o}C, induced with 0.1 mM IPTG (Sigma Aldrich, USA) for a further 4 h at 30 ^{o}C with shaking at 200 rpm. The bacterial culture was spun at 16,000 g for 10 min. The supernatant was discarded and the pellet was stored at -20 ^{o}C.

2.2.4.2 Nickel affinity chromatography

The bacterial pellet was resuspended in NTA buffer I supplemented with 1 % (v/v) Triton-X100 and 0.1 mM PMSF (Sigma Aldrich, USA). The cells were burst using a Misonix X2015 sonicator (3x 1 min bursts at maximum power with a 75 % pulse). The bacterial debris was pelleted by spinning at 16,000 g for 10 min at 4 ^{o}C and the lysate containing the thioredoxin-fusion protein was collected. Nickel-nitrilotriacetic acid (Ni-NTA) metal affinity chromatography was utilized to purify the thioredoxin-SSL10 fusion protein via its N-terminal poly-histidine tag. The lysate was passed through a 3 mL IDA Sepharose column. The resin was washed with 10 volumes of NTA buffer I and the fusion protein was eluted with 5 volumes NTA buffer II. The fusion protein was cleaved to release SSL10 using 3C protease (1 % (w/w) of estimated fusion protein; recombinant protein produced in house) in the presence of 1 mM DTT. The fusion protein was digested overnight at 4 °C and cleavage was confirmed by SDS-PAGE. The cleaved protein was dialysed into 20mM phosphate buffer pH 8.0, 300 mM NaCl O/N at 4 °C. Alternatively, the fusion protein was cut on the column. Following the NTAI wash, the column was equilibrated in NTAIII. The beads were resuspended in 3C protease (1 % (w/w) of estimated fusion protein) and 1.5 mM DTT, and incubated O/N at 4 °C. The

following day, SSL10 was eluted with 2 column volumes of NTAIII while thioredoxin and any uncleaved protein remained bound to the Sepharose column.

2.2.4.3 Cation exchange chromatography

Attempts to pass the cleaved protein back through the IDA Sepharose column resulted in SSL10 binding non-specifically to the Sepharose beads. Similar problems were encountered with cleavage of SSL10 on the column. Therefore, further purification of SSL10 from thioredoxin and any other contaminating proteins was performed using cation exchange chromatography on an AKTA FPLC (GE Healthcare, Sweden). To separate thioredoxin from SSL10, the protein preparation was passed through a MonoS column (GE Healthcare, Sweden) containing negatively charged carboxymethyl cellulose resin. The protein was dialysed into 20 mM sodium phosphate buffer pH 8.0 including 300 mM NaCl, which was used as the running buffer. The column was equilibrated with 5 column volumes of the running buffer at 2 mL/min before the protein sample was loaded onto the column. The column was washed with a further 10 column volumes and the bound SSL10 was eluted using a salt gradient of up to 1 M NaCl over 10 min. SSL10 was eluted at ~60 % of the NaCl gradient.

2.2.4.4 Size exclusion chromatography

Size exclusion chromatography was performed on a Sephadex 75 or 200 GL column (GE Healthcare, Sweden). The running buffer was typically PBS pH 7.4 or 20 mM Tris pH 8.0, 100 mM NaCl. A maximum sample of 500 µL was filtered and loaded onto the column. The column was run at 1 mL/min and fractions were collected at peak 280 nm absorbance.

2.2.4.5 IgG purification from plasma and ARH-77 cell line

Plasma from heparinised human blood was isolated using ficoll paque plus (GE Healthcare, Sweden) or Histopaque (Invitrogen, USA) and passed over a Protein A porous Sepharose column (Perseptive Biosystems, USA). The bound IgG was washed extensively in PBS pH 7.4 and eluted with 100 mM glycine pH 3.0 into 0.1 volumes of 1 M Tris pH 9.0 to neutralize the pH. For IgG3 purification the plasma was first passed over HiTrap Protein G Sepharose (GE Healthcare, Sweden). This was followed by a subsequent step using Protein A Sepharose where the unbound IgG3 was collected. The purified IgG was dialysed into PBS pH 7.4, filter sterilised and stored at 4 °C. For purification of monoclonal IgG1, ARH-77 cell line was grown in RPMI supplemented with 15 % FCS as per ATCC guidelines. The supernatant was collected after 5 days and the monoclonal IgG1 was purified over Protein A Sepharose as stated above.

2.2.4.6 Papain cleavage and purification of human IgG Fc

IgG (1.5 mg/ml) in PBS pH 7.4 was cleaved with papain (100 µg/mL; Sigma Aldrich, USA) in digest buffer (0.02 M EDTA, 0.02 M L-cysteine (Sigma Aldrich, USA), PBS pH 7.4) for 1h at 37 ^{o}C. The reaction was immediately quenched with fresh 0.01 volumes of 0.3 M idoacetamide (Sigma Aldrich, USA). The papain digested IgG was passed over rSSL10-coupled sepharose as described above to specifically purify the Fc domain of IgG. The fractions were analysed by SDS-PAGE under non-reducing conditions.

2.2.4.7 Prothrombin purification from plasma

Prothrombin was purified from blood collected in sodium citrate vacutainer tubes (Becton Dickinson, USA). Plasma was collected by spinning the tubes at 1500 g for 10 min. It was transferred to a small conical glass flask and PMSF (1 mM, Sigma Aldrich, USA) was added immediately. Proteins were precipitated using 1 M BaCl (0.8 mL/10 mL plasma) for 1 h at 4 ^{o}C. The precipitate was spun at 5000 g for 10 min at 4 ^{o}C. The large pellet was resuspended in 0.9 % NaCl (0.8 mL NaCl/ 10 mL plasma). The solution was transferred to an eppendorf, spun at 4 ^{o}C and washed in NaCl again. The precipitate was resuspended in 0.5 M EDTA pH 8 (1.5 mL/10 mL plasma) and rotated for 20 min at 4 ^{o}C. The resuspended protein solution was dialysed into 10 mM Tris pH 8.5 overnight at 4 ^{o}C. Prothrombin was purified on a MonoQ column (GE Healthcare, Sweden) using a NaCl gradient (0-1 M) over 10 min. Prothrombin was eluted at approximately 0.7 M NaCl (Dahlback, 1983).

2.2.5 Protein characterisation

2.2.5.1 Sodium dodecyl sulphate-polyacrylamide gel (SDS-PAGE)

The SDS-PAGE gels consist of a separating gel layered underneath a stacking gel. The separating gel was prepared first with Solution A, Solution B, TEMED (Biorad, UK), and ammonium persulphate (APS). The polymerisation agents, TEMED and ammonium persulphate were added immediately before pouring the gel. Water-saturated butanol was layered over the separating gel to ensure a level interface between the two sections. Once the separating gel was set the butanol was removed. The stacking gel was then prepared from Solution A, Solution C, TEMED, and 10% (v/v) ammonium persulphate (APS). It was poured over the separating gel and a comb was inserted to form the wells. Table 2.4 summarises the precise volumes added for the preparation of two 7.5 - 17 % SDS PAGE gels.

2.2.5.2 Protein electrophoresis

One dimensional discontinuous SDS-PAGE was performed using a Mighty Small II vertical gel electrophoresis unit (Hoefer, GE Healthcare, Sweden). The samples were mixed with an equal volume of 2x SDS-PAGE sample buffer. For the separation of proteins under reducing conditions 5 % β-mercaptoethanol was included in the loading buffer, whereas for non-reducing conditions the β-mercaptoethanol was omitted. The samples were denatured by heated at 95 ^{o}C for 2 min prior to loading onto the gel. Electrophoresis was performed at 200 V, 20 mA in SDS-PAGE running buffer. Proteins were visualised by staining the gels in Coomassie Brilliant Blue R250 stain and destaining in Coomassie destain solution.

Table 2.6: Running and stacking solutions for SDS-PAGE gel

	7.5 %	10 %	12.5 %	17 %	Stacking gel
Solution A	2.4 mL	3.3 mL	4.2 mL	5.7 mL	0.5 mL
Solution B	2.5 mL	2.5 mL	2.5 mL	2.5 mL	-
Solution C	-	-	-	-	0.83 mL
Water	5.1 mL	4.2 mL	3.3 mL	1.8 mL	2 mL
TEMED	8 µL	8 µL	8 µL	8 µL	3.3 µL
10% APS	60 µL	60 µL	60 µL	60 µL	40 µL

2.2.5.3 Silver staining

For improved resolution of polypeptide bands the destained SDS-PAGE gel was silver stained after rinsing well in water. The gel was soaked in 0.02% $Na_2S_2O_3$ for 3 min and rinsed in water for 20 s before adding 0.1 % $AgNO_3$ for 10 min. Fresh developing solution was prepared by mixing equal volumes of Silver nitrate developing solution A and developing solution B. The gel was rinsed in water for 20 s before adding the developing solution for 1 min. The reaction was halted by adding 0.05 vol of 2.3M citric acid to the developing solution.

2.2.5.4 Isoelectric focusing

An isoelectric focusing (IEF) gel was prepared using 1.4 mL 50 % (v/v) glycerol, 1.28 mL Solution A, 3.89 mL H_2O and 385 uL ampholines pH 3-10 (Biorad, UK). The polymerisation agents TEMED (14 µL) and 10 % APS (29 µL) were added immediately prior to pouring the gel. A comb was inserted to form the wells. Once set, the gel was placed in a Biorad Mini-PROTEAN II chamber. A catholyte solution (0.2 % NaOH) was added to the upper chamber. The lower chamber was checked to ensure there were no leakages from

the upper chamber before adding the anolyte solution (0.12 % glacial acetic acid). Protein samples (5 µg) were diluted 1:1 in 2x IEF loading buffer (30 % (v/v) glycerol, 15 % ampholines pH 3-10) and loaded. An IEF standard (Biorad, USA) was also loaded to ensure focusing of the gel. The gel was run at 150 V and slowly increased in increments of 50 V to a maximum of 250 V until the bottom blue phycocyanin band splits in two (~2 h). The gel was stained with IEF staining solution and destained in Coomassie destain solution.

2.2.6 Protein modification

2.2.6.1 Coupling of proteins to sepharose

CNBr-activated Sepharose 4B (GE Healthcare, Sweden) was resuspended in 1 mM HCl (1 g/3.5 mL) and washed in several aliquots of 1 mM HCl through a scintered glass filter. CNBr-activated Sepharose was stored 1:1 in 1 mM HCl. Protein (1 mL of 2 mg/mL) in PBS pH 8.0 was coupled to CNBr-activated Sepharose (600 µL 1:1 slurry washed in coupling buffer) by rotating overnight at 4 ^{o}C. The following day the supernatant was removed from the protein-coupled Sepharose beads and the absorbance of the supernatant (OD_{280nm}) was measured to ensure efficient protein coupling. The beads were washed in coupling buffer six times. The buffer was removed using a Hamilton syringe and the active sites were blocked in 100 mM Tris pH 8.0 for 2 h at RT. The beads were resuspended 1:1 in PBS pH 8.0 with 0.025 % NaN_3 and stored at 4 ^{o}C.

2.2.6.2 Coupling of proteins to fluorescein

The succinimidyl ester of 5-(6)-carboxyfluorescein diacetate (Molecular probes, Invitrogen, USA) was dissolved at 2 mg/mL in dimethyl sulfoxide (DMSO) immediately prior to use. The carboxyfluorescein solution (5 uL) was slowly added to protein (500 uL of 2 mg/mL in PBS pH 7.4). The reaction was incubated overnight at 4 ^{o}C in the dark. Unconjugated fluorescein was removed by gel filtration through a G25 sephadex column (10 times the volume being loaded). The protein was eluted in small aliquots and the absorbance was measured at OD_{495nm} and OD_{280nm} to determine the fraction containing the fluorescein-conjugated protein. Fractions with an optimal ratio of fluorescein:protein (OD_{495nm}:OD_{280nm}) between 0.3 and 0.7 were used for future experiments. Concentration (mg/mL) of labelled protein was calculated using the formula: OD_{280nm} - (OD_{495nm} x 0.3) / extinction coefficient of protein.

2.2.6.3 Coupling of proteins to Alexa 488

The same procedure was followed as in Section 2.2.6.2 for labelling of protein with Alexa 488 (Molecular probes, Invitrogen, USA). Concentration (mg/mL) of labelled protein was calculated using the formula: OD_{280nm} - (OD_{495nm} x 0.11) / extinction coefficient of protein.

2.2.6.4 Protein biotinylation

Protein (2 mg/mL) or WBC cells in PBS pH 8.0 were biotinylated with 10mM EZ-Link sulfo-NHS biotin (Pierce, USA) rotating for 1 h at 4^{o}C. Biotinylated proteins were dialysed into PBS pH 8.0 overnight at 4 ^{o}C to remove excess biotin. For preparation of biotinylated cell surface proteins, the biotin was quenched in 100 mM glycine pH 3.0 and the cells were washed three times in PBS pH 8.0, spinning down the cells each time at 400 g at 4 ^{o}C.

2.2.6.5 Deglycosylation of proteins

PNGase F (New England Biolabs, USA) was used to remove N-linked carbohydrates from non-denatured proteins. Proteins (100 µg) or serum (100 uL) were incubated with 500 U PNGaseF (diluted in 1x G7 reaction buffer supplied by the manufacturer) and incubated for 2 h at 37 ^{o}C. Alternatively Neuraminidase (New England Biolabs, USA) was used to remove N-acetyl neuraminic acid specifically in the supplied 1 x G1 buffer for 2 h at 37 ^{o}C.

2.2.6.6 Trichloroacetic acid protein precipitation

Proteins in the culture supernatant (1 mL) of *S.aureus* were precipitated with 10 % (v/v) ice cold Trichloroacetic acid (TCA). The supernatant was mixed well and incubated at 4 ^{o}C overnight. The following day the sample was spun at 16000 g for 10 min at 4 ^{o}C. The supernatant was discarded and the pellet was resuspended in SDS-PAGE reducing buffer and 0.1 volumes of 1M Tris pH 9.0. The proteins were separated by SDS-PAGE and transferred onto nitrocellulose membrane as described in Section 2.2.11.2.

2.2.7 Production and purification of anti-SSL10 antibodies

A New Zealand white rabbit was injected with 100 µg $SSL10_B$ in 0.5 mL PBS pH 7.4 and Freund's incomplete Adjuvant (1:1; Sigma Aldrich, USA) at the Vernon Jansen Unit (University of Auckland, NZ). The post-immune sera collected after immunisation with SSL10 twice was compared with pre immune sera and determined to have high levels of SSL10 reactive antibodies using Western blot. The rabbit was bled and

the serum collected was stored at -20 ^{o}C. Rabbit antibodies were purified from serum over a POROS Protein A Sepharose column (PerSpective biosystems) using FPLC (AKTA, GE Healthcare, Sweden). Antibodies specifically against SSL10 were subsequently isolated by affinity purification over an SSL10 Sepharose column (Section 2.2.6.1). The rabbit antibodies were eluted with 0.1 M glycine pH 3.0 as described in Section 2.2.4.5. The purified antibodies were dialysed into PBS pH 7.4 and stored at 4 ^{o}C.

2.2.8 Mass Spectrometry

Samples were either sent to Dr C Buchanan, Centre for Genomics and Proteomics, University of Auckland or were prepared for mass spectrometry according to the method reported by Shevchenko et al. with minor modifications (Shevchenko, Wilm, Vrm, & Mann, 1996). Specific bands of interest were excised from an SDS-PAGE gel and transferred to eppendorf tubes prewashed with 50 % acetonitrile (Merck, Germany)/ 0.1 % trifluoroacetic acid (Riedel-de Haen). The gel bands were cut into 1 mm cubes and washed in 200 µL 0.2 M NH_4HCO_3 /acetonitrile (1:1) for 45 min at 37 ^{o}C. The gel pieces were shrunk in 100 µL acetonitrile until completely white. The acetonitrile was removed and the gel pieces were dried in a SPDIIIV SpeedVac with a RVT40 Refrigerated Vapor Trap (ThermoSavant, USA) for 5 min at RT. The gel pieces were rehydrated in 20 mM DTT/0.1 M NH_4HCO_3 for 30 min at 56 ^{o}C. The excess liquid was removed and the pieces were shrunk with 100 µL acetonitrile. The acetonitrile was removed and the pieces were incubated with 50 µL 55 mM idoacetamide/ 0.1 M NH_4HCO_3 at RT in the dark for 15 min. The excess liquid was removed and the gel pieces were washed with 0.1 M NH_4HCO_3. The gel pieces were shrunk with acetonitrile, washed with water and shrunk again with acetonitrile. The acetonitrile was removed and the pieces were dried in the SpeedVac for 5 min at RT. Sequence grade modified trypsin (Promega, USA) was resuspended in its recommended buffer at 0.5 µg/mL and activated at 37 ^{o}C for 10 min immediately prior to use. The processed gel pieces were incubated with 10 µL trypsin solution for 10 min at RT. The gel was covered with 0.1 M Tris HCl pH 9.2, 10 % (v/v) acetonitrile and incubated at 37 ^{o}C in the dark overnight. The following day, the excess liquid was collected into a clean eppendorf tubes and the peptides were extracted twice from the gel pieces with 150 µL 0.1 % (v/v) TFA/60 % (v/v) ACN for 30 min at 37 ^{o}C. The fractions were combined and dried down to an invisible pellet using the SpeedVac. The pellets were stored at -20 ^{o}C.

For mass spectrometry, the pellets were resuspended in 20 µL Solvent A. The mixture was spun at 16,000 g for 5 min to remove any undissolved material and the liquid was transferred to StepVial II vials (SUN Sri, USA). Samples were analysed by LC/MSD Trap (Agilent 1100 Series) through a Zorbax SB-C18 column (150 mm x 0.5 mm; Agilent Technologies, Germany) using Solvent A and Solvent B gradient. The data was processed using an Agilent software programme and analysed using the MASCOT MS/MS ion search database (www.matrixsciences.com).

2.2.9 Cell culture

2.2.9.1 Preparation of serum

Blood was collected from healthy human volunteers in glass Vacutainer tubes (Becton Dikinson, USA). For serum preparation, blood was clotted at RT for 20-30 min and spun at 1,250 g for 20 min at 4 ^{o}C. Serum was immediately transferred to fresh tubes and stored at -80 ^{o}C.

2.2.9.2 Erythrocyte lysis with ammonium chloride

Blood was collected from healthy human volunteers in sodium heparin tubes (Becton Dickinson, USA) and added to 10 volumes of pre-warmed 1x erythrocyte lysis buffer. The erythrocytes were lysed at 37 ^{o}C with occasional mixing. Once the solution turned translucent the peripheral blood leukocytes (PBL) were immediately pelleted at 328 g for 5 min at RT and washed twice in PBS pH 7.4. Further lysis with erythrocyte lysis buffer was avoided to minimise damage to the PBLs. Alternatively, mild osmotic lysis was performed with 0.2 % (w/v) NaCl for 30 s followed by neutralisation with an equal volume of 1.6 % (w/v) NaCl. The cells were pelleted at 328 g for 5 min at 4 ^{o}C and washed twice in PBS pH 7.4.

2.2.9.3 Separation of PBMC and granulocytes

Blood was collected in sodium heparin or K_3EDTA vacutainer tubes (Becton Dickinson, USA) to inhibit coagulation and peripheral blood leukocytes were separated using Ficoll Paque Plus (GE Healthcare, Sweden) or a Histopaque (Invitrogen, USA) gradient. For Ficoll paque plus separation was by density centrifugation. An equal volume of blood was layered on top of Ficoll paque plus and spun at 800 g for 30 min at RT. The peripheral blood mononuclear cells were retained at the top interface of the plasma and ficoll paque plus media while the more dense granulocytes were layered on top of the erythrocytes at the bottom of the tube. Purification of granulocytes was ideally performed using a Histopaque gradient. Histopaque 1077 (2.5 mL) was carefully layered on top of Histopaque 1191 (2.5 mL). Blood (5 mL) was layered on top of the media and spun at 700 g for 30 min at RT. Peripheral blood mononuclear cells were present at the plasma-Histopaque 1077 interface where as the granulocytes were retained at the interface of the two Histopaque solutions well above the erythrocytes at the bottom of the tube. The PBLs collected were washed three times in PBS pH 7.4 and spun at 328 g for 10 min at 4 ^{o}C. Contaminating RBCs were removed by osmotic lysis (Section 2.2.9.2).

2.2.9.4 Lysis of blood leukocytes

Purified PBMCs and granulocytes were resuspended at $1x10^7$ cells/mL in WBC lysis buffer and incubated at 4 ^oC for 1 h. Insoluble material was spun down at 16000 g for 15 min at 4 ^oC. The soluble proteins were transferred to a fresh tube and stored at -80 ^oC.

2.2.10 Cellular interaction

2.2.10.1 Two colour staining of leukocytes with CD marker and SSL10-fluorescein

Purified peripheral blood leukocytes ($1x10^6$ cells/ml) were washed in FACs buffer and incubated with 5 µL fluorescein labeled -protein and 5 µL PE labeled specific antibodies against cluster differentiation surface markers (Serotec, UK): CD3, CD19, CD10, CD14 for 10 min at 4 ^oC in the dark. Cells were washed in FACs buffer to remove any unbound antibodies and resuspended in 500 µL FACS buffer. Control reactions containing unstained cells and cells with each stain alone were also included. For each sample 10000 events were analysed on a FacScan flow cytometer (Becton Dickinson, USA).

2.2.10.2 Competitive binding analysis

Polyclonal IgG1 or IgG3 purifed from human plasma using Protein A, Protein G and SSL10 Sepharose (Section 2.2.4.5) was labelled with fluorescein (Section 2.2.6.2). Fresh human peripheral blood mononuclear cells (PBMC) were purified from whole human blood (Section 2.2.9.3) and resuspended at $1x10^7$ cells/mL in FACS buffer. A two-fold dilution series of SSL10 or SSL7 (100 µg to 6.25 µg) was prepared in 50 µL FACS buffer. IgG-fluorescein (1 µg) was added to each dilution and incubated for 10 min. Fresh PBMCs ($5x10^6$ cells) were then added and incubated for a further 10 min before being washed three times with FACS buffer. Cells were resupspended in 0.5 mL FACs buffer and analysed for fluorescein staining FacScan or LSRII flow cytometer (Becton Dickinson, USA). Monocytes were selectively gated based on size and granularity, and 10000-30000 events were collected. All reactions were carried out in the dark at RT.

2.2.10.3 Confocal laser scanning microscopy and fluorescence microscopy

Freshly purified PBMCs were prepared and washed in PBS pH 7.4. PMBC ($1x10^6$ cells/mL) were incubated with 0.8 µM SSL10-Alexa 488 for confocal microscopy or SSL10-fluorescein for fluorescence microscopy for 10 mins at RT. Cells were washed three times in PBS pH 7.4 at 328 g for 5 min at 4 ^oC. Cells (50 uL) were spun onto a glass slide using Cytospin at 400 g for 2 min at RT and mounted in Prolong Gold with

DAPI. Cell were visualised by confocal laser scanning microscopy on a Leica TCS SP2 or fluorescence microscopy.

2.2.11 Analysis of protein interaction

2.2.11.1 Coprecipitation

The sample of interest (Serum/biotinylated protein/white blood cell lysate) (10-20 %) was diluted in TSA and mixed with 1 % (v/v) protein coupled-Sepharose beads for 1 hr at 4 ^{o}C. Beads were recovered by spinning at 16,000 g for 1 min and extensively washed in wash buffer and then once in TSA. Excess liquid was removed and the co-precipitated proteins were solubilised by boiling the beads in 10 µL SDS-PAGE sample buffer. The proteins were analysed by SDS-PAGE. For harsher wash conditions 1 % sodium deoxycholate was added to the wash buffer.

A modified two step coprecipitation method was also developed. SSL10 Sepharose was used to isolate biotinylated cell surface proteins of interest in the first round. Beads were washed as per standard method and bound proteins were eluted using 2 % SDS (w/v) at 55 ^{o}C and 65 ^{o}C. The eluted proteins were collected and incubated with Streptavidin agarose beads (Sigma Aldrich, USA) to specifically isolate biotinylated cell surface proteins. Bound proteins were solubilised by boiling in 10 µL SDS-PAGE buffer. The coprecipitated biotinylated proteins were analysed by Western blot (Section 2.2.11.2).

2.2.11.2 Western blot analysis

Proteins separated under reducing conditions on an SDS-PAGE gel were transferred onto a nitrocellulose (N+) membrane (Biotrace NT, Pall Life Sciences) in Towbin western transfer buffer using a Biorad transfer apparatus. Non-specific binding sites on the membrane were blocked with 5 % (w/v) non-fat milk powder in TBS-T. Antibodies against specific antigens of interest were incubated with the membrane in TBS-T for 1 h at RT. The membrane was washed twice in TBS-T for 5 min and twice in TBS for 15 min each. A peroxidase-conjugated antibody, specifically against the primary antibody was incubated with the membrane in TBS-T for 1 h at RT. Membranes were washed and developed using ECL chemiluminescence western blot detection kit (GE Healthcare, Sweden). Images captured using a Fujifilm LAS3000 imager (Alphatech, NZ) or developed on Kodak film (Kodak, USA). Membranes were stripped in Western stripping buffer for 10 min at 56 ^{o}C before being extensively washed and re-blocked overnight.

2.2.11.3 Enzyme-linked immunosorbent assay (ELISA)

Enzyme linked immunosorbent assays (ELISA) were performed on 96 well Maxisorb plates (Nunc, Denmark). Plates were coated with 50-100 µL antigen (1-25 µg/mL) diluted in sodium carbonate coupling buffer O/N at 4 ^{o}C. The plate was washed in TBS-T to remove any unbound antigen. The wells were blocked with 300 µL 0.5 % (w/v) BSA or 1 % (v/v) Tween in PBS pH 7.4 at RT for 1 h. Incubation of the test ligand or antibody was performed in 0.25 % (w/v) BSA or 0.5 % (v/v) Tween in PBS pH 7.4 for 1 h, followed by three washes in PBS-T. The captured antigen was subsequently detected with a specific primary antibody. The primary antibody was detected with a secondary antibody coupled to HRP. The bound complexes were detected with 50-100 uL OPD developing solution. Reactions were halted with an equal volume of 10 % (v/v) HCl. The absorbance was measured at OD_{490nm} on a µQuant spectrophotometer. For each assay, control wells without the immobilised antigen, ligand or the primary antibosy were also included to ensure the signal detected was not due to non-specific binding. All experiments were performed in duplicates and expressed as the average absorbance value $\pm$ s.d.

2.2.11.4 Analysis of glycan binding specificity by glycomics array

SSL10 labelled with carboxyfluorescein was submitted to the Consortium for Functional Glycomics (www.functionalglycomics.org) at the Scripps Research Institute (San Diego, California, USA) to test its interaction with 235 glycans on the Core H glycan array screen PA v3.2. SSL10 was analysed at 100 ug/mL in PBS pH 7.4.

2.2.12 Functional assays

2.2.12.1 *In vitro* PBMC proliferation assay

Purified PBMCs ($1x10^6$ cells/mL) were resuspended in RPMI media and added to titrated SSL proteins, PHA and SMEZ-2 (0-1 ug/mL) in a total volume of 200 µL in triplicate. Plates were incubated at 37 ^{o}C in 5 % CO_2 for three days before adding 10 % (v/v) AlamarBlue (Serotec, UK) and incubating at 37 ^{o}C in 5 % CO_2. OD_{570nm} and $OD6_{00nm}$ were measured and the ΔOD was calculated to determine the *in vitro* proliferation.

2.2.12.2 Phagocytosis assay

Two bacterial species were used in the phagocytosis assay: *Streptococcus pyogenes* (M1 strain ATCC700294), grown overnight in Todd Hewitt media under stationary anaerobic conditions or *S.aureus* (Wood 46), grown overnight in Trypic soy broth at 200 rpm under aerobic conditions. Cells were heat killed at 75 ^{o}C for 10 min and washed in PBS pH 7.4. Cells were resuspended to OD_{600nm} of 0.1 ($5x10^6$ cells/mL *S.pyogenes*; $5x10^7$ cells/mL *S.aureus*) and incubated with 1 µg fluorescein for 10 min at RT. Labelled cells were washed extensively with PBS until background was low and maintained on ice in the dark until use.

Polyclonal human IgG against Spy0128 pili protein on the cell surface of *S.pyogenes* were affinity purified from human plasma using recombinant Spy0128 protein (Dr H Kang, University of Auckland, NZ) coupled to sepharose beads. Human anti-spy0128 IgG (50 ug/mL) was incubated with 2 µM and 4 µM of SSL10 or SSL7, and 25 µL of *S.pyogenes*-fluorescien ($1.25x10^5$ cells) for 15 min at RT. Human monoclonal IgG1 purified from human lymphoblastoid cell line ARH-77 was also included as a negative control. For opsonisation of *S.aureus*-fluorescein ($1.25x10^6$ cells), purified human IgG1 pooled from patient sera (150 µg/mL) was used under the assumption that patients with *S.aureus* infections have high antibody titres against *S.aureus*. Bacterial cells were subsequently washed once in phagocytosis assay buffer.

Fresh human neutrophils were purified from blood obtained in EDTA collection tubes using Histopaque (Section 2.2.9.3). Cells were washed in FACS buffer and resuspended at $1x10^6$ cells/ml in phagocytosis assay buffer immediately prior to use. Neutrophils ($5x10^5$ cells) were added to opsonised bacteria and incubated for 10 min at 37 ^{o}C and then immediately washed in FACS buffer to remove any unbound *S.pyogenes*-fluorescein or *S.aureus*-fluorescein. Surface bound bacteria were quenched with 0.1% (v/v) Tryphan blue (Bjerknes & Bassoe, 1984) or lysed with lysostaphin (10 µg/mL; Sigma Aldrich, USA) for 20 min at 37 ^{o}C. Cells were washed and resuspended in 0.5 mL FACS buffer. The percentage of fluorescent neutrophils in 30000 events was measured using FacScan or LSRII flow cytometer (Becton Dickinson, USA). Higher concentrations of bacteria or lysostaphin caused lysis of neutrophils and thus were avoided.

2.2.12.3 Hemolytic complement assay

CH50 total complement haemolytic assay was performed in 96 well round bottom plates using opsonised sheep erythrocytes as the target antigen and guinea pig serum as the source of complement. Sheep erythrocytes (Gibco, Invitrogen, USA) were spun at 1250 g for 5 min at 4 ^{o}C and incubated with GHB^{++} buffer at 37 ^{o}C for 15 min to lyse any unstable erythrocytes. The erythrocytes were washed in GHB^{++} until the background supernatant was clear. A 1 % (v/v) suspension of sheep erythrocytes was sensitised with anti-sheep erythrocyte antibodies (1:3000), and incubated with guniea pig serum (1/300 dilution) and 0-2 µM of titrated protein for 1 h at 37 ^{o}C. Reactions were halted by pelleting the unlysed erythrocytes at 1250 g

for 5 min at 4 ^{o}C. The supernatant was transferred into a flat bottom 96 well plate and the absorbance at OD_{412nm} was measured. For the alternative pathway an identical procedure was used but with GHB/ MgEGTA buffer to remove the calcium required for activity of the classical and lectin complement pathways. Human RBC ($1x10^{7}$ cells; OD_{541nm} = 0.14 = $2x10^{8}$ cells/mL) was mixed with heterologous serum (25 %) for 1 hour and percentage of hemolysis measured at OD_{412nm}.

2.2.12.4 Wieslab ELISA

The classical, mannan-binding lectin and alternative pathways of complement were screened using a commercial Wieslab total complement ELISA (Wieslab, Sweden) that measures the formation of the end point C5b-9 complex (Seelen et al., 2005). The assays were performed according to the manufacturer's instructions. Complement activation by the control sera (pooled from five healthy individuals) in the presence and absence of SSL protein was compared.

2.2.12.5 Complement ELISA

Purified human IgG1 or IgG3 (10 mg/mL) was heat aggregated at 63 ^{o}C for 15 min. Precipitated proteins were spun and removed. Maxisorb ELISA plates (Nunc, Denmark) were coated 50 uL heat aggregated IgG at 25 ug/mL overnight at 4 ^{o}C. Wells were blocked with 1 % HSA in PBS pH 7.4. Fresh human serum was diluted to 5 % in GHB^{++} buffer and added to equal volume of titrated test protein. The mixture was added to the IgG coated wells and incubated for 30 min for detection of C3b deposition. Wells were washed in ELISA wash buffer three times and C3b was detected using rabbit anti-C3c antibody (1:4000) for 1 h. Wells were rinsed in wash buffer three times before adding anti-rabbit IgG coupled to HPR (1:10000). Bound secondary antibody was detected as described in Section 2.2.11.3. Controls without serum and primary antibody were also included.

2.2.12.6 Clotting assay

Blood from healthy volunteers was collected in sodium citrate vacutainer tubes (Becton Dickinson, USA) and spun at 1500 g for 15 min at 4 ^{o}C. Plasma was diluted to 50 % (v/v) in PBS pH 7.4 and incubated with 0-2 µM SSL for 5 min. The clotting process was initiated with 10 mM $CaCl_2$ and the absorbance at OD_{405nm} and OD_{620nm} was measured over 40 min on a spectrophotometer (Dawson et al., 1994). All assays were performed using fresh plasma to avoid precipitation of coagulation factors induced during the freeze-thaw process. Alternatively, coagulation was initiated using 0.1U activated thrombin (Sigma Aldrich, USA) diluted in PBS pH 7.4. Clot stability was also observed over three subsequent days.

2.2.13 Binding kinetics

2.2.13.1 Surface plasmon resonance

Biosensor anlaysis was performed using a BIAcore 2000 (BIAcore, GE Healthcare, Sweden). Purified monoclonal human IgG1 (ARH-77) was immoblised onto a CM5 caboxydextran chip (BIAcore, GE Healthcare, Sweden) using carbodiimide chemistry to ~300 response units (RU) as per manufacturer's instructions. An uncoupled control channel was also prepared for measuring the bulk and non-specific binding responses of the interaction. Freshly purified SSL10 (0.1-3 µM) was injected over the chip at 30 µL/min in HBS-EP (0.01 M HEPES pH 7.4, 0.3 M NaCl, 3 mM EDTA, 0.005 % Surfactant P20). The surface was regenerated using 1.5 M guanidine HCl, 17 % isopropanol and 10 mM glycine pH 3.0. Equilibrium binding response at 400 s was fitted to a single site binding model using the Hill equation as described previously (Chung et al., 2007): Req/*B*max = $([SSL10]^{nH})/(K_D + [SSL10]^{nH})$, where Req is the plateau binding response, K_D is the equilibrium dissociation constant, nH is the Hill coefficient, *B*max is the maximal bound analyte at calculated saturation, and Req/*B*max is the fraction of immobilized ligand bound.

2.2.13.2 Isothermal titration calorimetry (ITC)

Isothermal titration calorimetry was performed on a VP-ITC calorimeter (MicroCal, USA) at 25 ^{o}C in PBS pH 7.4. Prior to each experiment, the sample cell and syringe were rinsed in fresh MQ H_2O and the experimental buffer. The instrument was equilibrated to 25 ^{o}C with an initial delay of 300 s. The reference power and filter were set to 300 µcal/s and 2 s respectively. A typical experiment was preformed with approximately 1.4 mL 5-10 µM protein in the cell (stirring at 307 rpm) and approximately 150 uL 100-150 µM $SSL10_B$ in the syringe. A total of 30 10 µl protein injections at a speed of 0.5 µL/s were performed and the heat evolved was measured. An interval of 240 s between each consecutive injection was allowed for the heat signal to return to baseline. The heat evolved from the dilution of SSL10 into buffer alone was also measured as a background control. All data was fitted using the Origin software (OriginLab, USA).

2.2.14 Protein crystallography

2.2.14.1 Protein preparation

Highly pure protein was prepared for crystallography by affinity chromatography, cation exchange chromatography and size exclusion chromatography. The protein preparation was dialysed into 20 mM Tris HCl pH 7.4, 100 mM NaCl and passed through a 0.22 um filter (Milipore, USA). Dynamic light scattering (DynaPro, Protein Solutions, USA) was performed to determine polydispersity of protein preparation.

2.2.14.2 Crystallisation condition screening and data collection

Crystallisation conditions were screened using a Cartesian HONEYBEE nanaoliter dispensing robot (Genomic solutions). A 480 condition screen was used to set up 100nL sitting drops mixed with 100 nL of concentrated pure protein (Moreland et al., 2005). Crystals were grown at 18 ^{o}C in 96 well intelliplates. Fine screens were performed manually with 1 uL protein mixed with 1 uL precipitant solution in hanging and sitting drops. The SSL10 crystal was flash frozen in mother liquor containing 30% PEG 1500, 8 % MPD, 0.1 M Tris pH 8.5. X ray diffraction data from the SSL10 crystal was collected at School of Biological Sciences, University of Auckland, NZ using CuKα radiation (λ = 1.5418 Å) from a Rigaku RU300 rotating anode generator containing an Oxford cryostream, Mar345 imaging plate system and Osmic mirrors (Baker et al., 2007). Data was collected to 2.6 Å resolution. The data was truncated to 2.9 Å to obtain 81 % completion of the outer shell. The data was process using MOSFLM and SCALA from the CCP4 suite (Evans, 2006; Leslie, 1992).

2.2.14.3 Structure determination and refinement

The SSL10 crystal structure was solved by molecular replacement of SSL7 (pdb file 1V1O) at 2.9 Å using PHASER (McCoy, Grosse-Kunstleve, Storoni, & Read, 2005). Dr Paul Young University of Auckland, performed the initial rounds of manual building in COOT (Emsley & Cowtan, 2004) and refinement using Refmac5 (Murshudov, Vagin, & Dodson, 1997) at 2.9 Å. The electron density and overall fit of the model was poor. The original data was reprocessed at 2.75 Å and solved by molecular replacement with the 2.9 Å SSL10 model and rebuilt with Arp/wARP (Perrakis, Harkiolaki, Willson, & Lamzin, 2001). Subsequent cycles of manual building using COOT (Emsley & Cowtan, 2004) and refinement with Refmac5 (Murshudov et al., 1997) and BUSTER (Blanc et al., 2004) were performed. To improve the geometry of the model it was rebuilt using PHENIX (Adams et al., 2002). The quality of the geometry was routinely checked using MolProbity (Davis et al., 2007).

Chapter 3
Purification and Characterisation of Recombinant SSL10

3.1 Introduction

The *ssl10* gene is one of the few *ssl*s present in all the *S.aureus* strains and clinical isolates analysed to date (Aguiar-Alves et al., 2006; Sibbald et al., 2006). It contains a putative N-terminal signal sequence and cleavage site as determined by the SignalP algorithm (Nielsen, Engelbrecht, Brunak, & Heijne, 1997) and is thus predicted to exist as a secreted protein. An early study by Fitzgerald et al. analysed SSL10 from the sequenced *S.aureus* strains, NCTC8325, Sanger MSSA, Sanger MRSA, N315, Mu50, COL and MW2, and determined 95% homology at the nucleotide level and 94% homology at the amino acid level (Fitzgerald et al., 2003). The prevalence and strong sequence conservation of SSL10 suggests that it is of significant importance to the bacterium. In order to elucidate the role of SSL10 in staphylococcal pathogenesis it was cloned and expressed as a recombinant protein. This chapter outlines the purification and characterization of recombinant SSL10 and its C-terminal β-grasp domain.

3.2 Results

3.2.1 Analysis of *ssl10* from clinical isolates of *S.aureus*

To investigate the allelic variation of *ssl10* it was amplified by PCR from thirteen isolates of *S.aureus* originating from human infections. The primers were designed to amplify *ssl10* from the 31st residue Lysine (K), thus omitting the signal peptide sequence predicted by SignalP (Nielsen et al., 1997). All thirteen isolates had *ssl10* present (Fig. 3.1); nine of which were sequenced and determined to contain one of two SSL10 alleles. The first SSL10 allele ($SSL10_A$) was present in three of the sequenced isolates (ATCC25923, NU9485, 1137), while the remaining six isolates (MRSA33938, NU9325, US0440, RN4220, ATCC33593, 196) contained the second SSL10 allele ($SSL10_B$). Both groups had numerous nucleotide variations however these were not translated suggesting a mechanism of strict allelic conservation. At the amino acid level these two allelic forms display 81% identity.

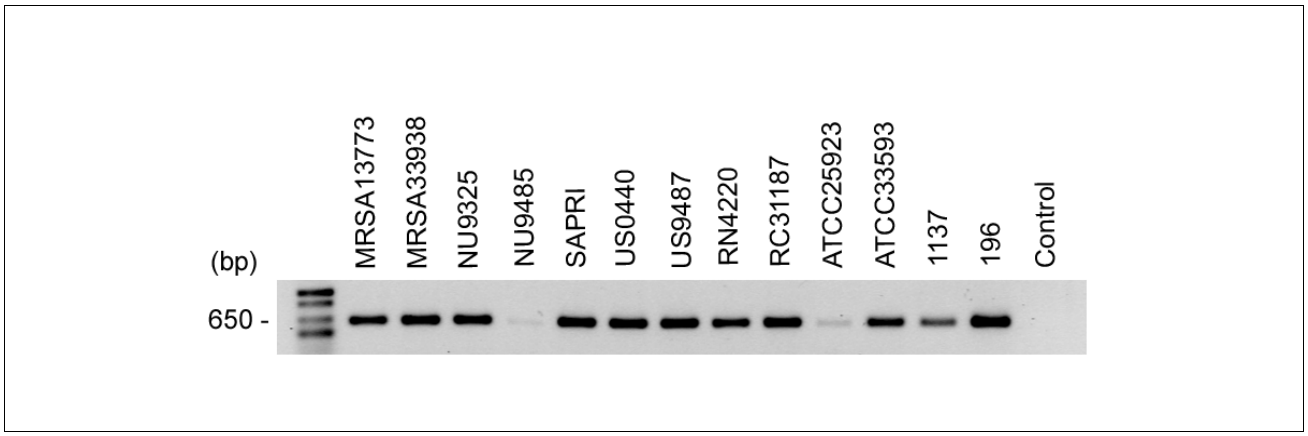

Figure 3.1: Amplification of *ssl10* from clinical isolates of *S.aureus* by PCR.

The *ssl10* gene product (591bp) was amplified using primers SSL10 Fwd and SSL10 Rev from the genomic DNA of thirteen clinical isolates of *S.aureus*. A reaction excluding template DNA was included as a negative control.

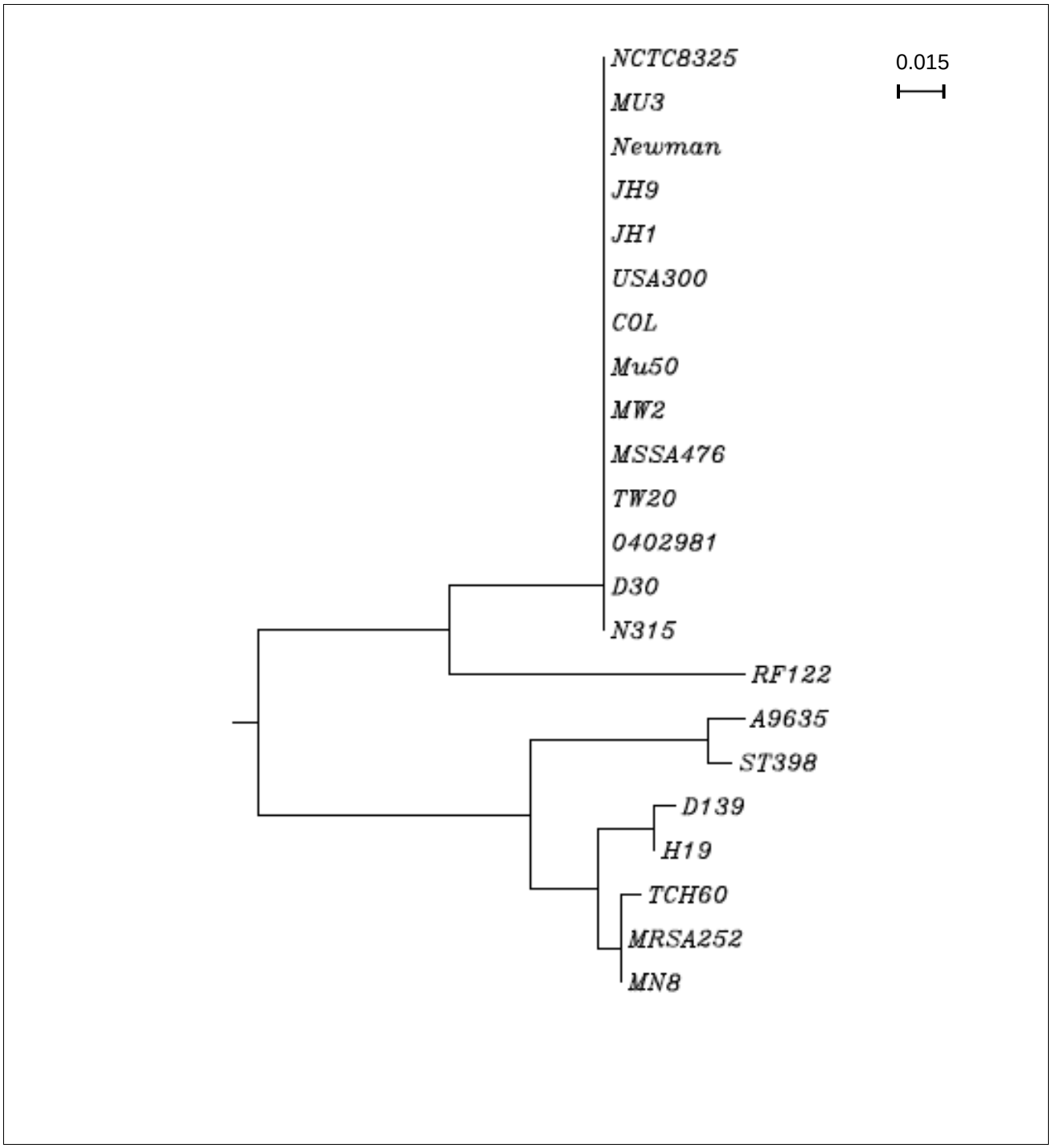

Figure 3.2: Neighbour-joining tree comparing SSL10 from the sequenced strains of *S.aureus*.

The amino acid sequences of SSL10 (excluding the signal peptide) from the publicly available sequenced genomes of *S.aureus* were aligned using Clustal W (Thompson et al., 1994) and a neighbour-joining tree was constructed. All the strains analysed originate from human infections except RF122, which is associated with bovine mastitis.

3.2.2 SSL10 from the publicly available sequenced strains of *S.aureus*

Amino acid alignment of SSL10 from the sequenced genomes of *S.aureus* show a further six allelic variants of SSL10, making a total of eight allelic variants in total (Fig. 3.2). The dominant SSL10 allele (formerly called SET14) is present in *S.aureus* NCTC8325, Mu3, Newman, JH9, JH1, USA300, COL, Mu50, MW2, MSSA476, TW20, 0404981, D30 and N315. The SSL10 alleles from *S.aureus* MSSA476 and MW2 (formerly called SET25) form a subset of this main allele with three amino acid variations present only in the N-terminal signal peptide sequence of the protein. The mature protein from these strains shows identity to $SSL10_B$ that was detected in the six clinical isolates of *S.aureus*. The bovine *S.aureus* strain RF122 contains the second allelic variant of SSL10, which displays strong similarities to $SSL10_B$ but considerable variations in the C-terminal portion of the protein (Fig. 3.3). The third allelic variant displays identity to $SSL10_A$ and is present in *S.aureus* MRSA252 and MN8 (formerly called SET4). Since the commencement of this study an increasing number of *S.aureus* strains have been sequenced and several alleles displaying close homology to $SSL10_A$ have been identified. The most striking are the two alleles of SSL10 from *S.aureus* A9635 and ST398 that have a number of unique variations compared to the other three alleles, again predominantly in the C-terminal domain (Fig. 3.3). These two alleles display the greatest variation from $SSL10_B$ with 78% identity (Table 3.1). The remaining three allelic variants of SSL10 from *S.aureus* TCH60, D139 and H19 display $\geq$ 97% identity to $SSL10_A$.

RF122	88						
A9635	78	74					
ST398	78	75	98				
D139	80	77	91	91			
H19	80	77	91	92	99		
TCH60	81	77	90	91	96	97	
MRSA252	81	78	90	92	97	97	99
	N315	**RF122**	**A9635**	**ST398**	**D139**	**H19**	**TCH60**

Table 3.1: Sequence identity of the eight allelic variants of SSL10.

Percentage of amino acid similarity between the different allelic variants of SSL10 (excluding the signal peptide) from the publicly available sequenced strains of *S.aureus*.

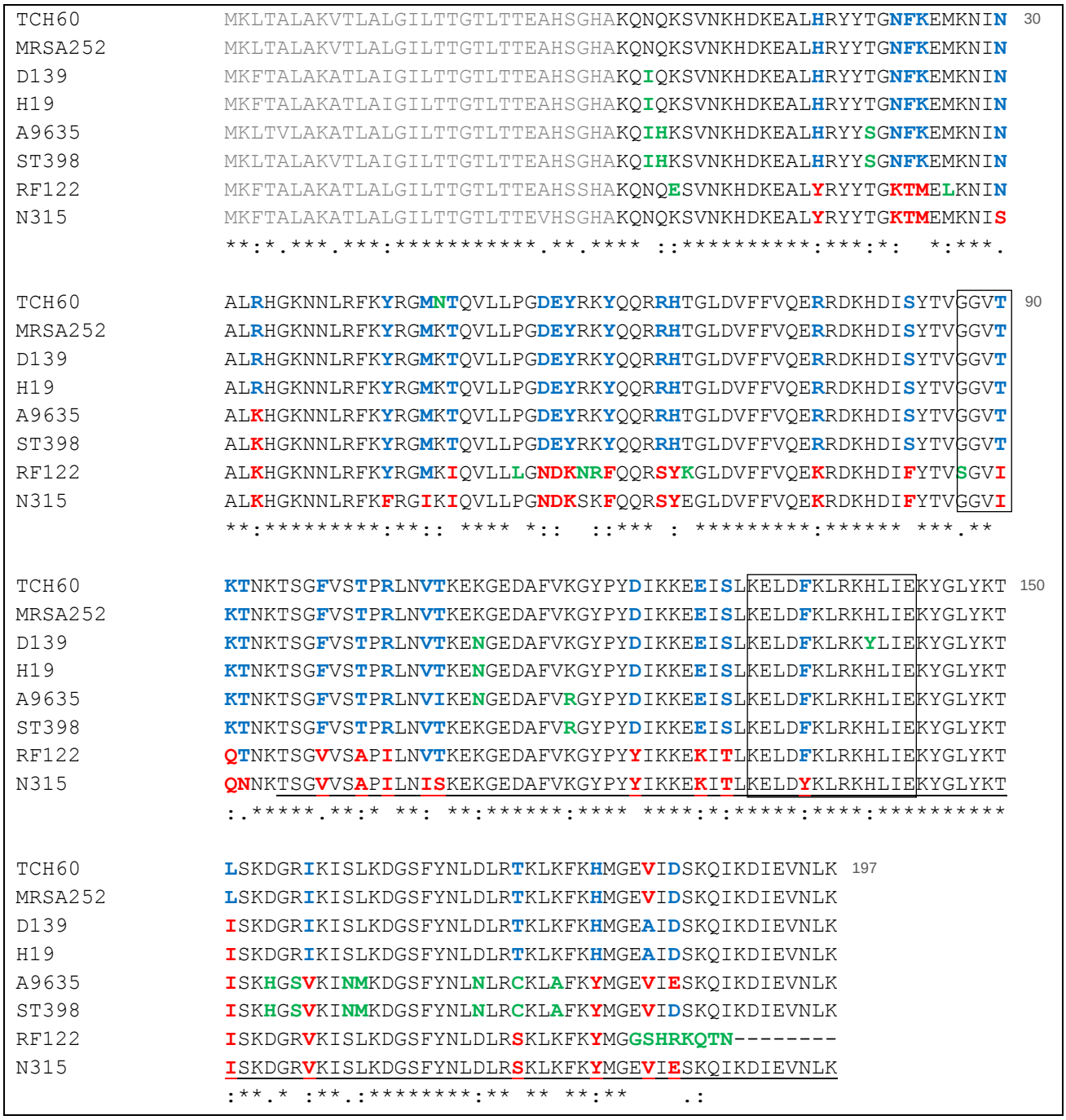

Figure 3.3: Amino acid sequence alignment of the eight allelic variants of SSL10 from the sequenced strains of *S.aureus* using ClustalW.

Amino acid identity (*), strong similarity (:) and weak similarity (.) are highlighted for each residue. Sequence in gray represents the predicted N-terminal signal sequence of *ssl10*. Residues in green are unique changes in sequence. Residues in blue or red are variations shared by the *ssl10* gene from MRSA252 or N315 respectively. The predicted β-grasp domain ($SSL10_{95-197}$) is underlined. The GGV/IT and central α4 helix sequence corresponding to the highly conserved staphylococcal/streptococcal exotoxin consensus sequences are highlighted (box).

3.2.3 Cloning and expression of recombinant SSL10

The genomic DNA of *S.aureus* ATCC25923 and *S.aureus* MRSA33938 were used to clone $ssl10_A$ and $ssl10_B$ respectively, for expression in the *E.coli* strain AD494(DE3)pLysS. In addition $ssl10_B$ was cloned from two alternative start sites. The first, from the 28th residue glycine (G) predicted by SignalP to be a lower probability signal peptide cleavage site. And the second, from the 41st residue aspartic acid (D) to exclude residues that correspond to those disordered in the crystal structure of related SSL proteins (V. L. Arcus et al., 2002; Chung et al., 2007). The truncated forms of $ssl10_B$ representing the N-terminal OB-fold domain ($SSL10_{23-91}$) and C-terminal β-grasp domain ($SSL10_{95-197}$) were also cloned to investigate their functional importance. These domains were predicted against the crystal structure of SSL11 (PDB file 2RDH) using the SWISS-MODEL modelling software (Arnold, Bordoli, Kopp, & Schwede, 2006). The genes were cloned into the pET32a.3C plasmid between the BamHI and EcoRI restriction sites, as previously established by Dr RJ Langley (University of Auckland, NZ) for several other SSLs.

The genes were expressed as a polyhistidine-tagged thioredoxin-fusion protein under IPTG control. The thioredoxin enhances protein solubility, while the polyhistidine tag allows for its purification using nickel (Ni^{2+}) affinity chromatography. The recombinant proteins were separated from the polyhistidine tagged N-terminal thioredoxin using a 3C protease from human rhinovirus, which efficiently cleaves at the sequence EVLFQ/GP (Walker et al., 1994). This leaves an extra four amino acids (GSGP) at the start of the expressed proteins inclusive of the remaining BamHI cleavage sequence. An additional glycine (G) residue was also included at the N-terminus of the β-grasp domain to increase its flexibility and enhance access for the 3C protease.

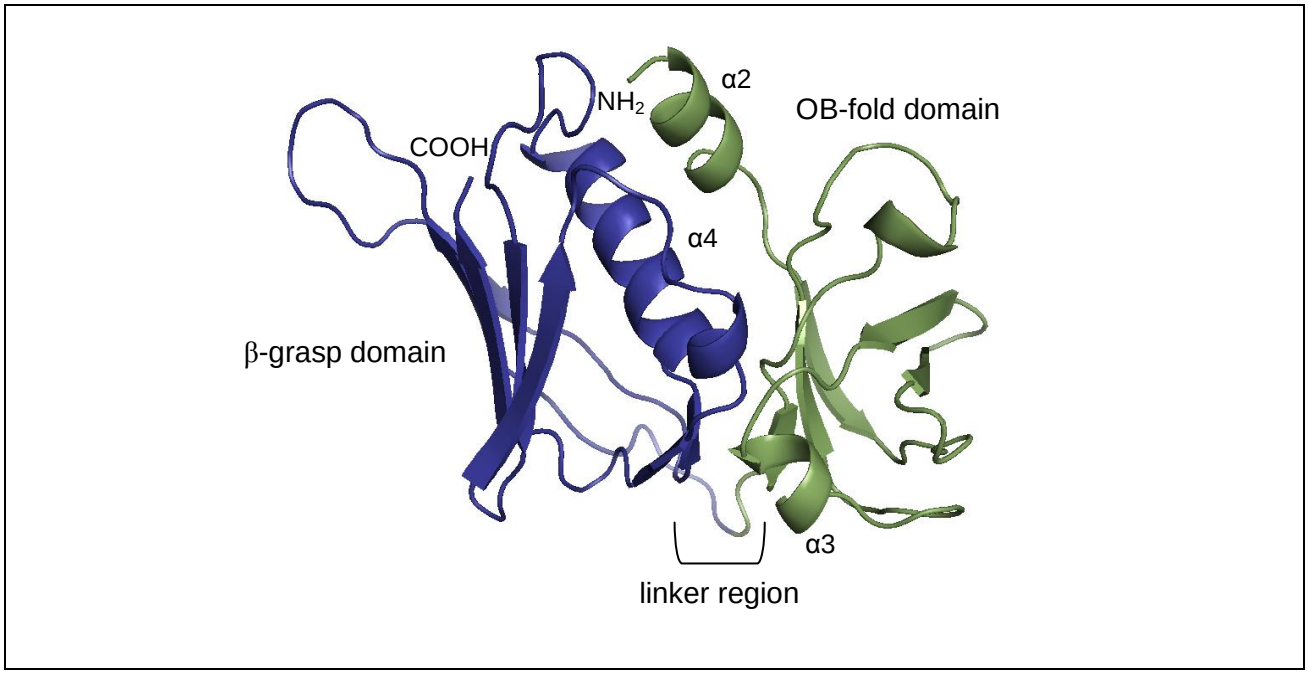

Figure 3.4: Structural model of SSL10 based on the crystal structure of SSL11.

Modelled structure of $SSL10_B$ against SSL11 (PDB file 2RDH) using SWISS-MODEL modelling software (Arnold et al., 2006). The C-terminal β-grasp domain (blue) and N-terminal OB-fold domain (green) are displayed. Primers were designed to amplify the N-terminal domain ($SSL10_{23-91}$) from the end of the second alpha helix (α2), and C-terminal domain ($SSL10_{95-197}$), while omitting the linker region between the domains.

3.2.4 Purification of recombinant SSL10

Identical methods were used for expression of the full length and truncated SSL10 proteins, however slightly different procedures were followed for their purification. The recombinant proteins were purified by Ni^{2+} affinity chromatography through the interaction of the polyhistidine tag on thioredoxin with nickel charged IDA Sepharose (Fig. 3.5a). Purification of full length SSL10 over Ni^{2+}-IDA Sepharose required competitive elution of the fusion protein with 100 mM imidazole and cleavage off the column with 3C protease. A subsequent purification step using cation exchange chromatography at pH 8.0 was necessary to remove the contaminating thioredoxin (Fig. 3.5b). Cleavage of SSL10 on the column overnight resulted in elution of majority of the SSL10 alongside thioredoxin, most likely due to non-specific interactions with thioredoxin. In contrast, the β-grasp domain $SSL10_{95\text{-}197}$ was cleaved overnight on the Ni^{2+}-IDA column and easily eluted off the column the next day without imidazole, thus separating it from the thioredoxin that remains bound to the column through its polyhistidine tag (Fig. 3.6). Further purification of the β-grasp domain was possible using cation exchange chromatography at pH 7.0 if required. High salt conditions of up to 300 mM NaCl were used during the purification procedure to inhibit non-specific interactions, in particular for the full length SSL10 molecule. All proteins were stored in PBS pH 7.4 without any notable stability concerns.

Each allelic variant of SSL10 was produced as a full length molecule of 201 amino acids, inclusive of the additional residues from the 3C protease and restriction enzyme sites. Two alternative SSL10 proteins, $SSL10_{11\text{-}197}$ and $SSL10_{\text{-}3\text{-}197}$ of the dominant allele were also successfully produced. Notably, the recombinant proteins consistently migrate higher on an SDS-PAGE gel at approximately 26 kDa compared to their predicted molecular weight of approximately 23.5 kDa (Protpram; (Gattiker, Duvaud, Wilkins, Appel, & Bairoch, 2005)). Typically 1 L of *E.coli* culture produced 40 mg of fusion protein and up to 5 mg of clean soluble SSL10 that was stable for extended periods at 4 ^{o}C irrespective of the start site (Fig 3.7a). A soluble 12 kDa C-terminal β-grasp domain was also produced, however the N-terminal OB-fold domain was unstable and immediately precipitated upon cleavage from thioredoxin. This is most likely due to the exposure of hydrophobic residues that are normally shielded by the β-grasp domain. For the β-grasp domain 1 L of *E.coli* culture produced approximately half the protein as the full length and was stable for at least several weeks at 4 ^{o}C. Isoelectric focusing was used to determine the experimental isoelectric points (pI) of recombinant SSL10 and $SSL10_{95\text{-}197}$ (Fig. 3.7b). $SSL10_{A}$, $SSL10_{B}$ and $SSL10_{\text{-}3\text{-}197}$ had a pI close to their predicted pI of 9.8-9.9, while $SSL10_{95\text{-}197}$ had a pI of approximately 9.0, lower than its predicted pI of 9.6.

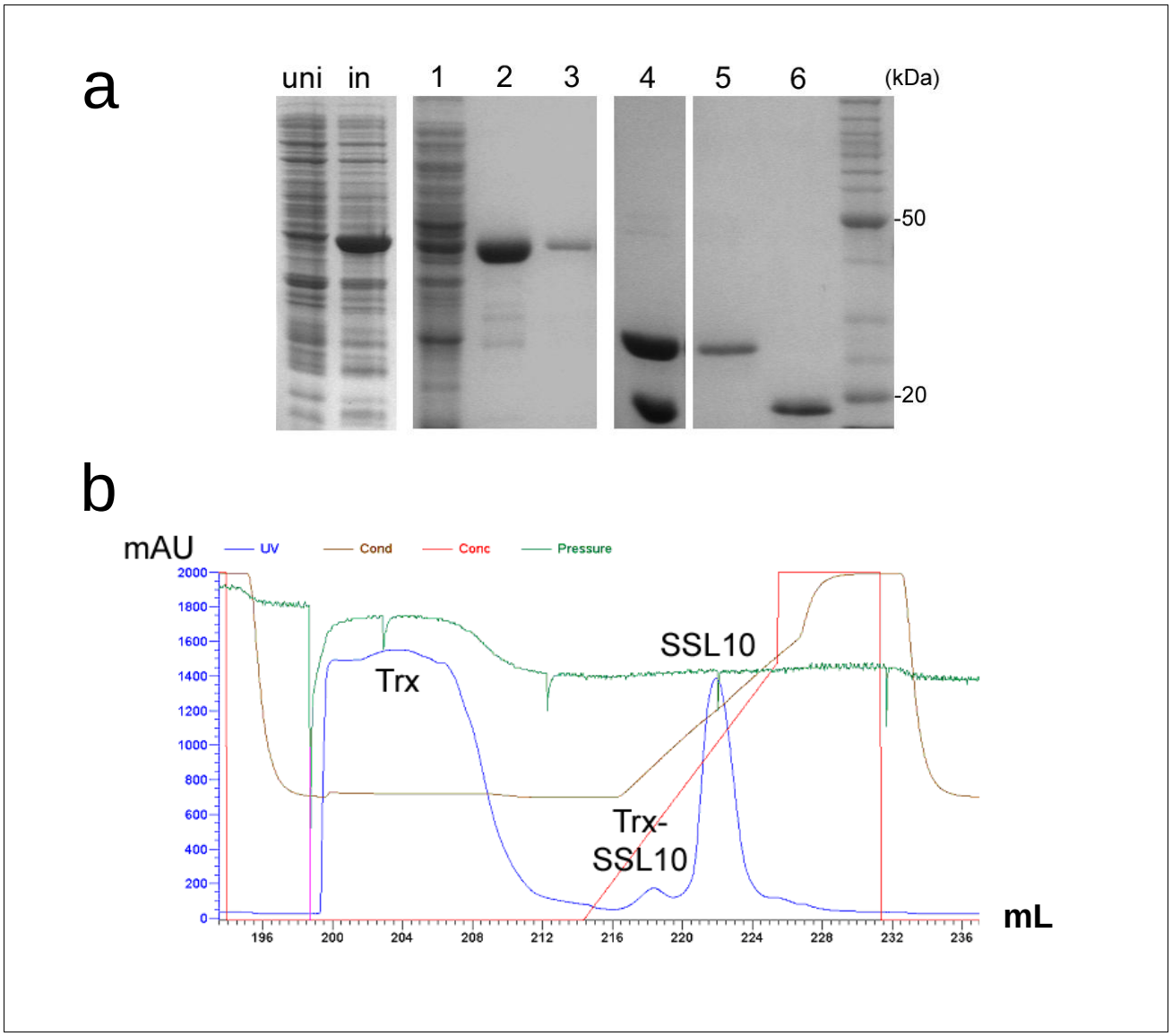

Figure 3.5: Expression of SSL10 in *E.coli* using the pET32a.3c expression system and purification using Ni^{2+} affinity chromatography and cation exchange chromatography.

(A) Reducing SDS-PAGE of uninduced (uni) and induced (in) *E.coli* cells expressing thioredoxin-SSL10 fusion protein (45 kDa). Flow-through from Ni^{2+} IDA column (1), elution of fusion protein with 100 mM imidazole (2-3), overnight cleavage of the fusion protein with 3C protease (4), and separation of SSL10 (5) and thioredoxin (6) using cation exchange chromatography.

(B) Profile of SSL10 purification from thioredoxin using cation exchange chromatography (20 mM sodium phosphate buffer pH 8.0). Thioredoxin (Trx) is removed in the flow-through. Any uncleaved thioredoxin-SSL10 fusion protein (Trx-SSL10) is eluted from the MonoS column with 0.3 M NaCl. Elution of SSL10 requires 0.6 M NaCl.

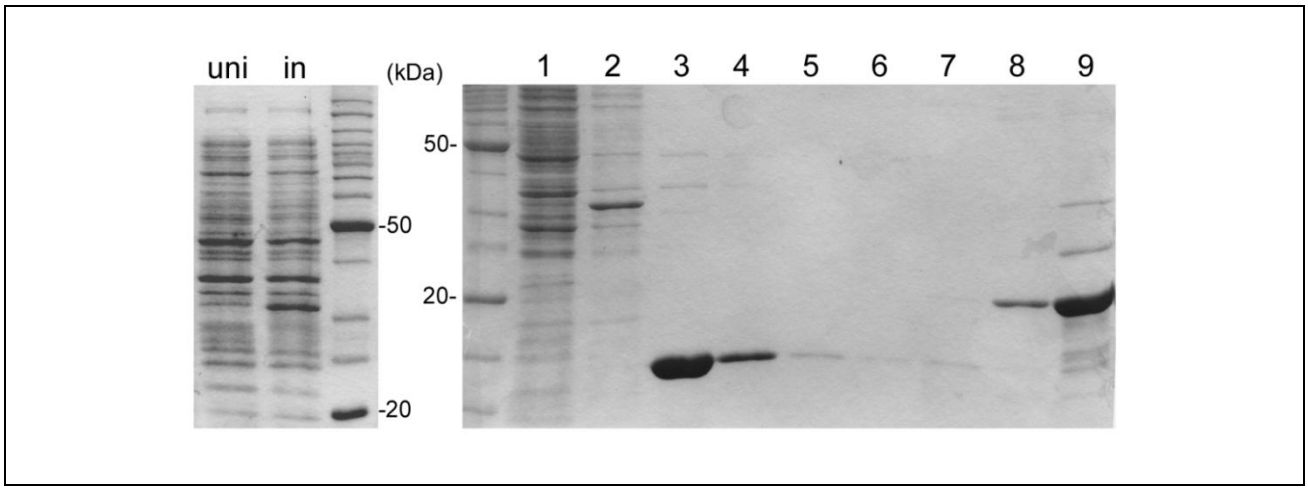

Figure 3.6: Purification of $SSL10_{95-197}$ using Ni^{2+} affinity chromatography

Reducing SDS-PAGE of uninduced (uni) and induced (in) *E.coli* cell culture expressing Thioredoxin-$SSL10_{95-197}$ fusion protein. Flow through from Ni^{2+} IDA column (1), wash with 10 mM imidazole (2) and elution of $SSL10_{95-197}$ following overnight cleavage of fusion protein with 3C protease in 0 mM imidazole (3-4), 5 mM imidazole (5-6), 10 mM imidazole (7-8) and 100 mM imidazole (9).

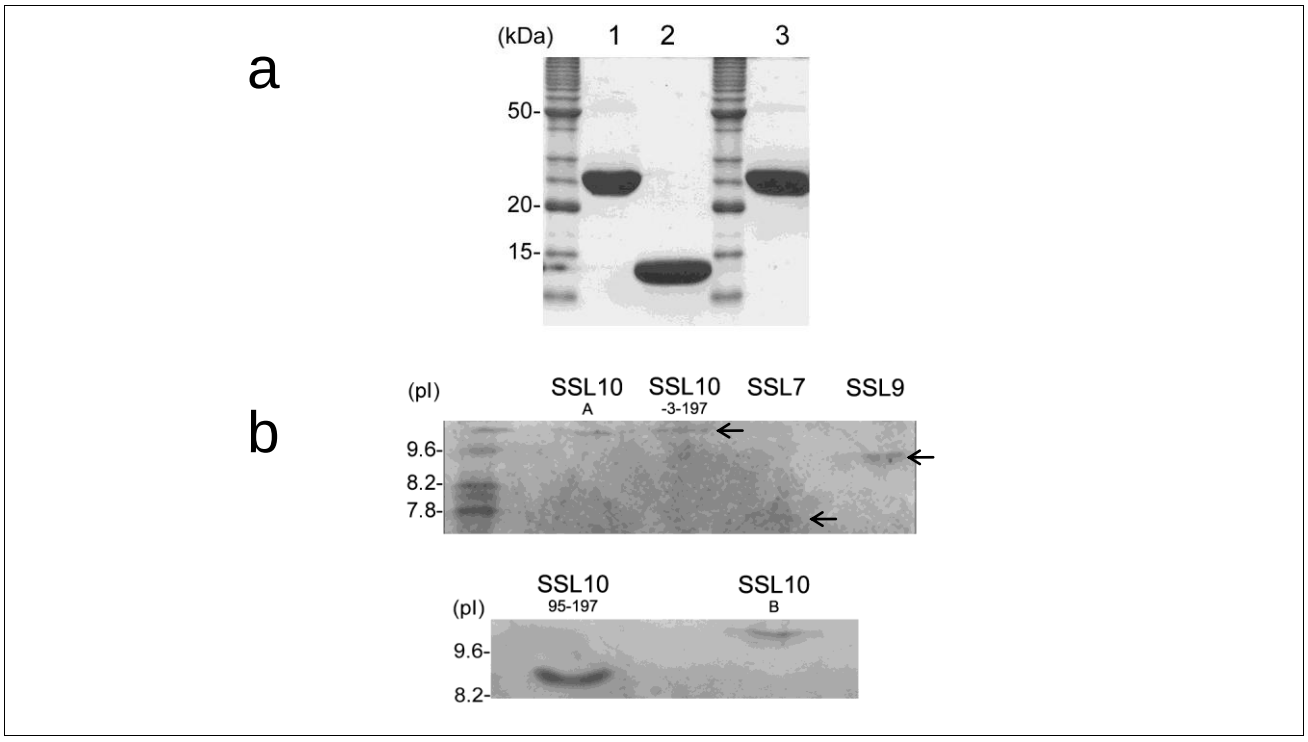

Figure 3.7: SDS-PAGE and isoelectric focusing of purified recombinant SSL10 and $SSL10_{95-197}$.

(a) A 15% reducing SDS-PAGE gel and (b) isoelectric focusing gel of purified $SSL10_B$ (1), $SSL10_{95-197}$ (2) and $SSL10_A$ (3). $SSL10_{-3-197}$, SSL7 and SSL9 were also included as controls for IEF.

Table: 3.2 Key properties of recombinant SSL10 proteins.

Theoretical values calculated using ProtPram (Gattiker et al., 2005) are reported for recombinant proteins that include additional residues from the 3C protease and BamHI restriction enzyme cleavage site. The observed experimental values are noted in brackets. *The molecular weight was observed by 12.5 % reducing SDS-PAGE.

Protein	Polypeptide Length (amino acid)	Molecular weight (kDa)	Extinction coefficient (Abs $_{280nm}$ 0.1%)	Isoelectric point (pI)
$SSL10_{A}$	201	23.6 (28.0*)	0.695	9.89 (9.9)
$SSL10_{B}$	201	23.4 (27.0*)	0.829	9.81 (9.9)
$SSL10_{B(-3-197)}$	204	23.6 (27.0*)	0.819	9.81 (9.9)
$SSL10_{B(11-197)}$	191	22.2 (27.0*)	0.837	9.74
$SSL10_{95-197}$	107	12.3 (12.5)	0.967	9.60 (9.3)

3.3 Discussion

The *ssl10* gene and the wider *ssl* gene locus are present in all the *S.aureus* isolates studied to date from both human and animal origins, emphasizing their importance in *S.aureus* pathogenesis (Aguiar-Alves et al., 2006; Fitzgerald et al., 2003; Sibbald et al., 2006). Comparison of SSL10 from the human strains and clinical isolates of *S.aureus* revealed strong sequence conservation between the allelic variants with $\geq$78% identity. The *ssl* gene cluster itself contains high levels of sequence diversification; most likely accumulated over time through horizontal gene transfer, recombination events and the loss of *ssl* genes (Fitzgerald et al., 2003). However, comparison of the silent substitutions in the *ssl* genes against the translated amino acid variations suggests that selective constraints are acting to maintain their individual functions (Fitzgerald et al., 2003).

There are two distinct groups of SSL10 alleles associated with human *S.aureus* infections. Two thirds of the sequenced *S.aureus* strains and isolates analysed produce $SSL10_B$. A subtype of $SSL10_B$ that only differs in the N-terminal signal sequence of the protein is present in the community acquired *S.aureus* strains MW2 and MSSA476, which interestingly also share strong sequence similarities in their core genomes (T Baba et al., 2008). In strong contrast, the second group displays greater diversity. It contains $SSL10_A$ from MRSA252, one of the most phylogenetically divergent *S.aureus* genomes sequenced to date (M T G Holden et al., 2004). As more *S.aureus* isolates have been sequenced, a number of other allelic variants have been uncovered. These alleles display unique variations predominantly across the β-grasp domain, which most likely reflects changes in antibody epitopes.

The greatest difference in SSL10 is seen with host species variations. The allele from RF122 shares strong similarities with $SSL10_B$ however it also differs in the last sixteen residues of the C-terminal domain. This could produce strong structural differences between the alleles that could confer an adaptive advantage to the diverse host conditions encountered during infection. Indeed comparative analysis of the bovine and human *S.aureus* genomes revealed extensive variations that favour infection in the different hosts (Herron-Olson, Fitzgerald, Musser, & Kapur, 2007).

Production of recombinant $SSL10_A$ and $SSL10_B$ using the pET32a expression system produced stable soluble protein. $SSL10_B$ has a high experimental isoelectric point of approximately 9.8-10 that is reflected in its elution profile from the cation exchange column at pH 8. Purification of the C-terminal β-grasp domain $SSL10_{95\text{-}197}$ also produced soluble stable protein with an experimental isoelectric point of approximately 9.0. In contrast to the full length protein the reduced net charge allows it to be successfully cleaved on the Ni^{2+} column and eluted without major thioredoxin contamination.

Chapter 4
Preliminary analysis of SSL10

4.1 Introduction

S.aureus produces an array of virulence and pathogenicity factors that target the cellular and molecular signalling systems of the immune response. The expression of these factors is largely influenced by cell density and environmental signals. Early studies of the SSL protein family by Fitzgerald et al. established constitutive expression of *ssl10* from the mid-exponential to stationary phase of staphylococcal growth (Fitzgerald et al., 2003). In contrast the other *ssl* genes from the same immune evasion cluster were detected to have strongest transcript levels during the stationary phase of growth; a trait typically observed with secreted immune evasion factors under the control of the *agr* regulator (Sibbald et al., 2006). Later studies investigating the response of *S.aureus* to heme toxicity detected a seven fold increase in *ssl10* along with eight other *ssl* genes (Stauff et al., 2008).

SSL10 has a predicted Sec-type signal peptide that is known to direct proteins through the commonly used Sec pathway to the cell wall or extracellular milieu (Sibbald et al., 2006). It lacks a typical cell wall anchoring domain thus is most likely secreted into the extracellular environment. Studies to date have not directly detected SSL10 in the extracellular milieu of *S.aureus* (Sibbald et al., 2006; Torres et al., 2007). However, immunoreactivity of recombinant SSL10 with sera specifically from patients with *S.aureus* bacteremia suggests that SSL10 is indeed produced during the infection process (Fitzgerald et al., 2003). This chapter outlines the preliminary studies undertaken to determine the expression profile of endogenous SSL10 and its potential cellular and molecular targets in the host environment.

4.2 Results

4.2.1 Expression of endogenous SSL10 by *S.aureus*

The cell surface and culture supernatant of *S.aureus* were analysed for the presence of endogenous SSL10 using western blot analysis. *S.aureus* Newman containing $ssl10_B$ was grown overnight in RPMI media supplemented with 2 % (w/v) Casamino acid. An *S.aureus* Newman Δ*hrtA* mutant was also grown under the same conditions in the presence and absence of 1 µM hemin. This mutant strain lacks a functional heme transporter thus confers increased susceptibility to heme toxicity and consequently increased expression of *ssl10* (Stauff et al., 2008). Proteins in the culture supernatant were precipitated with 10% TCA and the bacterial cells were washed in PBS before analysis by Western blot. Endogenous SSL10 was specifically detected using biotinylated anti-SSL10 rabbit IgG and any non-specific binding by staphylococcal Ig binding proteins was blocked with Igs in 10 % rabbit serum (Fig. 4.1).

SSL10 was present in the culture supernatant and cell surface of the Δ*hrtA* mutant in the presence and absence of hemin, while SSL10 was only detected in the culture supernatant of the wildtype. Hemin substantially retarded the growth of the Δ*hrtA* mutant thus was excluded in subsequent studies. A closer examination of the wildtype over a time course of 7 hr detected SSL10 expression from the late exponential phase. In contrast, the Δ*hrtA* mutant produced SSL10 from the early exponential phase; however its growth in RPMI media was notably retarded in comparison to the wildtype. Interestingly the growth of the ΔhrtA in TSB is not retarded (Torres et al., 2007). For both strains, SSL10 was present in the culture supernatant and not associated with the cell surface until the stationary phase. FACS analysis detected binding of SSL10-fluorescein to the cell surface of several *S.aureus* strains in the exponential and stationary phase; however the binding could not be competed with unlabelled SSL10 and thus was non-specific, most likely due to electrostatic interactions of the highly cationic SSL10 with the negatively charged bacterial surface (data not shown). *S.aureus* Newman, MRSA33938 and ATCC25923 were also grown over a time course of 8 hrs in TSB to mimic the conditions used in the study by Fitzgerald et al. (Fitzgerald et al., 2003). Very weak expression of SSL10 was noted only in the supernatant of *S.aureus* MRSA33938 from the mid-exponential to stationary phase of growth (data not shown).

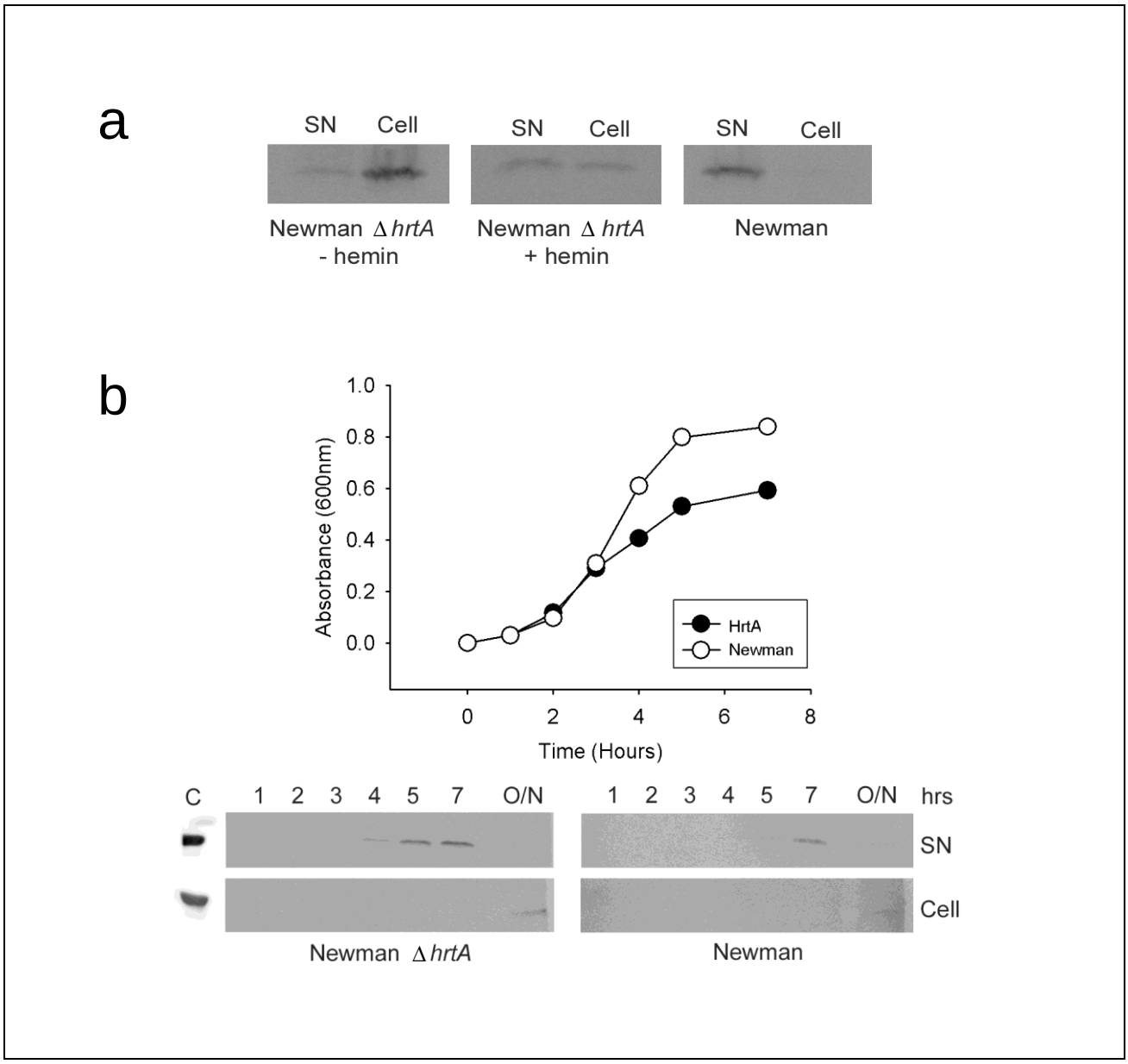

Figure 4.1: Immunoblot detecting the expression of endogenous SSL10 by S.*aureus* in RPMI.

Proteins from TCA-concentrated culture supernatant (SN) and cell surface (Cell) of *S.aureus* Newman Δ*hrtA* mutant and wildtype strains (a) grown overnight in RPMI +/- 1 µM hemin and (b) grown over a time course of 7 hr in RPMI. The overnight stationary culture (O/N) and recombinant SSL10 (C) were also included. The immunoblot was probed with biotinylated rabbit anti-SSL10 IgG (1:1000) in 10 % rabbit serum to block any Ig binding proteins. Biotinylated primary antibodies were specifically detected with streptavidin coupled to HRP (1:2000).

4.2.2 The interaction of SSL10 and human blood leukocytes

4.2.2.1 *In vitro* proliferation of human PBMCs

The SSL proteins were first identified through homology searches for the conserved regions of Sags (V. L. Arcus et al., 2002). To investigate if there are any functional similarities of SSL10 to Sags, the T cell proliferative capacity of SSL10 was measured using a standard colorimetric Alamar Blue proliferation assay (Ahmed, Gogal, & Walsh, 1994). The potent Sag, SMEZ-2 from *S.pyogenes* was used as a positive control (obtained from Dr F Radcliff, University of Auckland, NZ). It stimulated the proliferation of T cells at pg concentrations. Likewise, PHA, a known mitogen, also stimulated the proliferation of PBMCs in a dose dependent manner. In contrast, neither of the SSL10 alleles stimulated proliferation of PBMCs even at the highest concentrations tested (Fig. 4.2).

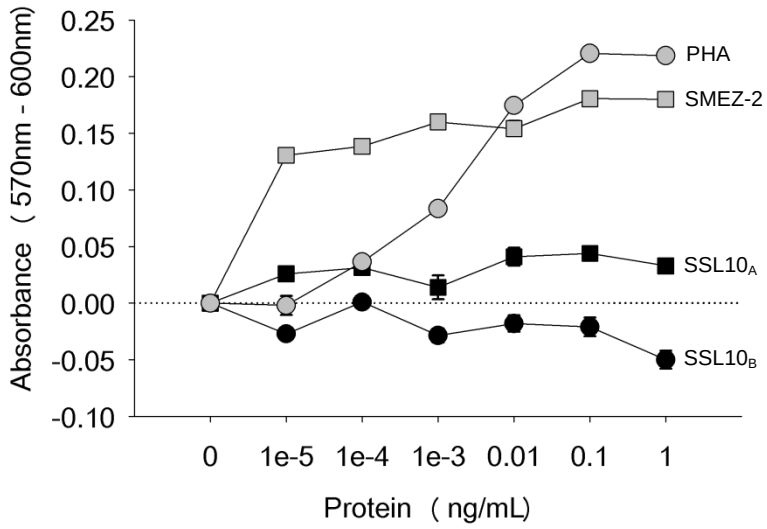

Figure 4.2: The *in vitro* proliferation of human PBMCs by SMEZ-2, PHA, $SSL10_A$ and $SSL10_B$.

Purified PBMCs ($5x10^5$ cells/well) were incubated with 10-fold dilutions of SMEZ-2, PHA, $SSL10_A$ and $SSL10_B$ (n=3). The proliferation of the PBMCs was measured after 72 hr using 10 % Alamar Blue. The data shown is a representative of three independent experiments using PBMCs from different donors.

4.2.2.2 SSL10 binds to the cell surface of blood monocytes

To assess if SSL10 has affinity for any of the different human leukocyte populations, FACS analysis was performed at 4 ^{o}C with fluorescein-labelled SSL10 (0.8 µM) and various PE-labelled cell surface markers (5 µL): CD3 (T-cells), CD19 (B-cells), CD14 (monocytes) and CD10 (granulocytes) (Fig. 4.3a). The specific cell populations (lymphocytes, monocytes and granulocytes) were first distinguished based on their size (forward scatter) and granularity (side scatter), and then analysed for staining by the specific cell surface CD-markers. SSL10-fluorescein strongly bound to monocytes with a ten-fold shift in fluorescence. This specific binding property was also observed in a total white blood cell preparation using fluorescence microscopy (Fig. 4.3b). Cells were incubated with SSL10 (0.8 µM) at 4 ^{o}C for 10 min, then washed twice and spun onto a glass slide. The individual cell populations were distinguished based on the shape of their nuclei, which were easily visualized after staining their chromosomal DNA with DAPI. Monocytes have horseshoe-shaped nuclei, whereas the nuclei of granulocytes are multi-lobed and lymphocytes are small and round. SSL10-fluorescein bound to monocytes in a dose-dependent manner and binding was saturated at higher concentrations (Fig 4.4a). Furthermore, increasing concentrations of unlabelled SSL10 was able to compete with SSL10-fluorescein for binding to monocytes (Fig. 4.4b). Similar levels of binding by SSL10-fluorescein were also observed with the monocyte cell lines THP-1 (Fig. 4.4c) and U937 (data not shown).

4.2.2.3 Internalisation of SSL10 by human blood monocytes

To determine if SSL10 remains on the cell surface or is internalised by blood monocytes, confocal microscopy was utilized (Fig. 4.5). Human PBMCs were incubated with Alexa488 labelled SSL10 at RT for 15 min. Cells were washed well and spun onto glass slides. Alternatively, cells were fixed with paraformaldehyde before immobilizing onto glass slides; however these cells displayed considerably higher background (data not shown). The chromosomal DNA was visualized by counter-staining the cells with DAPI. Z-series sections were taken on the Leica TCS SP2 confocal microscope (Leica, Germany). In both cell preparations SSL10-Alexa was detected throughout the cytosol in small discrete vesicles.

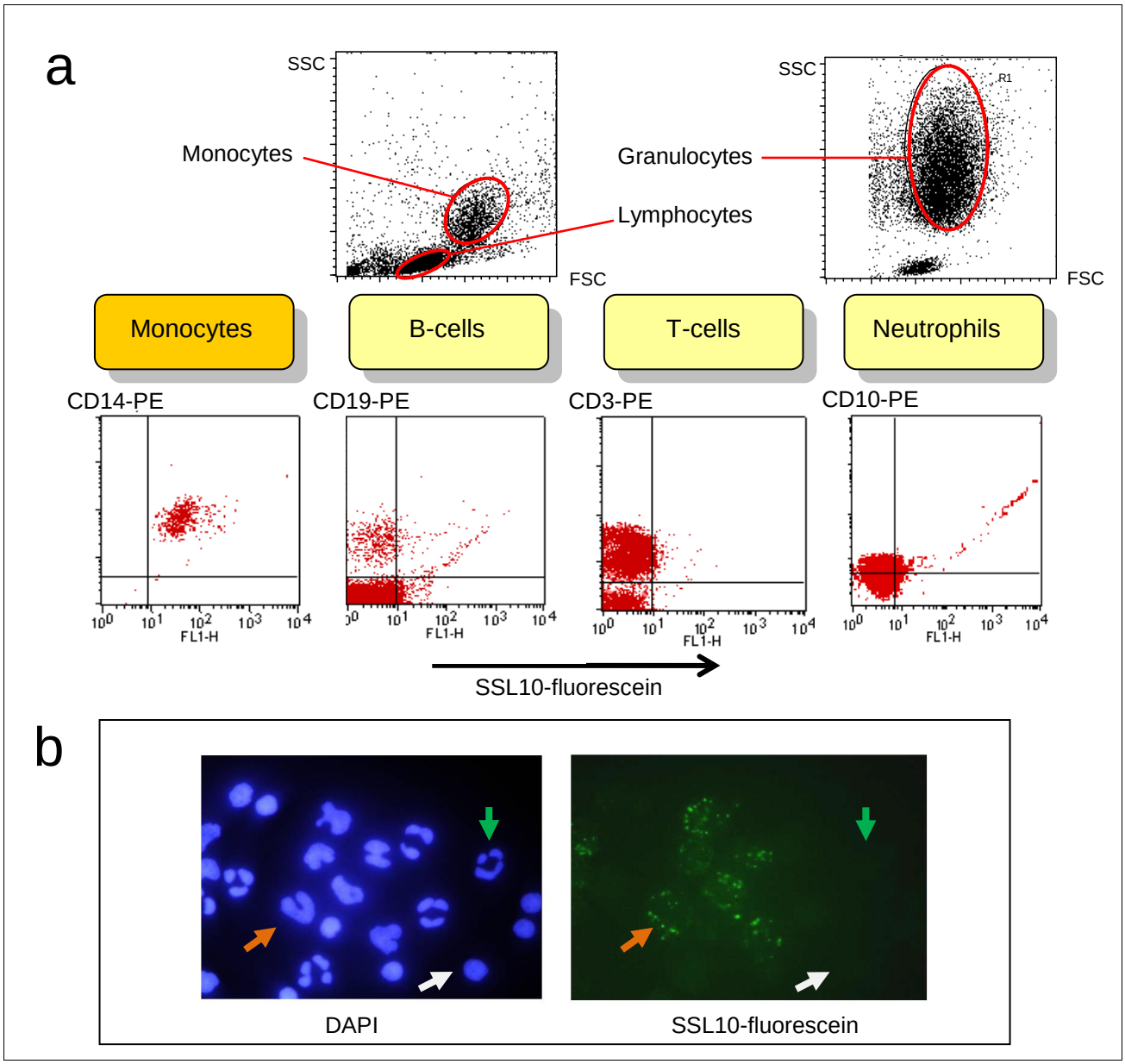

Figure 4.3: (a) FACS analysis and (b) fluorescence microscopy displaying binding of SSL10-fluorescein to human blood monocytes.

(a) Flow cytometry of purified human PBMC and granulocyte cell populations (2.5x10^5 cells). Cells were double stained with SSL10-fluorescein (0.8 µM) and a specific PE-labelled cell surface markers (5 µL): CD14 for monocytes; CD19 for B-cells; CD3 for T-cells; CD10 for neutrophils. The individual cell populations: monocytes (lymphocytes and granulocytes) were gated based on size (FSC) and granularity (SSC). Data shown is a representative of 3 individual experiments performed with cells from different donors.

(b) Fluorescence microscopy of purified human white blood cells labelled with SSL10-fluorescein (0.8 µM). Cells were co-stained with DAPI to distinguish the nuclei of the different cell populations: Horseshoe-shaped nuclei (orange arrow), small round nuclei (yellow arrow) and multi-globular nuclei (green arrow) highlighted are most likely monocytes, lymphocytes and granulocytes respectively.

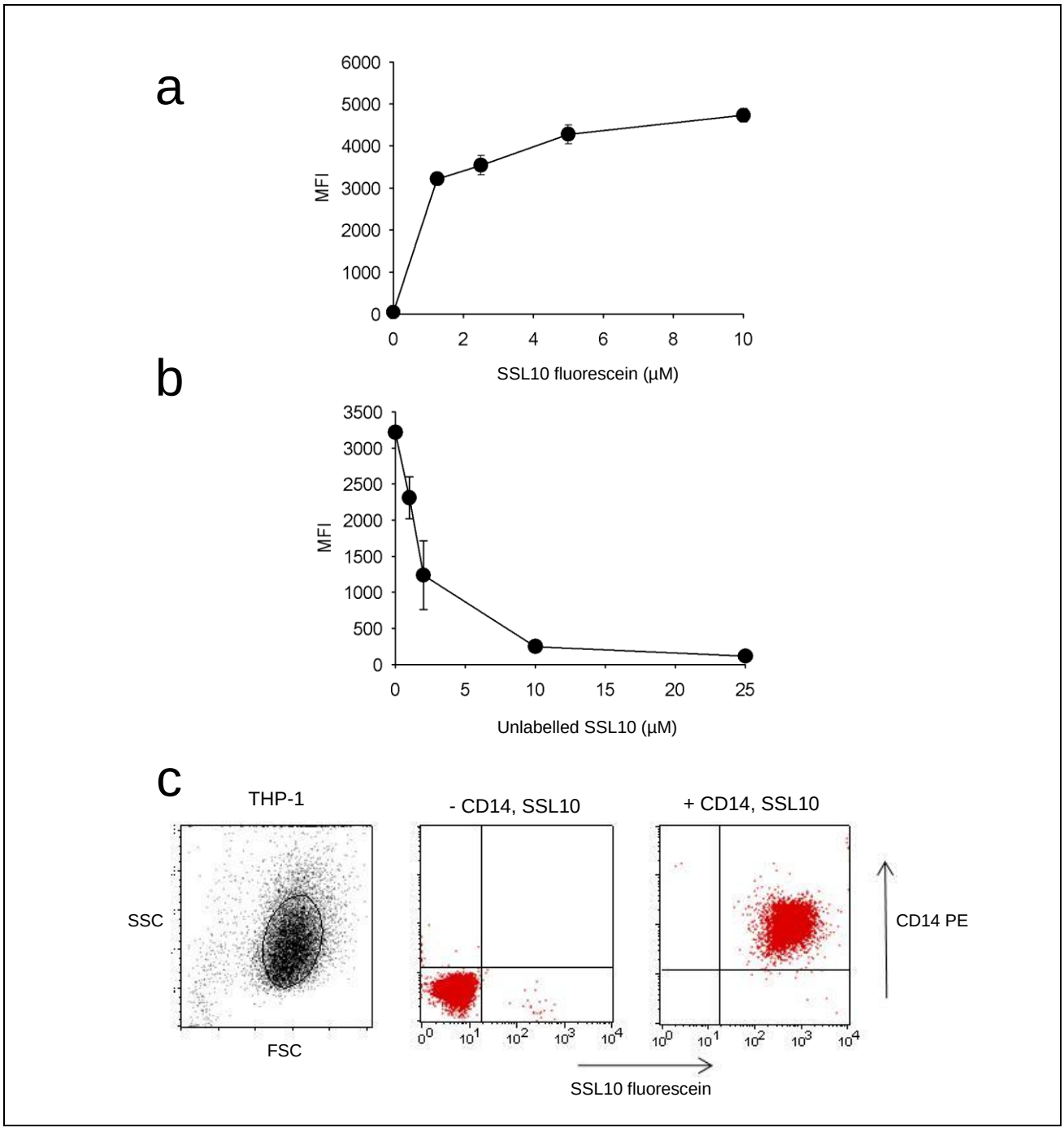

Figure 4.4: The interaction of SSL10-fluorescein with monocytes is saturable and competitive.

(a) Increasing concentrations of SSL10-fluorescein were incubated with human PBMCs ($2.5x10^5$ cells) in PBS pH 7.4, 0.5 % BSA at 4 ^oC for 10 min (n=2). (b) SSL10-fluorescein (1 µM) was incubated with PBMCs ($2.5x10^5$ cells) for 10 min in the presence of increasing concentrations of unlabelled SSL10 (n=2). Cells were washed and analysed by FACS to measure the mean fluorescence intensity (MFI). For each sample 10000 events were collected. (c) SSL10 also binds to the THP1 monocyte cell line. THP-1 cells were grown in RPMI with 10 % FCS and gated using forward (FSC) and side scatter (SSC) in the presence and absence of CD14 PE and SSL10-fluorescein.

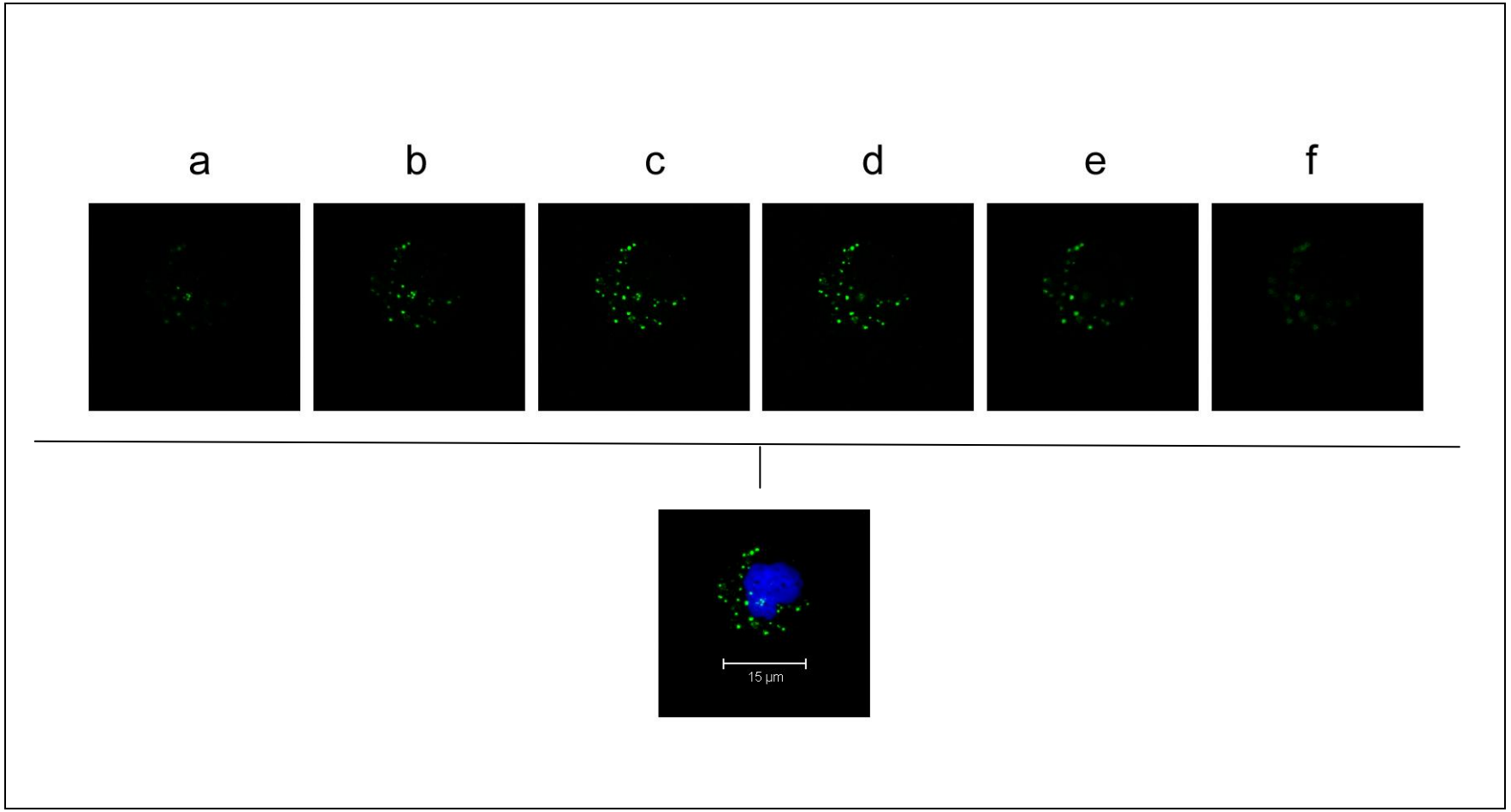

Figure 4.5: Confocal sections of a human PBMC incubated with SSL10-Alexa488.

SSL10 labelled with Alexa488 (0.8 µM) was incubated with human PBMC at RT in PBS pH 7.2, 0.5 % BSA for 15 min (green). Cells were washed twice and spun onto a glass slide. Z-series sections (a-f) were taken on the Leica TCS SP2 confocal microscope (Leica, Germany). Cells were counter stained with DAPI to visualize the chromosomal DNA (blue) and a larger cell with a horseshoe-shaped nucleus presumed to be a blood monocyte was selected. The Z-series sections were combined to form a stacked image (bottom).

4.2.2.4 Coprecipitation of monocyte surface proteins by SSL10 Sepharose

The cell surface of human PBMCs was biotinylated, and proteins in the cell lysate were affinity purified with SSL10 Sepharose and analysed by western blot. Several bands were repeatedly isolated by both alleles of SSL10 in the presence and absence of FCS (Fig. 4.6). Notably a single biotinylated disulfide linked heterodimeric surface protein with individual chains of approximately 140 and 120 kDa was purified. Following coomassie staining, numerous non-specific bands corresponding to intracellular or FCS proteins were present, thus a double coprecipitation method (Section 2.2.11.1) was adapted to specifically concentrate the cell surface proteins (data not shown). Despite repeated efforts these bands were not concentrated to sufficient quantities to visualize by coomassie staining for subsequent mass spectrometry; possibly due to weak receptor-ligand affinity.

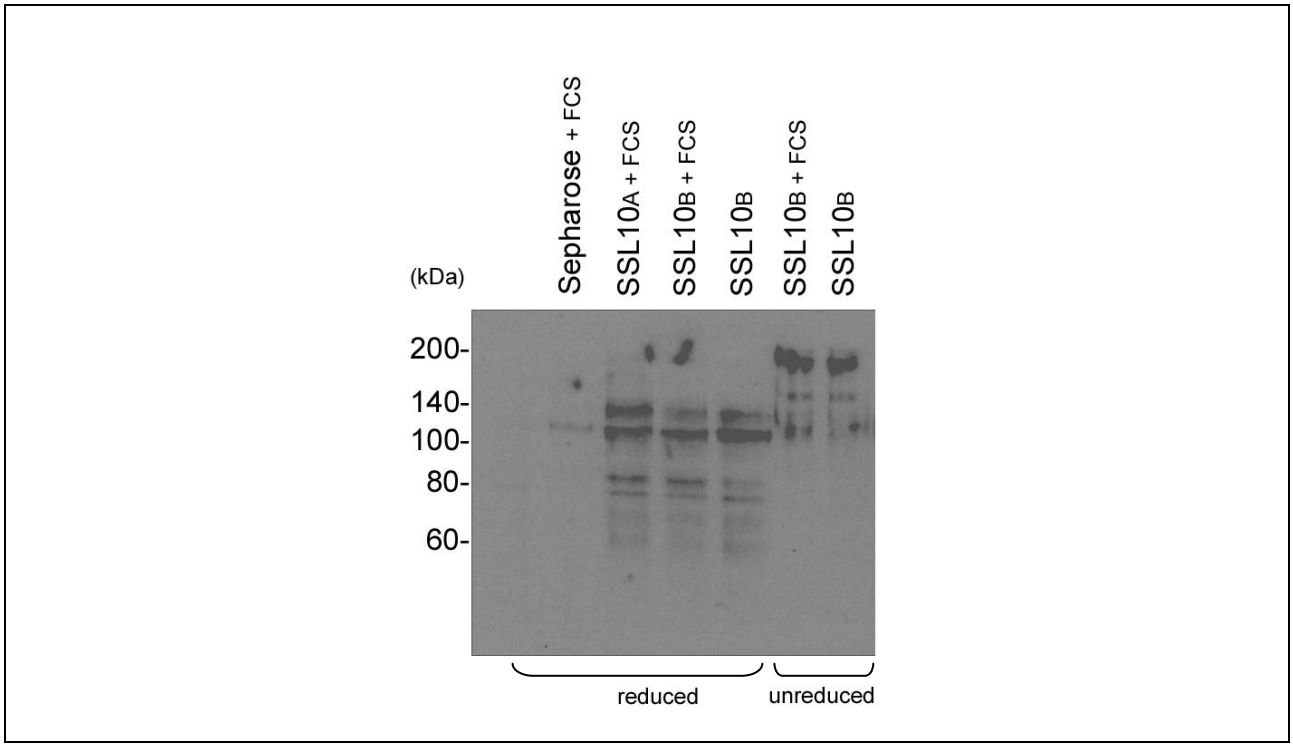

Figure 4.6: Affinity isolation of biotinylated cell surface proteins from PBMCs at 4 ^{o}C by SSL10.

Biotinylated cell lysate from purified PBMCs was incubated with Sepharose alone, $SSL10_A$ Sepharose or $SSL10_B$ Sepharose in the presence of 10 % FCS. $SSL10_B$ Sepharose was also incubated with biotinylated cell lysate in the absence of FCS. Bound proteins were analysed by reducing SDS-PAGE. Proteins bound by $SSL10_B$ Sepharose in the presence and absence of 10 % FCS were also analysed under non-reducing conditions. Biotinylated polypeptides were detected by Western blot analysis using Streptavidin coupled to HRP (1:1000).

4.2.3 Affinity isolation of plasma proteins by SSL10

To identify potential binding partners from the host immune system the interaction of SSL10 with plasma proteins was investigated. Proteins from fresh human plasma (10-20 %) were affinity purified with SSL10 Sepharose (10 µL of 1:1 suspension) and separated by reducing SDS-PAGE. Both alleles show similar binding profiles with two major polypeptide bands at approximately 50 kDa (E) and 25 kDa (G) and four weaker but significant bands at approximately 250 kDa (A), 65 kDa (C), 55 kDa (D) and 50 kDa (F) (Fig. 4.7). These polypeptides were identified by LC/MS mass spectrometry to be IgG1 heavy and immunoglobulin light chains, fibronectin, and fibrinogen α-, β- and γ- chains respectively (Appendix C.1-C.6). Weaker but consistent bands were also repeatedly observed at approximately 200 kDa (I) and 75 kDa (H). These were identified to be α2-macroglobulin and prothrombin respectively (Appendix C.7- C.8).

The β-grasp domain, $SSL10_{95-197}$, retained the ability to bind fibronectin and fibrinogen; however its ability to bind serum IgG was significantly reduced. This indicates that the IgG bound by SSL10 is not due to natural seroconversion against the protein alone. The β-grasp domain also binds plasminogen (B), which migrates as a sharp doublet (Fig 4.9b) distinct to the band observed with full length SSL10 (J) (Appendix C.9-C.10).

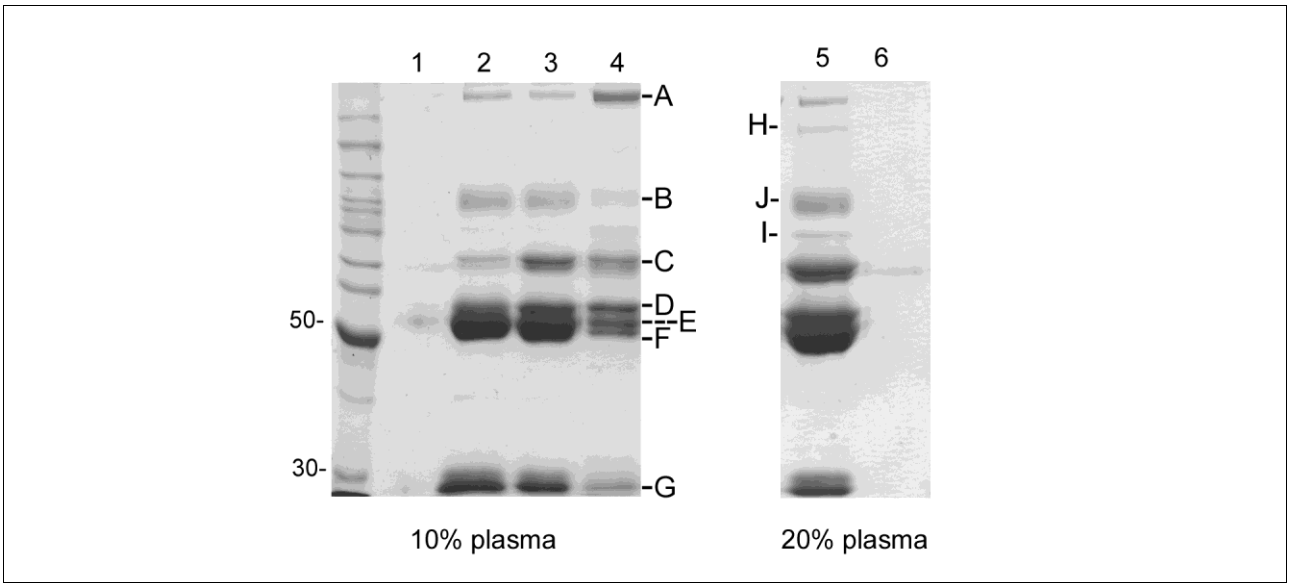

Figure 4.7: Affinity isolation of proteins from human plasma by $SSL10_A$, $SSL10_B$ and $SSL10_{95-197}$.
Sepharose alone (1,6), $SSL10_A$ (2) $SSL10_B$ (3,5) and $SSL10_{95-197}$ (4) Sepharose were individually incubated with 10% or 20% fresh human plasma at 4 ^oC. Bound proteins were analysed by reducing SDS-PAGE. Polypeptides were identified by mass spectrometry to be: fibronectin (A), plasminogen (B), fibrinogen α, β and γ chains (C,D,F respectively), IgG1 heavy chain (E), immunoglobulin light chain (G), α2-macroglobulin (H) and prothrombin (I). Identity of the 90 kDa band remains to be confirmed (J).

4.2.3.1 SSL10 interacts with IgG but not IgA or IgM

The 100 kDa polypeptide band (J) was consistently affinity purified by both alleles of SSL10 but its true identity remains to be determined. Mass spectrometry fingerprinting of tryptic peptides from 'J' were confirmed to be from both the IgG1 heavy chain and kappa/lambda Ig light chains on two separate occasions (Appendix C.10); however the apparent 100 kDa molecular mass of 'J' under reducing and denaturing SDS-PAGE is inconsistent with the classical heavy and light chains of IgG1 that migrate at 50 and 25 kDa. An anti-IgG,A,M antibody detected a high molecular weight band (x) affinity purified by SSL10 and Protein A of approximately 100 kDa from fresh plasma that is presumed to be band 'J' (Fig 4.8a). Intriguingly this band was absent in frozen plasma (Fig 4.8b). As expected Protein A also bound IgG, IgA and IgM while SSL7 specifically bound to IgA. Of the three human Ig classes, SSL10 only bound to IgG.

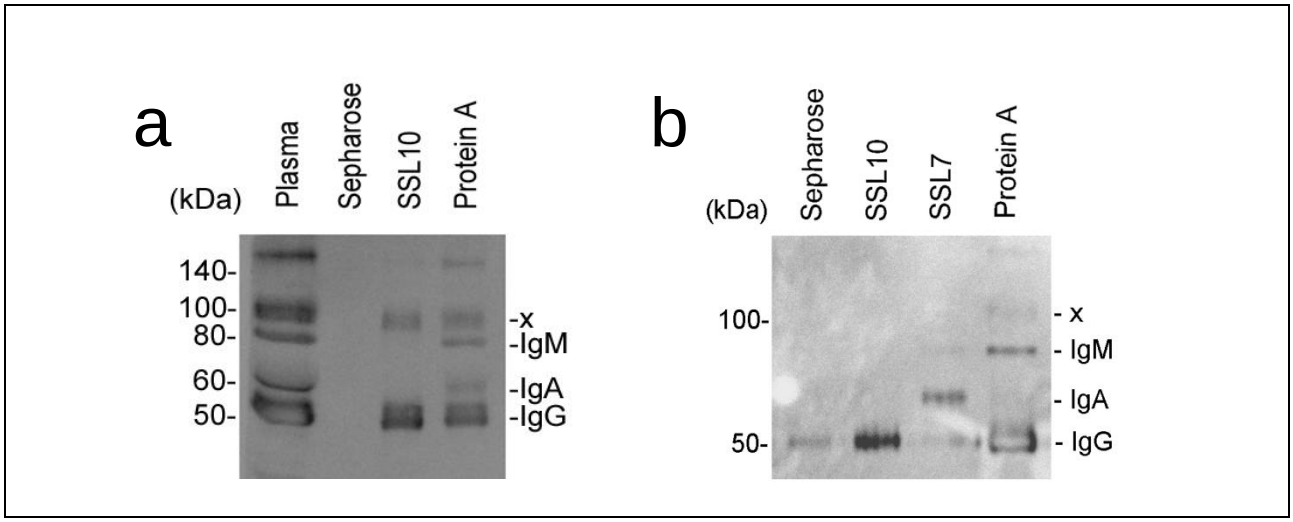

Figure 4.8: Western blot analysis of proteins affinity purified by Protein A, SSL10 and SSL7.
Proteins from (a) fresh and (b) frozen plasma were affinity purified with Sepharose alone or Sepharose coupled with Protein A, SSL10 or SSL7. Immunoblots were probed with an anti-IgG,A,M antibody (1:10000) coupled to HRP.

4.2.3.2 SSL10 directly interacts with purified fibrinogen

Fibrinogen is a large 340 kDa dimeric protein comprised of duplicate 50, 55 and 65 kDa chains. Affinity isolation studies of purified fibrinogen were performed with 10 µL (1:1 suspension) SSL10 or $SSL10_{95\text{-}197}$ Sepharose in the presence of 0.3 M NaCl and 0.1 % (v/v) Tween to inhibit non-specific binding. SSL10 bound strongly to purified fibrinogen but only weakly through the β-grasp domain (Fig. 4.9a). SSL10 also bound to three polypeptides bands of approximately 50, 55 and 65 kDa from mouse, cow and sheep plasma (Fig. 4.10a). The 65 kDa bands from cow, 55 kDa band from mouse and sheep and 50kDa band

from mouse were verified by mass spectrometry to the fibrinogen α, β and γ chains respectively. Under the same conditions the control, Protein A only bound to IgG (Fig. 4.10b). Analysis by western blot did not detect binding of SSL10-biotin to the α, β or γ- chains of fibrinogen separated by reducing SDS-PAGE (data not shown); possibly due to targeting of structural epitopes on fibrinogen that are not detected under reducing conditions. Alternatively, the fibrinogen binding site on SSL10 could be blocked by biotinylation.

4.2.3.3 SSL10 binds to purified plasminogen

Plasminogen is the inactive form of the fibrinolytic enzyme plasmin. It was easily affinity purified from fresh plasma using Lysine Sepharose chromatography (Deutsch & Mertz, 1970). The purified 90 kDa polypeptide band was verified by mass spectrometry to be plasminogen (Appendix C.9). Purified plasminogen (0.3 mg/mL) was the only protein that bound equally strongly to both the full-length and β-grasp domain of SSL10 (10 uL 1:1 suspension) by affinity isolation (Fig. 4.9b). Incubation of SSL10 with purified plasminogen in solution overnight at 37 ^{o}C did not induce the formation of plasmin or promote the cleavage of purified human IgG1 by plasminogen (data not shown).

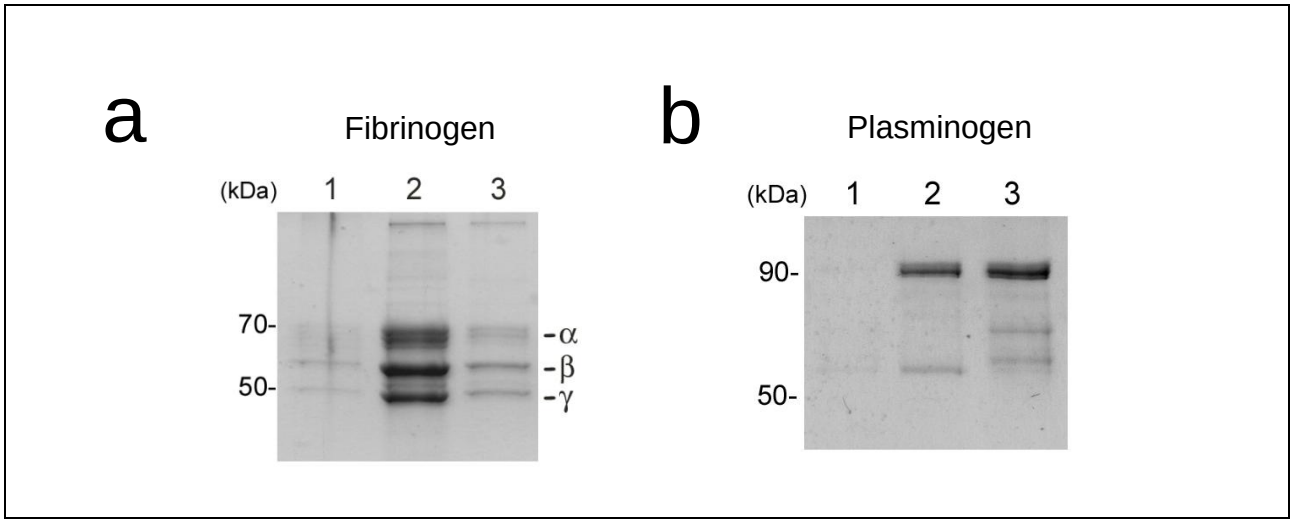

Figure 4.9: Affinity isolation of purified human fibrinogen and plasminogen by SSL10 and SSL10$_{95-197}$ Sepharose.

(a) Purified fibrinogen (0.2 mg/mL) and (b) Lysine Sepharose-purified plasminogen (0.3 mg/mL) were mixed with Sepharose alone (Lane 1), SSL10 Sepharose (Lane 2) or SSL10$_{95-197}$ Sepharose (Lane 3). After extensive washing bound proteins were separated by 10 % reducing SDS-PAGE and detected using Coomassie Blue stain.

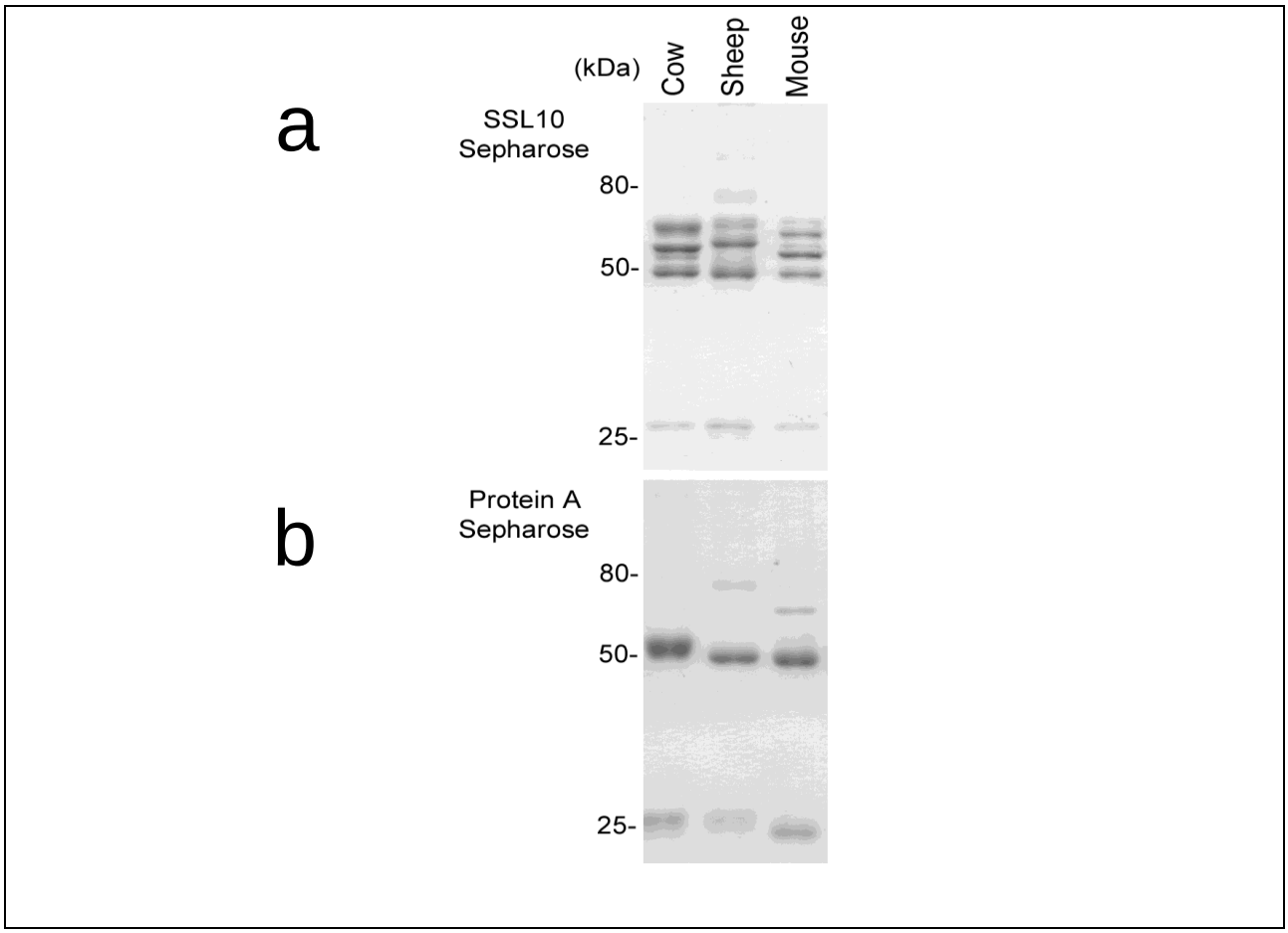

Figure 4.10: Affinity isolation of proteins from cow, sheep and mouse plasma using (a) SSL10 Sepharose and (b) Protein A Sepharose.

Cow, sheep and mouse plasma (10 %) was mixed with (a) SSL10 Sepharose or (b) Protein A Sepharose at 4 ^{o}C. The bound polypeptide bands were separated by 12 % reducing SDS-PAGE and detected by Coomassie Blue stain.

4.2.3.4 SSL10 directly binds to the coagulation factor prothrombin

Prothrombin is the inactive precursor of thrombin, a potent serine protease at the heart of the coagulation cascade. This 72 kDa protein was purified from sodium citrate human plasma using barium chloride precipitation (Dahlback, 1983) followed by anion exchange chromatography (Fig 4.11a Lane 8). Prothrombin was eluted from the anion exchange MonoQ column with 0.7 M NaCl in 20 mM Tris pH 7.5 and dialysed into PBS pH 7.4. Freshly purified biotinylated prothrombin directly bound to immobilized SSL10 by ELISA however it did not bind to SSL7 or the β-grasp domain of SSL10 (Fig 4.11b). It is possible the size and/or orientation of immobilized $SSL10_{95\text{-}197}$ interferes with prothrombin binding. Reverse binding studies by ELISA were unsuccessful due to high levels of non-specific binding of SSL10 and $SSL10_{95\text{-}197}$ to the plate surface.

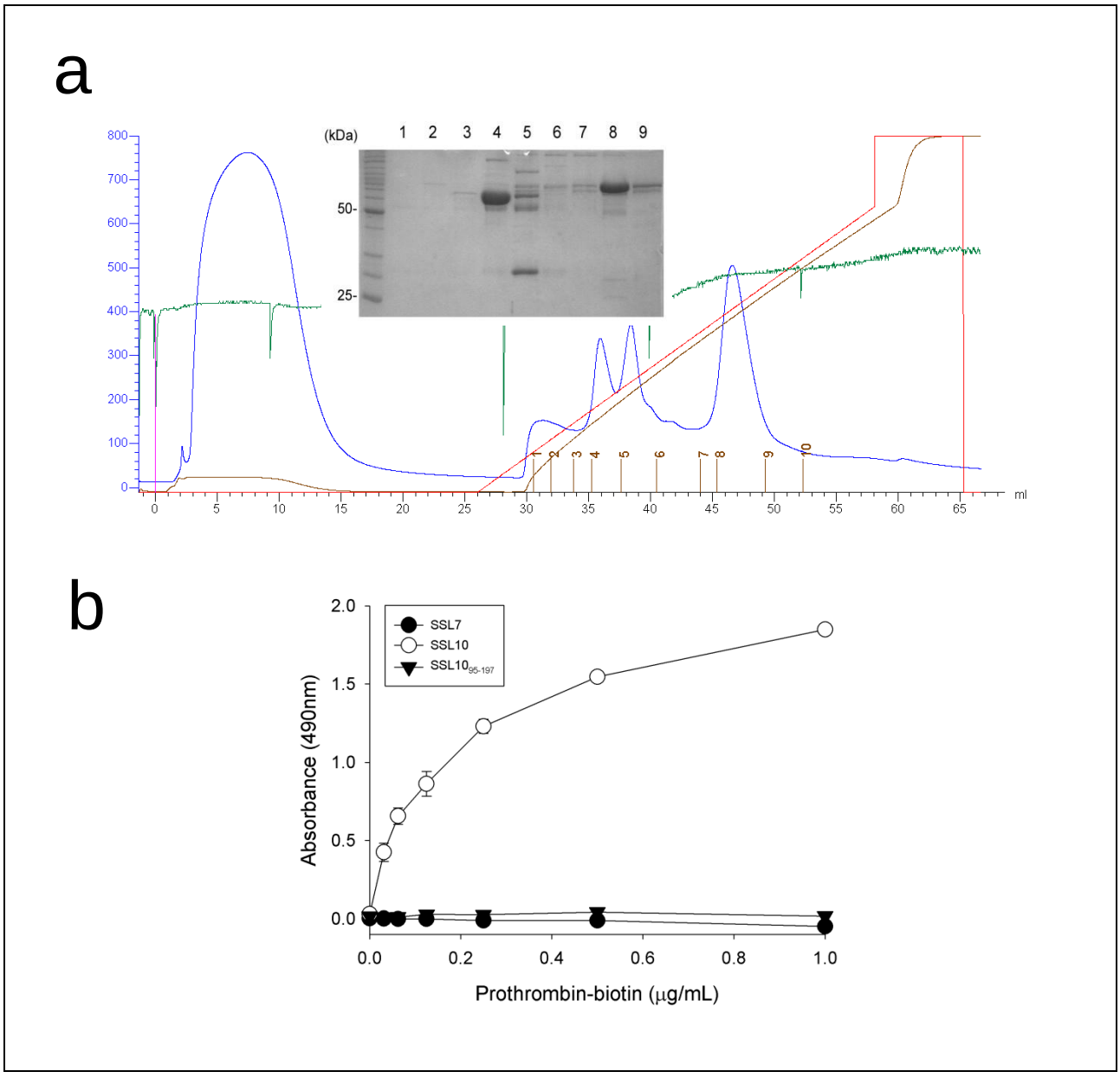

Figure 4.11: Direct interaction of SSL10 with BaCl-purified Prothrombin by ELISA.

(a) Profile of prothrombin purification using Anion exchange chromatography (MonoQ, GE Healthcare) in 20 mM Tris pH 7.5. Prothrombin was precipitated from 15 mL sodium citrate human plasma using BaCl prior to loading on the Mono Q column. Bound proteins were eluted and the collected fractions (1-8) were analysed by 10 % reducing SDS-PAGE (Lanes 1-9). The major peak collected in fraction 8 (lane 8) was verified by mass spectrometry to contain prothrombin (Appendix C.17). Approximately 0.7 M NaCl was required to elute prothrombin from the MonoQ column.
(b) ELISA analysis of biotinylated prothrombin and immobilized SSL10, $SSL10_{95\text{-}197}$ and SSL7 (0.5 µg/mL). Data shown is a representative of two independent experiments (n=2).

4.2.4 SSL10 interferes with clot formation

Fibrinogen and prothrombin are central molecules involved in the formation of insoluble fibrin clots. To investigate if SSL10 interferes with their activity, fibrin formation was measured using a plasma turbidity assay. The intrinsic pathway of the calcium-dependent coagulation cascade was initiated by replacing the calcium removed in platelet poor sodium citrate plasma. After 15 mins a clear inhibition of coagulation was noted in the presence of SSL10 (Fig. 4.12a). Clot formation was followed over time at OD_{405nm} with OD_{620nm} measured as a background reference. In the absence of SSL10, fibrin fibres aggregated over 40 mins following an initial 10 min lag during which time the cascade activates and forms protofibrils without increasing the turbidity (Fig. 4.12b). The inclusion of 0.5 µM SSL10 in 50 % plasma extended the lag phase to 40 mins. The β-grasp domain also displayed equivalent effects to the full length protein while SSL7 did not interfere with clot formation (Fig. 4.13). In contrast, SSL10 or its β-grasp domain did not inhibit clot formation in the presence of preactivated thrombin (Fig 4.12c). The resulting clots were monitored over the following 3 days for any alterations in stability; however no changes were noted.

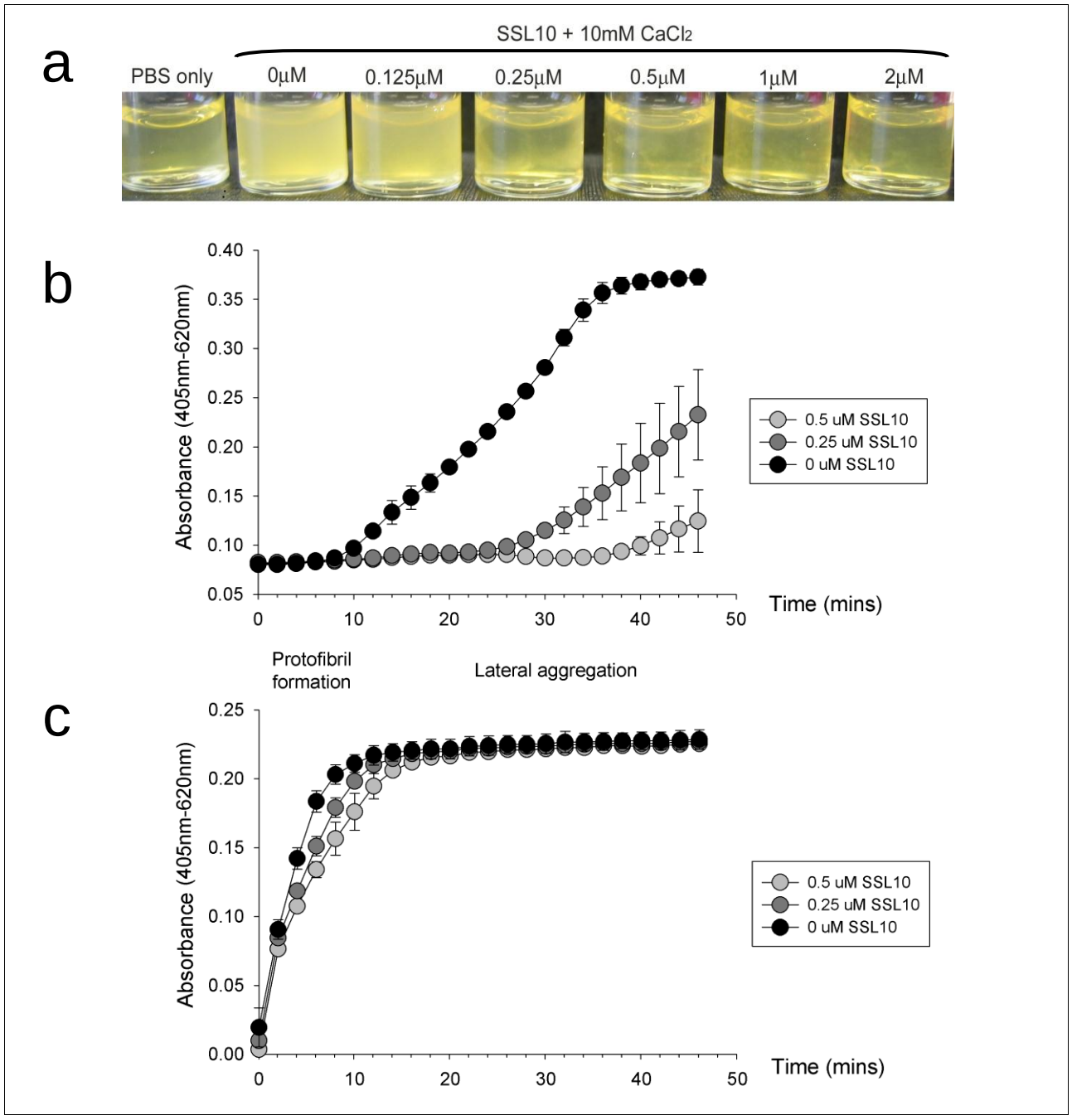

Figure 4.12: SSL10 inhibits clot formation in platelet poor human plasma.

(a) Platelet poor sodium citrate plasma diluted in PBS pH 7.4 and/or activated with 10 mM CaCl in the presence of 0, 0.125, 0.25, 0.5, 1 or 2 μM $SSL10_B$. The image was taken 15 mins following activation to assess turbidity as a measure of fibrin clot formation. (b) Under the same conditions, clot formation for 0, 0.25 and 0.5 μM SSL10 was also measured at OD_{405nm} (OD_{620nm} as reference) over 46 mins following activation with (b) 10 mM CaCl or (c) 0.1 U thrombin. The data shown is a representative of three independent experiments using plasma from different healthy donors (n=2).

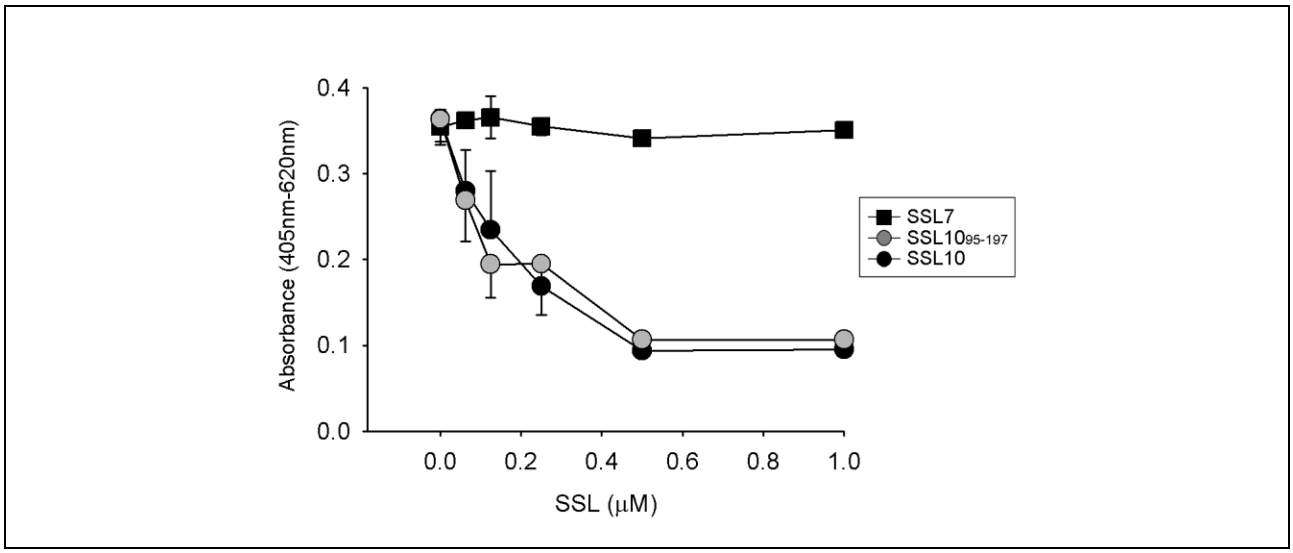

Figure 4.13: Clot formation in the presence of SSL10, $SSL10_{95-197}$ and SSL7 at 40 min following activation with 10 mM CaCl.

Platelet poor plasma (50 %) was incubated with various concentrations of SSL10, $SSL10_{95-197}$ or SSL7 (0-1 μM) for 10 min and the coagulation cascade was activated with 10 mM CaCl. The OD_{405} nm (OD_{620} nm as reference) 40 min following activation was plotted against the concentration of protein. The data is a representative of two independent experiments using plasma from different healthy donors (n=2).

4.3 Discussion

SSL10 is a widely distributed but tightly regulated protein. It is not readily detected in the extracellular milieu of *S.aureus* grown in TSB (Sibbald et al., 2006) or LB media (data not shown). However, studies have reported upregulation of *ssl10* following exposure to hypochloride (M. W. Chang et al., 2007) and uptake of *S.aureus* into neutrophils (Voyich et al., 2005) and epithelial cells (Garzoni et al., 2007). Furthermore, Stauff et al. detected a 7-fold increase in *ssl10* expression by exponential-phase *S.aureus* lacking the ATPase HrtA, which together with the permease HrtB, protects the organism against heme toxicity (Stauff et al., 2008). These studies suggest there are additional environmentally-regulated control mechanisms that govern SSL10 expression.

In the current study, SSL10 was detected by western blot in the culture supernatant of *S.aureus* grown in RPMI media. The Δ*hrtA* mutant expressed SSL10 from the early exponential phase; in strong contrast to the weak expression displayed by the wildtype from the late-exponential to stationary phase of growth. This response is atypical for secreted factors under the control of the *agr* regulator that are generally expressed during the stationary phase to aid in immune evasion (Dunman et al., 2001; Sibbald et al., 2006). Even in the absence of hemin the growth of the Δ*hrtA* mutant was retarded compared to the wildtype suggesting the timely expression of SSL10 was a stress-related response. This is further supported in a recent study by Attia et al. where immunomodulatory factors, including the SSLs, were upregulated in *S.aureus* that had reduced membrane integrity due to the absence of HrtA, rather than in response to deficiencies in HrtA activity against heme toxicity (Attia, Benson, Stauff, & Skaar, 2010). Thus it has been proposed that these factors are upregulated to provide protection from the host defences when *S.aureus* perceives membrane damage (Attia et al., 2010). It is tempting to speculate that this is also the scenario faced during physiological exposure to hypochloride (M. W. Chang et al., 2007) and uptake into host cells (Garzoni et al., 2007; Voyich et al., 2005) that upregulates *ssl10* expression.

Despite structural homology to superantigens, SSL10 does not exhibit any superantigen-like hyper-stimulatory activity in a lymphocyte proliferation assay suggesting it has a unique role. Cellular analysis by FACS detected specific binding of SSL10-fluorescein to a cell surface receptor on monocytes but not lymphocytes or granulocytes. Furthermore it was rapidly internalized into discrete vesicles in the monocyte cytoplasm at 37 °C. Whether internalisation is observed at 4 °C remains to be determined. Regardless, white blood cells play a prominent role in the clearance of *S.aureus* thus calculated targeting of these early phagocytic precursors could dictate the fate of multiple downstream responses. The identity of its receptor and the potential destination within the cell remains to be characterized. Walenkamp et al. detected SSL10 binding to CXCR4-expressing Jurket cells and direct competition with antibodies specifically against CXCR4 (CD184) (Walenkap et al., 2009). However CXCR4 is widely distributed on blood monocytes and lymphocytes (B. Lee, Sharron, Montaner, Weissman, & Doms, 1999; L. Patel et al.,

2001). Furthermore, the 140/120 kDa heterodimeric protein identified in surface proteins selectively bound by SSL10 is not consistent with the known size of CXCR4. It is possible binding of SSL10 to other white blood cell populations is blocked by amine coupling of fluorescein; however this would suggest differential binding characteristics of SSL10 to different cell populations with respect to the monocyte population.

SSL10 binds to fibrinogen from multiple species including man, mouse, cow and sheep. It is one of many fibrinogen-binding proteins produced by *S.aureus*, highlighting the key importance and complexity of the 340 kDa fibrinogen protein. Clumping factor A and B (ClfA, ClfB) are cell wall anchored fibrinogen-binding proteins that promote clumping of *S.aureus* in blood (Eidhin et al., 1998; Espersen, Clemmensen, & Barkholt, 1985). ClfA is constitutively expressed and recognises the carboxy-terminus of the fibrinogen γ chain (C.-Z. Liu, Shih, & Tsai, 2005). It binds in close proximity to the binding site of the platelet integrin $\alpha_{IIb}\beta_3$ and inhibits fibrinogen-dependent platelet aggregation (Foster & Hook, 1998; C. Liu et al., 2005). In contrast, ClfB binds to the fibrinogen α and β chains and is only expressed during the peak stages of *S.aureus* invasion (Eidhin et al., 1998). S.aureus also produces the secreted protein Efb, which binds to the fibrinogen α chain through two distinct sites located on its amino and carboxy-terminus (Palma, Wade, Flock, & Flock, 1998). The exact binding site of SSL10 on fibrinogen is not known however its inability to bind to the reduced fibrinogen chains by Western blot suggests that it potentially targets a structural epitope. Intriguingly, SSL10 also displays affinity for fibronectin, another extracellular matrix protein involved in wound healing (Mosher, 1975) and *S.aureus* colonization (Clarke, Harris, Richards, & Foster, 2002; Ingham et al., 2004). For secreted *S.aureus* proteins such as SSL10, fibrinogen and fibronectin could serve as means to stay concentrated at the site of infection where it can be most effectively utilised.

SSL10 also directly binds to the 72 kDa coagulation factor prothrombin. Positioned at the heart of the coagulation cascade, its activation into thrombin promotes the cleavage of fibrinogen into fibrin fibres that rapidly aggregate into an insoluble clot. *S.aureus* is well known for its unique coagulase protein that forms a complex with prothrombin to promote the cleavage of fibrinogen while bypassing thrombin formation (Boden & Flock, 1992). SSL10 does not exhibit coagulase activity; instead it dramatically hinders clot formation through predominant interactions in its β-grasp domain. This effect is not observed in the presence of preactivated thrombin suggesting SSL10 activity is directed at prothrombin rather than fibrinogen. As little as 0.5-1.0 μM SSL10 or $SSL10_{95\text{-}197}$ can delay coagulation in 50 % plasma by a further 30 min *in vitro*. This correlates well with a 1:1 stoichiometry interaction between SSL10 and prothrombin, which is present in 50% blood at approximately 0.75 μM (Ahsen, Lewczuk, Schutz, Oellerich, & Ehrenreich, 2000). Under *in vivo* conditions, even the smallest extension of the clotting process would provide ample opportunity for *S.aureus* to escape and spread. Curiously immobilized $SSL10_{95\text{-}197}$ does not bind to biotinylated prothrombin by ELISA; however it is possible that in this orientation the binding site on the smaller immobilized SSL10 domain is inaccessible to prothrombin. ELISA analysis is limited in the

reverse orientation due to strong non-specific binding of SSL10 and $SSL10_{95-197}$ to the plate surface, even under various blocking conditions.

Obstructing the generation of the serine protease thrombin is strategically beneficial for *S.aureus* on multiple levels. Thrombin is at the heart of both the intrinsic and extrinsic coagulation pathways thus is a key force for maintaining homeostasis and supporting the inflammatory process (Esmon, 2004). It intensifies the clotting process by activating platelets that reinforce the fibrin seal (Kahn et al., 1998). Furthermore thrombin forms an intimate link with the complement cascade through the cleavage of complement C5 and release of the potent anaphylatoxin C5a (Huber-Lang et al., 2006). Thrombin generation requires the formation of the Ca^{2+} dependent prothrombinase complex, comprising of coagulation factors Factor Xa, Factor V and prothrombin (Esmon, 2004). The interaction of SSL10 with prothrombin could directly block the formation or activity of the prothrombinase complex. Alternatively, it could be sterically hindered by a complex of SSL10 with prothrombin and another plasma protein, such as fibrinogen. Intriguingly SSL9 and SSL12 both bind fibrinogen and affect clot stability over time (Dr N. Jackson, Dr A Taylor, Personal communication). Combined activity of all three related proteins *in vivo* could have a dramatic impact on how well the initial breach is sealed to restrict *S.aureus* and furthermore, how the inflammatory process is localized and managed.

SSL10 also displays affinity for several other plasma proteins that play important roles in the host defences against *S.aureus*. It makes prominent interactions with human IgG but not IgA or IgM (described in detail in Chapter 5). The 100 kDa band identified by mass spectrometry to be IgG1 is puzzling; it could reflect ineffective reduction of the disulfide bonds by β-mercaptoethanol. SSL10 and its β-grasp domain also directly bind to plasminogen, a precursor of the fibrinolytic enzyme plasmin. Plasmin degrades fibrin clots and inactivates host factors such as surface bound IgG and complement factors (S. H. M. Rooijakkers, van Wamel, Ruyken, van Kessel, & Van Srijp, 2005). The *S.aureus* secreted protein staphylokinase hijacks and activates plasminogen by inducing a conformational change that exposes the catalytic domain (Shibata et al., 1994). SSL10 did not cleave purified plasminogen into plasmin in solution, nor did it activate plasminogen to cleave purified human IgG1. Plasminogen displays strong affinity for lysine residues (Deutsch & Mertz, 1970), which could dictate its interaction with the lysine rich SSL10 protein. SSL10 also binds weakly to α2 macroglobulin, a proteinase inhibitor that traps a wide range of endopeptidases. Whether its interaction with SSL10 is direct remains to be determined. Given the enormous number of proteins in sera, the affinity profile of SSL10 itself reflects a level of specificity. Further studies are required to investigate the interaction of SSL10 with the individual host proteins and also their combined activities.

The extreme cationic nature of the SSL10 further highlights its versatility and may be an important feature in its ability to bind to a range of anionic plasma proteins. SSL10 was associated specifically with the cell

surface of stationary phase overnight *S.aureus* cultures. Affinity isolation of biotinylated *S.aureus* surface proteins did not detect any specific polypeptide bands (data not shown). Furthermore, binding of SSL10-fluorescein to the cell surface of *S.aureus* detected by FACS analysis was not competed by excess unlabelled SSL10 (data not shown). Thus association of SSL10 to the bacterial cell surface most likely reflects non-specific binding due to its highly cationic nature. *S.aureus* secretes two other highly cationic proteins, Sbi (Atkins et al., 2008) and Eap (Chavakis et al., 2002), which lack the typical LPXTG cell wall anchoring motif but bind to unknown sites on the *S.aureus* cell surface. All three proteins also display affinity for multiple plasma proteins. Binding back of these highly cationic secreted proteins to the bacterial surface adds another dimension to the *S.aureus* defence strategy. It permits *S.aureus* to bridge with host components and exploits them as immunological camouflage. But more importantly it reduces the net negative charge of the *S.aureus* surface thereby avoiding the lethal effects of host cationic antimicrobial factors without imposing structural modifications that can alter *S.aureus* integrity.

Chapter 5
Human IgG1 and SSL10

5.1 Introduction

Immunoglobulin G forms an integral part of the systemic host defences, linking antigen recognition through the Fab domain to an array of downstream effector functions through the Fc domain. Several host proteins bind to the IgG Fc domain, including complement C1q, which activates the classical complement pathway (Idusogie et al., 2000); the neonatal Fc receptor, which prevents catabolism of maternal IgG during transport to the fetus (B. Wines, Powell, Parren, Barnes, & Hogarth, 2000); and multiple FcγRs, which trigger a range of immune responses including phagocytosis, antibody dependent cellular cytotoxicity and secretion of inflammatory mediators (Gessner et al., 1998). Despite strong homology between the four human IgG subclasses, each displays a unique profile of biological activities and *in vivo* response to infection (Barrett & Ayoub, 1986; R Jefferis & Kumararatne, 1990). Given the versatility of this molecule it is not surprising that Ig binding proteins are a common feature in the evasion strategies of many pathogenic organisms.

S.aureus has several Ig binding proteins at its disposal. The best characterized is the cell wall anchored Protein A that binds the Cγ2-Cγ3 elbow of IgG from a range of species (Deisenhofer, 1981) and indirectly inhibits FcγR and C1q binding. In addition, it forms interactions with the Fab domain of V_H3^+ Igs and acts as a potent B cell superantigen (Anderson et al., 2006). Intriguingly, the secreted IgG binding protein Sbi displays strong similarities to Protein A. Both protein bind through multiple domains and share residues involved in IgG Fc binding that dictate affinity for all the human IgG subclasses except IgG3 (Atkins et al., 2008). *S.aureus* also secretes SSL7, which targets the Cα2-Cα3 interface of IgA and directly competes with FcαRI (B. D. Wines et al., 2006). In this study SSL10, a close homologue of SSL7, was found to bind human IgG1 from plasma. This chapter confirms and further characterizes the unique specificity, kinetics, mechanisms and functional implications of the interaction of SSL10 and human IgG1.

5.2 Results

5.2.1 SSL10 exclusively binds to human IgG1

The human IgG population is comprised of four subclasses, of which IgG1 is the major form present in blood. To confirm the interaction of SSL10 with human IgG and determine if it has affinity towards all the IgG subclasses, coprecipitation analysis was performed with purified proteins. Commercially purified human IgG1, IgG2, IgG3 and IgG4 were individually mixed with SSL10 Sepharose, or as a control Protein A Sepharose. The captured proteins were separated by reducing SDS-PAGE and transferred to nitrocellulose membrane for subsequent detection with biotinylated mouse anti-human IgG subclass-specific antibodies (Fig.5.1a). Protein A lacks affinity for IgG3 and as expected coprecipitated all the IgG subclasses except IgG3. In contrast, SSL10 exclusively bound IgG1. This interaction was also consistent in the reverse orientation, where SSL10 was specifically captured by IgG1 Sepharose (Fig. 5.1b).

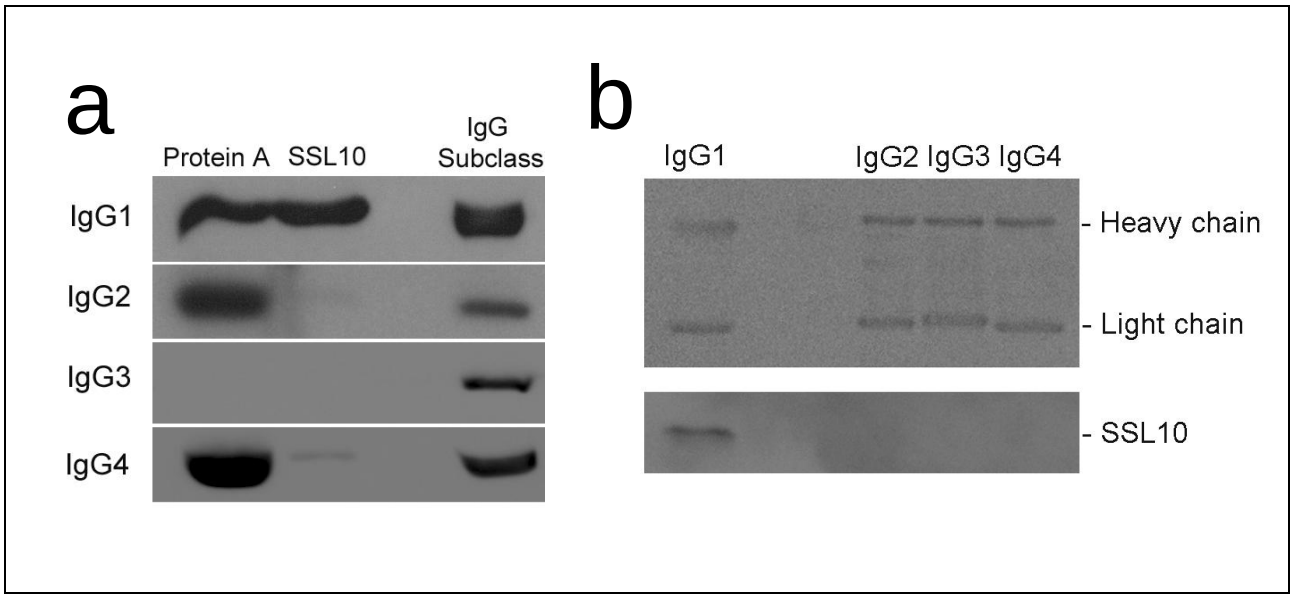

Figure 5.1: Immunoblot displaying the specificity of SSL10 for human IgG1

(a) Affinity isolation of purified human IgG1, IgG2, IgG3 and IgG4 (25 µg) with 5 µL Protein A Sepharose (lane 1) or SSL10 Sepharose (lane 2). The individual IgG subclasses were included as positive controls (lane 3). The IgG heavy chain was detected using biotinylated mouse monoclonal antibodies against the specific IgG subclass (1:2000).

(b) Human IgG subclass-specific Sepharose (5 µL) was incubated with either their respective biotinylated mouse anti-human IgG subclass specific antibodies to confirm efficient coupling of the IgG subclasses onto sepharose (top panel) or 2 µM SSL10 (bottom panel) for 1 h at 4 °C. SSL10 was detected using biotinylated mouse monoclonal anti-SSL10 antibodies. All biotinylated antibodies were detected using Streptavidin coupled to HRP. This data is a representative of two independent experiments.

5.2.2 SSL10 binds to the IgG1 Fc domain

The Fab (~50 kDa) and Fc (~55 kDa) domains of Protein A-purified IgG were produced using papain, which cleaves between histidine 224 and threonine 225, and glutamic acid 233 and leucine 234 (Wang & Wang, 1977) The cleaved fragments were incubated with SSL10 Sepharose. Of these two fragments only the Fc domain was coprecipitated by SSL10 (Fig 5.2). This strict specificity of SSL10 for the invariant region of IgG also confirms that IgG is not bound to SSL10 due to natural seroconversion against SSL10. Notably, SSL10 coprecipitated the individual 25 kDa domains of the Fc fragment produced by papain cleavage between His^{224} and Thr^{225} (Fig. 5.2).

The central cavity of the IgG Fc domain is stabilized by complex carbohydrates attached to the asparagine 297 residue on the Cγ2 domains (Krapp et al., 2003). The core motif comprises of the heptasaccharide $GlcNAc_2Man_3GlcNAc_2$, which can be further extended by the addition of fucose, galactose or sialic acid residues (Wuhrer et al., 2007). Absence of these carbohydrate structures significantly alters the affinity and biological activity of host Fc receptors, C1q and FcγR. Removal of the carbohydrates from native IgG1 Fc by the endopeptidase PNGaseF, which cleaves between the innermost GlcNAc and asparagine residue, did not interfere with the ability of SSL10 Sepharose to affinity purify IgG1 Fc (Fig. 5.2 lane 5). This suggests SSL10 does not bind to IgG1 Fc through N-linked carbohydrate moieties.

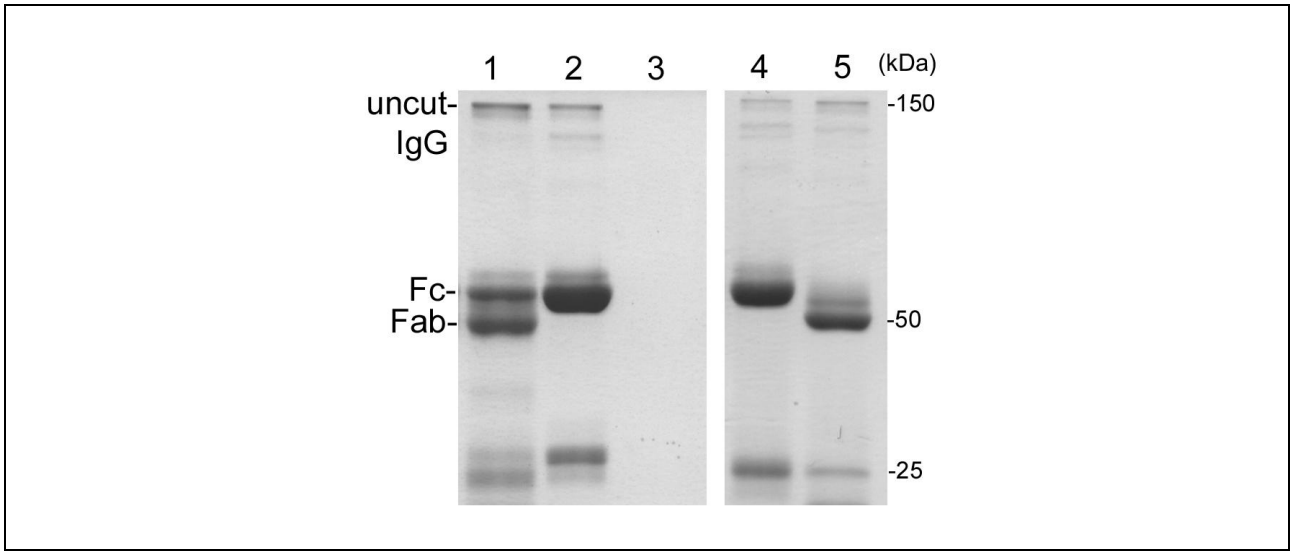

Figure 5.2: Coprecipitation of the Fc domain of human IgG1 by SSL10 Sepharose.

Non-reducing SDS-PAGE gel of Protein A-purified human IgG cleaved with papain to yield the Fc (55 kDa) and Fab (50 kDa) domains (1). Non-specific papain cleavage also induces formation of individual 25 kDa subunits of Fc (1). The digested IgG was coprecipitated with SSL10 Sepharose (2) or Sepharose alone (3). The native Fc domain affinity purified by SSL10 Sepharose before (4) and after (5) treatment with PNGaseF to remove the Cγ2 domain linked carbohydrates. Data is a representative of two independent experiments.

5.2.3 SSL10 binds to a single site on human IgG1

The binding affinity of SSL10 towards a monoclonal human IgG1 was investigated using Surface Plasmon Resonance. Purified human monoclonal IgG1 from the ARH-77 lymphoblastoid cell line (Drewinko, Mars, Minowada, Burk, & Trujillo, 1984) was immobilized onto a CM5 Biacore biosensor chip using carbodiimide chemistry to approximately 300 RU. $SSL10_A$, $SSL10_B$ and $SSL10_{95\text{-}197}$ (0-3 µM) were used as the analyte at various concentrations and the equilibrium binding response was measured. $SSL10_A$ and $SSL10_B$ bound to IgG1 in a dose dependent manner. In contrast, freshly purified $SSL10_{95\text{-}197}$ did not display affinity for immobilized human IgG1. This suggests key residues promoting stabilized binding to IgG1 are located in the N-terminal OB fold domain. The IgG bound by $SSL10_{95\text{-}197}$ from human plasma is likely to be due to natural seroconversion against the C-terminal domain of SSL10 (Fig. 4.7, lane 4). Varying levels of IgG against $SSL10_{95\text{-}197}$ have been detected in the sera of four *S.aureus* infected patients (Appendix D).

The equilibrium binding response for $SSL10_A$ and $SSL10_B$ were analysed using the BIAevaluation 3.1 software and fitted to a single binding site model using the Hill plot: $R_{eq}/B_{max}=([rSSL10]^{nH})/(K_D+[rSSL10]^{nH})$, where R_{eq} is the plateau binding response, B_{max} is the maximum analyte bound at saturation, nH is the hill coefficient and K_D is the equilibrium dissociation constant. For $SSL10_A$ the K_D was 0.64 ± 0.07 µM (± SEM, Chi^2 = 1.2) with a hill coefficient of 0.6 (n=2). Similarly, for $SSL10_B$ the K_D was 0.92 ± 0.08 µM (± SEM, Chi^2 = 5) with a hill coefficient of 0.85 (n=2). A hill coefficient below 1 suggests negative cooperativity where affinity for the receptor decreases as more ligand is bound. However, it is difficult to ascertain if these results reflect a normal physiological response as these analyses were conducted in the presence of 0.3 M NaCl to reduce the large non-specific electrostatic interactions that occurred between the highly cationic SSL10 protein and the anionic dextran surface. Nevertheless it confirms specific binding of SSL10 to human IgG1, most likely involving a single site interaction. These kinetic analyses were also attempted in the reverse orientation with immobilized SSL10 (data not shown). However, IgG1 did not bind to SSL10 as well as expected. A similar effect also observed with ELISA analysis where a notably large excess of IgG to SSL10 was required for saturation (data not shown). This is most likely due to the orientation of SSL10 on the surface or steric hindrance caused by immobilization.

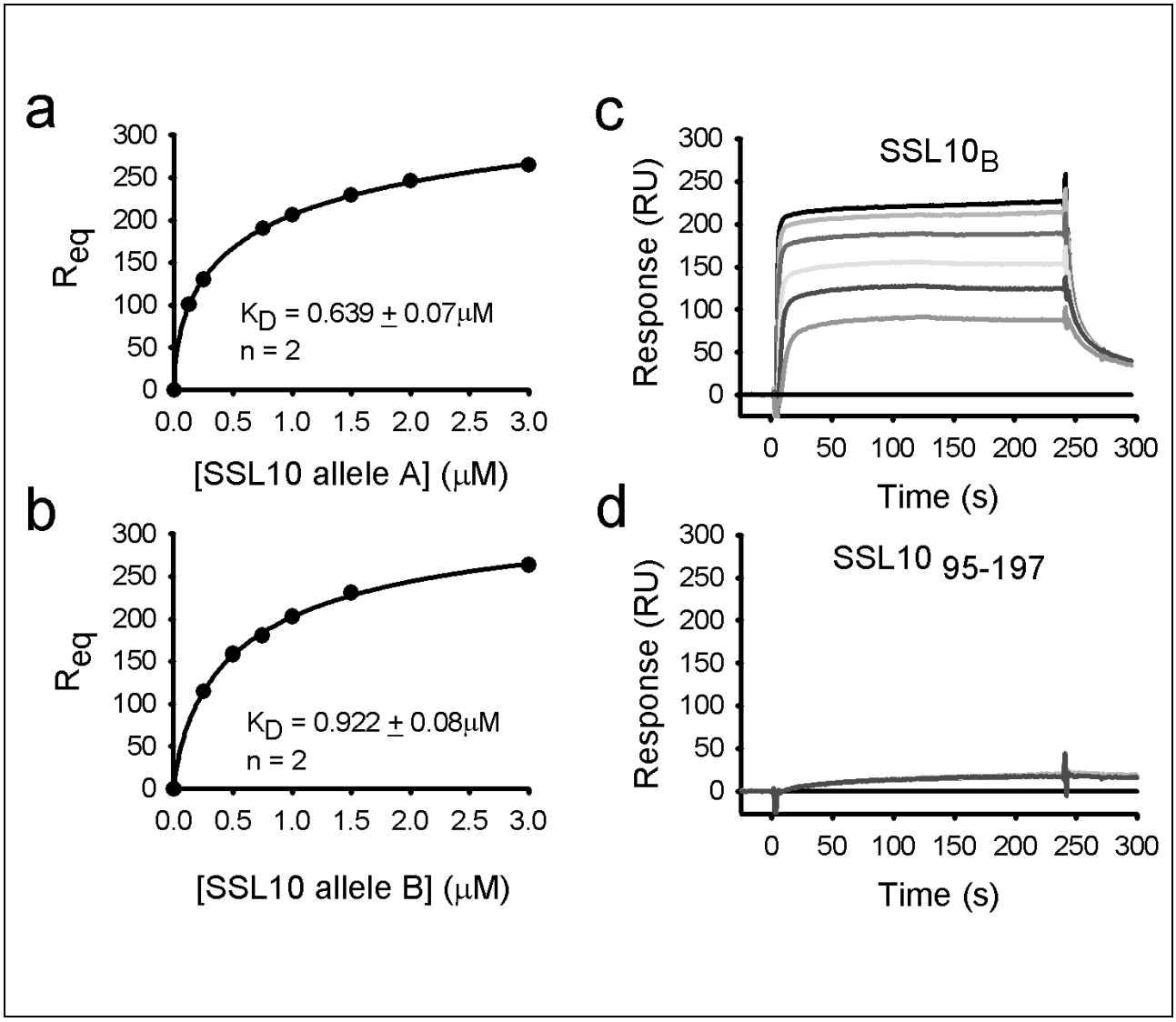

Figure 5.3: Kinetic analysis of SSL10 binding to human IgG1 using surface plasmon resonance.

(a-b) Equilibrium binding response of (a) $SSL10_A$ and (b) $SSL10_B$ binding to immobilized monoclonal human IgG1 on CM5 BIAcore biosensor chip. The data was fitted to the single site model using the Hill plot and dissociation constant (K_D) ± SEM calculated (n = 2).

(c-d) Sensogram of $SSL10_B$ at 0 μM, 0.06 μM, 0.125 μM, 0.25 μM, 0.5 μM and 1 μM, and $SSL10_{95-197}$ at 0 μM, 0.5 μM, 1 μM, 1.5 μM (ascending order) reacted with monoclonal human IgG1.

5.2.4 Isothermal titration calorimetry analysis of SSL10 and IgG1

Isothermal titration calorimetry (ITC) was performed to further investigate the binding kinetics of SSL10 and IgG1. ITC eliminates the need for immobilization and the associated non-specific electrostatic interactions that were highly problematic with Surface Plasmon Resonance and ELISA analysis. Purified polyclonal human IgG1, monoclonal human IgG1 (ARH-77) and IgG1 Fc were analysed for binding to $SSL10_B$ at 25 °C in PBS pH 7.4. The heat evolved upon periodic 10 µL injections of $SSL10_B$ into IgG1 Fc or IgG1 was measured using a VP-ITC MicroCal calorimeter (USA). The background heat evolved from SSL10 dilution into the experimental buffer was also measured and removed. The corrected heat released in the exothermic reaction was fitted to a single site model using the MicroCal Origin software (USA) supplied by the manufacturer. Interestingly, a stoichiometry of 1:1 (N= 0.7-1.0) was determined with a calculated dissociation constant of 0.2 ± 0.002 µM for polyclonal human IgG1 and 0.3 $\pm$ 0.024 µM for monoclonal human IgG1 (± SEM). In comparison, the IgG1 Fc displayed a higher dissociation constant of 1.2 ± 0.14 µM (± SEM), most likely due to heterogenicity of the Fc population introduced during papain cleavage. The variation in stoichiometry for the polyclonal IgG1 and Fc could be due to inaccurate measurements of protein concentration or impurity of the protein preparation. Both SPR and ITC suggest the affinity of SSL10 for IgG1 is in the high nanomolar range; much weaker than the other *S.aureus* IgG binding proteins but approximately 10 fold stronger then the low affinity FcγRs (Table 5.1).

5.2.5 Cleavage of Fcγ1 Asn^{297}-linked carbohydrates

The complex of SSL10 and human IgG1 Fc was analysed by size exclusion chromatography in PBS pH 7.4. SSL10 (520 µM) was mixed with IgG1 Fc (130 µM) purified from plasma and loaded onto a Superdex 200 column (Fig. 5.5a). Two peaks at 9.5 mL and 11.5 mL were eluted from the column. Approximately 0.5 mL elution fractions (a-i) of the peaks were collected and analysed by non-reducing SDS-PAGE. Western blot performed with biotinylated rabbit anti-SSL10 IgG indicates SSL10 is not eluted from the column in complex with the Fc domain. SSL10 alone is typically eluted from the column at 12.5 mL, thus its premature elution at 11.5 mL suggests SSL10 does bind to the IgG1 Fc domain but dissociates at some stage during its migration due to low affinity interaction. SSL10 (360 µM) was also analysed in complex with IgG1 Fc treated with PNGase F (180 µM) to remove the N-linked carbohydrates from Asn^{297} (Fig. 5.5b). In strong contrast, approximately half of the SSL10 was eluted from the column in complex with the deglycosylated Fc domain. This suggests the removal of N-linked carbohydrates alters the structure of the Fc domain to a state which favors stronger binding of SSL10.

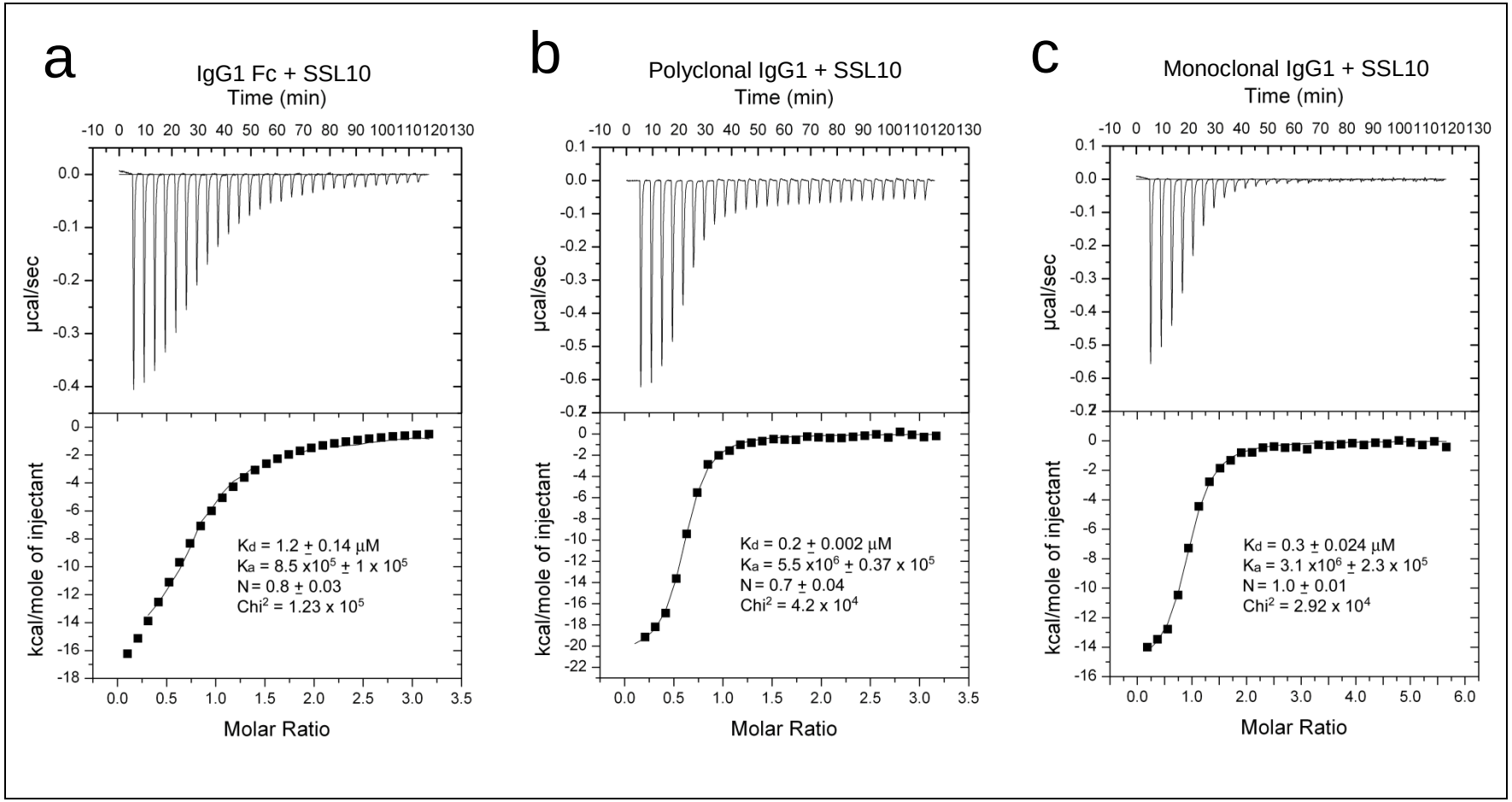

Figure 5.4: Isothermal titration calorimetry profiles for the binding of SSL10 to human IgG1 and IgG1 Fc at 25 ^{o}C in PBS pH 7.4.

The raw data from sequential 10 µl injections of (a) 90 µM SSL10 into 6 µM human IgG1 Fc, (b) 105 µM SSL10 into 7 µM human polyclonal IgG1 and (c) 142 µM SSL10 into 5 µM human monoclonal IgG1 (Top). The plot of the heat evolved (kcal) per mole of SSL10 added against the molar ratio of SSL10 to IgG1. The data was fitted to a single site binding model and the solid line represents the best fit. The best fit parameters for dissociation constant (K_d), association constant (K_a), stoichiometry (N) and Chi^2 is listed.

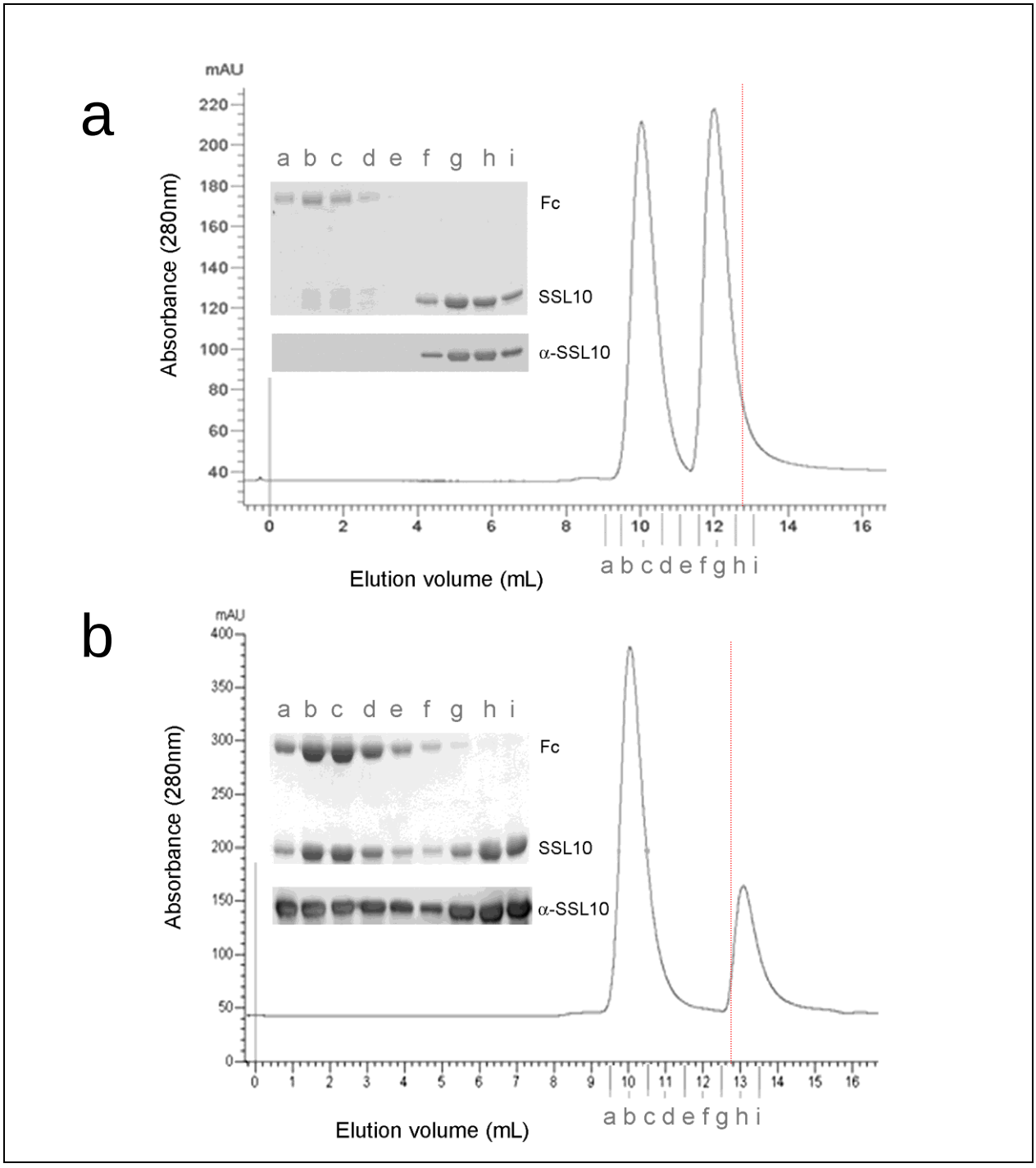

Figure: 5.5 Size exclusion profile of SSL10 and IgG1 Fc before and after PNGase F treatment.

Size exclusion chromatography elution profile of SSL10 mixed with (a) human IgG1 Fc (4:1) or (b) PNGase F-treated human IgG1 Fc (2:1). Fractions a-i were separated by 12.5 % non-reducing SDS-PAGE and analysed by western blot. The elution fractions on coomassie stained protein gel (top) and following transfer to nitrocellulose membrane for detection with biotinylated anti-SSL10 rabbit IgG and Streptavidin coupled to HRP (bottom). The dotted line indicates the expected elution volume (12.5 mL) of SSL10 alone. Premature elution of SSL10 (11.5 mL) indicates it binds to glycosylated IgG1 Fc but dissociates during migration down the column due to low affinity. SSL10 binds stronger upon removal of the IgG1 Fc carbohydrates, most likely due to alterations in the structure of the Fc domain.

Table 5.1: Summary of the kinetic properties of IgG binding proteins

Name	Ligand	Assay	Association constant (M^{-1})	Details
Bacterial proteins				
Protein A	Fc IgG1	SPR,ITC	10^7-10^8	Hydrophobic interactions (Jendeberg et al., 1995)
Protein G	IgG1	^{125}I binding assay	~10^9	Hydrophilic interactions, neutral pH (Akerstrom & Bjorck, 1986)
Sbi domain I	IgG1	SPR	$3.5x10^7$	(Atkins et al., 2008)
Sbi domain II	IgG1	SPR	$4.3x10^7$	(Atkins et al., 2008)
Sbi domain I	IgG2	SPR	$4x10^7$	(Atkins et al., 2008)
Sbi domain II	IgG2	SPR	$3x10^6$	(Atkins et al., 2008)
Sbi domain I	IgG4	SPR	$7.6x10^6$	(Atkins et al., 2008)
Sbi domain II	IgG4	SPR	$6.3x10^6$	(Atkins et al., 2008)
$SSL10_A$	Monoclonal IgG1	SPR	$1.08x10^6$	0.3 M NaCl, K_D=0.6 µM
$SSL10_B$	Monoclonal IgG1	SPR	$1.56x10^6$	0.3 M NaCl, K_D=0.9 µM
$SSL10_B$	Monoclonal IgG1	ITC	$3.1x10^6$	K_d=0.3 µM
$SSL10_B$	Serum IgG1	ITC	$5.5x10^6$	K_d=0.2 µM
$SSL10_B$	Fc	ITC	$8.5x10^5$	K_d=1.2 µM
Host proteins				
IgG1	FcγRI	Enzymatic assay	10^8-10^9	High affinity monomeric IgG receptor (Canfield & Morrison, 1991; Gessner et al., 1998)
IgG1	FcγRII	SPR	10^6-10^7	(Gessner et al., 1998; Maenaka, van der Merwe, Stuart, Jones, & Sondermann, 2001)
IgG1	FcγRIII	SPR	10^6-10^7	(Gessner et al., 1998; Maenaka et al., 2001)
C1q	IgG1	Competition assay	$5x10^4$	(Hughes-Jones, 1977)
C1q	Aggregated IgG1	competition assay	$0.5\text{-}2.5x10^8$	(Hughes-Jones, 1977)

5.2.6 Proteins precipitated from human and animal sera by SSL10

To determine if the specificity of SSL10 for IgG extends to other species, sera (25 µL) from various species was mixed with 5 µL SSL10 Sepharose or Protein A Sepharose. The sera were first pre-absorbed on $SSL10_{95-197}$ Sepharose to remove as many naturally occurring antibodies as possible. SSL10 bound strongly to IgG from human, chimpanzee (Appendix C.16), orangutan and macaque, and weakly to the more distantly related primate spider monkey (Fig. 5.6). SSL10 also bound strongly to IgG from baboon (Appendix C.15, data not shown). SSL10 did not show strong affinity for cow, sheep, mouse, rabbit, guinea pig or pig IgG. Amino acid alignment of the IgG subtypes highlights two potential residues, lysine K274 and leucine L358 that could dictate the specificity of SSL10 for IgG1 (Fig 5.7). Of these two residues only K274, on the upper Cγ2 domain, is unique to human, chimpanzee, baboon and macaque (Fig. 5.8).

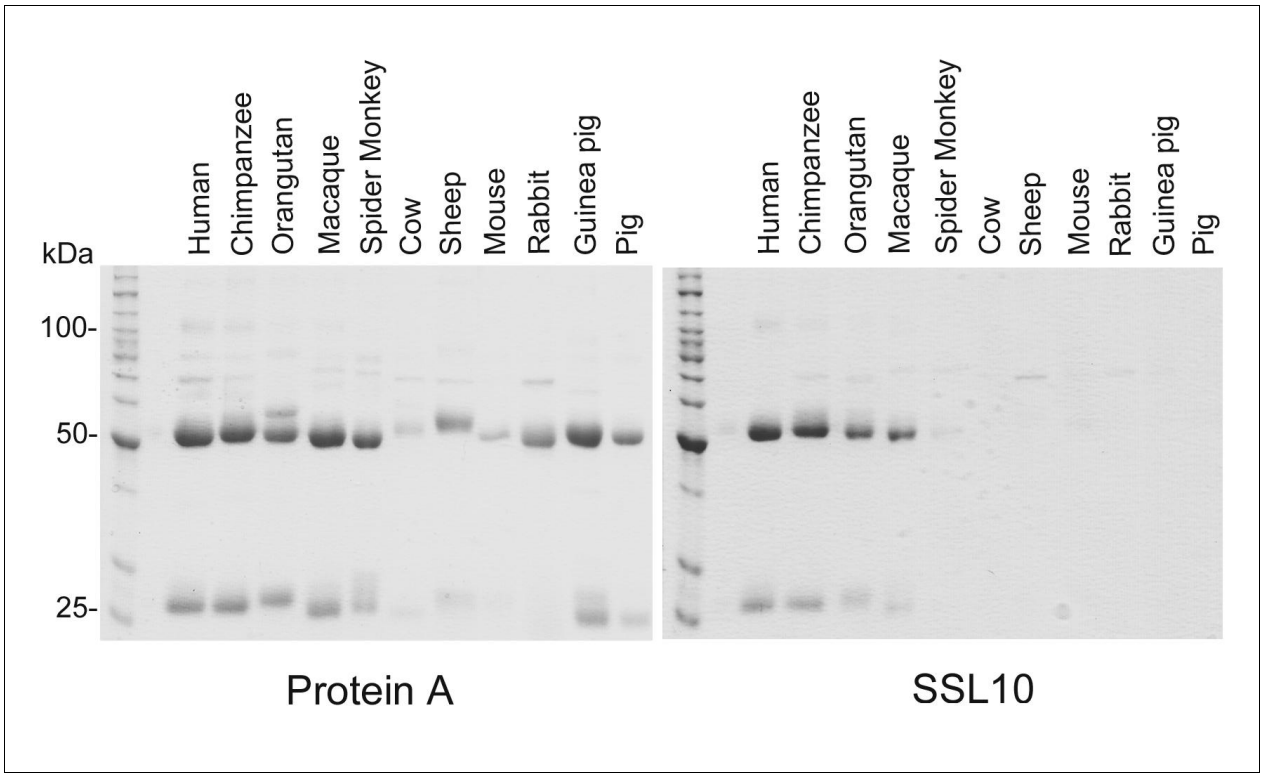

Figure 5.6: Affinity isolation of proteins from human and animal sera using Protein A or SSL10 Sepharose

Human and animal sera (25 µL) were preabosorbed on $SSL10_{95-197}$ Sepharose prior to incubating with 5 µL Protein A or SSL10 Sepharose for 1 h at 4 °C. Bound proteins were separated by 10 % reducing SDS-PAGE. IgG heavy chain migrates at 50 kDa and light chain migrates at 25 kDa. SSL10 migrates at approximately 27 kDa.

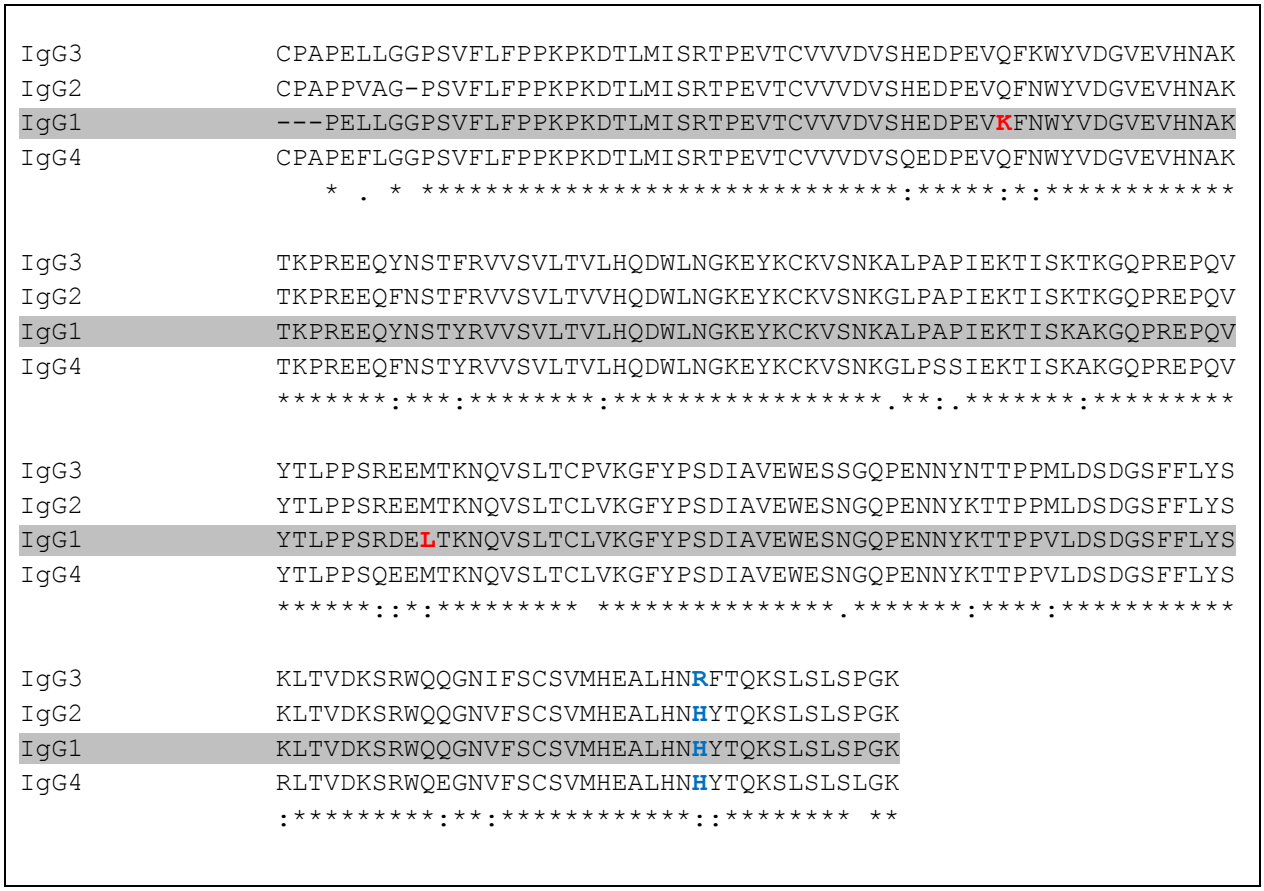

Figure 5.7: Amino acid alignment of the Fc domain of human IgG1-4.

Amino acid alignment of the Fc domain of human IgG1-4 (Accession number: CAC20454-57) using Clustal W. Residues unique to human IgG1, K274 and L358, are highlighted in red. The change in residue 434 from histidine to arginine is predicted to dictate the loss of Protein A affinity for IgG3.

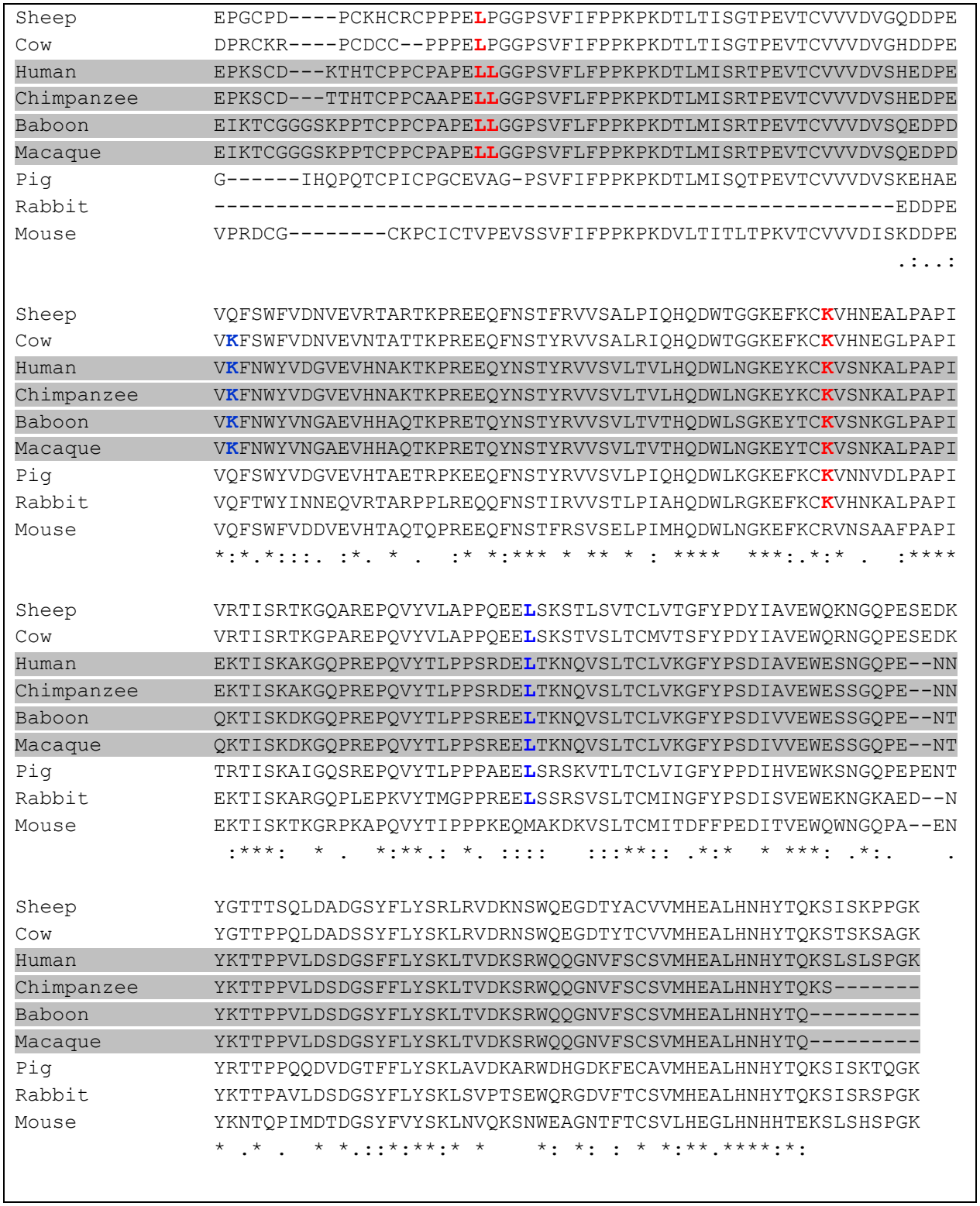

Figure 5.8: Amino acid alignment comparing Fc domain of IgG1 from different species.

Amino acid sequence alignment of the IgG1 Fc domain from human (Accession number: CAC204540), chimpanzee (PT0207), baboon (AAM93486), macaque (AAQ57555), sheep (CAA49451), cow (AB568619), pig, (I47158), rabbit (I46732) and mouse (BAC44885). SSL10 specifically binds to human IgG1 and primate IgG (shaded). Two residues unique to human IgG1 (blue) could contribute to the IgG1 subclass specificity. Mutation of L234.L235 and K322 (red) dramatically reduces SSL10 affinity (Dr BD Wines, Personal communications).

5.2.7 SSL10 inhibits IgG1 binding to the cell surface of monocytes

FcγRs are present on the surface of nearly all human leukocytes. Flow cytometry was utilised to determine whether the interaction of SSL10 with the Fc region of human IgG1 impacts on its ability to bind to cell surface FcγRI on monocytes. Increasing concentrations of unlabelled SSL10 or SSL7 (0 µg-100 µg) were incubated with fluorescein-labelled polyclonal human IgG1 or IgG3 (1 µg) prior to incubation with freshly isolated peripheral blood mononuclear cells ($5x10^5$ cells) (Fig. 5.9). Blood monocytes were specifically gated based on size and granularity and 10000 events were collected. SSL7 has strong specificity for IgA and as expected did not interfere with the binding of either IgG1-fluorescein or IgG3-fluorescein to the cell surface of monocytes. SSL10 also did not inhibit the binding of IgG3-fluorescein to the cell surface but displayed strong dose dependent inhibition of IgG1-fluorescein. This was also observed on neutrophils and a subset of lymphocytes (data not shown).

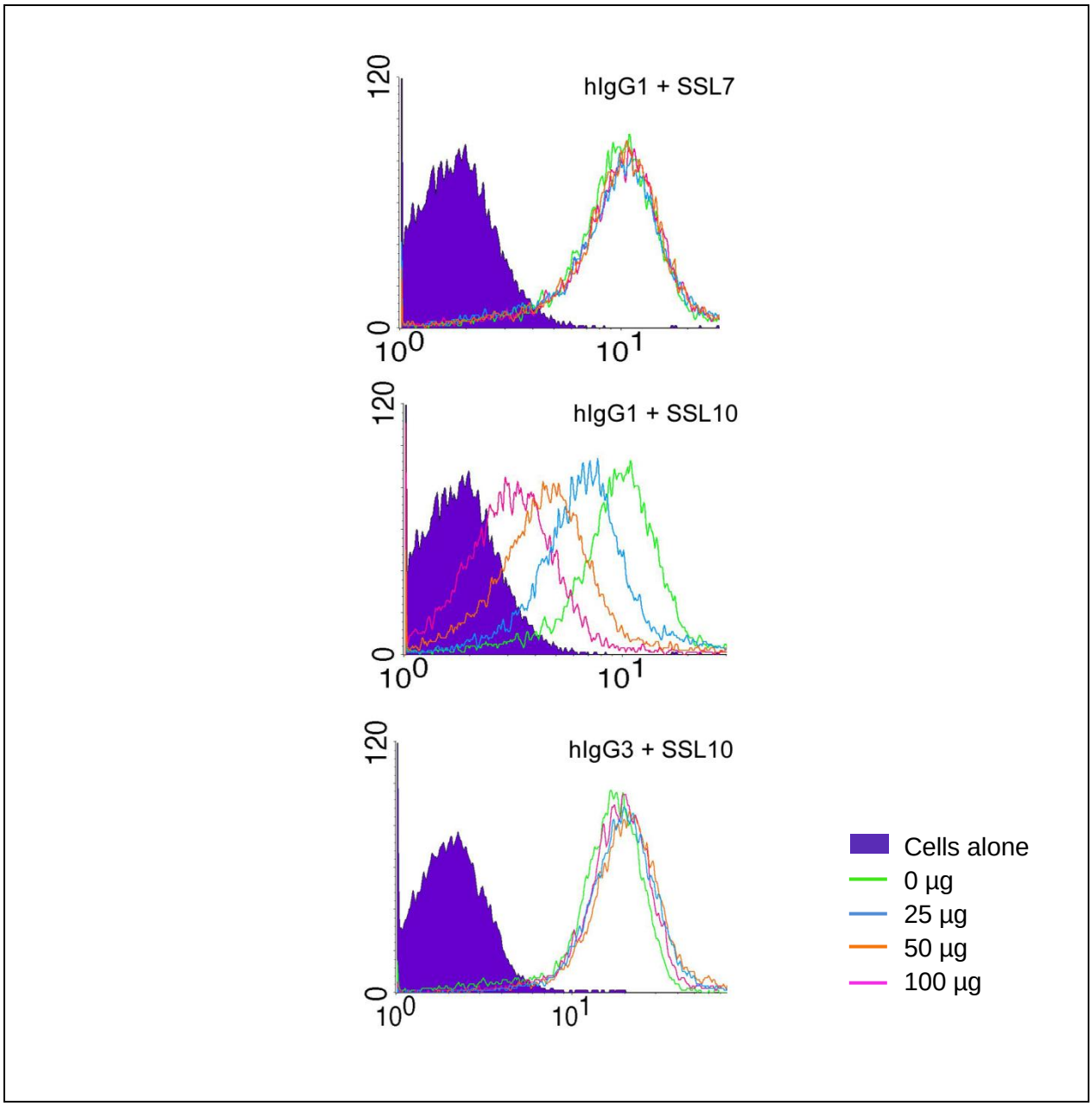

Figure 5.9: Competition of fluorescein-labelled human IgG1 or IgG3 with SSL10 or SSL7

IgG1 or IgG3 fluorescein (1 µg) was incubated with increasing concentrations of SSL10 or SSL7 (0-100 µg) for 10 min followed by PBMCs ($5x10^5$ cells). The percentage of fluorescent monocytes were detected using FACS. The monocyte population was gated based on size and granularity and 10000 events were collected. Data is a representative of at least three independent experiments using monocytes from different donors.

5.2.8 Phagocytosis of IgG-opsonised bacteria by human neutrophils

Phagocytosis of IgG-opsonised bacteria by human neutrophils was investigated using FACS. Heat-killed *S.pyogenes* (ATCC700294) or *S.aureus* (Wood46) were labelled with fluorescein and opsonised with human IgG in the presence of SSL10, SSL7 or Protein A. *S.pyogenes*-fluorescein was opsonised with affinity purified human IgG (50 µg/mL) against the major cell wall Spy0128 pilus protein. In contrast *S.aureus*-fluorescein was opsonised with SSL10-purified human IgG1 (150 µg/mL) from the pooled sera of patients with staphylococcal infections under the assumption that high titres of anti-staphylococcal antibodies are present. Phagocytosis by freshly purified human neutrophils was allowed to proceed for only 10 min to reduce the background observed through IgG independent uptake (Gu, Saunders, Jursik, & Wiley, 2010). The fluorescent extracellular bacteria were quenched with tryphan blue (Bjerknes & Bassoe, 1984) or lysed with lysostaphin, and the percentage of fluorescent neutrophils were measured by FACS. With appropriate IgG opsonisation, bacteria were rapidly phagocytosed by neutrophils (Fig. 5.10). However in the presence of a purified monoclonal human IgG1 (ARH-77) not directed at the bacterium (data not shown) or in the absence of the opsonising IgG, phagocytosis was not observed. Both Protein A and SSL10 inhibited phagocytosis of IgG-opsonised bacteria in a dose dependent manner, however Protein A displayed greater efficiency due to its multiple immunoglobulin binding domains (Fig. 5.11). In contrast, SSL7 did not interfere with IgG-mediated phagocytosis in either model.

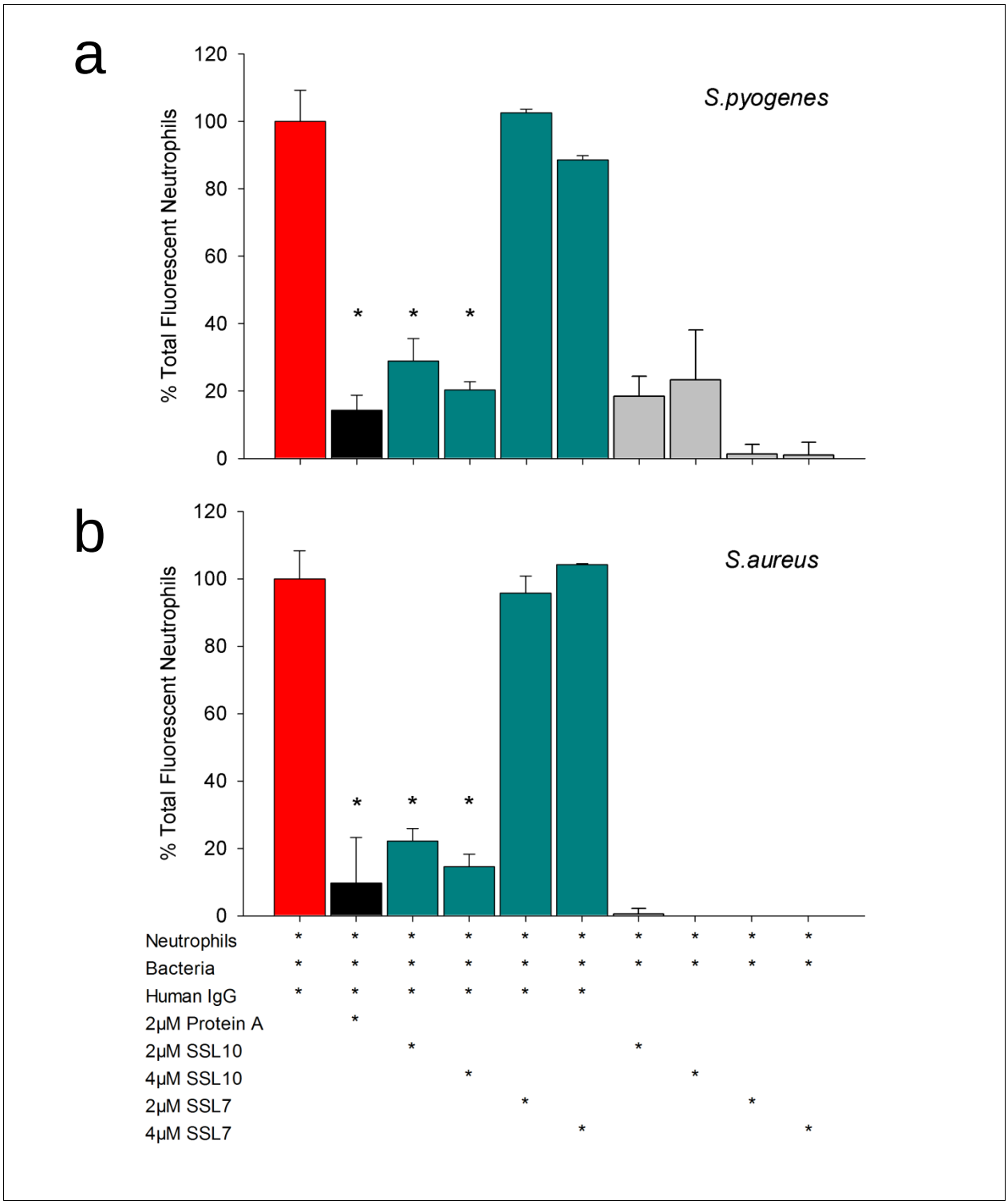

Figure 5.10: Phagocytosis of fluorescent *S.pyogenes* and *S.aureus* by human neutrophils.

Bar graph representing the percentage of total fluorescent neutrophils following uptake of (a) heat-killed fluorescent *S.pyogenes* (ATCC700294) opsonised with human anti-Spy0128 or (b) heat-killed fluorescent *S.aureus* (Wood 46) opsonised with human IgG1 from the sera of patients with *S.aureus* infection. SSL10, SSL7 or Protein A was included during opsonisation of bacteria. Neutrophils were analysed by FACS and 10000 events were collected. (n=2 *p<0.05, statistical significance as determined by Student's t test).

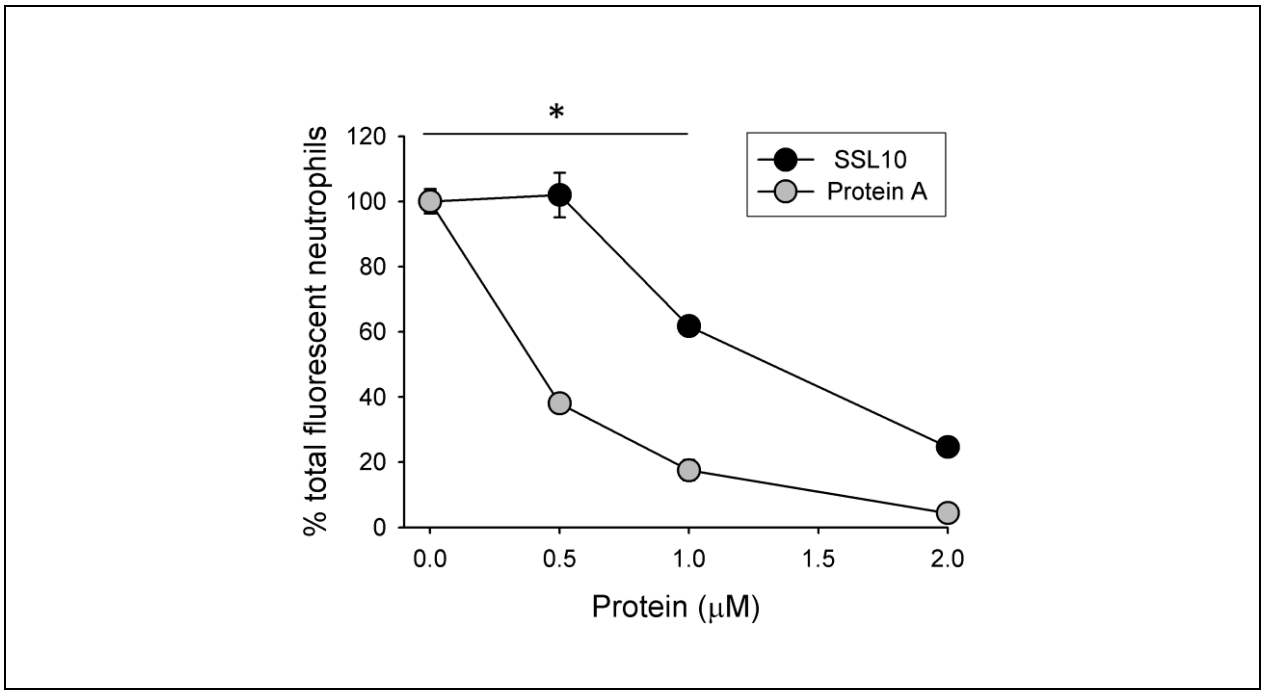

Figure 5.11: Phagocytosis of IgG-opsonised *S.pyogenes* by human neutrophils in the presence of SSL10 and Protein A.

FACS measuring the percentage of total fluorescent neutrophils following uptake of IgG-opsonised fluorescent *S.pyogenes* in the presence of 0-2 μM SSL10 or Protein A. 10000 events were collected (n=4, *p<0.002, statistical significance as determined by Student's t test)

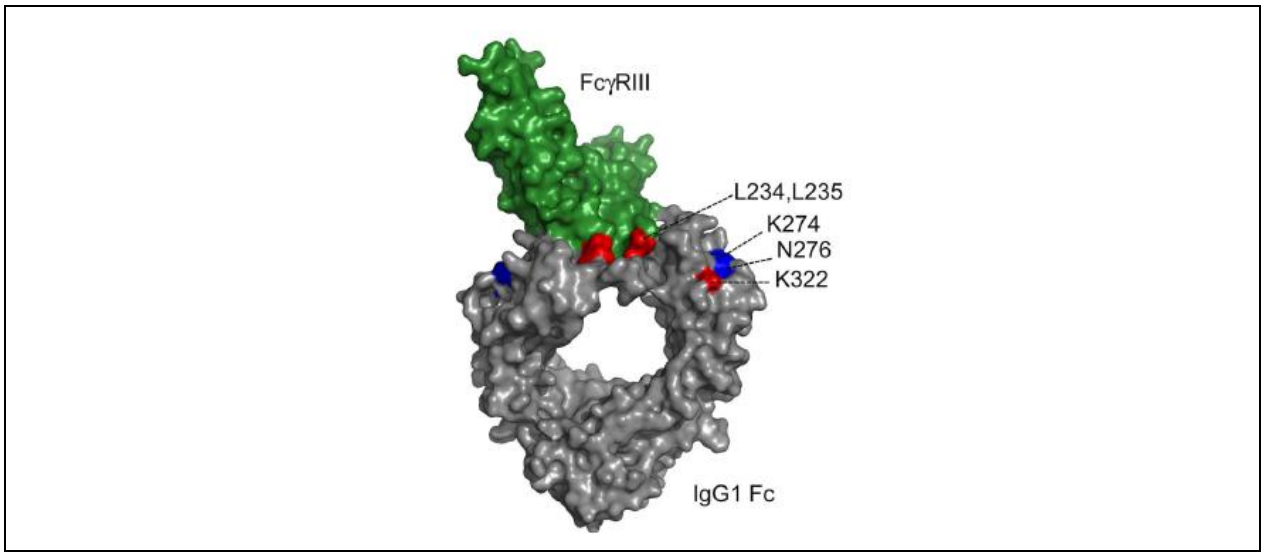

Figure 5.12: Crystal structure of FcγRIII binding to human IgG1 Fc domain

FcγRIII binds to the lower hinge and upper Cγ2 domain of human IgG1 Fc and structurally dislocates the Cγ2 domain with respect to the Cγ3 domain (PDB file 1EK4). Mutation of L234.L235 and K322 significantly reduces SSL10 binding (Dr BD Wines, Burnett Institute, Australia, Personal communications). Adjacent to K322 is the K274 residue unique to the IgG1 Fc domain.

5.3 Discussion

SSL10 binds to the Fc domain of human IgG1, the major systemic immunoglobulin and primary γ-subclass responder against protein antigens and bacterial polysaccharides (Barrett & Ayoub, 1986; R Jefferis & Kumararatne, 1990). The IgG Fc domain is a key ligand for several host proteins including complement C1q (Hughes-Jones, 1977), the neonatal Fc receptor (Burmeister et al., 1994; B. Wines et al., 2000) and multiple FcγRs (Gessner et al., 1998). Of the four subclasses of human IgG, the γ1 subclass is the predominant form, displaying strong affinity for several FcγRs (Canfield & Morrison, 1991; Gessner et al., 1998; Maenaka et al., 2001) and highly efficient complement activation (Bruggemann et al., 1987). All individuals have antibodies against S.*aureus* (Dryla et al., 2005) and indeed administration of neutralising antibodies against staphylococcal toxins forms an effective treatment (Takei, Arora, & Walker, 1993). However, this adaptive response only governs part of the protective effects of Igs. The crucial importance of the Fc domain is clearly demonstrated in macaques where neutralizing antibodies engineered to be defective in FcγR and complement binding activities were dramatically reduced in their ability to effectively and efficiently clear HIV (Hessell et al., 2007). It is thus not surprising that numerous bacterial proteins also target the IgG Fc domain including Staphylococcal Protein A (Deisenhofer, 1981) and Sbi (Atkins et al., 2008), and Streptococcal Protein G (Akerstrom & Bjorck, 1986; Sauer-Eriksson, Kleywegt, Uhlen, & Jones, 1995) and Protein M (Lewis, Meehan, Owen, & Woof, 2008).

The affinity of SSL10 for IgG extends across primate species. IgG from human, baboon, chimpanzee, orangutan and macaque were all bound strongly by SSL10. IgG from spider monkey was also bound by SSL10 but to a weaker degree. In comparison the IgG from rabbit, mouse, pig, guinea pig and cow lacked the same robust binding observed with the IgG from primate species reflecting the strict specificity of SSL10. This is in strong contrast to the other Ig binding proteins of *S.aureus*, including Protein A, Sbi and SSL7 that interact with Igs across a wide range of mammalian species through the CH2-CH3 interface. Interestingly, SSL10 from the bovine *S.aureus* isolate RF122 is considerably different in its primary sequence, which could reflect an adaptation to the host and potentially variations in its IgG binding profile to include bovine IgG.

The interaction of SSL10 with the Fcγ1 domain inhibits IgG1 binding to the cell surface of myeloid cells, most likely by interfering with its ability to bind FcγRs. The dramatic functional consequence is evident in the failure of neutrophils to effectively phagocytose IgG1-opsonised bacteria in the presence of SSL10. The FcγRIII binding site on human IgG1 Fc has been mapped to a single site on the lower hinge region adjacent to the upper Cγ2 domain; a common model for all the FcγR subtypes (R Jefferis & Lund, 2002). Both Protein A and Protein G also inhibit FcγR activity despite clear evidence from their respective crystal structures that their binding sites are distinctly different to that of FcγRIII. Interestingly upon FcγRIII binding the Cγ2 domain undergoes a dramatic dislocation with respect to the Cγ3 domain (Sondermann et al., 2000). It is proposed that receptors that bind at the Cγ2-Cγ3 interface such as Protein A, stabilize the Cγ2-Cγ3 elbow and prevent FcγR binding; an allosteric mechanism also of

potential physiological significance in the activation of different host receptors such as FcnR (Sondermann et al., 2000). Alternatively interaction of these bacterial proteins with multiple IgG molecules simultaneously, indirectly prevents access of the FcγRs.

SSL10 predominantly utilises residues on its N-terminal OB-fold domain to interact with a single site on human IgG1 with high nanomolar affinity (K_D = 250 nM). This correlates well with its ability to compete with low affinity FcγRs for antigen bound IgG1 (K_D = 100-1000 nM) and also explains the large excess of SSL10 to IgG1 required for competition with high affinity FcγRI on monocytes (K_D = 1-10 nM). Interestingly, the thermodynamic data suggests SSL10 forms a 1:1 stoichiometry interaction with human IgG1 at 25 °C in PBS pH 7.4. A recent study conducted by Dr BD Wines (Burnett Institute, Australia) using human IgG1 mutants, localized the binding site of SSL10 to the upper Cγ2 domain and lower hinge region, in close proximity to the FcγR (Roy Jefferis et al., 1998; Shields et al., 2001) and C1q binding sites (Idusogie et al., 2000). Sequence comparison of the different IgG subclasses revealed two distinct residues on the Fc domain that could contribute to the specificity of SSL10 for IgG1; of these only lysine K274 is located specifically in the upper Cγ2 region of Fcγ1 from human and primate species. SSL10 binding to the upper Cγ2 domain in close proximity to the hinge region and axis of symmetry could produce an allosteric effect or conformational change that renders the other site non-functional, thereby preventing another SSL10 molecule from binding; in a similar manner to that of FcγRIII (R Jefferis & Lund, 2002).

An intriguing aspect of host effector functions is the role of IgG Fc glycosylation. The central cavity between the Cγ2 domains is filled with carbohydrates that stem from asparagine 297 and stabilize the IgG Fc domain in an open conformation that promotes FcγR and complement C1 binding (Krapp et al., 2003). The glycosylation profile changes in response to physiological and pathological circumstances such as age and disease state, without altering the overall conformation of the Fc domain (Wuhrer et al., 2007). Upon cleavage of this central carbohydrate bridge, the Cγ2 domains converge to form a closed conformation. The Cγ3 domain remains relatively rigid thus does not alter Protein A binding at the Cγ2-Cγ3 interface, whereas the Cγ2 domain varies dramatically in the hinge proximal region thus is no longer able to support the binding of host receptors (Roy Jefferis et al., 1998; Krapp et al., 2003; Prabakaran et al., 2008; Yamaguchi et al., 2006). This is in strong contrast to SSL10, which binds with notably higher affinity to deglycosylated IgG1 Fc. IgG1 binding to an antigen could induce a similar conformational change in the lower hinge and upper CH2 domain that allows SSL10 to bind with higher affinity or induce a localised structural change itself upon binding that inhibits FcγR and potentially C1 binding.

SSL10 is a unique new addition to the *S.aureus* IgG binding family. Its tight regulatory control coupled with a strict specificity for human and non-human primate IgG1 sets it apart from the other IgG binding proteins. Unlike many bacterial IgG binding proteins SSL10 binds to a single site on each Fcγ1 in close proximity to the upper Cγ2 domain (Dr BD Wines, Burnett Institute, Australia, Personal communications). The cell surface anchored Protein A and secreted Sbi display affinity for a wider

repertoire of IgG subclasses and species (Atkins et al., 2008). Both proteins target the Cγ2-Cγ3 interface, which is a common feature shared by many Ig binding proteins from various bacterial species (Lewis et al., 2008). The specificity of SSL10 for Fcγ1 further highlights the importance of IgG1-mediated immunity in the recognition and clearance of *S.aureus*.

Chapter 6
Complement and SSL10

6.1 Introduction

The complement system is an intricate immune surveillance system. It has evolved in higher organisms from a basic two factor system to an elaborate cascade linking multiple recognition mechanisms and effector functions (Dodds, 2002). Over recent years novel functions have been discovered, clearly demonstrating a wider role for complement in homeostasis, development and immunity (Markiewski et al., 2007; Prodeus et al., 1998; Rutkowski et al., 2010). The complement system forms complex interactions with the coagulation system, enhancing platelet activation, tissue factor expression and procoagulant modification of the endothelium (Hamilton, Hattori, Esmon, & Sims, 1990; Sims & Wiedmer, 1991; Tedesco et al., 1997). Complement has also been implicated in the proliferation and regeneration of damaged tissues throughout the body (Rutkowski et al., 2010; Strey et al., 2003). Its importance is clearly highlighted, with defective activation, execution or consumption of complement being linked to recurrent staphylococcal infections and severe diseases such as systemic lupus erythematosus (M. B. Fischer et al., 1996; P. Morgan & Walport, 1991; Prodeus et al., 1998).

SSL7, a close homologue of SSL10, binds to complement C5 and inhibits C5a production and bactericidal activity through endpoint MAC formation (Langley et al., 2005; Laursen et al., 2010). SSL7 also simultaneously binds to human IgA and inhibits FcαR activity (B. D. Wines et al., 2006). Given the shared immunoglobulin-binding property of SSL7 and SSL10, the functional impact of SSL10 on the complement cascade was investigated. This chapter describes the interaction of SSL10 with the complement system and its potential targets for interference.

6.2 Results

6.2.1 Inhibition of complement pathways by SSL10

The impact of SSL10 on the three individual pathways of the human complement system was measured using a Wielisa Total Complement System Screen (Wieslab, Sweden) (Seelen et al., 2005) (Fig. 6.1). This ELISA based assay utilizes IgM for activation of the classical pathway, mannan for activation of the MBL pathway and LPS for activation of the alternative pathway. End-point MAC formation through each pathway was quantitated using a monoclonal antibody against a unique neoepitope on the C5b-9 complex. For the purpose of this assay, the supplied control serum pooled from several human donors was used as the source of complement to avoid donor differences and ensure standard complement activation. Both SSL10 and its β-grasp domain $SSL10_{95\text{-}197}$ (0-2 µM) specifically inhibited the classical and MBL pathways with no substantial effects on the alternative pathway. Notably, its effects on the MBL pathway were more prominent compared to the classical pathway. However, SSL10 had greater inhibitory effects on the classical pathway following preincubation with serum; reducing end point MAC formation by approximately 70 % in the presence of 1 µM SSL10 (Dr N Jackson, University of Auckland, NZ, Personal communications,).

To determine if these effects were carbohydrate mediated, SSL10 was sent to the Consortium for Functional Glycomics (Core H, USA). SSL10 was tested on a glycan array comprising of over 406 unique samples (Version 3.2); however it did not display significant affinity for any of the glycans including those containing mannose (<400 relative fluorescence units, data not shown). Given the classical pathway in this assay is activated by IgM and both the classical and MBL pathways are inhibited by predominant interactions through the SSL10 β-grasp domain, it is highly likely SSL10 has a specific target in the complement cascade that is separate from its IgG1 binding property.

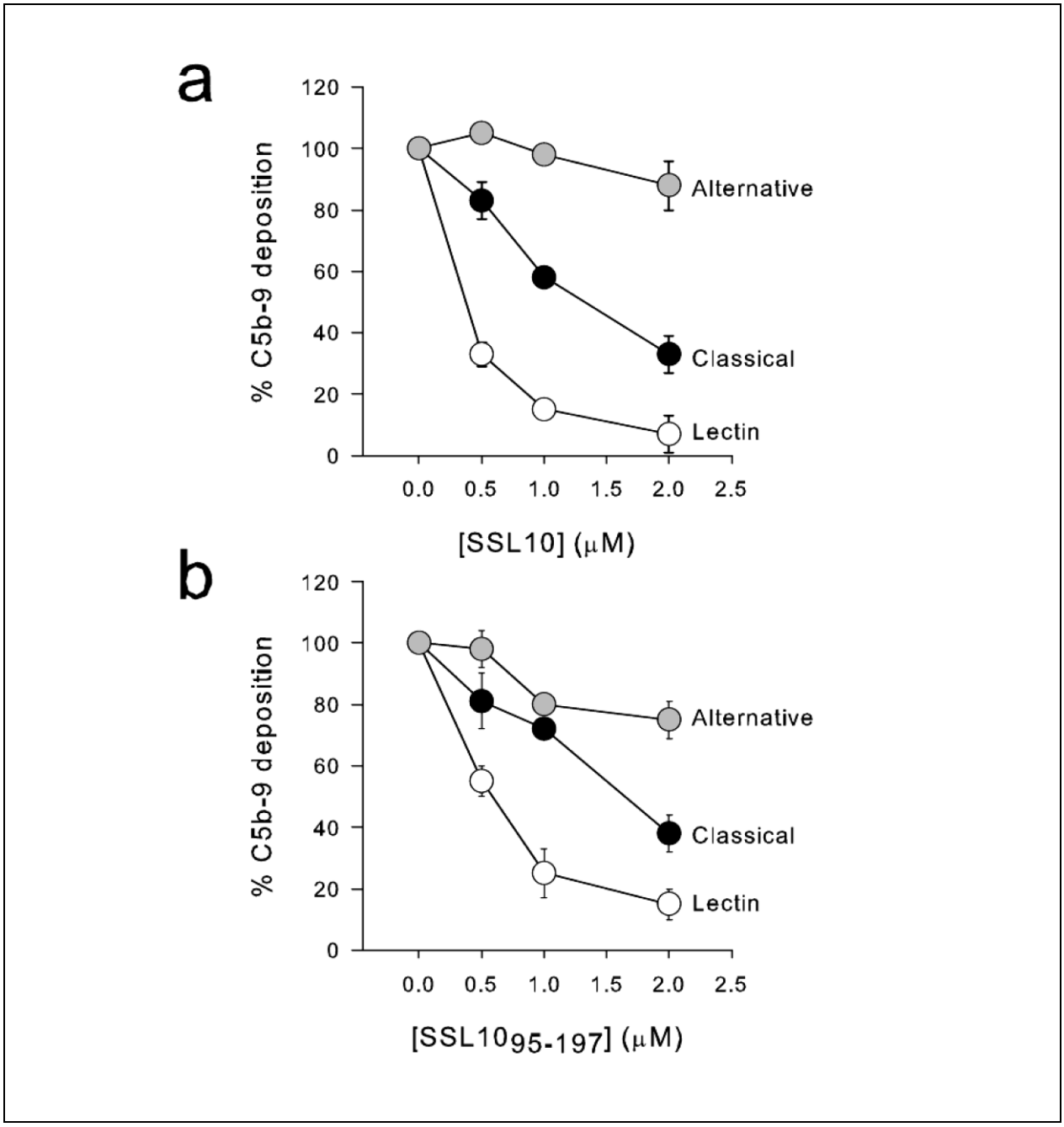

Figure 6.1: Impact of SSL10 and SSL10$_{95-197}$ on endpoint MAC formation through the classical, alternative and lectin pathway of the human complement cascade.

A Weislab ELISA total complement screen was used to measure the activity of the alternative, classical and lectin (MBL) pathways of the human complement system in the presence of a) SSL10 and b) SSL10$_{95-197}$. LPS was utilized for activation of the alternative pathway, IgM for the classical pathway and mannan for the MBL pathway. The percentage of total C5b-9 deposition was detected using an antibody against a neoepitope on C5b-9 (n=3).

6.2.2 SSL10 inhibits the hemolysis of RBC by complement

Complement inhibition by SSL10 was confirmed using a traditional hemolytic assay that measures the lysis of red blood cells as an indicator of complement activity. Total complement activation predominately through the classical pathway was measured using guinea pig serum as a rich source of complement to lyse Ig-opsonised sheep red blood cells. The serum was diluted to 0.33 % in buffer containing calcium and magnesium, which are essential for the cleavage of C4 (Valet & Cooper, 1974) and formation of the C3 convertase (Fishelson et al., 1983) respectively. In contrast, for the alternative pathway 25 % human serum was used to lyse heterologous human RBC (Langley et al., 2005) in the presence of EGTA, which chelates calcium and blocks the classical and lectin pathways (Fine, Marney, Colley, Sergent, & Des Prez, 1972). SSL7, a potent inhibitor of total complement activity, was used as a control. It efficiently blocked hemolysis through the alternative pathway but displayed weak inhibition in the total complement assay due to weaker affinity for guinea pig C5 (Appendix E). In contrast, SSL10 and $SSL10_{95\text{-}197}$ blocked hemolysis in the total complement assay but not in the alternative pathway assay (Fig. 6.2). This supports the Wieslab ELISA data where complement inhibition by SSL10 was independent of the alternative pathway (Fig. 6.1). Notably a two-fold greater concentration of SSL10 was required for the inhibition of guinea pig complement (Fig. 6.2a) compared with human complement (Fig. 6.1) reflecting potential species specificity in its target or mechanism of inhibition.

6.2.3 SSL10 inhibits C3b deposition

All three complement pathways converge at the formation of C3b and progress through the common terminal cascade. To confirm SSL10 targets a specific stage in the human complement cascade prior to C3b deposition, an ELISA based assay was performed using human serum and immobilised heat-aggregated polyclonal human IgG1 or IgG3 (Fig. 6.3). Complement activation was detected using an antibody against the C3c domain of activated C3b (Janssen, Christodoulidou, McCarthy, Lambris, & Gros, 2006). C3b is stable for several hours thus forms an ideal target for detection. SSL10 displays comparable inhibition of C3b deposition following complement activation with human IgG1 and IgG3. In contrast SSL7, which targets C5 on the terminal complement cascade, does not interfere with C3b formation.

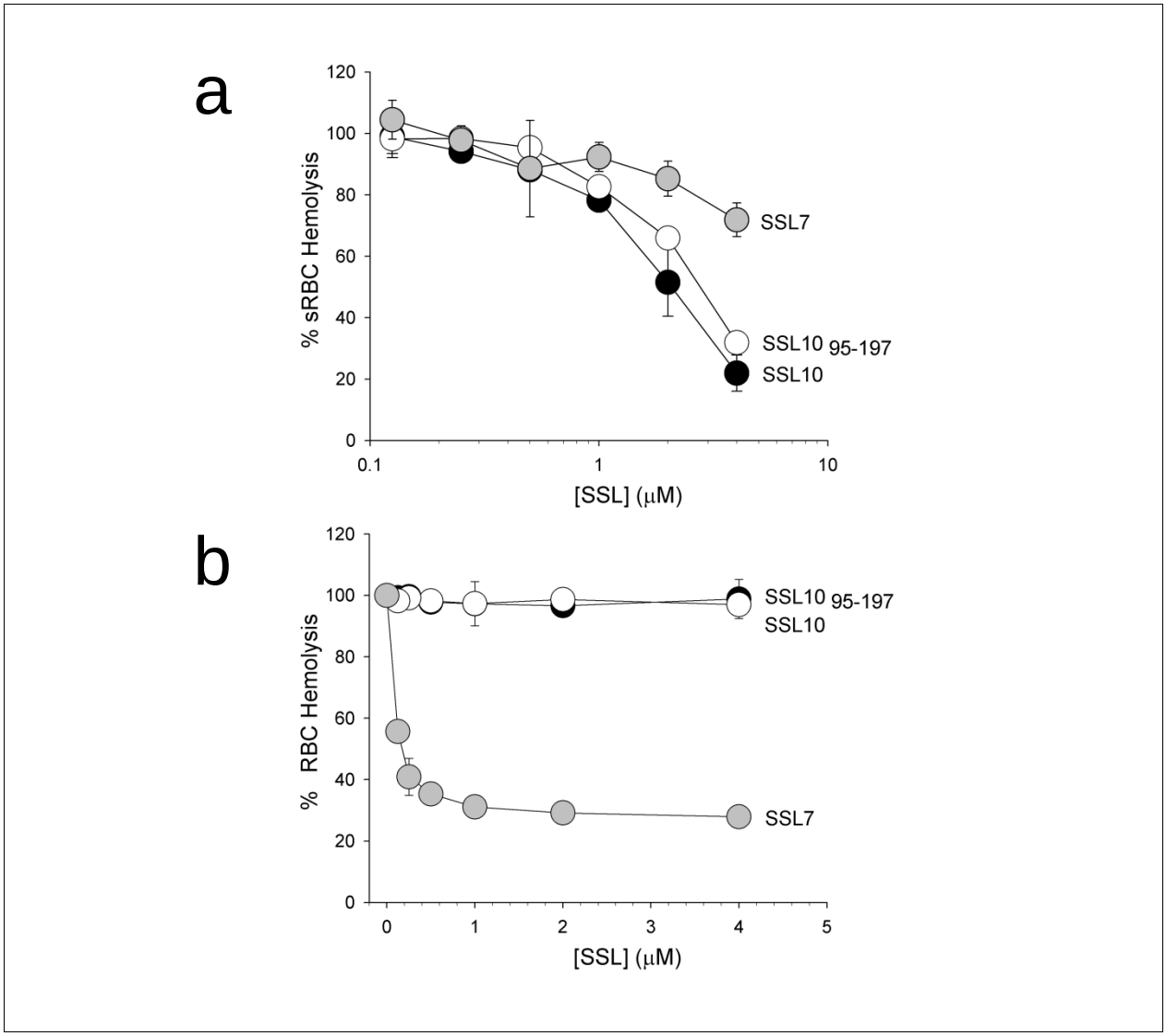

Figure 6.2: Complement-mediated hemolysis of RBC in the presence of SSL10, $SSL10_{95-197}$ and SSL7.

The impact of SSL10, $SSL10_{95-197}$ and SSL7 on a) total complement activity measured through the hemolysis of Ig-opsonised sheep RBC by guinea pig complement and b) alternative pathway complement activity measured through the hemolysis of human RBC and heterologous serum in the presence of $MgCl_2$ and EGTA (n=2).

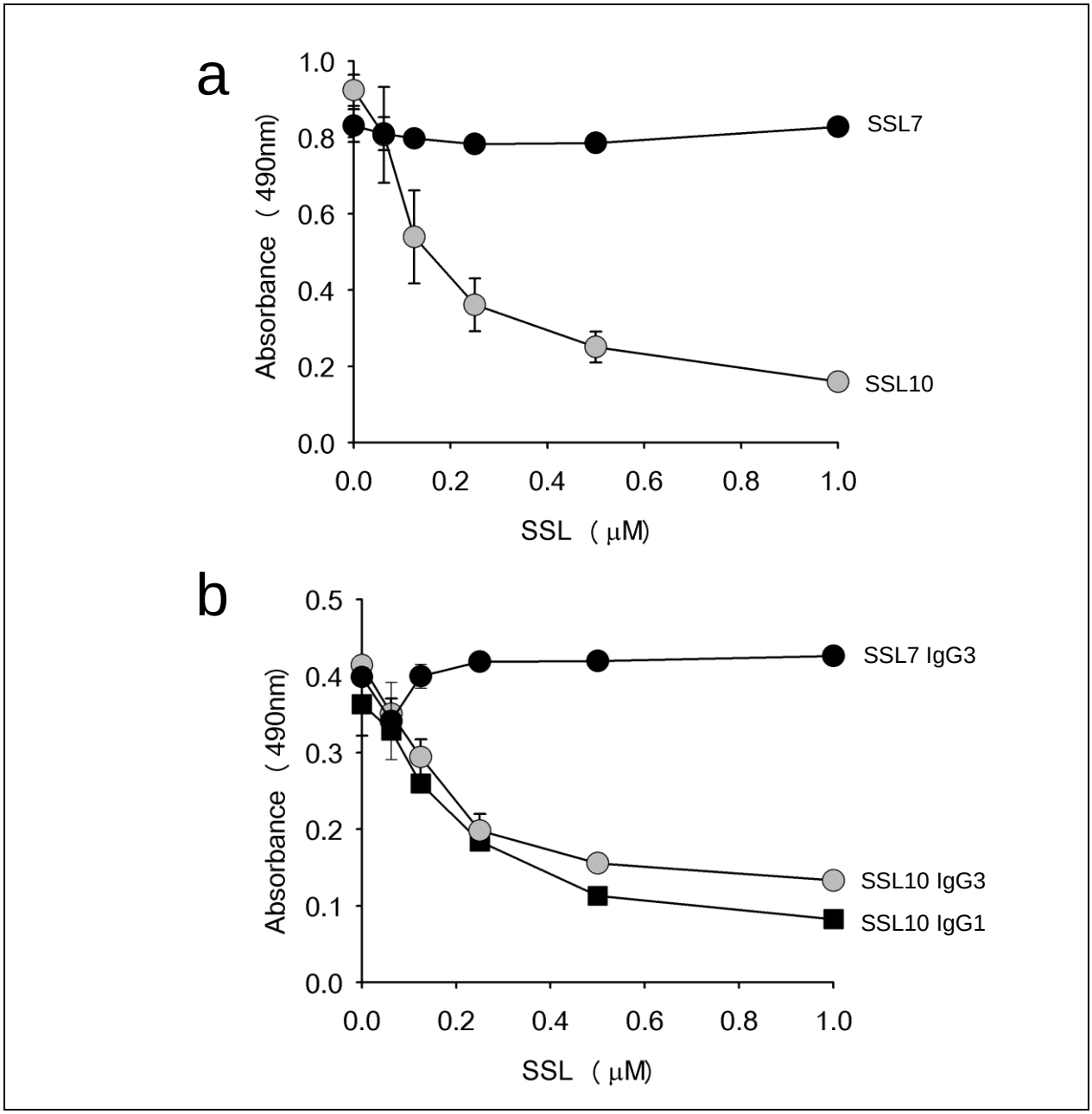

Figure 6.3: ELISA analysis of C3b deposition following IgG1 or IgG3-mediated complement activation.

a) Immobilised heat aggregated human IgG1 (25 µg/mL) incubated with 2.5 % human serum and SSL10 or SSL7 in the presence of CaCl and MgCl. b) Comparison of SSL10 mediated complement inhibition following activation with heat-aggregated IgG1 or IgG3 (25 µg/mL). C3b deposition was detected using a monoclonal antibody against C3c (n=2).

6.2.4 SSL10 affinity purifies complement C4 from human serum

The classical and MBL lectin pathways converge at the cleavage of complement factors C4 and C2, and subsequent formation of the C3 convertase, C4b2a. To investigate if SSL10 displays affinity for either of these factors Western blot analysis was performed on proteins affinity purified from human serum at 4 °C (Fig. 6.4). Fresh human serum (10%) was incubated with Sepharose alone or Sepharose coupled to SSL10, $SSL10_{95\text{-}197}$, SSL7, SSL11 or Protein A (10 µL of 1:1 suspension). The affinity purified proteins were separated by reducing SDS-PAGE and blotted onto nitrocellulose membrane. To eliminate natural deposition of complement proteins through complement activation, freshly collected human serum was immediately incubated with 10 mM EDTA prior to affinity purification studies. In addition to C2 and C4, the membranes were also probed with antibodies against complement C5 as a control from the terminal cascade that is common to all three complement pathways.

In the presence of EDTA, C2, C4 or C5 were not detected on Sepharose alone (Fig. 6.4 lane 1) excluding any indirect interactions from the Sepharose beads. As expected, C5 was purified by SSL7 Sepharose (Fig. 6.4 lane 4; 120kDa α-chain and 70kDa β-chain). C4 (93kDa α-chain and 70kDa β-chain; the predominant chains detected by anti-C4) and C2 (93kDa) contain complex biantennary glycans with varying degrees of sialyation (Gigli, von Zabern, & Porter, 1977; Ritchie et al., 2002) thus were both affinity purified by the sialic acid binding protein SSL11 (Fig. 6.4 lane 6) (Chung et al., 2007). In addition, SSL11 did not affinity purify either of these proteins following removal of the carbohydrates in PNGase F-treated serum (Fig. 6.5). Protein A, an IgG binding protein was also included as a control to exclude any effects arising from clustered IgG. Protein A did not bind C2, C4 or C5 (Fig. 6.4 lane 5) whereas SSL10 (Fig. 6.4 lane 2) and $SSL10_{95\text{-}197}$ (Fig 6.4 lane 3) specifically bound to C4 (93kDa α-chain and 70kDa β-chain). In the absence of EDTA, activated C4 covalently bound to IgG (Campbell, Dodds, & Porter, 1980). This was evident from the high molecular weight bands specifically purified by the IgG binding proteins SSL10 (Fig. 6.4 lane 2) and Protein A (Fig. 6.4 lane 5). This band was absent in the presence of EDTA confirming SSL10 forms specific interactions with C4 in the absence of complement activation.

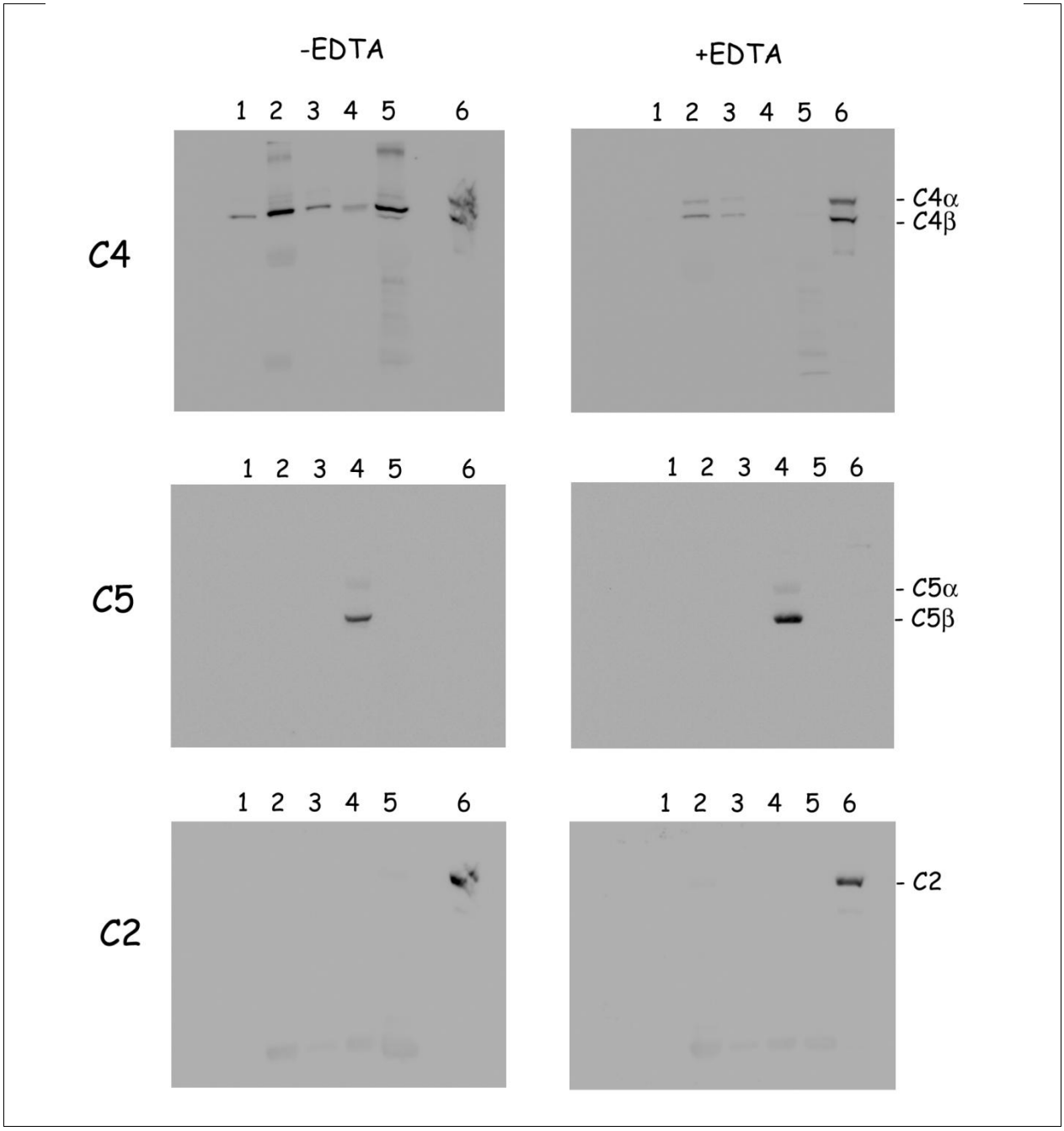

Figure 6.4: Western blot of complement C2, C4 and C5 affinity purified from human serum.

Sepharose alone (1) or SSL10 (2), $SSL10_{95-197}$ (3), SSL7 (4), Protein A (5) and SSL11 (6) coupled to Sepharose were incubated with fresh human serum with or without 10 mM EDTA for 1 h at 4 °C. Bound proteins were separated by reducing SDS-PAGE and transferred to nitrocellulose membrane. Complement C4, C2 and C5 were detected using goat anti-C4 (1:10000), goat anti-C2 (1:10000) or rabbit anti-C5 (1:5000) IgG respectively. Primary antibodies were detected with secondary antibodies coupled to HRP against goat (1:15000) or rabbit (1:2500) IgG. The membranes were stripped and reprobed between each detection antibody.

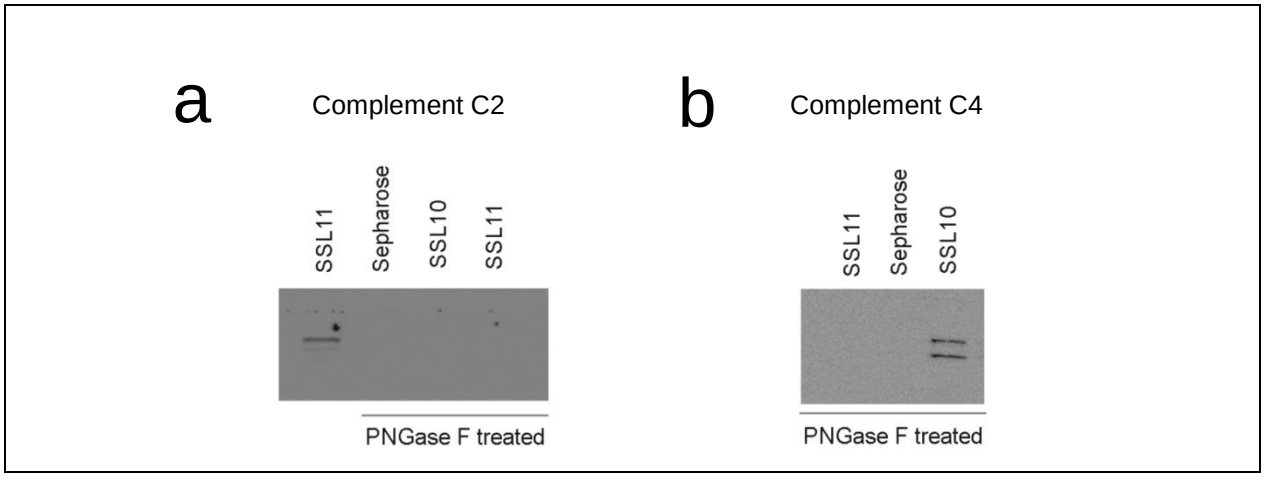

Figure 6.5: Western blot of proteins isolated from PNGase F-treated serum by SSL10 and SSL11. Serum was treated with PNGase F (50 U / µL serum) for 1 h at 37 °C in the absence of detergent. SSL10 or SSL11 coupled to Sepharose and Sepharose alone was incubated with PNGase F treated serum (10 %) for 1 h at 4 °C. SSL11 was also incubated with untreated sera as a positive control. The bound proteins were transferred to nitrocellulose membrane and detected with goat anti-C4 or anti-C2 IgG (1:10000) and anti-goat IgG coupled to HRP (1:15000).

6.2.4 SSL10 directly binds to complement C4 and C4b

To investigate the interaction of SSL10 and C4 further, direct binding experiments were performed using ELISA. The binding of purified human C2, C4, C4a and C4b (0-50 nM) to immobilized SSL10, $SSL10_{95-197}$, SSL7 and SSL11 (1 µM) was measured (Fig. 6.6). As expected, SSL7 did not bind to any of the complement factors tested. SSL10 and to a weaker extent $SSL10_{95-197}$ displayed specific binding to C4 but not C2. Analysis of the cleaved components of C4 (Fig. 6.6), C4a and C4b, identified C4b as the primary binding target of SSL10 although its binding was weaker compared to the complete C4 molecule. Only background binding to C4a was detected with both SSL10 and $SSL10_{95-197}$. As noted in the coprecipitation studies, SSL11 bound to C4 and C2 through carbohydrate mediated interactions (Fig. 6.4, 6.5). Interestingly SSL11 also bound to the non-glycosylated C4a fragment (Moon et al., 1981) by ELISA displaying a potentially unique function independent of its carbohydrate binding property (Fig. 6.6). C4a is not only an anaphylatoxin but also a potent antimicrobial peptide (Klickstein, Barbashov, Liu, Jack, & Nicholson-Weller, 1997; van den Elsen et al., 2002). Only background binding of the primary and secondary antibodies to the SSLs and the plate surface was detected in each experiment verifying direct protein-protein interactions.

Comparatively, SSL10 bound to C4 and C4b with weaker affinity compared to SSL11. Complement C4 purified from human serum is a combination of two isotypes C4A and C4B (Table 6.1). Any differential specificity of SSL10 for either isotype could also account for the reduced binding. Alternatively, immobilisation of the 24 kDa SSL10 protein could influence its binding to the larger 200 kDa C4 protein.

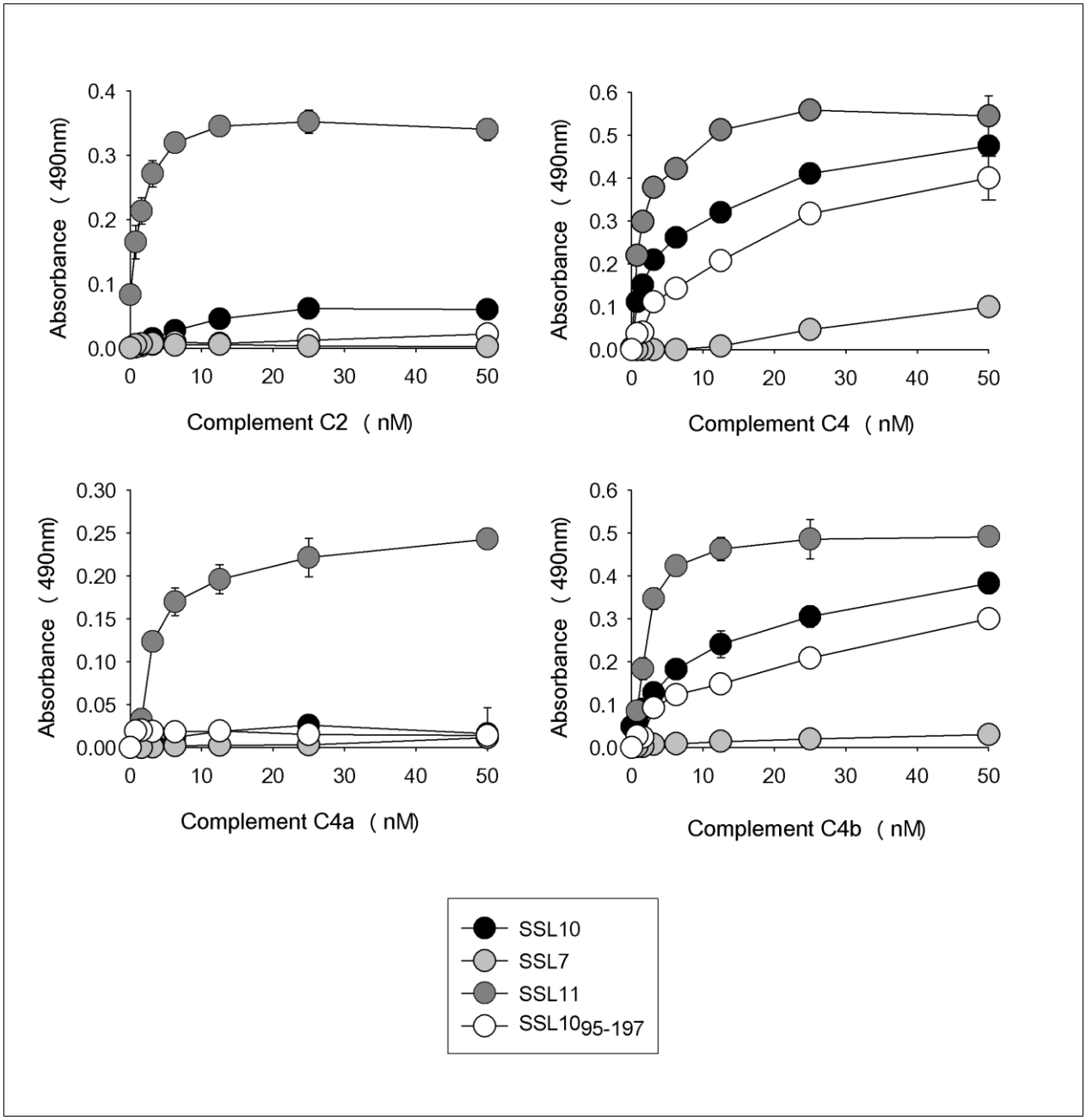

Figure 6.6: Direct interaction of complement C2, C4, C4a and C4b with SSL10, SSL10$_{95-197}$, SSL11 or SSL7 by ELISA.

SSL10, SSL10$_{95-197}$, SSL7 or SSL11 (1 µM) were immobilised on Maxisorp plates and incubated with increasing concentrations of purified complement C2, C4, C4a or C4b (0-50 nM). Bound proteins were specifically detected with goat polyclonal anti-C2 or anti-C4 IgG (1:10000). Primary antibodies were detected with anti-goat IgG coupled to HRP (1:15000). Data is a representative of two independent experiments (n=2).

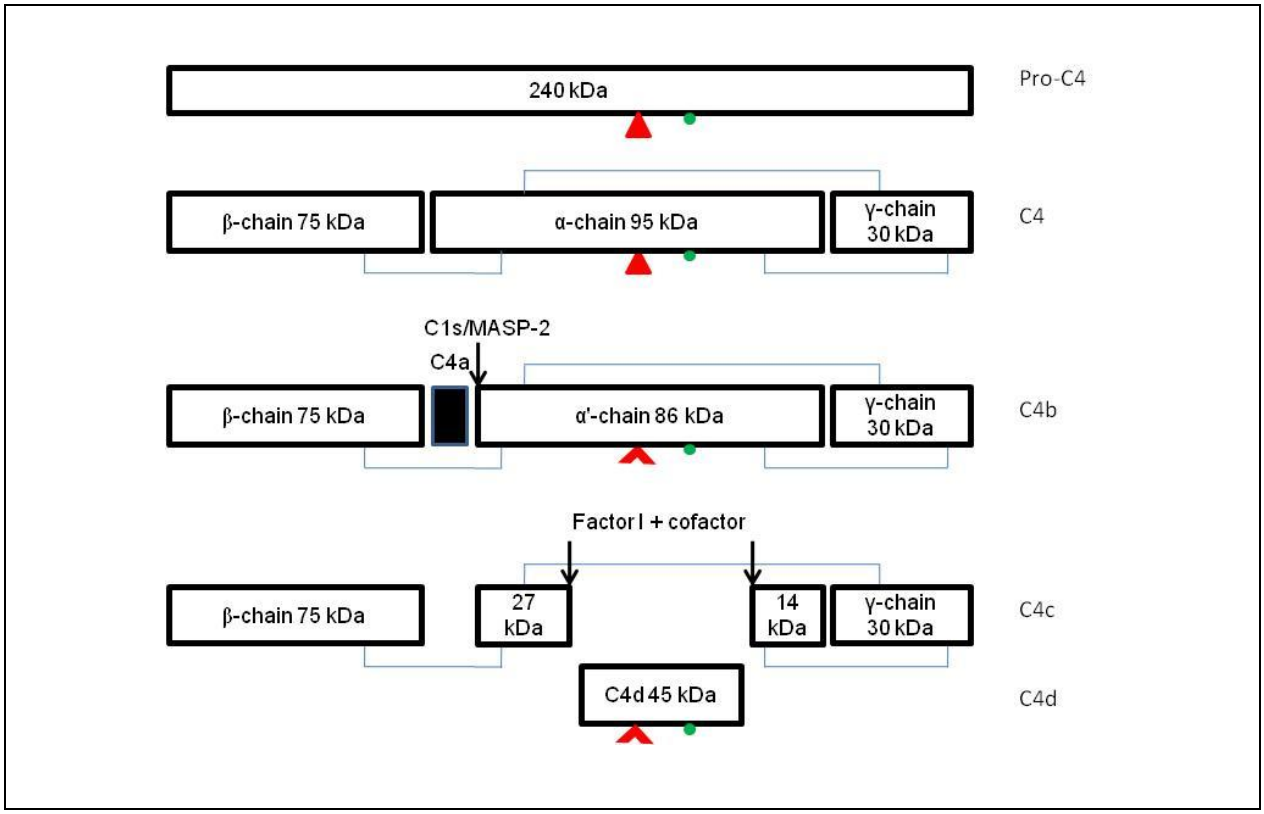

Figure 6.7: Schematic diagram of complement C4 and its activation products

The single polypeptide precursor of C4 (Pro-C4) is cleaved by intracellular enzymes into C4 α, β, and γ chains and linked by interchain disulphide bonds (lines). The C4 α-chain contains the internal thioester (triangle) and isotype specific residues (circle). Cleavage of the α-chain by activated C1s or MASP-2 releases the anaphylatoxin C4a (9 kDa) and exposes the reactive thioester on C4b that is involved in covalent bond formation (open triangle). C4b is inactivated into C4c and C4d by regulatory protein Factor I thus can no longer participate in convertase formation or CR1 mediated phagocytosis (A. Law & Dodds, 1997).

Table 6.1: Isotype specific residues on complement C4 involved in covalent bond formation.

The four key residues involved in covalent bond formation on human C4 are highlighted in bold. The corresponding residues on C4 from different species and related proteins C3 and α2-macroglobulin are also included. *Determined by mutation of recombinant human C4 (Carroll, Tathallah, Bergamaschini, Alicot, & Isenman, 1990; A. Law & Dodds, 1997).

Protein	Species	Residues 1101-1106	Bond formed
C4A	Human	**P C** P V **L D**	Amide
C4B	Human	**L S** P V **I H**	Ester
C4	Guinea pig	**P C** P V **I H**	Amide*
C4	Mouse	P C P V I H	Amide*
C3	Human	D A P V I H	Ester
α2-macroglobulin	Human	S G S L L N	Amide

6.3 Discussion

SSL10 binds to complement C4 and specifically inhibits the classical and mannan-binding lectin (MBL) pathways of complement. The classical pathway is activated through antigen-bound IgM, IgG1 or IgG3, while the lectin pathway recognises specific carbohydrate motifs on foreign surfaces (Walport, 2001). Although these two pathways differ in their mode of activation they converge at the cleavage of C4 and C2, and formation of the proteolytic C3 convertase complex, C4b2a; providing an ideal site for microbial interference. This key branch of the cascade triggers the inflammatory process through the generation of C4a and C3a, two small peptides that display potent antimicrobial and anaphylactic activities (Peter F Zipfel & Reuter, 2009). It also promotes the deposition of opsonins C4b and C3b, which mark foreign surfaces for recognition and clearance by phagocytic cells through CR1 (CD35) (Klickstein et al., 1997). Dysfunction of this process in humans due to complete C4 deficiency is associated with recurrent bacterial infections and the severe autoimmune disease systemic lupus erythematosus (P. Morgan & Walport, 1991). In mice, C4 deficiency alters the humoral response, with B cells unable to undergo isotype switching or maintain tolerance to self antigens (M. B. Fischer et al., 1996; P. Morgan & Walport, 1991; Prodeus et al., 1998).

SSL10 directly binds to complement C4 and its cleaved C4b fragment through predominant interactions in its C-terminal β-grasp domain ($SSL10_{95\text{-}197}$). It shows preferential binding to the full length C4 molecule over C4b. While the structural conformation of native C4 and C4b is not known, it can be predicted based on the crystal structure of its C4d fragment (van den Elsen et al., 2002) and the current structural model of homologues C3 and C5 (Hammel et al., 2007a; Janssen et al., 2006; Janssen et al., 2005; Laursen et al., 2010). C3, C4 and C5 are all members of the α_2-macroglobulin family of proteins and intriguingly C4Ad shares a distinctly superimposable fold with C3d (van den Elsen et al., 2002). The central core of these proteins is formed by an N-terminal macroglobulin domain (MG1-MG6) superhelix that is crowned by the MG7 and MG8 domains (Janssen et al., 2005; Laursen et al., 2010). Upon cleavage of the anaphylatoxin, the superhelix remains largely unchanged while the MG8-CUB superdomain undergoes a sharp structural alteration, exposing the thioester moiety and shifting the distant isotype specific residues towards the reactive thioester for bond formation (van den Elsen et al., 2002). This dramatic change in conformation could explain the specificity and differential binding of SSL10 towards C4 and C4b. While $SSL10_{95\text{-}197}$ mirrors these effects its interaction with C4 and inhibition of endpoint complement is weaker suggesting the involvement of the OB fold domain in maintaining either direct affinity with C4 or structural integrity of the β-grasp domain.

The exact mechanism of SSL10 action still remains to be determined. By preferentially binding to C4 it is possible SSL10 inhibits the formation of C4a. The activated serine proteases C1s and MASP-2 of the classical and lectin complement pathways respectively, cleave a single peptide bond on C4 through their serine protease domain to release C4a. Interestingly the loop diversity in this domain supports enhanced cleavage of C4 by MASP-2 (Harmat et al., 2004). Both serine proteases also interact with C4 through an accessory site on their CCP2 domain (Kardos et al., 2001); however, unlike SSL10, the

complexes binds to both C4 and the activated C4b fragment through similar affinities (Harmat et al., 2004), suggesting the binding surface is maintained following the large structural change induced from release of C4a and thus unlikely to be the SSL10 target. These protease complexes are also proposed to undergo significant structural changes and flexibility during C4 cleavage (Harmat et al., 2004), which could provide SSL10 ample opportunity for indirect interference. Indeed the involvement of other SSL10 ligands that demonstrate affinity for the OB-fold domain such as IgG1, fibrinogen, fibronectin and prothrombin, can not be excluded. SSL7 eloquently demonstrates how dual interaction with C5 and IgA forms a supercomplex that inhibits multiple functions through remote sites on C5 (Laursen et al., 2010). SSL10 could fulfil a similar role in the inhibition of C4 activity; extending its influence to inhibit C4b interaction with C2, C3 convertase function and/or detection of C4b by phagocytic complement receptor CR1.

There are two isotypes of C4 in humans, C4A and C4B (S. K. A. Law, Dodds, & Porter, 1984). Notably SSL10 only binds to a fraction of total complement C4 by ELISA thus could exhibit specificity for a particular isotype. Overall C4A and C4B are highly homologous but show striking differences in their reactivity. C4A forms covalent amide bonds with a half life of ~10 s (A. Law & Dodds, 1997), which makes it more efficient at opsonisation and immune complex clearance (Reilly, 1999; Reilly & Mold, 1997). C4Ab also displays greater affinity for CR1 and thus enhanced phagocytosis (Reilly & Mold, 1997). In contrast, C4B forms a covalent ester bond with a dramatically shorter half life of ~1 s (A. Law & Dodds, 1997). It is more efficient at driving the classical and lectin complement pathways (A. Law & Dodds, 1997; S. K. A. Law et al., 1984). These characteristic differences have been attributed to four isotype-specific residues Pro^{1101}, Cys^{1102}, Leu^{1105}, Asp^{1106} on C4A, and Leu^{1101}, Ser^{1102}, Ile^{1105} and His^{1106} on C4B (Table 6.1) (Carroll et al., 1990; A. Law & Dodds, 1997). These residues reside on the central portion of the alpha chain of C4d, which forms part of the larger activated C4b fragment (Carroll et al., 1990). Preferential binding of SSL10 to a specific C4 isotype could dictate its overall functional impact on the innate immune response. Interestingly both guinea pig and mouse C4 have a combination of these isotype specific residues (PCPVIH) (A. Law & Dodds, 1997), which could account for the higher concentration of SSL10 required for inhibition of guinea pig complement compared to human complement.

Itoh et al. recently reported inhibition of the classical complement pathway by SSL10 through direct competition with C1q for IgG1 (Itoh et al., 2010). Although the involvement of IgG1 is not excluded there are several strong indications that support the impact of SSL10 on the complement cascade is supplementary to its IgG1 binding property. Firstly, the truncated C-terminal β-grasp domain $SSL10_{95\text{-}197}$ inhibits both the classical and MBL pathways, however SSL10 requires the N-terminal OB-fold domain to stably bind to human IgG1. Secondly, activation of the classical pathway in the Weislab ELISA kit was IgM driven. There has been no evidence in this current study to suggest SSL10 has affinity for any of the Ig isotypes other than IgG. And thirdly, both the classical and MBL pathways were specifically inhibited by SSL10 despite their independent modes of activation. The Wieslab ELISA kit has been extensively tested using sera with well defined complement deficiencies that demonstrate exclusive

activation of each pathway through their respective recognition complexes (Seelen et al., 2005) and the profile of SSL10 interference most closely reflects sera deficient in C4 or C2.

Complement evasion strategies have evolved with the host over millions of years and interference of C4 activity is a key feature of many diverse organisms. The secreted *flavivirus* NS1 protein forms a complex with C1s and C4 in solution to accelerate C4 consumption (Avirutnan et al., 2010), while the human parasite species *Schistosoma* and *Trypanosoma* produce a C2 receptor trispanning protein (CRIT) that directly prevents C2 cleavage and subsequent C3 convertase formation (Inal et al., 2005). *Salmonella enterica* produces the protease PgtE, which degrades C3b, C4b and C5 (Ramu et al., 2007). Most microbial evasion strategies against C4 entail hijacking of the host regulatory protein C4-binding protein. This regulatory protein is involved in Factor I-mediated cleavage of activated C4 and subsequent destabilization of the C3 convertase C4b2a (Bloom, Webb, Villoutreix, & Dalback, 1999). *Streptococcus pyogenes* bind to C4BP using the cell surface immunoglobulin binding proteins Arp and Sir (Thern, Stenberg, Dahlback, & Lindahl, 1995), while *Neisseria gonorrhoeae* binds to the α-chain of C4BP through its type IV pili (A M Blom et al., 2001).

S.aureus has a wide arsenal of complement inhibitor proteins that ensure effective defence against the rapid and multifaceted complement system. From the early stages of activation, the classical complement pathway is plagued by the Ig binding protein Protein A, which blocks C1q binding to IgG (Kishore & Reid, 2000). Further along at the heart of the cascade Efb (Hammel et al., 2007a), Ecb (I Jongerius et al., 2007), SCIN (S. H. Rooijakkers et al., 2009) and another IgG-binding protein Sbi (Burman et al., 2008) target complement factor C3 and disable all three complement pathways. Intriguingly these diverse factors interact through a shared three-helix bundle motif (Upadhyay et al., 2008). Two close homologues of SSL10, SSL7 and SSL9, also interfere with the complement system through their C-terminal β-grasp domains. SSL7 binds to complement C5 through Asp^{147} on its C-terminal β6-β7 loop and inhibits all three complement pathways (Laursen et al., 2010). In contrast SSL9 specifically inhibits the classical and mannan-binding lectin pathways; the exact mechanisms of which still remain to be determined (Dr N Jackson, University of Auckland, NZ, Personal communications). SSL10 is the first *S.aureus* protein identified to directly target complement C4. Future studies investigating the exact binding sites of C4 and IgG1 on SSL10 will allow comprehensive understanding of the mechanism by which SSL10 achieves this task.

Chapter 7
Structural and Mutational Analysis of SSL10

7.1 Introduction

The classic superantigen fold comprising of a C-terminal β-grasp domain and smaller N-terminal OB-fold domain (V. Arcus, 2002; Proft & Fraser, 2003) has been evolutionary maintained in the SSL protein family to support a diverse range of ligands and functional roles (V. L. Arcus et al., 2002; Baker et al., 2007), (Chung et al., 2007) Superantigens utilise their two domain structure to simultaneously bind MHCII and TCR (Fraser et al., 2000). SSL7 displays similar characteristics, simultaneously binding to C5 through its β-grasp domain and IgA predominantly through its OB-fold domain to effectively inhibit complement and FcαR activity (Langley et al., 2005). In contrast, SSL11 displays defined affinity for the common terminal trisaccharide sialyllactosamine thus targeting a broad repertoire of host glycoproteins (Chung et al., 2007). It effectively prevents P-selectin mediated leukocyte recruitment to the site of infection and has also been implicated in interfering with actin polymerisation within the cell itself. Structural and mutational characterisation of the sialic acid binding site on SSL11 subsequently identified a wider subset of SSL proteins, SSL2-SSL6, that also share this sialic acid binding site (Baker et al., 2007; Chung et al., 2007).

This chapter describes the crystallisation and structure determination of recombinant SSL10. Given the strong sequence and functional similarities between SSL10 and SSL7, alanine mutation screening of SSL10 based on the orthologous residues forming the IgA binding site on SSL7 was used to investigate the residues involved in IgG1 binding.

7.2 Results

7.2.1 Crystallography

7.2.1.1 Protein purification and initial crystallisation condition screen

Recombinant $SSL10_B$ was produced and purified for crystallography as outlined in Section 3.2.3 and 3.2.4. It was further purified by size exclusion chromatography on a Sephadex 200 size exclusion column (GE Healthcare, Sweden) as a single monomeric peak. The shoulder and lag sections of the peak were excluded from the solution used for crystallography. Dynamic light scattering of the protein preparation at 2 mg/mL in 20 mM Tris pH 7.4, 100 mM NaCl determined a polydispersity index (Cp/Rh) of 10.8 %. This indicates monodispersity of the protein, which is ideal for crystal formation. A total of 480 conditions were screened for crystallisation (Moreland et al., 2005) of $SSL10_B$ at 15 mg/mL using a Cartesian HONEYBEE nanoliter robot. Sitting drops were set up at 18 °C (100 nL protein + 100 nL crystallisation reagent). Within 7 days a single elongated rectangular crystal was formed in 30 % PEG1500, 8 % MPD, 0.1 M Tris pH 8.5 (Fig. 7.1). This crystal grew in size over the following week.

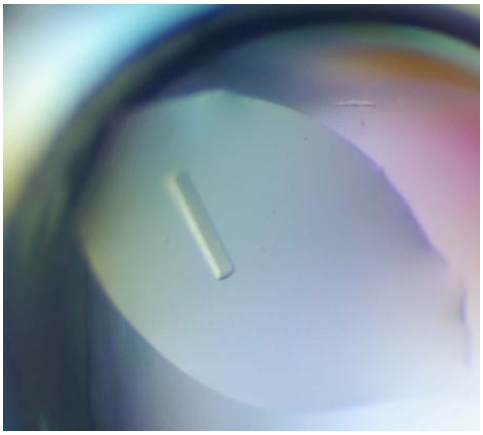

Figure 7.1: The crystal of recombinant $SSL10_B$ under polarised light.

A Cartesian Honeybee nanoliter dispensing robot was used to set up 200 nL sitting drops of a 480 condition screen mixed 1:1 with 15 mg/mL recombinant $SSL10_B$ in 20 mM Tris pH 7.4, 100 mM NaCl. After 7 days a single rectangular crystal was formed in 30 % PEG1500, 8 % MPD, 0.1 M Tris pH 8.5.

7.2.1.2 Fine screening around optimal crystallisation condition

Fine screening was performed using: 20, 25, 30 or 35 % PEG 1500; 0, 2, 4, 6, 8 or 10 % MPD; and 0.1 M Tris pH 8.5 or pH 9.0, in sitting (100 µL reservoir solution) or hanging drops (500 µL reservoir solution). Drops of 1 µL SSL10 (15 mg/mL) and 1 µL crystallisation solution were set up at 18 °C. Different protein preparations at different concentrations (5, 10, 12 and 18 mg/mL) or different ratios of SSL10 to crystallisation solution (1:2 or 2:1) were tested. SSL10 frozen at -80 °C or freshly purified was also tested at 15 mg/mL. Sitting and hanging drops were streak-seeded with fine SSL10 crystal fragments using a cat's whisker. The original conditions on the Cartesian HONEYBEE robot were also re-created. These screens did not produce any crystals; however the single crystal from the initial crystallisation screen grew to a sufficient size for x-ray diffraction.

7.2.1.3 X-ray diffraction and data collection

The SSL10 crystal was removed from the drop and immediately flash frozen in liquid nitrogen by Dr Paul Young, University of Auckland. The mother liquor (30 % PEG1500, 8 % MPD, 0.1 M Tris pH 8.5) was pre-tested and found be an ideal cryo-protectant. The crystal was sent to the Australian Synchrotron (Melbourne, Australia). The data collected were of very low resolution (6-10 Å) and hindered by ice formation. With the assistance of Dr Paul Young, the crystal was recovered for further analysis at the School of Biological Sciences, University of Auckland. The crystal was washed in liquid nitrogen to remove a large portion of the contaminating ice. Subsequent annealing of the crystal by removing it from the cryostream for 1 s, then re-freezing, improved the resolution of the data. Data were collected to 2.6 Å resolution after one round of annealing. Further annealing did not improve the data resolution.

7.2.1.3 Molecular refinement of the 2.9 Å $SSL10_B$ model

The crystal structure of SSL10 was solved by molecular replacement using the determined structure of SSL7 (PDB file 1V1O), which displays 39 % identity to SSL10. The data were initially indexed in space group P4 and integrated using MOSFLM (Leslie, 1992), then scaled and merged using SCALA (Evans, 2006). The data were restricted to 2.9 Å to give 81 % completeness of the outer shell and reindexed to space group $P4_32_12$. Manual rounds of building and molecular refinement for the 2.9 Å model were performed by Dr Paul Young using COOT (Emsley & Cowtan, 2004) and Refmac5 (Murshudov et al., 1997). The moderate resolution and low number of unique reflections limited data refinement.

7.2.1.4 Molecular refinement of the 2.75 Å $SSL10_B$ model

The original data were reprocessed to 2.75 Å, increasing the number of unique reflections available for refinement from 4690 to 5523. The 2.9 Å model of SSL10 was used for molecular replacement and the

structure was automatically built using ARP/wARP (Perrakis et al., 2001). Manual building using COOT (Emsley & Cowtan, 2004) and multiple rounds of refinement were performed using Refmac5 (Murshudov et al., 1997) and then BUSTER (Blanc et al., 2004). The solved crystal structures of homologues SSL7 (PDB file 1V1O) and SSL11 (PDB file 2RDH) were used as a guide during manual building and the geometry was routinely assessed using MolProbity (Davis et al., 2007). To improve the structural geometry, the model was re-built using PHENIX (Adams et al., 2002) and refined using BUSTER.

SSL10 crystallised as a single molecule per asymmetric unit with unit cell dimensions of a = 91.4, b = 91.4, c = 46.48, α = β = γ = 90°. In the crystal lattice it forms a dimer with the neighbouring molecule through the C-terminal β7 strand (Fig. 4). The final model of SSL10 includes residues Ser^{6} to Leu^{196} with a highly disordered loop region missing from residues Asn^{55} and Ser^{64}. The final R/Rfree is 0.2538/0.2846. The model displays excellent geometry with 95% of the residues in the most favoured region of the Ramachandran plot and no outliers as determined by MolProbity (Davis et al., 2007). The overall MolProbity score of 1.68 is in the 100^{th} percentile in relation to structures of comparable resolution. This score is calculated based on geometrical criteria's including Ramachandran and rotamer outliers, and clashes between atoms. The clash-score between atoms is 4.53 (100^{th} percentile) and poor rotamers are 1.34 %. The complete data collection and refinement statistics are reported in Table 7.1.

7.2.1.4 The SSL10 structure

SSL10 adopts the typical two domain SSL fold with an N-terminal OB-fold domain and C-terminal β-grasp domain (Fig. 7.2). It displays extensive similarities and differences compared to the structures of SSL5, SSL7 and SSL11 (Fig. 3). Interestingly SSL10 has greatest sequence identity to SSL7 but some features of the structure have more in common with SSL5, in particular the loop between the β4b and β5, which is defined in SSL5 but disordered in SSL7 and SSL11. Furthermore the loop between the β1 and β2 is notably shorter in SSL10 and SSL11 compared with SSL7 and SSL5. Both these loop regions form the major target site for IgA on SSL7 (Ramsland et al., 2007). Interestingly SSL10 is missing the loop between β3 and β4a, which is present in SSL5, SSL7 and SSL11. The α2 helix capping the β-barrel of the OB-fold domain is also shorter than in the other SSLs. The most prominent difference is the loop between the β6 and β7 in the C-terminal domain, which is rotated almost 90° from all the other SSLs. This β7 region in SSL7 forms key interactions with a parallel β-strand from complement C5 (Laursen et al., 2010).

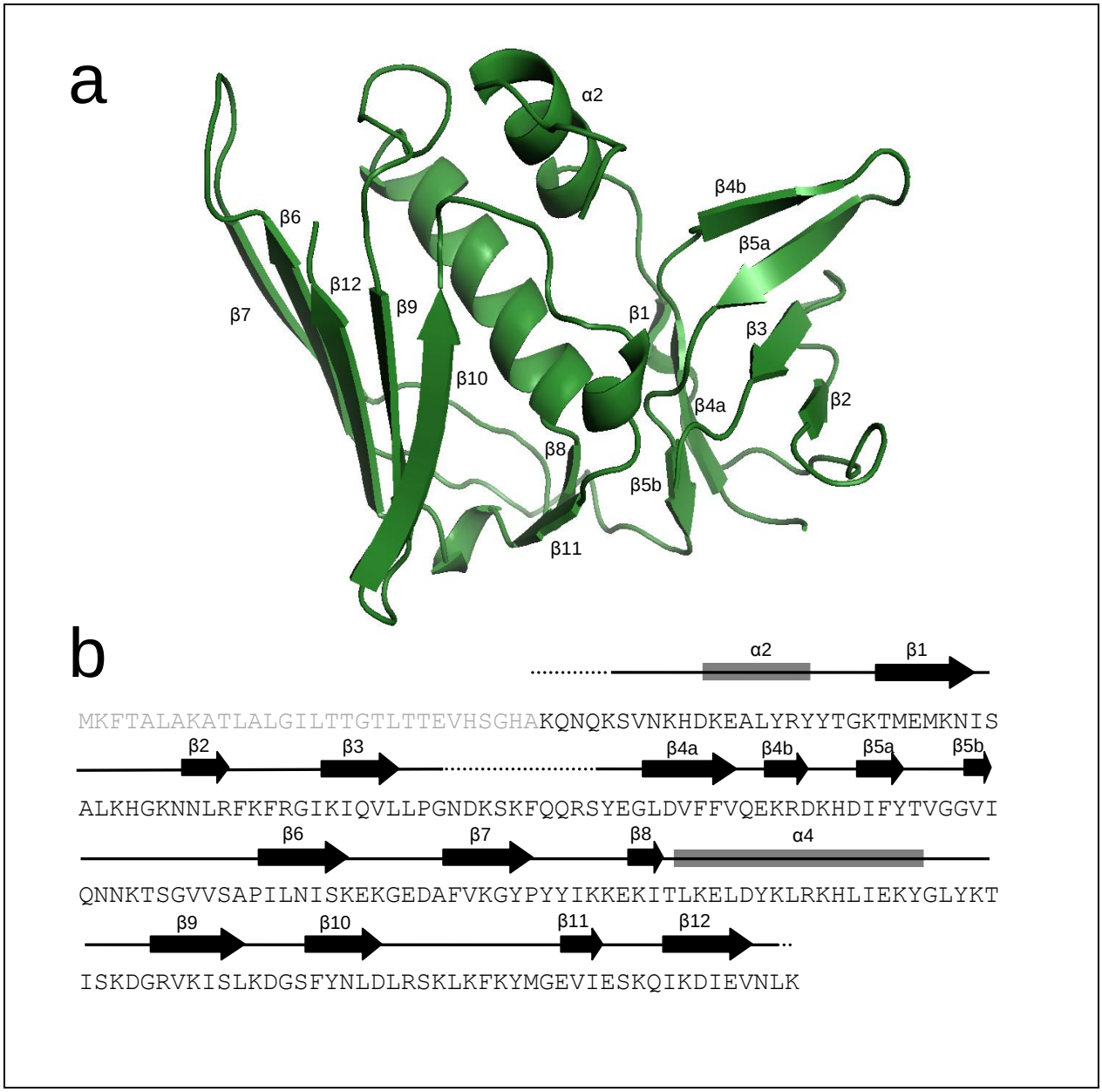

Figure 7.2: Crystal structure of $SSL10_B$

(a) Ribbon diagram of $SSL10_B$ displaying the N-terminal OB-fold domain (β1-β5b) and C-terminal β-grasp domain (β6-β12). Residues in the N-terminus (1-5), C-terminus (197) and loop region between β3 and β4a strands (55-64) are absent in the structure. (b) Amino acid sequence of $SSL10_B$ displaying the corresponding secondary structural elements: α-helix, gray box; β-sheets, black arrow. Missing residues are shown with dotted lines.

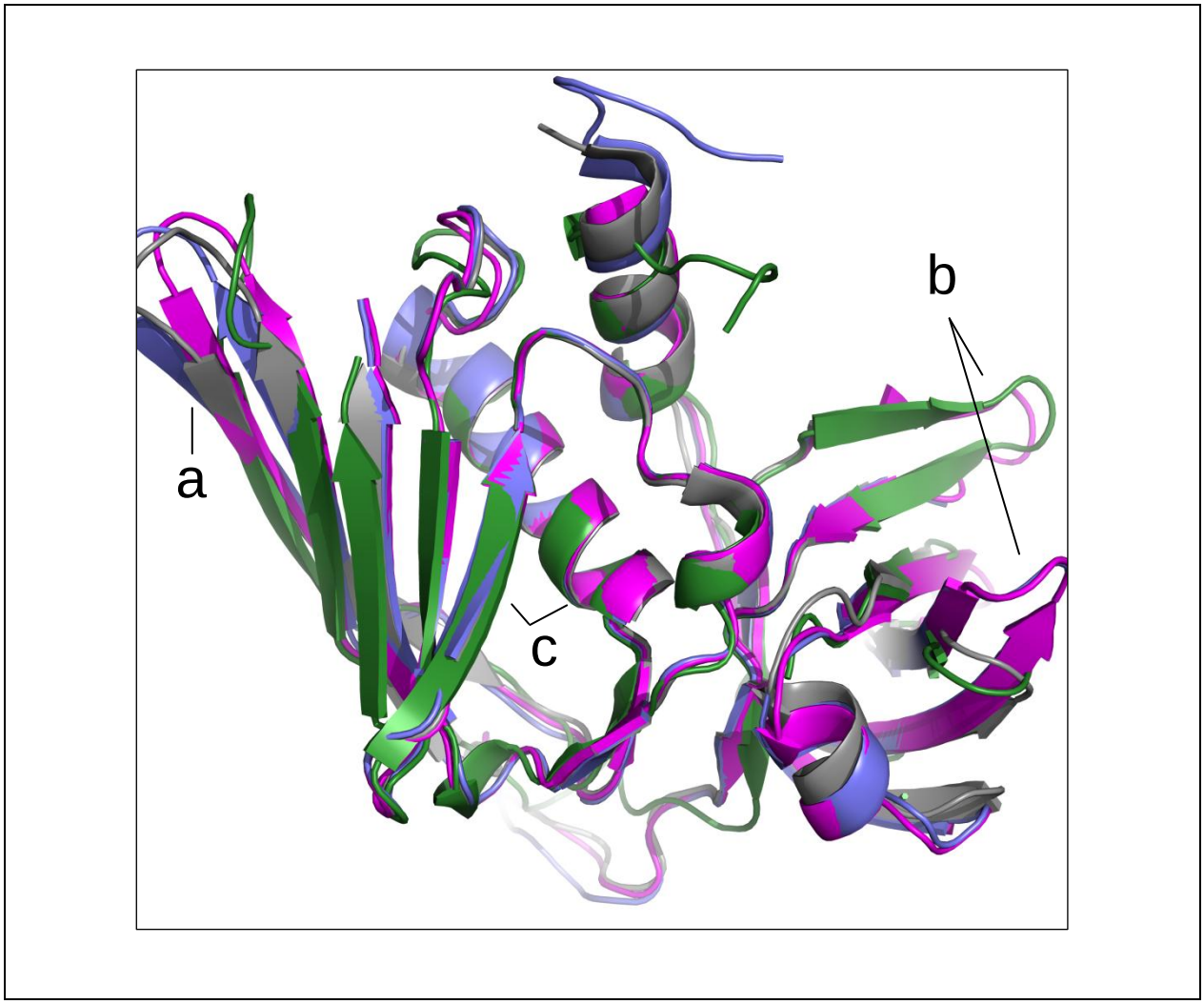

Protein overlayed	Number of residues	rmsd for Cα (Å)	% Sequence identity	PDB file
SSL5/SSL10	162	1.37	34	1M4V
SSL7/SSL10	172	1.45	39	1V10
SSL11/SSL10	163	1.39	38	2RDH

Figure 7.3: Structural comparison of SSL5, SSL7, SSL11 and SSL10

Ribbon diagram comparing the structures of SSL5 (pink, PDB file: 1M4V), SSL7 (blue, PBD file: 1V1O), SSL11 (gray, PDB file: 2RDH) and SSL10 (green). All four proteins share the same two domain structure with a highly conserved central alpha helix (α4). (a) SSL7 interacts with complement C5 through Asp^{147} on its β7 strand (Laursen et al., 2010). (b) It simultaneously binds to IgA Fc through its OB-fold domain utilising multiple residues on loop regions (Ramsland et al., 2007). (c) SSL5 and SSL11 utilises the interface of the β-grasp domain, predominantly through Thr^{168}, to bind sialyl-$Lewis^X$ (Baker et al., 2007; Chung et al., 2007). The similarity between SSL10 and the published SSL structures was determined by calculating the root mean square difference (rmsd) between the Cα positions (bottom). The number of residues aligned, sequence similarities and PBD file are stated.

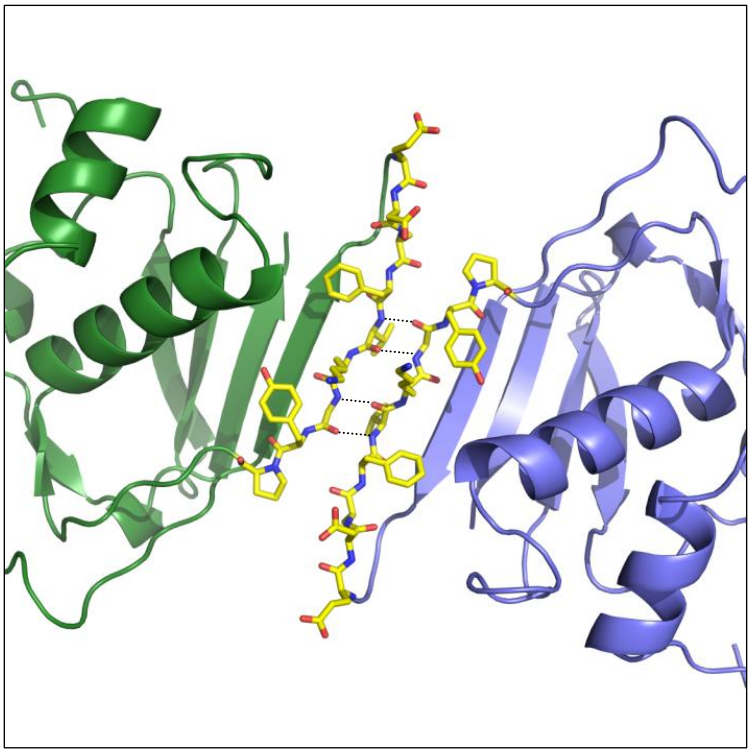

Figure 7.4: The dimer interface between adjacent SSL10 molecules

As observed with all the other SSLs crystalised to date SSL10 forms a dimer through the β7 strand on the C-terminal domain creating an extended 10 stranded β-sheet between two anti-parallel molecules. Hydrogen bonds of 2.75 to 3 Å are shown as black dotted lines.

Table 7.1: X-ray data collection and refinement statistics for the crystal structure of $SSL10_B$

	SSL10
Crystal data	
Space group	$p4_32_12$
Cell axial lengths (Å)	91.4, 91.4, 46.59
Cell angles (°)	90, 90, 90
Data collection	
Resolution range (Å)	30-2.75 (2.9-2.75)
Data collection temperature (K)	110
Unique reflections	5523 (778)
Completeness (%)	99.9 (100)
Rmerge (%)	0.134(0.793)
I/σ_I	14.1 (2.7)
Multiplicity	9.2 (8.6)
Refinement	
Resolution range (Å)	28.97-2.75
R/R_{free}	0.2538/0.2846
Protein atoms (mean B values ($Å^2$))	49.16
Water molecules (mean B values ($Å^2$))	30.013
rms deviations from standard values	
Bond lengths (Å)	0.007
Bond angles (°)	0.85
Ramachandran plot	
% residues in most favoured regions	94.92
Outliers	0
Cβ deviations	0
Poor rotamers (%)	1.34
MolProbity score	1.65 (100^{th} percentile)
Clashscore, all atoms	4.18 (100^{th} percentile)

7.2.1.5 Optimisation of crystal formation

Numerous approaches were employed in an attempt to grow quality crystals (Table 7.2). Both alleles of SSL10, $SSL10_A$ and $SSL10_B$ were screened for crystal formation (up to 30 mg/mL). Two alternate forms of $SSL10_B$ were also produced for screening; one from the second high probability start site ($SSL10_{B\ -3-197}$) predicted by SignalP (Nielsen et al., 1997) and the other truncated to omit orthologous residues disordered in related SSL crystal structures ($SSL10_{B\ 11-197}$). To aid crystal growth, streak-seeding with fine SSL5 or SSL10 crystals was carried out. A library of small molecules (HT screen 138, Hampton Research, CA, USA) was also utilized to manipulate the solubility of the sample. Given the large number of lysine residues in SSL10 (35/197), reductive methylation of $SSL10_B$ was carried out to reduce surface entrophy by modifying the flexible solvent exposed side chains of lysine that can disrupt the crystal lattice (Walter et al., 2006). Alternatively, mutational modification of $SSL10_B$ was performed to eliminate specific residues that might impede intermolecular contacts that are essential for assembly of protein molecules into a crystal lattice. The SERsever (Goldschmidt, Cooper, Derewenda, & Eisenberg, 2007) predicted a specific site at Lys^{125}, Glu^{126} and Lys^{127} to contain high conformational entropy thus these three residues were simultaneously mutated (HM Baker, University of Auckland, NZ, Personal communications). Despite these various approaches crystals of SSL10 did not readily form in any of the conditions screened.

7.2.1.6 Co-complex of SSL10 and human IgG1 Fc

Crystallisation conditions for a 1:1 co-complex of SSL10 and human IgG1 Fc in 20 mM Tris pH 7.4, 100 mM NaCl, were also screened using sitting drops prepared by the Cartesian HONEYBEE robot. Fcγ1 from monoclonal IgG1 produced by the ARH-77 cell line was prepared using papain and multiple rounds of size exclusion chromatography. The protein preparation was mixed with $SSL10_B$ in solution at a final concentration of 5 mg/mL or 10 mg/mL. Crystals were readily formed at 5 mg/mL. Clusters of plates formed in 0.2 M potassium iodide, 20 % PEG 3350 were tested using 30 % glycerol as a cryoprotectant. These were subsequently identified to be the Fc domain alone. Several conditions were also identified at 10 mg/mL. Crystals grown in 0.2 M imidazole malate, 20 % PEG 4000 pH 7.0 were tested in cryo containing 15 % glycerol, however the crystal did not diffract well. Fine screening around numerous other conditions were unsuccessful and the crystals from the initial screen were ultimately too small for X-ray diffraction.

Fcγ1 domain from polyclonal IgG1 was also prepared using papain and treated with PNGase F to remove the extending carbohydrates from the Cγ2 domain. Cleavage of these carbohydrate residues increased the affinity of SSL10 for the Fc domain to level sufficient for purification by size exclusion chromatography (Section 5.2.5). Purified SSL10 and Fc were mixed at a ratio of 2:1 15 min prior to size exclusion chromatography. Peaks were collected at 0.25 mL intervals and analysed by Western blot for the presence of SSL10. The peaks containing the complex of SSL10 and Fc were combined and concentrated to 7 mg/mL or 8 mg/mL for crystallisation screening in 20 mM Tris HCl pH 7.4, 100 mM

NaCl as previously described. Long elongated rods were formed after 2 weeks in 20 % PEG4000, 0.2 M imidazole malate pH 7.0, however they diffracted poorly. Small thin crystals formed after 4 weeks in 1.6 M ammonium sulphate, 0.1 M NaCl, 0.1 M HEPES pH 7.5, however fine screens around this condition were unsuccessful with the same protein preparation flash frozen at -80 °C.

Table 7.2: Conditions for optimisation of SSL10 crystallisation

All proteins were produced using standard procedures (Section 3.2.3) in 20 mM Tris pH 7.4, 100 mM NaCl.

Condition tested	Concentration (mg/mL)	Details
$SSL10_A$	30	Second SSL10 allele (pI = 9.9)
$SSL10_B$	15	Successfully produced SSL10 crystal
$SSL10_{B\ (-3-197)}$	10	Second high probability signal sequence start site
$SSL10_{B\ (-3-197)}$	30	Second high probability signal sequence start site
$SSL10_{B\ (11-197)}$	15	Truncated to remove commonly disordered residues in other SSL crystal structures
$SSL10_B$ additive screen	15	HT Additive screen HR2-138 (Hampton Research, USA)
$SSL10_B$ reductive methylation	7	To reduce net charge, addition of 10 % glycerol. (Walter et al., 2006)
$SSL10_B$ + SSL5 crystal	40	Seeding with SSL5 crystals
$SSL10_B$ K125,E126,K127A	10	Mutation of problematic site identified in C-terminal β-grasp domain
$SSL10_B$ Fcγ1 co-complex	5-10	Complex with monoclonal Fcγ1 and polyclonal PNGase F-treated Fcγ1

7.2.2 Mutagenesis of SSL10

Alanine mutation screening was performed to isolate the regions of potential functional importance on SSL10. The β-grasp domain alone does not bind IgG1 as seen in affinity isolation and SPR studies, thus residues residing on the N-terminal OB-fold domain were targeted. Overall SSL10 is highly conserved with its alleles displaying up to 78 % identity however there are key differences in its binding to IgG1 with $SSL10_A$ displaying higher affinity then $SSL10_B$.

Given the strong sequence identity and functional homology of SSL10 to SSL7 their amino acid sequence were compared to identify potential regions for mutagenesis (Fig. 7.5). SSL7 utilises residues on loops L1 and L4 of its OB-fold domain to bind IgA at a site also targeted by FcαRI (B. D. Wines et al., 2006). Mutagenesis of leucine L79, proline P82, and asparagine N38 on SSL7 reduces its interaction with IgA (Ramsland et al., 2007); even more so in combination. Arginine R44 and

asparagine N83 also make notable interactions (Laursen et al., 2010; Ramsland et al., 2007). Initially, the equivalent residues: histidine H34, lysine K76, lysine K79 and histidine H80 on SSL10 were mutated to alanine. These mutants were analysed for their ability to affinity purify IgG1 from plasma and compete for IgG1 with FcγRs on the cell surface of monocytes, however none of the four mutants displayed any differences from the wildtype.

Other surface exposed residues on loops L1 and L4 of SSL10 were also mutated. Of particular interest was loop region L1, which has three less residues in SSL10 compared to SSL7. A third loop in close proximity to loops L1 and L4 has an additional residue, Arg^{63}, which was also investigated. In general point mutations were produced however several double mutations were also produced to scan specific regions in an attempt to isolate a potential area for focus. The most prominent effect was observed with D78A over three independent competition experiments (Fig. 7.6). D81A in the same region also exhibited reduced competition for IgG1. On the opposite face of the protein, there was a reduction in IgG1 competition with R63A and double mutation of the neighbouring glutamine residues. These results are summarized in Table 7.3. Affinity isolation of IgG1 from plasma and serum was also performed with all the mutants however no significant differences were observed in comparison to the wildtype SSL10 (data not shown).

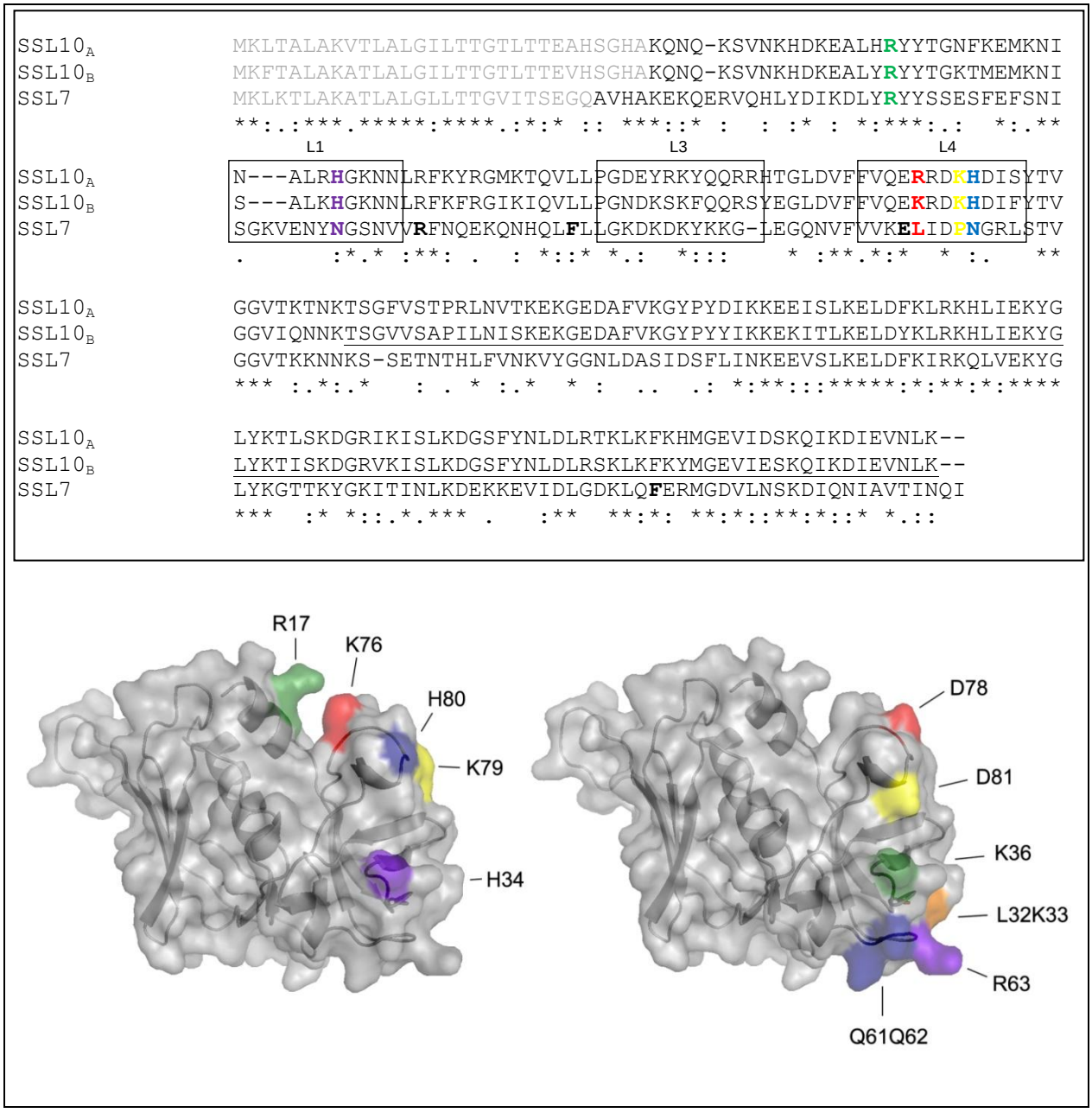

Figure 7.5: Comparison of SSL10 and SSL7 highlights key residues for mutagenesis.

The amino acid sequence of $SSL10_A$ and $SSL10_B$ was aligned with SSL7 using Clustal W (Thompson et al., 1994). The sequence corresponding to the β-grasp domain of $SSL10_B$ is underlined. The orthologous residues on SSL10 corresponding to key SSL7 residues involved in IgA binding are displayed in colour on the amino acid sequence alignment (top) and predicted structure of SSL10 (lower left). The predicted structure based on SSL11 was produced using SWISS-MODEL (Arnold et al., 2006) and depicted to include key regions that are missing from the crystal structure of SSL10. Additional residues selected for mutagenesis in loop regions of the OB fold domain are also highlighted (lower right). The regions of loops L1, L3 and L4 based on the native crystal structure of SSL10 are highlighted (box).

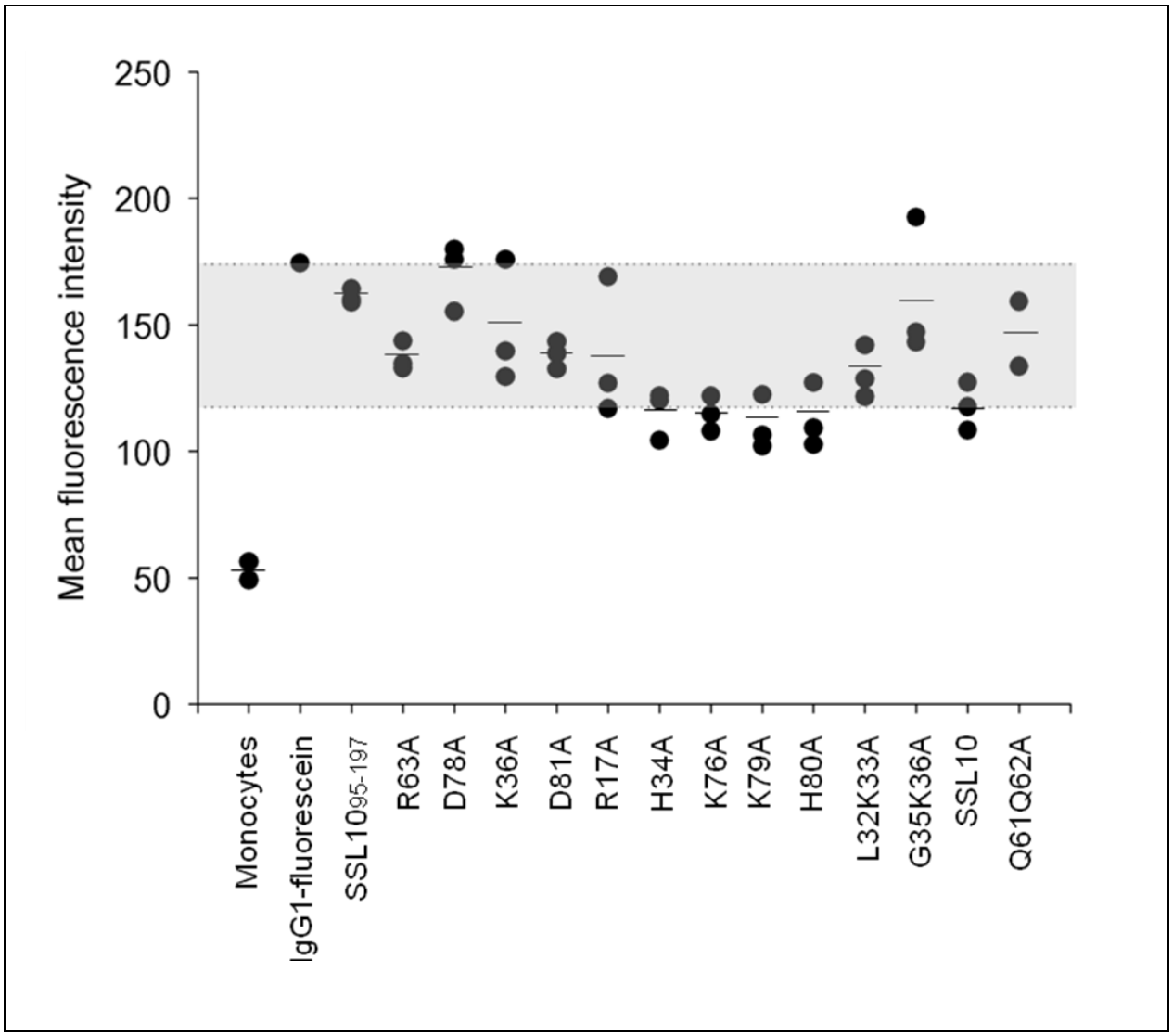

Figure: 7.6 Competition with cell surface FcγRs on monocytes for binding to IgG1-fluorescein by $SSL10_B$, $SSL10_{95-197}$ and SSL10 mutants.

IgG1-fluorescein (1 µg) was incubated with 50 µg SSL10, $SSL10_{95-197}$ or SSL10 mutants for 10 min prior to adding freshly purified PBMCs ($5x10^5$ cells) at 4 °C. Cells were washed and analysed for IgG1-fluorescein binding by FACS. A total of 10000 events were collected (n=3). The shaded region represents the maximum competition exhibited by 50 µg wildtype SSL10. In contrast $SSL10_{95-197}$ does not effectively compete for IgG1 as expected. The data display the mean MFI and are representative of three independent experiments.

Table 7.3: Alanine mutation screening of $SSL10_B$

Summary of results based on three independent IgG1 competition experiments.

Mutagenesis	Comment	Impact of mutagenesis
R17A	On SSL7 forms minor interaction with IgA	Marginal reduction in competition with FcγRs for IgG1
L32K33A	On Loop 1, close to N38 implicated in SSL7 binding to IgA [4]	Marginal reduction in competition with FcγRs for IgG1
H34A	Equivalent to N38 on SSL7 Loop 1 [4]	No change
G35K36A	On Loop 1, close to N38 implicated in SSL7 binding to IgA [4]	Marginal reduction in competition with FcγRs for IgG1
K36A	On Loop 1, close to N38 implicated in SSL7 binding to IgA [4]	Marginal reduction in competition with FcγRs for IgG1
N37N38A	On Loop 1, close to N38 implicated in SSL7 binding to IgA [4]	No change
Q61Q62A	On Loop 3 located close to Loops 1 and 4, additional residue compared to homologs SSL7 and SSL9	Reduction in competition with FcγRs for IgG1
R63A	On Loop 3 located close to Loops 1 and 4, additional residue compared to homologs SSL7 and SSL9	Reduction in competition with FcγRs for IgG1
K76A	Equivalent to L79 on SSL7 Loop 4; Arginine in $SSL10_A$ [5]	No change
D78A	On Loop 4, close to residues implicated in SSL7 binding to IgA [5,6,7]	Substantial reduction in competition with FcγRs for IgG1; no change in affinity isolation of IgG1
K79A	Equivalent to P82 on SSL7 Loop 4 [6]	No change
H80A	Equivalent to N83 on SSL7 on Loop 4 [7]	No change
D81A	On Loop 4, close to residues implicated in SSL7 binding to IgA [5,6,7]	Reduction in competition with FcγRs for IgG1; no change in affinity isolation of IgG1

[4] Mutation of N38 on SSL7 reduces affinity for IgA by 35-fold
[5] Mutation of L79 on SSL7 reduces affinity for IgA by 91-fold
[6] Mutation of P82 on SSL7 reduces affinity for IgA by 35-fold
[7] Mutation of N83 on SSL7 reduces affinity for IgA by 4-fold

7.3 Discussion

SSL10 adopts the same stable Sag motif as all the other SSLs crystalised to date and similarly also maintains its functional diversity despite the conserved fold (V. L. Arcus et al., 2002; Baker et al., 2007; Chung et al., 2007), (Dr N. Jackson, S. Hermans, University of Auckland, NZ, Personal communications). The N-terminal OB-fold domain contains a β-barrel linked to a larger C-terminal β-grasp domain, which wraps its five β-strands around a central amphiphatic α-helix. In the crystal lattice SSL10 is aligned antiparallel with the adjacent molecule forming a dimer interface through its β7 strand. Four hydrogen bonds are formed between the main chain atoms of each molecule. SSL10 does not form a dimer in solution thus at the high protein concentrations used for crystallisation the dimer could represent a crystallisation artefact. However, a natural tendency for all the SSLs to dimerise at this precise interface at high concentrations could represent functional relevance at physiologically high concentrations such as at the cell surface.

The central α-helix from all the SSL structures is well defined and the diversity between the proteins is mainly located in the loop regions. Intriguingly, SSL10 displays greatest structural homology to SSL5 although it has greatest sequence identity to SSL7. SSL10 has a defined loop between the β4b and β5 strands of the OB-fold domain, which is missing in the SSL7 and SSL11 monomers. Interestingly this region has a key importance in SSL7 binding to IgA, which could explain its enhanced flexibility and thus disordered nature (Ramsland et al., 2007). Furthermore the loop between the β1 and β2 strands is notably shorter in SSL10 and SSL11 compared with SSL7. This loop forms the second major contact site for IgA (Ramsland et al., 2007). Interestingly SSL10 is missing the loop between β3 and β4a strands, which is present in SSL5, SSL7 and SSL11. And finally in the OB-fold domain, the α2 helix capping the β-barrel is also shorter than the other SSLs. In the C-terminal domain, the most prominent difference is the loop between the β6 and β7 strands, which is rotated almost 90° from all the other SSLs. The β7 strand from SSL7 forms key interactions with a parallel β-strand from complement C5 (Laursen et al., 2010). This marked structural difference could be functionally relevant in SSL10 binding to complement C4, a close homolog of complement C5.

Crystallisation and refinement of SSL10 has been challenging. Attempts to promote crystallisation of SSL10 by modifying the protein sample, reducing surface entropy for improved crystal lattice formation, providing scaffolding for crystal growth or forming a co-complex with Fcγ1 (a readily crystallisable ligand binding partner) have been unsuccessful. As with any recombinant protein the methods of expression and purification can also have a dramatic impact on protein folding and three-dimensional structure. Only a single crystal was produced from all the screens, which was further plagued by ice formation and poor diffraction. Annealing improved the data resolution from 6 Å to 2.9 Å. Re-indexing the original data to 2.75 Å increased the number of unique reflections and improved the electron density maps for manual building. These factors combined with multiple rounds of refinement using Buster greatly improved the geometry of the model.

The two domains of SSL10 display different functional properties. The OB-fold domain is required for IgG1 binding while predominant interactions through the β-grasp domain inhibit the complement and coagulation cascades. Mutational analysis of the OB-fold domain was performed to determine the IgG1 binding site. Orthologous residues to the IgA binding site on SSL7 comprising asparagine N38, leucine L79, proline P82 and asparagine N83 (Ramsland et al., 2007) were used as an initial guide. Surface exposed residues on loop regions in close proximity to the IgA binding site were also mutated. Aspartic acid residue D78 makes dominant contributions to the ability of SSL10 to compete with FcγRs for IgG1. Nearby, aspartic acid D81 and several other residues on adjacent loops including lysine K36, arginine R63 and glutamine Q61 and Q62 also make notable contributions. However point mutation of these residues did not alter the capacity of SSL10 to affinity purify IgG1 from plasma (data not shown) suggesting several key residues are involved in stabilized binding of SSL10 to IgG1. Further mutational studies employing methods for affinity analysis, such as ITC, are necessary to investigate the combined effects of these point mutations and fully characterize the IgG1 binding site on SSL10.

Chapter 8
Discussion

8.1 Introduction

The human immune system is as an interactive network of cellular and molecular signalling systems, thus it is not surprising *S.aureus* produces a large assortment of cell surface and secreted proteins that act as a cohesive force to drive infection. This study outlines the contribution of the 24 kDa secreted protein SSL10 to *S.aureus* pathogenesis.

SSL10 shares the stable structural architecture of Sags and SSL proteins crystallised to date (Al-Shangiti et al., 2004; Baker et al., 2007; Chung et al., 2007; Fraser et al., 2000). The N-terminal OB-fold domain linked to the larger C-terminal β-grasp domain typically embraces large functional diversity. Thus despite structural homology to superantigens SSL10 does not stimulate lymphocyte proliferation. Instead it interacts with multiple plasma proteins in cases through defined domains. SSL10 is also a characteristically cationic protein (pI = 9.8), which potentially contributes to the repertoire of host proteins it targets. It interacts with human IgG1, prothrombin and α2-macroglobulin through interactions in its OB-fold domain and complement C4, plasminogen, fibrinogen and fibronectin through interactions in its C-terminal β-grasp domain. Intriguingly it also interacts with the cell surface of monocytes through a multi-chain cell surface receptor. SSL10 has a dramatic functional impact on complement, coagulation and FcγR activity. Thus this highly conserved, tightly regulated protein is recruited to provide *S.aureus* with a distinct survival advantage through immunological disguise, dissemination, adherence to extracellular matrix factors and escape from phagocytic cells.

Unlike typical secreted immune evasion factors that are produced during the late exponential and stationary phase of growth, SSL10 expression was detected from the mid-exponential phase in an *S.aureus* Δ*hrtA* mutant with reduced membrane integrity and not in the wildtype under normal growth conditions. It has been proposed that *ssl10* is upregulated by *S.aureus* in response to membrane damage (Attia et al., 2010); a potential scenario faced during physiological exposure to hypochloride (M. W. Chang et al., 2007) and internalisation into host cells (Garzoni et al., 2007; Voyich et al., 2005) that also upregulate *ssl10* expression.

8.2 SSL10 and IgG1

SSL10 demonstrates high nanomolar affinity for human IgG1 (K_D = 250 nM) through a single site 1:1 stiochiometry interaction. IgG1 is the primary responder against protein antigens and bacterial polysaccharides (Barrett & Ayoub, 1986; R Jefferis & Kumararatne, 1990). This major systemic Ig displays a unique profile of biological activities encompassing FcγR-mediated activity and highly efficient complement activation (Bruggemann et al., 1987; Canfield & Morrison, 1991). Unlike the typical Ig-binding proteins that target the CH2-CH3 interface (Atkins et al., 2008; Deisenhofer, 1981; Ramsland et al., 2007), SSL10 binds to the lower hinge and upper Cγ2 domain of the Fcγ1 domain (Dr BD Wines, Personal communications). Its subclass specificity is likely to be provided by lysine 274 that is specific to human IgG1 and conserved across non-human primates.

SSL10 interferes with IgG1 binding to cell-surface FcγRs. It also binds to the antigen-bound form of IgG1 and interferes with FcγR-mediated phagocytosis by neutrophils. FcγRs are widely distributed on blood leukocytes (Gessner et al., 1998) thus depending on the cell type influenced, targeting of FcγR activity could have dramatic implications on the host response. Certainly specific targeting of FcγRIIa-activated platelets combined with the anti-coagulative properties of SSL10 would have dramatic consequences on the restriction and elimination of bacterial cells. However, the impact of SSL10 on FcγR-mediated phagocytosis is clearly not as effective as Protein A, which has multiple high affinity IgG-binding domains suggesting SSL10 must also be conserved in the rapidly evolving *S.aureus* genome for a supplementary purpose.

Whether SSL10 displays differential binding characteristics toward antigen-bound or unbound IgG1 is a key question that remains to be answered to fully understand its functional motivation. The interaction of surface-associated SSL10 with IgG1 could aid in immunological disguise of *S.aureus*; in particular during circumstances that triggers membrane damage, which upregulates SSL10 expression (Attia et al., 2010). However, given the abundance of IgG1 during infection it is expected SSL10 would preferentially bind to antigen-bound IgG1. Removal of the extending carbohydrates from the IgG1 Cγ2 domain clearly enhances SSL10 affinity for the Fc domain. This could mimic the structural changes between the IgG1 Cγ2 domain and hinge region that transpires upon antigen binding and also provide a possible explanation for why IgG3, with its extended hinge region, is not an ideal ligand for SSL10.

8.3 SSL10 and complement

SSL10 specifically inhibits the classical and mannan-binding lectin pathways of complement through direct interactions with complement C4. Its inhibition of both guinea pig complement and IgM-activated classical pathway support a target independent of its IgG1 binding property. Itoh et al. reported inhibition of the classical pathway through direct competition of C1q to IgG1 in the presence of SSL10 (Itoh et al., 2010). However in this current study, despite repeated efforts SSL10 was not able to directly

inhibit purified C1q binding to IgG1. Indeed a 1:1 stoichiometry binding of SSL10 would leave the second C1q binding site free due to the homodimeric structure of IgG1. It is not yet clear whether antigen-bound IgG1 displays an altered conformation that allows a second SSL10 molecule to bind. SSL10 also interacts with fibrinogen and fibronectin thus under physiological circumstances dual binding of SSL10 to IgG1 and either fibrinogen, fibronectin or C4 could equally well inhibit access to the second C1q binding site.

8.4 Multi-protein complexes

The crystal structure of SSL10 displays a distinctive two domain Sag fold capable of simultaneously binding multiple ligands. The potential of this conserved fold to form a supercomplex is eloquently depicted by simultaneous binding of SSL7 to IgA and C5 (Laursen et al., 2010). SSL10 predominantly binds to IgG1 through its OB-fold domain while anti-complement and anti-coagulation activities are predominantly mediated through the β-grasp domain. Numerous other *S.aureus* proteins exhibit similar characteristics to manipulate the immune response. For example clumping factor A interacts with fibrinogen, IgG and complement to activate platelets (Loughman et al., 2005); in an analogous manner to FnBP which utilises fibronectin and IgG (Fitzgerald, Loughman et al., 2006). Direct one to one interactions are certainly capable of eliciting strong effects, but on a wider scale the formation of complexes introduces another dimension to bacterial strategies against the host response. It is also possible the specificity of SSL10 for IgG1 could be driven by a requirement to fit a certain conformational state that otherwise wouldn't be possible due to the extended hinge region of IgG3.

8.5 Multifaceted targeting of the immune response

S.aureus has co-evolved with the human host to develop multifaceted strategies against established microbial clearance mechanisms; in many cases making multiple points of interference with host factors. Remarkably SSL10 interacts with fibrinogen, fibronectin and precursors of the proteolytic enzymes thrombin and plasmin. In addition to its inhibitory effects on complement and IgG1-mediated immunity SSL10 also interferes with the coagulation cascade.

The question remains: how does a small protein achieve such as diverse range of tasks? The exact mechanisms still need to be addressed however there are several observations that suggest plasminogen could play a role. Staphylokinase effectively hijacks plasminogen to cleave human IgG in the hinge region at Lys^{222} and the α and β chains of complement-derived opsonins (S H M Rooijakkers, Willem J B van Wamel et al., 2005). Intriguingly staphylokinase displays structural homology to the β-grasp domain of SSL10, with a five stranded β-sheet cradling a single α-helix (Rabijns, De Bondt, & De Ranter, 1997). The dual interaction of SSL10 with plasminogen through its C-terminal β-grasp domain and the lower hinge region of IgG1 through its OB-fold domain could allow removal of the Fc domain. SSL10 also binds to complement C4 and C4b thus it could use plasminogen to inactivate C4 or C4b

and inhibit the classical and mannan-binding lectin pathways. Furthermore, the effects of SSL10 on delaying clot formation could be promoted by plasminogen-mediated cleavage of fibrinogen fibrils in the presence of low concentrations of thrombin during the early stages of coagulation. It is clear SSL10 is not effective in the presence of pre-activated thrombin. The interaction of SSL10 with prothrombin through the OB-fold domain and plasminogen through the C-terminal domain could also act to inhibit prothrombin cleavage into thrombin thereby further hindering clot formation, in a similar manner to the inhibition of C5 cleavage by the SSL7-IgA complex (Laursen et al., 2010). SSL10 does not cleave plasminogen into plasmin in solution (data not shown). Whether it induces a structural change to activate plasminogen in a similar manner to staphylokinase remains to be investigated. Alternatively plasminogen could be activated by another factor, possibly even another SSL protein. Both SSL9 and SSL12 promote the lysis of fibrinogen clots (Dr N Jackson, Dr A Taylor, Personal communication).

8.6 The impact of SSL10 on the inflammatory response

SSL10 acts on different levels to disrupt the inflammatory response. Although the coagulation cascade is not a classical immune response it plays a vital role in containment of bacteria and the inflammatory response and any inhibition to the central enzyme thrombin can have a dramatic impact on multiple systems. Coagulation and complement are also closely involved, forming a well interconnected system. Thrombin, for example, has been linked to complement activation, bypassing the standard means of activation to generate C5a (Huber-Lang et al., 2006). Intriguingly, these factors all share a central role in vasodilation that supports the migration of phagocytic cells to the site of infection.

SSL10 also extends its activity to monocytes, the early precursors of phagocytic macrophages. The specific receptor involved has been elusive. Although a previous study implicated CXCR4 as being the primary receptor (Walenkap et al., 2009), this study has observed key contradictions including the strict cellular specificity and coprecipitation of multiple high molecular weight polypeptide chains. Whether SSL10 acts in a complex with other serum factors such as fibrinogen or fibronectin, to activate or inhibit the innate cellular response of monocytes is a key question that remains to be addressed.

8.7 Future directions

SSL10 interferes with IgG1-mediated immunity, complement and coagulation. Preliminary analysis of key IgG1 binding residues on the SSL10 OB-fold domain identified aspartic acid D78 as a potential candidate. Several other key residues have also been identified in neighbouring loop regions including aspartic acid D83, lysine K36, arginine R63 and glutamine residues Q61 and Q62. The binding affinities of these mutants still need to be determined using thermodynamic analysis. Studies investigating the precise link between the different host proteins targeted by SSL10 also needs to characterised. The 2.75 Å crystal structure of SSL10 will provide a better indication of localised regions of importance.

Although the IgG1 binding property of SSL10 is human specific, its interaction with other ligands could display reactivity across species and thus be characterised in *in vivo* studies. Like many of the other SSLs, SSL10 has distinctive functional traits that could be analysed in a gain of function assay using *Lactococcus bacillus*. Similarly, analysis for a loss of function using *S.aureus* mutants of SSL10 could also be utilized. Furthermore, host adaptation of bovine *S.aureus* strains has established diverse SSL10 alleles that could be used as a tool for comparison.

The aggressive versatility of *S.aureus* is a huge clinical and social concern. The era of antibiotics provided us with a luxury that has been short lived due to the emergence of antibiotic resistant strains. The sequencing of *S.aureus* genomes has already provided us with great insights and advancement into this bacterium; but it has also highlighted the incredible complexity of host-pathogen interactions. Thus a comprehensive understanding of this bacterium is vital if we are to successfully develop alternative therapeutics in the future.

Appendix A
Sequenced *S.aureus* strains

Strain	Source	Details	SSL10 locus tag	Reference
N315	Pharynx, Japan	Hospital acquired MRSA ST5, VSSA	SA0390	(Kuroda et al., 2001)
Mu50	Japan	Hospital acquired VISA, Related to N315 ST5	SAV0429	(Kuroda et al., 2001)
MW2	Fatal Pediatric bacteremia, USA	Community acquired invasive MRSA ST1	MW0391	(Tadashi Baba et al., 2002)
MRSA252	Fatal bacteremia, UK	Hospital acquired epidemic MRSA ST36	SAR0429	(M T G Holden et al., 2004)
COL	Hospital acquired MRSA, USA	Hospital acquired MRSA ST250	SACOL0474	(Gill et al., 2005)
MSSA476	Osteomyelitis, UK	Community acquired invasive MSSA, Penicillin and fusidic acid resistant ST1	SAS0393	(M T G Holden et al., 2004)
RF122	Bovine mastitis, USA	ET3-1 strain is ST151	SAB0383	(Herron-Olson et al., 2007)
USA300	Wrist abscess, USA	Community acquired MRSA, Epidemic in Canada and Europe	SAUSA300_0404	(Highlander et al., 2007)
Mu3	Japan	VISA ST5	SAHV_0427	(Neoh et al., 2008)
NCTC8325	Corneal ulcer, USA	Hospital acquired MSSA, Laboratory strain parent of non-lysogneic 8325-4 ST8	SAOUHSC_00395	(Iandolo et al., 2002)
Newman	Japan	MRSA, Laboratory strain, truncated FnBPs	NWMN_0397	(T Baba et al., 2008)
04-02981	Europe	MRSA, haplotype H225-01, ST225	SA2981_0405	(Nubel et al., 2010)
D30	Nasal isolate	Healthy donor	SAD30_0191	(Sivaraman, Venkataraman, Tsai, Dewell, & Cole, 2008)

Strain	Source	Details	SSL10 locus tag	Reference
TW20	London	MRSA, outbreak in intensive care unit	SATW20_05060	(Matthew T G Holden et al., 2010)
JH1	Blood culture, USA	MRSA, VSSA, ST105	SaurJH1_0465	(Mwangi et al., 2007)
JH9	USA	VISA ST105	SaurJH9_0453	(Mwangi et al., 2007)
A9635	Clinical strain	ST45	SALG_00493	Unpublished
ST398	-	MRSA	SAPIG0498	Unpublished
D139	-	ST145	SATG_02469	Unpublished
H19	-	ST10	SAUG_02157	Unpublished
TCH60	-	ST30	HMPREF0772_0204	Human genome sequencing center
MN8	-	ST30	HMPREF0769_1991	Human genome sequencing center

Appendix B
pET32a.3c plasmid map

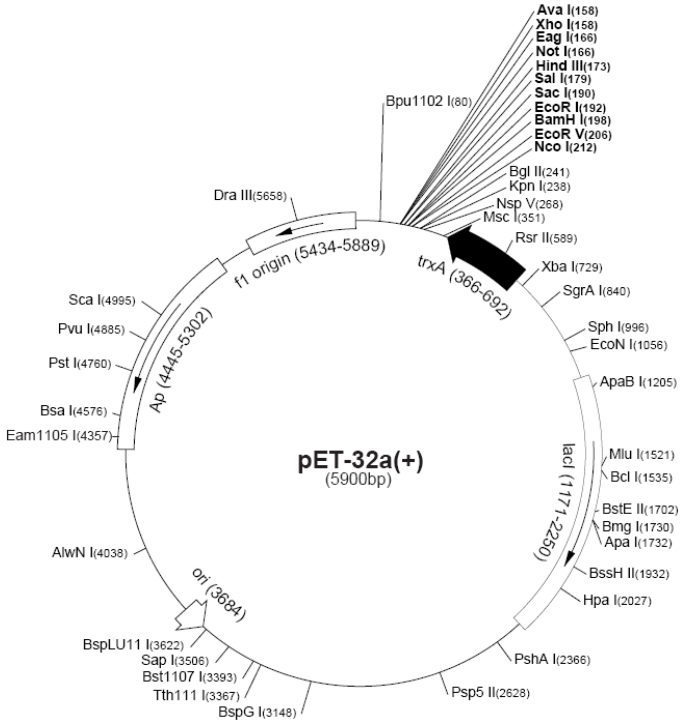

The pET32a (+) plasmid (Novagen, USA) was modified to include a 3C protease recognition and cleavage site followed by a T-cell receptor gene (TCR). The TCR gene can be removed using the restriction enzymes BamHI and EcoRI and replaced with another gene in its place. The plasmid has an ampicillin resistance marker and can be selected for using 50 µg/mL ampicillin. The pET32a plasmid map was taken from www.merck-chemicals.co.nz/life-science-research/vector-table-novagen-pet-

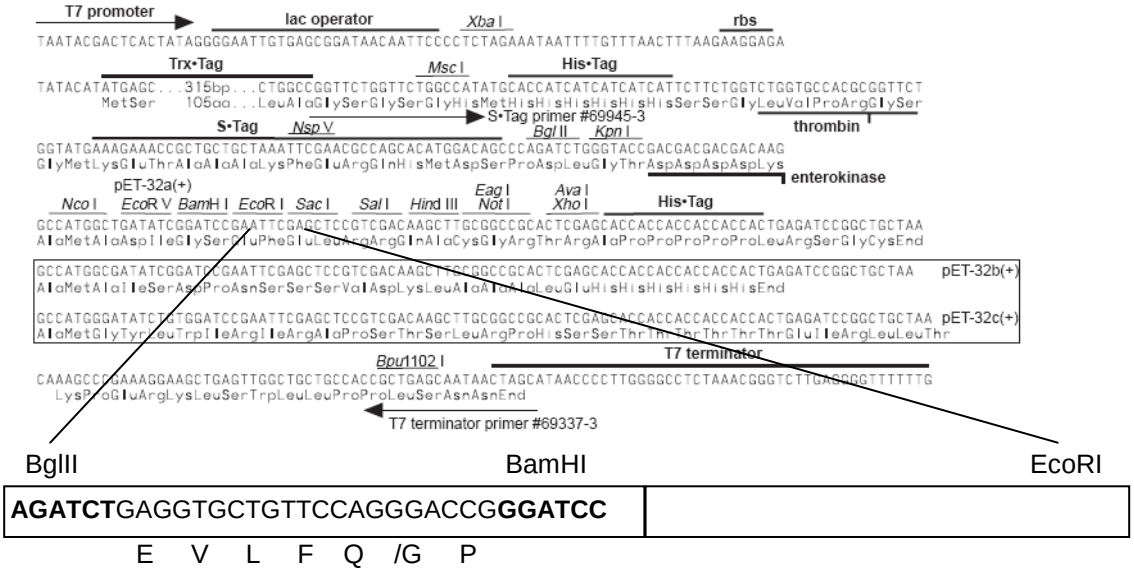

BglII BamHI EcoRI

AGATCTGAGGTGCTGTTCCAGGGACCG**GGATCC**	
E V L F Q /G P	

3C protease linker and recognition sequence — T-cell receptor insert

Appendix C
Mass spectrometry

Peptides from mass spectrometry were identified by Mascot (MS/MS Ion search) using the SwissProt database (www.matrixscience.com).

C.1 Human IgG1 Heavy chain

Match to: **IGHG1_HUMAN** Score: **107**
Ig gamma-1 chain C region - Homo sapiens (Human)
Found in search of P:\mass spec\Mass spec 27jun08\DP260608\Compounds 260608\3.mgf

Nominal mass (M_r): **36596**; Calculated pI value: **8.46**
NCBI BLAST search of IGHG1_HUMAN against nr
Unformatted sequence string for pasting into other applications

Taxonomy: Homo sapiens

Fixed modifications: Carbamidomethyl (C)
Variable modifications: Oxidation (M)
Cleavage by Trypsin: cuts C-term side of KR unless next residue is P
Sequence Coverage: **32%**

Matched peptides shown in **Bold Red**

```
     1 ASTKGPSVFP LAPSSKSTSG GTAALGCLVK DYFPEPVTVS WNSGALTSGV
    51 HTFPAVLQSS GLYSLSSVVT VPSSSLGTQT YICNVNHKPS NTKVDKKVEP
   101 KSCDKTHTCP PCPAPELLGG PSVFLFPPKP KDTLMISRTP EVTCVVVDVS
   151 HEDPEVKFNW YVDGVEVHNA KTKPREEQYN STYRVVSVLT VLHQDWLNGK
   201 EYKCKVSNKA LPAPIEKTIS KAKGQPREPQ VYTLPPSRDE LTKNQVSLTC
   251 LVKGFYPSDI AVEWESNGQP ENNYKTTPPV LDSDGSFFLY SKLTVDKSRW
   301 QQGNVFSCSV MHEALHNHYT QKSLSLSPGK
```

Probability Based Mowse Score

Ions score is -10*Log(P), where P is the probability that the observed match is a random event.

Individual ions scores **> 36 indicate identity or extensive homology** (p<0.05).

Protein scores are derived from ions scores as a non-probabilistic basis for ranking protein hits.

Start - End	Observed	Mr(expt)	Mr(calc)	Delta	Miss	Sequence
17 - 30	661.3600	1320.7054	1320.6708	0.0347	0	K.STSGGTAALGCLVK.D (Ions score 17)
17 - 30	661.3600	1320.7054	1320.6708	0.0347	0	K.STSGGTAALGCLVK.D (Ions score 14)
139 - 157	713.9900	2138.9482	2138.0202	0.9280	0	R.TPEVTCVVVDVSHEDPEVK.F (Ions score 30)
158 - 171	839.4300	1676.8454	1676.7947	0.0507	0	K.FNWYVDGVEVHNAK.T (Ions score 62)

158 - 171	560.2200	1677.6382	1676.7947	0.8435	0	K.FNWYVDGVEVHNAK.T (Ions score 45)
185 - 200	904.3600	1806.7054	1806.9992	-0.2938	0	R.VVSVLTVLHQDWLNGK.E (Ions score 43)
185 - 200	603.4900	1807.4482	1806.9992	0.4489	0	R.VVSVLTVLHQDWLNGK.E (Ions score 23)
185 - 200	603.5500	1807.6282	1806.9992	0.6289	0	R.VVSVLTVLHQDWLNGK.E (Ions score 25)
228 - 238	643.8600	1285.7054	1285.6666	0.0388	0	R.EPQVYTLPPSR.D (Ions score 10)
228 - 243	624.9600	1871.8582	1871.9629	-0.1047	1	R.EPQVYTLPPSRDELTK.N (Ions score 24)
228 - 243	625.2000	1872.5782	1871.9629	0.6153	1	R.EPQVYTLPPSRDELTK.N (Ions score 20)
244 - 253	581.4100	1160.8054	1160.6223	0.1831	0	K.NQVSLTCLVK.G (Ions score 40)
276 - 292	937.4700	1872.9254	1872.9146	0.0109	0	K.TTPPVLDSDGSFFLYSK.L (Ions score 16)
276 - 292	625.3500	1873.0282	1872.9146	0.1136	0	K.TTPPVLDSDGSFFLYSK.L (Ions score 33)
276 - 292	625.5900	1873.7482	1872.9146	0.8336	0	K.TTPPVLDSDGSFFLYSK.L (Ions score 24)

C.2 Human IgG1 Light chain

User : Deepa Patel

E-mail : d.patel@auckland.ac.nz

MS data file : P:\mass spec\27_5_10\9.mgf

Database : SwissProt 2010_06 (517,100 sequences; 182,146,551 residues)

Taxonomy : Homo sapiens (human) (20,295 sequences)

Timestamp : 28 May 2010 at 05:36:24 GMT

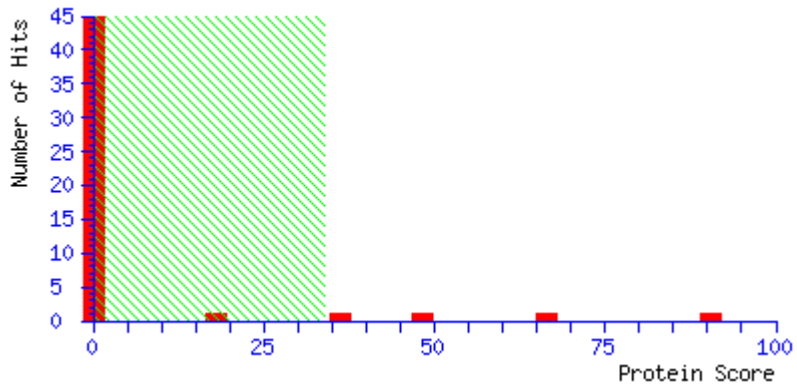

Peptide score distribution. Ions score is $-10\log(P)$, where P is the probability that the observed match is a random event. Individual ions scores **> 34 indicate identity** or **extensive homology** ($p<0.05$).

Dupes	Expect	Rank	U	1	2	Peptide	
	0.037	▶2				GAYSLSLR	Significant
	9	▶1				GFFLFVEGGR	top ranking
	6.4e-05	▶1				GSSIFGLAPGK	significant and top ranking
	1.3e-06	▶1		■		SSGTSYPDVLK	peptide is found in all proteins in family member 1
	6.2e-07	▶1			■	VCNYVSWIK	peptide is found in some but not all proteins in family member 2
	6.4e-05	▶1	U			GSSIFGLAPGK	Unique
▶2	5.7e-05	▶1				LNTLETEEWFFK	peptide has two duplicates
	0.18	▶1				LNTLETEEWFFK	duplicate peptide

Protein Family Summary

▶**1**
IGKC_HUMAN 90 Ig kappa chain C region OS=Homo sapiens GN=IGKC PE=1 SV=1

▶**2**
KV201_HUMAN 6 Ig kappa chain V-II region Cum OS=Homo sapiens PE=1 9SV=1

▶**3**
KV309_HUMAN 4 Ig kappa chain V-III region VG (Fragment) OS=Homo sapiens 6PE=1 SV=1

▶**4**
KV302_HUMAN 3 Ig kappa chain V-III region SIE OS=Homo sapiens PE=1 5SV=1

▶**5**
LUZP1_HUMAN 16 Leucine zipper protein 1 OS=Homo sapiens GN=LUZP1 PE=1 SV=2

C.3 Fibronectin

Match to: **FINC_HUMAN** Score: **151**
Fibronectin OS=Homo sapiens GN=FN1 PE=1 SV=3
Found in search of P:\mass spec\Mass spec 29july08\New Folder\16a.mgf

Nominal mass (M_r): **266034**; Calculated pI value: **5.45**
NCBI BLAST search of FINC_HUMAN against nr
Unformatted sequence string for pasting into other applications

Taxonomy: Homo sapiens

Fixed modifications: Carbamidomethyl (C)
Variable modifications: Oxidation (M)
Cleavage by Trypsin: cuts C-term side of KR unless next residue is P
Sequence Coverage: **12%**

Matched peptides shown in **Bold Red**

1 MLRGPGPGLL LLAVQCLGTA VPSTGASKSK RQAQQMVQPQ SPVAVSQSKP
51 GCYDNGKHYQ INQQWERTYL GNALVCTCYG GSRGFNCESK PEAEETCFDK
101 YTGNTYRVGD TYERPKDSMI WDCTCIGAGR GRISCTIANR CHEGGQSYKI
151 GDTWRRPHET GGYMLECVCL GNGKGEWTCK PIAEKCFDHA AGTSYVVGET
201 WEKPYQGWMM VDCTCLGEGS GRITCTSRNR CNDQDTRTSY RIGDTWSKKD
251 NRGNLLQCIC TGNGRGEWKC ER**HTSVQTTS SGSGPFTDVR** AAVYQPQPHP
301 QPPPYGHCVT DSGVVYSVGM QWLKTQGNKQ MLCTCLGNGV SCQETAVTQT
351 YGGNSNGEPC VLPFTYNGRT FYSCTTEGRQ DGHLWCSTTS NYEQDQKYSF
401 CTDHTVLVQT QGGNSNGALC HFPFLYNNHN YTDCTSEGRR DNMKWCGTTQ
451 NYDADQKFGF CPMAAHEEIC TTNEGVMYRI GDQWDKQHDM GHMMRCTCVG
501 NGRGEWTCIA YSQLRDQCIV DDITYNVNDT FHKRHEEGHM LNCTCFGQGR
551 GRWKCDPVDQ CQDSETGTFY QIGDSWEKYV HGVRYQCYCY GRGIGEWHCQ
601 PLQTYPSSSG PVEVFITETP SQPNSHPIQW NAPQPSHISK YILRWRPKNS
651 VGRWKEATIP GHLNSYTIKG LKPGVVYEGQ LISIQQYGHQ EVTRFDFTTT
701 STSTPVTSNT VTGETTPFSP LVATSESVTE ITASSFVVSW VSASDTVSGF
751 RVEYELSEEG DEPQYLDLPS TATSVNIPDL LPGRKYIVNV YQISEDGEQS
801 LILSTSQTTA PDAPPDPTVD QVDDTSIVVR WSRPQAPITG YRIVYSPSVE
851 GSSTELNLPE TANSVTLSDL QPGVQYNITI YAVEENQEST PVVIQQETTG
901 TPRSDTVPSP RDLQFVEVTD VKVTIMWTPP ESAVTGYRVD VIPVNLPGEH
951 **GQR**LPISRNT FAEVTGLSPG VTYYFKVFAV SHGR**ESKPLT AQQTTK**LDAP
1001 TNLQFVNETD STVLVRWTPP RAQITGYR**LT VGLTR**RGQPR QYNVGPSVSK
1051 YPLR**NLQPAS EYTVSLVAIK** GNQESPKATG VFTTLQPGSS IPPYNTEVTE
1101 TTIVITWTPA PRIGFK**LGVR PSQGGEAPR**E VTSDSGSIVV SGLTPGVEYV
1151 YTIQVLRDGQ ERDAPIVNKV VTPLSPPTNL HLEANPDTGV LTVSWER**STT**
1201 **PDITGYR**ITT TPTNGQQGNS LEEVVHADQS SCTFDNLSPG LEYNVSVYTV
1251 KDDKESVPIS DTIIPAVPPP TDLRFTNIGP DTMRVTWAPP PSIDLTNFLV
1301 **R**YSPVKNEED VAELSISPSD NAVVLTNLLP GTEYVVSVSS VYEQHESTPL
1351 RGRQKTGLDS PTGIDFSDIT ANSFTVHWIA PRATITGYRI RHHPEHFSGR
1401 PREDRVPHSR NSITLTNLTP GTEYVVSIVA LNGREESPLL IGQQSTVSDV
1451 PRDLEVVAAT PTSLLISWDA PAVTVRYYR**I TYGETGGNSP VQEFTVPGSK**
1501 STATISGLKP GVDYTITVYA VTGR**GDSPAS SKPISINYR**T EIDKPSQMQV
1551 TDVQDNSISV KWLPSSSPVT GYRVTTTPKN GPGPTKTKTA GPDQTEMTIE
1601 GLQPTVEYVV SVYAQNPSGE SQPLVQTAVT NIDRPKGLAF TDVDVDSIKI
1651 AWESPQGQVS RYRVTYSSPE DGIHELFPAP DGEEDTAELQ GLRPGSEYTV
1701 SVVALHDDME SQPLIGTQST AIPAPTDLKF TQVTPTSLSA QWTPPNVQLT
1751 GYRVRVTPKE KTGPMKEINL APDSSSVVVS GLMVATKYEV SVYALKDTLT
1801 SRPAQGVVTT LENVSPPRRA RVTDATETTI TISWRTKTET ITGFQVDAVP
1851 ANGQTPIQRT IKPDVRSYTI TGLQPGTDYK IYLYTLNDNA RSSPVVIDAS
1901 TAIDAPSNLR FLATTPNSLL VSWQPPRARI TGYIIKYEKP GSPPREVVPR
1951 PRPGVTEATI TGLEPGTEYT IYVIALKNNQ KSEPLIGRKK TDELPQLVTL
2001 PHPNLHGPEI LDVPSTVQKT PFVTHPGYDT GNGIQLPGTS GQQPSVGQQM

```
2051 IFEEHGFRRT TPPTTATPIR HRPRPYPPNV GEEIQIGHIP REDVDYHLYP
2101 HGPGLNPNAS TGQEALSQTT ISWAPFQDTS EYIISCHPVG TDEEPLQFRV
2151 PGTSTSATLT GLTRGATYNI IVEALKDQQR HKVREEVVTV GNSVNEGLNQ
2201 PTDDSCFDPY TVSHYAVGDE WERMSESGFK LLCQCLGFGS GHFRCDSSRW
2251 CHDNGVNYKI GEKWDRQGEN GQMMSCTCLG NGKGEFKCDP HEATCYDDGK
2301 TYHVGEQWQK EYLGAICSCT CFGGQRGWRC DNCRRPGGEP SPEGTTGQSY
2351 NQYSQRYHQR TNTNVNCPIE CFMPLDVQAD REDSRE
```

Probability Based Mowse Score

Ions score is -10*Log(P), where P is the probability that the observed match is a random event.

Individual ions scores **> 36 indicate identity or extensive homology** (p<0.05).

Protein scores are derived from ions scores as a non-probabilistic basis for ranking protein hits.

Start - End	Observed	Mr(expt)	Mr(calc)	Delta	Miss	Sequence
273 - 290	621.9700	1862.8882	1862.8759	0.0123	0	R.HTSVQTTSSGSGPFTDVR.A (Ions score 30)
912 - 922	646.9400	1291.8654	1291.6660	0.1994	0	R.DLQFVEVTDVK.V (Ions score 57)
939 - 953	815.4300	1628.8454	1628.8635	-0.0180	0	R.VDVIPVNLPGEHGQR.L (Ions score 16)
939 - 953	544.2500	1629.7282	1628.8635	0.8647	0	R.VDVIPVNLPGEHGQR.L (Ions score 32)
985 - 996	666.4200	1330.8254	1330.7092	0.1162	0	R.ESKPLTAQQTTK.L (Ions score 16)
1029 - 1035	380.3400	758.6654	758.4650	0.2004	0	R.LTVGLTR.R (Ions score 22)
1055 - 1070	578.4600	1732.3582	1731.9407	0.4175	0	R.NLQPASEYTVSLVAIK.G (Ions score 36)
1117 - 1129	662.4100	1322.8054	1322.7055	0.1000	0	K.LGVRPSQGGEAPR.E (Ions score 20)
1198 - 1207	555.8300	1109.6454	1109.5353	0.1101	0	R.STTPDITGYR.I (Ions score 33)
1275 - 1284	584.2600	1166.5054	1166.5390	-0.0336	0	R.FTNIGPDTMR.V Oxidation (M) (Ions score 28)
1285 - 1301	642.7700	1925.2882	1925.0411	0.2471	0	R.VTWAPPPSIDLTNFLVR.Y (Ions score 25)
1480 - 1500	723.3400	2166.9982	2167.0433	-0.0452	0	R.ITYGETGGNSPVQEFTVPGSK.S (Ions score 38)
1525 - 1539	531.3900	1591.1482	1590.8002	0.3480	0	R.GDSPASSKPISINYR.T (Ions score 13)
1767 - 1787	711.7800	2132.3182	2132.1035	0.2147	0	K.EINLAPDSSSVVVSGLMVATK.Y Oxidation (M) (Ions score 22)
1788 - 1796	536.3700	1070.7254	1070.5648	0.1607	0	K.YEVSVYALK.D (Ions score 27)
1867 - 1880	772.3900	1542.7654	1542.7566	0.0089	0	R.SYTITGLQPGTDYK.I (Ions score 22)
1881 - 1891	678.3800	1354.7454	1354.6881	0.0574	0	K.IYLYTLNDNAR.S (Ions score 30)
1892 - 1910	638.6200	1912.8382	1911.9902	0.8480	0	R.SSPVVIDASTAIDAPSNLR.F (Ions score 32)
1911 - 1927	643.4100	1927.2082	1926.0363	1.1718	0	R.FLATTPNSLLVSWQPPR.A (Ions score 30)
1930 - 1936	404.4800	806.9454	806.4902	0.4553	0	R.ITGYIIK.Y (Ions score 11)
2150 - 2164	731.4300	1460.8454	1460.7835	0.0620	0	R.VPGTSTSATLTGLTR.G (Ions score 69)
2165 - 2176	646.4200	1290.8254	1290.7183	0.1071	0	R.GATYNIIVEALK.D (Ions score 56)

C.4 Fibrinogen α-chain

Match to: **FIBA_HUMAN** Score: **173**
Fibrinogen alpha chain precursor [Contains: Fibrinopeptide A] - Homo sapiens (Human)
Found in search of P:\mass spec\Mass spec 27jun08\DP260608\Compounds 260608\9.mgf

Nominal mass (M_r): **95656**; Calculated pI value: **5.70**
NCBI BLAST search of FIBA_HUMAN against nr
Unformatted sequence string for pasting into other applications

Taxonomy: Homo sapiens

Fixed modifications: Carbamidomethyl (C)
Variable modifications: Oxidation (M)
Cleavage by Trypsin: cuts C-term side of KR unless next residue is P
Sequence Coverage: **19%**

Matched peptides shown in **Bold Red**

```
   1 MFSMRIVCLV LSVVGTAWTA DSGEGDFLAE GGGVRGPRVV ERHQSACKDS
  51 DWPFCSDEDW NYKCPSGCRM KGLIDEVNQD FTNRINKLKN SLFEYQKNNK
 101 DSHSLTTNIM EILRGDFSSA NNRDNTYNRV SEDLRSRIEV LKRKVIEKVQ
 151 HIQLLQKNVR AQLVDMKRLE VDIDIKIRSC RGSCSRALAR EVDLKDYEDQ
 201 QKQLEQVIAK DLLPSRDRQH LPLIKMKPVP DLVPGNFKSQ LQKVPPEWKA
 251 LTDMPQMRME LERPGGNEIT RGGSTSYGTG SETESPRNPS SAGSWNSGSS
 301 GPGSTGNRNP GSSGTGGTAT WKPGSSGPGS TGSWNSGSSG TGSTGNQNPG
 351 SPRPGSTGTW NPGSSERGSA GHWTSESSVS GSTGQWHSES GSFRPDSPGS
 401 GNARPNNPDW GTFEEVSGNV SPGTRREYHT EKLVTSKGDK ELRTGKEKVT
 451 SGSTTTTRRS CSKTVTKTVI GPDGHKEVTK EVVTSEDGSD CPEAMDLGTL
 501 SGIGTLDGFR HRHPDEAAFF DTASTGKTFP GFFSPMLGEF VSETESRGSE
 551 SGIFTNTKES SSHHPGIAEF PSRGKSSSYS KQFTSSTSYN RGDSTFESKS
 601 YKMADEAGSE ADHEGTHSTK RGHAKSRPVR DCDDVLQTHP SGTQSGIFNI
 651 KLPGSSKIFS VYCDQETSLG GWLLIQQRMD GSLNFNRTWQ DYKRGFGSLN
 701 DEGEGEFWLG NDYLHLLTQR GSVLRVELED WAGNEAYAEY HFRVGSEAEG
 751 YALQVSSYEG TAGDALIEGS VEEGAEYTSH NNMQFSTFDR DADQWEENCA
 801 EVYGGGWWYN NCQAANLNGI YYPGGSYDPR NNSPYEIENG VVWVSFRGAD
 851 YSLRAVRMKI RPLVTQ
```

Probability Based Mowse Score

Ions score is -10*Log(P), where P is the probability that the observed match is a random event.

Individual ions scores **> 36 indicate identity or extensive homology** (p<0.05).

Protein scores are derived from ions scores as a non-probabilistic basis for ranking protein hits.

Start - End	Observed	Mr(expt)	Mr(calc)	Delta	Miss	Sequence
72 - 84	**760.8700**	**1519.7254**	**1519.7267**	**-0.0012**	**0**	**K.GLIDEVNQDFTNR.I** (Ions score 59)
72 - 84	**507.5900**	**1519.7482**	**1519.7267**	**0.0215**	**0**	**K.GLIDEVNQDFTNR.I** (Ions score 40)
90 - 97	**514.7900**	**1027.5654**	**1027.4974**	**0.0680**	**0**	**K.NSLFEYQK.N** (Ions score 32)
101 - 114	**815.3000**	**1628.5854**	**1628.8192**	**-0.2337**	**0**	**K.DSHSLTTNIMEILR.G** (Ions score 32)
101 - 114	**549.3000**	**1644.8782**	**1644.8141**	**0.0641**	**0**	**K.DSHSLTTNIMEILR.G** Oxidation (M) (Ions score 24)
101 - 114	**823.4500**	**1644.8854**	**1644.8141**	**0.0713**	**0**	**K.DSHSLTTNIMEILR.G** Oxidation (M) (Ions score 21)

115 - 123	484.2300	966.4454	966.4155	0.0299	0	R.GDFSSANNR.D (Ions score 37)
149 - 157	553.9100	1105.8054	1105.6608	0.1447	0	K.VQHIQLLQK.N (Ions score 41)
149 - 157	369.6500	1105.9282	1105.6608	0.2674	0	K.VQHIQLLQK.N (Ions score 10)
168 - 176	550.7600	1099.5054	1099.6237	-0.1183	1	K.RLEVDIDIK.I (Ions score 34)
191 - 202	755.8100	1509.6054	1508.6994	0.9060	1	R.EVDLKDYEDQQK.Q (Ions score 39)
203 - 210	464.8600	927.7054	927.5389	0.1665	0	K.QLEQVIAK.D (Ions score 22)
226 - 238	721.4800	1440.9454	1440.7799	0.1655	0	K.MKPVPDLVPGNFK.S (Ions score 33)
226 - 238	729.3700	1456.7254	1456.7748	-0.0494	0	K.MKPVPDLVPGNFK.S Oxidation (M) (Ions score 33)
250 - 258	547.7700	1093.5254	1093.4896	0.0358	0	K.ALTDMPQMR.M 2 Oxidation (M) (Ions score 27)
259 - 271	501.2700	1500.7882	1500.7354	0.0527	0	R.MELERPGGNEITR.G (Ions score 14)
259 - 271	759.3400	1516.6654	1516.7304	-0.0649	0	R.MELERPGGNEITR.G Oxidation (M) (Ions score 6)
259 - 271	506.7200	1517.1382	1516.7304	0.4078	0	R.MELERPGGNEITR.G Oxidation (M) (Ions score 22)
272 - 287	786.8100	1571.6054	1571.6700	-0.0645	0	R.GGSTSYGTGSETESPR.N (Ions score 54)
548 - 558	570.7700	1139.5254	1139.5459	-0.0204	0	R.GSESGIFTNTK.E (Ions score 30)
559 - 573	546.5700	1636.6882	1636.7594	-0.0712	0	K.ESSSHHPGIAEFPSR.G (Ions score 49)
559 - 573	819.3600	1636.7054	1636.7594	-0.0539	0	K.ESSSHHPGIAEFPSR.G (Ions score 32)
582 - 591	595.6700	1189.3254	1189.5364	-0.2109	0	K.QFTSSTSYNR.G (Ions score 23)

C.5 Fibrinogen β-chain

User : C Buchanan
Email : c.buchanan@auckland.ac.nz
Search title : SSL10 E
Database : SwissProt 54.0 (276256 sequences; 101466206 residues)
Taxonomy : Homo sapiens (human) (16974 sequences)
Timestamp : 20 Aug 2007 at 01:28:11 GMT
Top Score : 121 for FIBB_HUMAN, Fibrinogen beta chain precursor [Contains: Fibrinopeptide B] - Homo sapiens (Human)

Probability Based Mowse Score

Protein score is -10*Log(P), where P is the probability that the observed match is a random event. Protein **scores greater than 55 are significant** (p<0.05).

FIBB_HUMAN **Mass:** 56577 **Score:** 121 **Expect:** 1.3e-08 **Queries matched:** 15

1. Fibrinogen beta chain precursor [Contains: Fibrinopeptide B] - Homo sapiens (Human)

C.6 Fibrinogen γ-chain

User : C Buchanan
Email : c.buchanan@auckland.ac.nz
Search title : SSL10 F
Database : SwissProt 54.1 (277883 sequences; 101975253 residues)
Taxonomy : Homo sapiens (human) (17062 sequences)
Timestamp : 26 Aug 2007 at 20:39:36 GMT
Top Score : 135 for Mixture 1, IGHG1_HUMAN + FIBG_HUMAN

Probability Based Mowse Score

Protein score is -10*Log(P), where P is the probability that the observed match is a random event. Protein **scores greater than 55 are significant** (p<0.05).

Mixture 1 Total score: 135 Expect: 5.4e-10 **Queries matched:** 14

1.

Components (only one family member shown for each component):

IGHG1_HUMAN **Mass:** 36596 **Score: 72 Expect:** 0.0011 **Queries matched:** 7

Ig gamma-1 chain C region - Homo sapiens (Human)

FIBG_HUMAN **Mass:** 52106 **Score: 61 Expect:** 0.014 **Queries matched:** 7

Fibrinogen gamma chain precursor - Homo sapiens (Human)

---

2. IGHG1_HUMAN **Mass:** 36596 **Score: 72 Expect:** 0.0011 **Queries matched:** 7

Ig gamma-1 chain C region - Homo sapiens (Human)

IGHG2_HUMAN **Mass:** 36489 **Score:** 26 **Expect:** 46 **Queries matched:** 3

Ig gamma-2 chain C region - Homo sapiens (Human)

PHOS_HUMAN **Mass:** 28513 **Score:** 19 **Expect:** 2.4e+02 **Queries matched:** 2

Phosducin - Homo sapiens (Human)

---

3. FIBG_HUMAN **Mass:** 52106 **Score: 61 Expect:** 0.014 **Queries matched:** 7

Fibrinogen gamma chain precursor - Homo sapiens (Human)

C.7 α2-macroglobulin

Match to: **A2MG_HUMAN** Score: **84**

Alpha-2-macroglobulin precursor - Homo sapiens (Human)
Found in search of P:\mass spec\Mass spec 27jun08\DP260608\Compounds 260608\7.mgf

Nominal mass (M_r): **164600**; Calculated pI value: **6.00**
NCBI BLAST search of A2MG_HUMAN against nr
Unformatted sequence string for pasting into other applications

Taxonomy: Homo sapiens

Fixed modifications: Carbamidomethyl (C)
Variable modifications: Oxidation (M)
Cleavage by Trypsin: cuts C-term side of KR unless next residue is P
Sequence Coverage: **16%**

Matched peptides shown in **Bold Red**

```
   1 MGKNKLLHPS LVLLLLVLLP TDASVSGKPQ YMVLVPSLLH TETTEKGCVL
  51 LSYLNETVTV SASLESVRGN RSLFTDLEAE NDVLHCVAFA VPKSSSNEEV
 101 MFLTVQVKGP TQEFKKRTTV MVKNEDSLVF VQTDKSIYKP GQTVKFRVVS
 151 MDENFHPLNE LIPLVYIQDP KGNRIAQWQS FQLEGGLKQF SFPLSSEPFQ
 201 GSYKVVVQKK SGGRTEHPFT VEEFVLPKFE VQVTVPKIIT ILEEEMNVSV
 251 CGLYTYGKPV PGHVTVSICR KYSDASDCHG EDSQAFCEKF SGQLNSHGCF
 301 YQQVKTKVFQ LKRKEYEMKL HTEAQIQEEG TVVELTGRQS SEITRTITKL
 351 SFVKVDSHFR QGIPFFGQVR LVDGKGVPIP NKVIFIRGNE ANYYSNATTD
 401 EHGLVQFSIN TTNVMGTSLT VRVNYKDRSP CYGYQWVSEE HEEAHHTAYL
 451 VFSPSKSFVH LEPMSHELPC GHTQTVQAHY ILNGGTLLGL KKLSFYYLIM
 501 AKGGIVRTGT HGLLVKQEDM KGHFSISIPV KSDIAPVARL LIYAVLPTGD
 551 VIGDSAKYDV ENCLANKVDL SFSPSQSLPA SHAHLRVTAA PQSVCALRAV
 601 DQSVLLMKPD AELSASSVYN LLPEKDLTGF PGPLNDQDDE DCINRHNVYI
 651 NGITYTPVSS TNEKDMYSFL EDMGLKAFTN SKIRKPKMCP QLQQYEMHGP
 701 EGLRVGFYES DVMGRGHARL VHVEEPHTET VRKYFPETWI WDLVVVNSAG
 751 VAEVGVTVPD TITEWKAGAF CLSEDAGLGI SSTASLRAFQ PFFVELTMPY
 801 SVIRGEAFTL KATVLNYLPK CIRVSVQLEA SPAFLAVPVE KEQAPHCICA
 851 NGRQTVSWAV TPKSLGNVNF TVSAEALESQ ELCGTEVPSV PEHGRKDTVI
 901 KPLLVEPEGL EKETTFNSLL CPSGGEVSEE LSLKLPPNVV EESARASVSV
 951 LGDILGSAMQ NTQNLLQMPY GCGEQNMVLF APNIYVLDYL NETQQLTPEV
1001 KSKAIGYLNT GYQRQLNYKH YDGSYSTFGE RYGRNQGNTW LTAFVLKTFA
1051 QARAYIFIDE AHITQALIWL SQRQKDNGCF RSSGSLLNNA IKGGVEDEVT
1101 LSAYITIALL EIPLTVTHPV VRNALFCLES AWKTAQEGDH GSHVYTKALL
1151 AYAFALAGNQ DKRKEVLKSL NEEAVKKDNS VHWERPQKPK APVGHFYEPQ
1201 APSAEVEMTS YVLLAYLTAQ PAPTSEDLTS ATNIVKWITK QQNAQGGFSS
1251 TQDTVVALHA LSKYGAATFT RTGKAAQVTI QSSGTFSSKF QVDNNNRLLL
1301 QQVSLPELPG EYSMKVTGEG CVYLQTSLKY NILPEKEEFP FALGVQTLPQ
1351 TCDEPKAHTS FQISLSVSYT GSRSASNMAI VDVKMVSGFI PLKPTVKMLE
1401 RSNHVSRTEV SSNHVLIYLD KVSNQTLSLF FTVLQDVPVR DLKPAIVKVY
1451 DYYETDEFAI AEYNAPCSKD LGNA
```

Probability Based Mowse Score

Ions score is -10*Log(P), where P is the probability that the observed match is a random event.

Individual ions scores **> 36 indicate identity or extensive homology** (p<0.05).

Protein scores are derived from ions scores as a non-probabilistic basis for ranking protein hits.

Start - End	Observed	Mr(expt)	Mr(calc)	Delta	Miss	Sequence
136 - 145	**560.8100**	**1119.6054**	**1119.6288**	**-0.0234**	**0**	**K.SIYKPGQTVK.F**
(Ions score 19)						
215 - 228	**558.6900**	**1673.0482**	**1671.8508**	**1.1973**	**0**	**R.TEHPFTVEEFVLPK.F**
(Ions score 57)						

320 - 338	704.3100	2109.9082	2109.0702	0.8380	0	K.LHTEAQIQEEGTVVELTGR.Q (Ions score 32)
540 - 557	615.7200	1844.1382	1844.0295	0.1087	0	R.LLIYAVLPTGDVIGDSAK.Y (Ions score 12)
587 - 598	636.8000	1271.5854	1271.6656	-0.0802	0	R.VTAAPQSVCALR.A (Ions score 43)
705 - 715	630.2600	1258.5054	1258.5652	-0.0598	0	R.VGFYESDVMGR.G (Ions score 29)
720 - 732	515.9600	1544.8582	1544.7947	0.0635	0	R.LVHVEEPHTETVR.K (Ions score 15)
812 - 820	509.9000	1017.7854	1017.5859	0.1996	0	K.ATVLNYLPK.C (Ions score 21)
824 - 841	628.6500	1882.9282	1883.0404	-0.1122	0	R.VSVQLEASPAFLAVPVEK.E (Ions score 19)
854 - 863	558.7300	1115.4454	1115.5975	-0.1521	0	R.QTVSWAVTPK.S (Ions score 20)
935 - 945	605.8700	1209.7254	1209.6353	0.0901	0	K.LPPNVVEESAR.A (Ions score 16)
1004 - 1014	628.2600	1254.5054	1254.6357	-0.1302	0	K.AIGYLNTGYQR.Q (Ions score 22)
1020 - 1031	709.7500	1417.4854	1417.5899	-0.1044	0	K.HYDGSYSTFGER.Y (Ions score 21)
1082 - 1092	552.3700	1102.7254	1102.5982	0.1272	0	R.SSGSLLNNAIK.G (Ions score 40)
1148 - 1162	522.7600	1565.2582	1564.8249	0.4333	0	K.ALLAYAFALAGNQDK.R (Ions score 26)
1241 - 1263	796.5400	2386.5982	2386.1877	0.4105	0	K.QQNAQGGFSSTQDTVVALHALSK.Y (Ions score 11)
1298 - 1315	682.3000	2043.8782	2044.0914	-0.2133	0	R.LLLQQVSLPELPGEYSMK.V (Ions score 25)
1408 - 1421	539.9600	1616.8582	1616.8410	0.0172	0	R.TEVSSNHVLIYLDK.V (Ions score 13)

C.8 Prothrombin

Match to: **THRB_HUMAN** Score: **54**
Prothrombin precursor - Homo sapiens (Human)
Found in search of P:\mass spec\Mass spec 27jun08\DP260608\Compounds 260608\6.mgf

Nominal mass (M_r): **71475**; Calculated pI value: **5.64**
NCBI BLAST search of THRB_HUMAN against nr
Unformatted sequence string for pasting into other applications

Taxonomy: Homo sapiens

Fixed modificatihons: Carbamidomethyl (C)
Variable modifications: Oxidation (M)
Cleavage by Trypsin: cuts C-term side of KR unless next residue is P
Sequence Coverage: **15%**

Matched peptides shown in **Bold Red**

```
   1 MAHVRGLQLP GCLALAALCS LVHSQHVFLA PQQARSLLQR VRRANTFLEE
  51 VRKGNLEREC VEETCSYEEA FEALESSTAT DVFWAKYTAC ETARTPRDKL
 101 AACLEGNCAE GLGTNYRGHV NITRSGIECQ LWRSRYPHKP EINSTTHPGA
 151 DLQENFCRNP DSSTTGPWCY TTDPTVRRQE CSIPVCGQDQ VTVAMTPRSE
 201 GSSVNLSPPL EQCVPDRGQQ YQGRLAVTTH GLPCLAWASA QAKALSKHQD
 251 FNSAVQLVEN FCRNPDGDEE GVWCYVAGKP GDFGYCDLNY CEEAVEEETG
 301 DGLDEDSDRA IEGRTATSEY QTFFNPRTFG SGEADCGLRP LFEKKSLEDK
 351 TERELLESYI DGRIVEGSDA EIGMSPWQVM LFRKSPQELL CGASLISDRW
 401 VLTAAHCLLY PPWDKNFTEN DLLVRIGKHS RTRYERNIEK ISMLEKIYIH
 451 PRYNWRENLD RDIALMKLKK PVAFSDYIHP VCLPDRETAA SLLQAGYKGR
 501 VTGWGNLKET WTANVGKGQP SVLQVVNLPI VERPVCKDST RIRITDNMFC
 551 AGYKPDEGKR GDACEGDSGG PFVMKSPFNN RWYQMGIVSW GEGCDRDGKY
 601 GFYTHVFRLK KWIQKVIDQF GE
```

Probability Based Mowse Score

Ions score is -10*Log(P), where P is the probability that the observed match is a random event.

Individual ions scores **> 36 indicate identity or extensive homology** (p<0.05).

Protein scores are derived from ions scores as a non-probabilistic basis for ranking protein hits.

Start - End	Observed	Mr(expt)	Mr(calc)	Delta	Miss	Sequence
225 - 243	665.9500	1994.8282	1994.0408	0.7874	0	R.LAVTTHGLPCLAWASAQAK.A (Ions score 39)
248 - 263	655.6100	1963.8082	1962.9007	0.9075	0	K.HQDFNSAVQLVENFCR.N (Ions score 37)
354 - 363	597.7700	1193.5254	1193.5928	-0.0673	0	R.ELLESYIDGR.I (Ions score 43)
487 - 498	626.2900	1250.5654	1250.6506	-0.0852	0	R.ETAASLLQAGYK.G (Ions score 23)
501 - 508	437.7700	873.5254	873.4709	0.0546	0	R.VTGWGNLK.E (Ions score 17)
518 - 537	744.8300	2231.4682	2231.2460	0.2222	0	K.GQPSVLQVVNLPIVERPVCK.D (Ions score25)
600 - 608	595.2900	1188.5654	1188.5716	-0.0062	0	K.YGFYTHVFR.L (Ions score 24)

C.9 Plasminogen

Match to: **PLMN_HUMAN** Score: **52**
Plasminogen OS=Homo sapiens GN=PLG PE=1 SV=2
Found in search of P:\mass spec\17_6_09\1.mgf

Nominal mass (M_r): **93247**; Calculated pI value: **7.04**
NCBI BLAST search of PLMN_HUMAN against nr
Unformatted sequence string for pasting into other applications

Taxonomy: Homo sapiens

Fixed modifications: Carbamidomethyl (C)
Variable modifications: Oxidation (M)
Cleavage by Trypsin: cuts C-term side of KR unless next residue is P
Sequence Coverage: **4%**

Matched peptides shown in **Bold Red**

```
    1 MEHKEVVLLL LLFLKSGQGE PLDDYVNTQG ASLFSVTKKQ LGAGSIEECA
   51 AKCEEDEEFT CRAFQYHSKE QQCVIMAENR KSSIIIRMRD VVLFEKKVYL
  101 SECKTGNGKN YRGTMSKTKN GITCQKWSST SPHRPRFSPA THPSEGLEEN
  151 YCRNPDNDPQ GPWCYTTDPE KRYDYCDILE CEEECMHCSG ENYDGKISKT
  201 MSGLECQAWD SQSPHAHGYI PSKFPNKNLK KNYCRNPDRE LRPWCFTTDP
  251 NKRWELCDIP RCTTPPPSSG PTYQCLKGTG ENYRGNVAVT VSGHTCQHWS
  301 AQTPHTHNRT PENFPCKNLD ENYCRNPDGK RAPWCHTTNS QVRWEYCKIP
  351 SCDSSPVSTE QLAPTAPPEL TPVVQDCYHG DGQSYRGTSS TTTTGKKCQS
  401 WSSMTPHRHQ KTPENYPNAG LTMNYCRNPD ADKGPWCFTT DPSVRWEYCN
  451 LKKCSGTEAS VVAPPPVVLL PDVETPSEED CMFGNGKGYR GKRATTVTGT
  501 PCQDWAAQEP HRHSIFTPET NPRAGLEKNY CRNPDGDVGG PWCYTTNPRK
  551 LYDYCDVPQC AAPSFDCGKP QVEPKKCPGR VVGGCVAHPH SWPWQVSLRT
  601 RFGMHFCGGT LISPEWVLTA AHCLEKSPRP SSYKVILGAH QEVNLEPHVQ
  651 EIEVSRLFLE PTRKDIALLK LSSPAVITDK VIPACLPSPN YVVADRTECF
  701 ITGWGETQGT FGAGLLKEAQ LPVIENKVCN RYEFLNGRVQ STELCAGHLA
  751 GGTDSCQGDS GGPLVCFEKD KYILQGVTSW GLGCARPNKP GVYVRVSRFV
  801 TWIEGVMRNN
```

Probability Based Mowse Score

Ions score is -10*Log(P), where P is the probability that the observed match is a random event.

Individual ions scores **> 36 indicate identity or extensive homology (p<0.05).**

Protein scores are derived from ions scores as a non-probabilistic basis for ranking protein hits.

Start - End	Observed	Mr(expt)	Mr(calc)	Delta	Miss	Sequence
90 - 96	424.9100	847.8054	848.4644	-0.6589	0	R.DVVLFEK.K (Ions score 12)
513 - 523	649.4200	1296.8254	1297.6415	-0.8160	0	R.HSIFTPETNPR.A (Ions score 42)
513 - 523	649.4400	1296.8654	1297.6415	-0.7760	0	R.HSIFTPETNPR.A (Ions score 28)
513 - 523	433.6900	1298.0482	1297.6415	0.4067	0	R.HSIFTPETNPR.A (Ions score 7)
657 - 663	437.9200	873.8254	874.4912	-0.6658	0	R.LFLEPTR.K (Ions score 31)
657 - 663	437.9300	873.8454	874.4912	-0.6458	0	R.LFLEPTR.K (Ions score 34)
671 - 680	515.4300	1028.8454	1029.5706	-0.7252	0	K.LSSPAVITDK.V (Ions score 42)

C.10 Band 'J'

Peptide score distribution. Ions score is $-10\log(P)$, where P is the probability that the observed match is a random event. Individual ions scores **> 34 indicate identity** or **extensive homology** (p<0.05).

Ig gamma-1 chain C region OS=Homo sapiens GN=IGHG1 PE=1 SV=1
Found in search of P:\mass spec\15_12_09\15dec09\1.mgf

Nominal mass (M_r): **36596**; Calculated pI value: **8.46**
NCBI BLAST search of IGHG1_HUMAN against nr
Unformatted sequence string for pasting into other applications

Taxonomy: Homo sapiens

Fixed modifications: Carbamidomethyl (C)
Variable modifications: Oxidation (M)
Cleavage by Trypsin: cuts C-term side of KR unless next residue is P
Sequence Coverage: **40%**

Matched peptides shown in **Bold Red**

```
     1 ASTKGPSVFP LAPSSKSTSG GTAALGCLVK DYFPEPVTVS WNSGALTSGV
    51 HTFPAVLQSS GLYSLSSVVT VPSSSLGTQT YICNVNHKPS NTKVDKKVEP
   101 KSCDKTHTCP PCPAPELLGG PSVFLFPPKP KDTLMISRTP EVTCVVVDVS
   151 HEDPEVKFNW YVDGVEVHNA KTKPREEQYN STYRVVSVLT VLHQDWLNGK
   201 EYKCKVSNKA LPAPIEKTIS KAKGQPREPQ VYTLPPSRDE LTKNQVSLTC
   251 LVKGFYPSDI AVEWESNGQP ENNYKTTPPV LDSDGSFFLY SKLTVDKSRW
   301 QQGNVFSCSV MHEALHNHYT QKSLSLSPGK
```

Start - End	Observed	Mr(expt)	Mr(calc)	Delta	Miss	Sequence
5 - 16	593.8600	1185.7054	1185.6394	0.0661	0	K.GPSVFPLAPSSK.S (Ions score 48)
17 - 30	661.3600	1320.7054	1320.6708	0.0347	0	K.STSGGTAALGCLVK.D (Ions score 32)
132 - 138	418.3000	834.5854	834.4269	0.1585	0	K.DTLMISR.T (Ions score 31)
132 - 138	426.3400	850.6654	850.4218	0.2436	0	K.DTLMISR.T Oxidation (M) (Ions score 31)
139 - 157	714.0000	2138.9782	2138.0202	0.9580	0	R.TPEVTCVVVDVSHEDPEVK.F (Ions score 13)
158 - 171	839.4600	1676.9054	1676.7947	0.1107	0	K.FNWYVDGVEVHNAK.T (Ions score 36)
158 - 171	560.0600	1677.1582	1676.7947	0.3635	0	K.FNWYVDGVEVHNAK.T (Ions score 37)
158 - 171	560.3200	1677.9382	1676.7947	1.1435	0	K.FNWYVDGVEVHNAK.T (Ions score 50)
185 - 200	603.2700	1806.7882	1806.9992	-0.2111	0	R.VVSVLTVLHQDWLNGK.E (Ions score 21)
210 - 217	419.8200	837.6254	837.4960	0.1295	0	K.ALPAPIEK.T (Ions score 15)
228 - 238	643.7900	1285.5654	1285.6666	-0.1012	0	R.EPQVYTLPPSR.D (Ions score 19)
228 - 238	643.7900	1285.5654	1285.6666	-0.1012	0	R.EPQVYTLPPSR.D (Ions score 21)
228 - 238	643.8100	1285.6054	1285.6666	-0.0612	0	R.EPQVYTLPPSR.D (Ions score 16)

228 - 238	429.6200	1285.8382	1285.6666	0.1715	0	R.EPQVYTLPPSR.D (Ions score 20)
228 - 243	625.1600	1872.4582	1871.9629	0.4953	1	R.EPQVYTLPPSRDELTK.N (Ions score 11)
244 - 253	581.3300	1160.6454	1160.6223	0.0231	0	K.NQVSLTCLVK.G (Ions score 40)
276 - 292	625.3100	1872.9082	1872.9146	-0.0064	0	K.TTPPVLDSDGSFFLYSK.L (Ions score 11)
276 - 292	937.5200	1873.0254	1872.9146	0.1109	0	K.TTPPVLDSDGSFFLYSK.L (Ions score 18)
276 - 292	625.4900	1873.4482	1872.9146	0.5336	0	K.TTPPVLDSDGSFFLYSK.L (Ions score 26)

Match to: **LAC2_HUMAN** Score: **86**
Ig lambda-2 chain C regions OS=Homo sapiens GN=IGLC2 PE=1 SV=1
Found in search of P:\mass spec\27_5_10\8.mgf

Nominal mass (M_r): **11458**; Calculated pI value: **6.92**
NCBI BLAST search of LAC2_HUMAN against nr
Unformatted sequence string for pasting into other applications

Taxonomy: Homo sapiens

Fixed modifications: Carbamidomethyl (C)
Variable modifications: Oxidation (M)
Cleavage by Trypsin: cuts C-term side of KR unless next residue is P
Sequence Coverage: **74%**

Matched peptides shown in **Bold Red**

```
     1 GQPKAAPSVT LFPPSSEELQ ANKATLVCLI SDFYPGAVTV AWKADSSPVK
    51 AGVETTTPSK QSNNKYAASS YLSLTPEQWK SHRSYSCQVT HEGSTVEKTV
   101 APTECS
```

Start - End	Observed	Mr(expt)	Mr(calc)	Delta	Miss	Sequence
5 - 23	662.7600	1985.2582	1985.0105	0.2476	0	K.AAPSVTLFPPSSEELQANK.A (Ions score 18)
5 - 23	662.8400	1985.4982	1985.0105	0.4876	0	K.AAPSVTLFPPSSEELQANK.A (Ions score 23)
5 - 23	662.9900	1985.9482	1985.0105	0.9376	0	K.AAPSVTLFPPSSEELQANK.A (Ions score 19)
24 - 43	738.0700	2211.1882	2210.1446	1.0436	0	K.ATLVCLISDFYPGAVTVAWK.A (Ions score 48)
51 - 60	495.7700	989.5254	989.5029	0.0225	0	K.AGVETTTPSK.Q (Ions score 21)
51 - 60	495.8200	989.6254	989.5029	0.1225	0	K.AGVETTTPSK.Q (Ions score 54)
66 - 80	872.4500	1742.8854	1742.8515	0.0339	0	K.YAASSYLSLTPEQWK.S (Ions score 31)
66 - 80	582.2700	1743.7882	1742.8515	0.9367	0	K.YAASSYLSLTPEQWK.S (Ions score 22)
84 - 98	856.3900	1710.7654	1710.7519	0.0135	0	R.SYSCQVTHEGSTVEK.T (Ions score 42)
84 - 98	571.5400	1711.5982	1710.7519	0.8462	0	R.SYSCQVTHEGSTVEK.T (Ions score 9)

Match to: **IGHG3_HUMAN** Score: **47**
Ig gamma-3 chain C region OS=Homo sapiens GN=IGHG3 PE=1 SV=2
Found in search of P:\mass spec\15_12_09\15dec09\1.mgf

Nominal mass (M_r): **42287**; Calculated pI value: **8.23**
NCBI BLAST search of IGHG3_HUMAN against nr

Unformatted sequence string for pasting into other applications

Taxonomy: Homo sapiens

Fixed modifications: Carbamidomethyl (C)
Variable modifications: Oxidation (M)
Cleavage by Trypsin: cuts C-term side of KR unless next residue is P
Sequence Coverage: **18%**

Matched peptides shown in **Bold Red**

```
     1 ASTKGPSVFP LAPCSRSTSG GTAALGCLVK DYFPEPVTVS WNSGALTSGV
    51 HTFPAVLQSS GLYSLSSVVT VPSSSLGTQT YTCNVNHKPS NTKVDKRVEL
   101 KTPLGDTTHT CPRCPEPKSC DTPPPCPRCP EPKSCDTPPP CPRCPEPKSC
   151 DTPPPCPRCP APELLGGPSV FLFPPKPKDT LMISRTPEVT CVVVDVSHED
   201 PEVQFKWYVD GVEVHNAKTK PREEQYNSTF RVVSVLTVLH QDWLNGKEYK
   251 CKVSNKALPA PIEKTISKTK GQPREPQVYT LPPSREEMTK NQVSLTCLVK
   301 GFYPSDIAVE WESSGQPENN YNTTPPMLDS DGSFFLYSKL TVDKSRWQQG
   351 NIFSCSVMHE ALHNRFTQKS LSLSPGK
```

Start - End	Observed	Mr(expt)	Mr(calc)	Delta	Miss	Sequence
17 - 30	661.3600	1320.7054	1320.6708	0.0347	0	R.STSGGTAALGCLVK.D (Ions score 32)
179 - 185	418.3000	834.5854	834.4269	0.1585	0	K.DTLMISR.T (Ions score 31)
179 - 185	426.3400	850.6654	850.4218	0.2436	0	K.DTLMISR.T Oxidation (M) (Ions score 31)
232 - 247	603.2700	1806.7882	1806.9992	-0.2111	0	R.VVSVLTVLHQDWLNGK.E (Ions score 21)
257 - 264	419.8200	837.6254	837.4960	0.1295	0	K.ALPAPIEK.T (Ions score 15)
275 - 285	643.7900	1285.5654	1285.6666	-0.1012	0	R.EPQVYTLPPSR.E (Ions score 19)
275 - 285	643.7900	1285.5654	1285.6666	-0.1012	0	R.EPQVYTLPPSR.E (Ions score 21)
275 - 285	643.8100	1285.6054	1285.6666	-0.0612	0	R.EPQVYTLPPSR.E (Ions score 16)
275 - 285	429.6200	1285.8382	1285.6666	0.1715	0	R.EPQVYTLPPSR.E (Ions score 20)
275 - 290	635.5400	1903.5982	1903.9349	-0.3368	1	R.EPQVYTLPPSREEMTK.N (Ions score 28)
275 - 290	635.5500	1903.6282	1903.9349	-0.3068	1	R.EPQVYTLPPSREEMTK.N (Ions score 23)
291 - 300	581.3300	1160.6454	1160.6223	0.0231	0	K.NQVSLTCLVK.G (Ions score 40)

Match to: **IGKC_HUMAN** Score: **56**
Ig kappa chain C region OS=Homo sapiens GN=IGKC PE=1 SV=1
Found in search of P:\mass spec\15_12_09\15dec09\1.mgf

Nominal mass (M_r): **11773**; Calculated pI value: **5.58**
NCBI BLAST search of IGKC_HUMAN against nr
Unformatted sequence string for pasting into other applications

Taxonomy: Homo sapiens

Fixed modifications: Carbamidomethyl (C)
Variable modifications: Oxidation (M)
Cleavage by Trypsin: cuts C-term side of KR unless next residue is P
Sequence Coverage: **49%**

Matched peptides shown in **Bold Red**

```
     1 TVAAPSVFIF PPSDEQLKSG TASVVCLLNN FYPREAKVQW KVDNALQSGN
    51 SQESVTEQDS KDSTYSLSST LTLSKADYEK HKVYACEVTH QGLSSPVTKS
   101 FNRGEC
```

Start - End	Observed	Mr(expt)	Mr(calc)	Delta	Miss	Sequence
1 - 18	649.3700	1945.0882	1945.0197	0.0685	0	-
.TVAAPSVFIFPPSDEQLK.S (Ions score 27)						
1 - 18	649.5900	1945.7482	1945.0197	0.7285	0	-
.TVAAPSVFIFPPSDEQLK.S (Ions score 35)						
42 - 61	712.5500	2134.6282	2134.9614	-0.3333	0	
K.VDNALQSGNSQESVTEQDSK.D (Ions score 25)						
62 - 75	751.8600	1501.7054	1501.7512	-0.0457	0	K.DSTYSLSSTLTLSK.A
(Ions score 51)						

Match to: **LAC2_HUMAN** Score: **50**
Ig lambda-2 chain C regions OS=Homo sapiens GN=IGLC2 PE=1 SV=1
Found in search of P:\mass spec\15_12_09\15dec09\1.mgf

Nominal mass (M_r): **11458**; Calculated pI value: **6.92**
NCBI BLAST search of LAC2_HUMAN against nr
Unformatted sequence string for pasting into other applications

Taxonomy: Homo sapiens

Fixed modifications: Carbamidomethyl (C)
Variable modifications: Oxidation (M)
Cleavage by Trypsin: cuts C-term side of KR unless next residue is P
Sequence Coverage: **41%**

Matched peptides shown in **Bold Red**

```
     1 GQPKAAPSVT LFPPSSEELQ ANKATLVCLI SDFYPGAVTV AWKADSSPVK
    51 AGVETTTPSK QSNNKYAASS YLSLTPEQWK SHRSYSCQVT HEGSTVEKTV
   101 APTECS
```

Start - End	Observed	Mr(expt)	Mr(calc)	Delta	Miss	Sequence
5 - 23	662.7000	1985.0782	1985.0105	0.0676	0	
K.AAPSVTLFPPSSEELQANK.A (Ions score 21)						
5 - 23	662.7000	1985.0782	1985.0105	0.0676	0	
K.AAPSVTLFPPSSEELQANK.A (Ions score 16)						
5 - 23	662.9500	1985.8282	1985.0105	0.8176	0	
K.AAPSVTLFPPSSEELQANK.A (Ions score 17)						
51 - 60	495.7500	989.4854	989.5029	-0.0175	0	K.AGVETTTPSK.Q
(Ions score 28)						
51 - 60	495.7700	989.5254	989.5029	0.0225	0	K.AGVETTTPSK.Q
(Ions score 55)						
66 - 80	582.0000	1742.9782	1742.8515	0.1267	0	K.YAASSYLSLTPEQWK.S
(Ions score 18)						

C.11 Cow Fibrinogen α-chain

User : Deepa Patel
Email : d.patel@auckland.ac.nz
Search title :
MS data file : P:\mass spec\Mass spec 29july08\New Folder\5.mgf
Database : SwissProt 56.0 (392667 sequences; 141217034 residues)
Taxonomy : Mammalia (mammals) (63154 sequences)
Timestamp : 13 Aug 2008 at 06:42:37 GMT
Protein hits : FIBA_BOVI Fibrinogen alpha chain OS=Bos taurus GN=FGA PE=1 **N** SV=5

Probability Based Mowse Score

Ions score is -10*Log(P), where P is the probability that the observed match is a random event.

Individual ions scores > 40 indicate identity or extensive homology (p<0.05).

Protein scores are derived from ions scores as a non-probabilistic basis for ranking protein hits.

Match to: **FIBA_BOVIN** Score: **260**
Fibrinogen alpha chain OS=Bos taurus GN=FGA PE=1 SV=5
Found in search of P:\mass spec\Mass spec 29july08\New Folder\5.mgf

Nominal mass (M_r): **67484**; Calculated pI value: **6.73**
NCBI BLAST search of FIBA_BOVIN against nr
Unformatted sequence string for pasting into other applications

Taxonomy: Bos taurus

Fixed modifications: Carbamidomethyl (C)
Variable modifications: Oxidation (M)
Cleavage by Trypsin: cuts C-term side of KR unless next residue is P
Sequence Coverage: **39%**

Matched peptides shown in **Bold Red**

```
     1 MFSVRDLCLV LSLVGAIKTE DGSDPPSGDF LTEGGGVRGP RLVERQQSAC
    51 KETGWPFCSD EDWNTKCPSG CRMKGLIDEV DQDFTSRINK LRDSLFNYQK
   101 NSKDSNTLTK NIVELMRGDF AKANNNDNTF KQISEDLRSR IEILRRKVIE
   151 QVQRIKVLQK NVRDQLVDMK RLEVDIDIKI RSCKGSCSRA LEHKVDLEDY
   201 KNQQKQLEQV IAINLLPSRD IQYLPLIKMS TITGPVPREF KSQLQEAPLE
   251 WKALLEMQQT KMVLETFGGD GHARGDSVSQ GTGLAPGSPR KPGTSSIGNV
   301 NPGSYGPGSS GTWNPGRPEP GSAGTWNPGR PEPGSAGTWN PGRPEPGSAG
   351 TWNPGRPEPG SAGTWNPGRP EPGSAGTWNT GSSGSSSFRP DSSGHGNIRP
   401 SSPDWGTFRE EGSVSSGTKQ EFHTGKLVTT KGDKELLIDN EKVTSGHTTT
   451 TRRSCSKVIT KTVTNADGRT ETTKEVVKSE DGSDCGDADF DWHHTFPSRG
   501 NLDDFFHRDK DDFFTRSSHE FDGRTGLAPE FAALGESGSS SSKTSTHSKQ
   551 FVSSSTTVNR GGSAIESKHF KMEDEAESLE DLGFKGAHGT QKGHTKARPA
   601 RGIHTSPLGE PSLTP
```

C.12 Sheep Fibrinogen β-chain

User : **Deepa Patel**
Email : **d.patel@auckland.ac.nz**
Search title :
MS data file : **P:\mass spec\Mass spec 29july08\New Folder\13.mgf**
Database : **SwissProt 56.0 (392667 sequences; 141217034 residues)**
Taxonomy : **Mammalia (mammals) (63154 sequences)**
Timestamp : **13 Aug 2008 at 06:45:29 GMT**
Protein hits : **FIBG_BOVI** Fibrinogen gamma-B chain OS=Bos taurus GN=FGG PE=1 SV=1

Probability Based Mowse Score

Ions score is -10*Log(P), where P is the probability that the observed match is a random event.

Individual ions scores **> 40 indicate identity or extensive homology** (p<0.05).

Protein scores are derived from ions scores as a non-probabilistic basis for ranking protein hits.

1. FIBG_BOVIN **Mass:** 50850 **Score:** 102 **Queries matched:** 7 **emPAI:** 0.18
Fibrinogen gamma-B chain OS=Bos taurus GN=FGG PE=1 SV=1

Query	Observed	Mr(expt)	Mr(calc)	Delta	Miss	Score	Expect	Rank	Peptide
14	399.1900	796.3654	796.4192	-0.0537	0	26	2	1	K.IHDVTGR.D
134	541.4100	1080.8054	1080.5200	0.2855	1	77	1e-05	1	K.VTGENDKYR.L
136	545.9200	1089.8254	1089.4978	0.3276	0	52	0.0039	1	R.TSTADYASFK.V
145	566.3600	1130.7054	1129.5516	1.1538	0	26	1.7	1	R.IQLEDWNGR.T
207	661.9100	1321.8054	1321.7394	0.0661	0	36	0.14	1	K.ESGLYFIRPLK.A
208	661.9400	1321.8654	1321.7394	0.1261	0	(31)	0.4	1	K.ESGLYFIRPLK.A
41	441.8200	1322.4382	1321.7394	0.6988	0	(23)	3.4	1	K.ESGLYFIRPLK.A

C.13 Mouse Fibrinogen β-chain

User : Deepa Patel
Email : d.patel@auckland.ac.nz
Search title :
MS data file : P:\mass spec\250708\DP250708\exported compounds\25708 9.mgf
Database : SwissProt 56.0 (392667 sequences; 141217034 residues)
Taxonomy : Mus musculus (house mouse) (15819 sequences)
Timestamp : 30 Jul 2008 at 00:38:04 GMT
Protein hits : FIBB_MOUS Fibrinogen beta chain OS=Mus musculus GN=Fgb PE=2 **E** SV=1

Match to: **FIBB_MOUSE** Score: **228**
Fibrinogen beta chain OS=Mus musculus GN=Fgb PE=2 SV=1
Found in search of P:\mass spec\250708\DP250708\exported compounds\25708 9.mgf

Nominal mass (M_r): **55402**; Calculated pI value: **6.68**
NCBI BLAST search of FIBB_MOUSE against nr
Unformatted sequence string for pasting into other applications

Taxonomy: Mus musculus

Fixed modifications: Carbamidomethyl (C)
Variable modifications: Oxidation (M)
Cleavage by Trypsin: cuts C-term side of KR unless next residue is P
Sequence Coverage: **44%**

Matched peptides shown in **Bold Red**

```
     1 MRHLWLLLLL CVFSVQTQAA DDDYDEPTDS LDARGHRPVD RRKEEPPSLR
    51 PAPPPISGGG YRARPAKATA NQKKVERRPP DAGGCLHADT DMGVLCPTGC
   101 TLQQTLLNQE RPIKSSIAEL NNNIQSVSDT SSVTFQYLTL LKDMWKKKQA
   151 QVKENENVIN EYSSILEDQR LYIDETVNDN IPLNLRVLRS ILEDLRSKIQ
   201 KLESDISAQM EYCRTPCTVS CNIPVVSGKE CEEIIRKGGE TSEMYLIQPD
   251 TSIKPYRVYC DMKTENGGWT VIQNRQDGSV DFGRKWDPYK KGFGNIATNE
   301 DAKKYCGLPG EYWLGNDKIS QLTRMGPTEL LIEMEDWKGD KVKAHYGGFT
   351 VQNEASKYQV SVNKYKGTAG NALMDGASQL VGENRTMTIH NGMFFSTYDR
   401 DNDGWVTTDP RKQCSKEDGG GWWYNRCHAA NPNGRYYWGG LYSWDMSKHG
   451 TDDGVVWMNW KGSWYSMRRM SMKIRPFFPQ Q
```

Probability Based Mowse Score

Ions score is -10*Log(P), where P is the probability that the observed match is a random event.

Individual ions scores > **35 indicate identity or extensive homology** (p<0.05).

Protein scores are derived from ions scores as a non-probabilistic basis for ranking protein hits.

Start - End	Observed	Mr(expt)	Mr(calc)	Delta	Miss	Sequence
44 - 62	659.9800	1976.9182	1976.0116	0.9066	0	K.EEPPSLRPAPPPISGGGYR.A (Ions score 30)
154 - 170	684.7600	2051.2582	2050.9443	0.3139	0	K.ENENVINEYSSILEDQR.L (Ions score 40)
171 - 186	951.4900	1900.9654	1900.9894	-0.0240	0	R.LYIDETVNDNIPLNLR.V (Ions score 24)
171 - 186	634.9600	1901.8582	1900.9894	0.8688	0	R.LYIDETVNDNIPLNLR.V (Ions score 25)

190 - 196 **423.4200** **844.8254** **844.4654** **0.3600** **0** **R.SILEDLR.S** (Ions score 34)
202 - 214 **809.3600** **1616.7054** **1616.6810** **0.0244** **0** **K.LESDISAQMEYCR.T** Oxidation (M) (Ions score 44)
215 - 229 **809.8600** **1617.7054** **1617.7855** **-0.0800** **0** **R.TPCTVSCNIPVVSGK.E** (Ions score 21)
230 - 236 **474.9000** **947.7854** **947.4382** **0.3472** **0** **K.ECEEIIR.K** (Ions score 29)
237 - 257 **810.3900** **2428.1482** **2428.1944** **-0.0462** **1** **R.KGGETSEMYLIQPDTSIKPYR.V** Oxidation (M) (Ions score 4)
238 - 257 **767.7100** **2300.1082** **2300.0994** **0.0087** **0** **K.GGETSEMYLIQPDTSIKPYR.V** Oxidation (M) (Ions score 55)
264 - 275 **687.9200** **1373.8254** **1373.6688** **0.1567** **0** **K.TENGGWTVIQNR.Q** (Ions score 40)
264 - 275 **687.9400** **1373.8654** **1373.6688** **0.1967** **0** **K.TENGGWTVIQNR.Q** (Ions score 47)
264 - 275 **688.3100** **1374.6054** **1373.6688** **0.9367** **0** **K.TENGGWTVIQNR.Q** (Ions score 49)
264 - 275 **688.3400** **1374.6654** **1373.6688** **0.9967** **0** **K.TENGGWTVIQNR.Q** (Ions score 50)
276 - 284 **490.8900** **979.7654** **979.4359** **0.3295** **0** **R.QDGSVDFGR.K** (Ions score 34)
319 - 324 **359.4600** **716.9054** **716.4181** **0.4874** **0** **K.ISQLTR.M** (Ions score 30)
325 - 338 **575.3700** **1723.0882** **1722.7844** **0.3037** **0** **R.MGPTELLIEMEDWK.G** 2 Oxidation (M) (Ions score 23)
325 - 341 **670.2100** **2007.6082** **2006.9329** **0.6753** **1** **R.MGPTELLIEMEDWKGDK.V** Oxidation (M) (Ions score 22)
344 - 357 **754.9000** **1507.7854** **1507.7056** **0.0799** **0** **K.AHYGGFTVQNEASK.Y** (Ions score 50)
344 - 357 **503.7000** **1508.0782** **1507.7056** **0.3726** **0** **K.AHYGGFTVQNEASK.Y** (Ions score 23)
401 - 411 **638.3600** **1274.7054** **1274.5528** **0.1527** **0** **R.DNDGWVTTDPR.K** (Ions score 35)
417 - 426 **620.3200** **1238.6254** **1238.5105** **0.1150** **0** **K.EDGGGWWYNR.C** (Ions score 14)
449 - 461 **772.7600** **1543.5054** **1543.6878** **-0.1824** **0** **K.HGTDDGVVWMNWK.G** (Ions score 40)
449 - 461 **515.6900** **1544.0482** **1543.6878** **0.3604** **0** **K.HGTDDGVVWMNWK.G** (Ions score 25)
449 - 461 **780.8500** **1559.6854** **1559.6827** **0.0027** **0** **K.HGTDDGVVWMNWK.G** Oxidation (M) (Ions score 29)
449 - 461 **521.0800** **1560.2182** **1559.6827** **0.5354** **0** **K.HGTDDGVVWMNWK.G** Oxidation (M) (Ions score 39)
474 - 481 **516.9300** **1031.8454** **1031.5553** **0.2902** **0** **K.IRPFFPQQ.-** (Ions score 27)

C.14 Mouse Fibrinogen γ-chain

User : Deepa Patel
Email : d.patel@auckland.ac.nz
Search title :
MS data file : P:\mass spec\250708\DP250708\exported compounds\250708 10.mgf
Database : SwissProt 56.0 (392667 sequences; 141217034 residues)
Taxonomy : Mus musculus (house mouse) (15819 sequences)
Timestamp : 30 Jul 2008 at 00:41:17 GMT
Protein hits : FIBG_MOUS Fibrinogen gamma chain OS=Mus musculus GN=Fgg PE=2 **E** SV=1

Probability Based Mowse Score

Ions score is -10*Log(P), where P is the probability that the observed match is a random event.

Individual ions scores **> 35 indicate identity or extensive homology** (p<0.05).

Protein scores are derived from ions scores as a non-probabilistic basis for ranking protein hits.

Match to: **FIBG_MOUSE** Score: **199**
Fibrinogen gamma chain OS=Mus musculus GN=Fgg PE=2 SV=1
Found in search of P:\mass spec\250708\DP250708\exported compounds\250708 10.mgf

Nominal mass (M_r): **50044**; Calculated pI value: **5.54**
NCBI BLAST search of FIBG_MOUSE against nr
Unformatted sequence string for pasting into other applications

Taxonomy: Mus musculus

Fixed modifications: Carbamidomethyl (C)
Variable modifications: Oxidation (M)
Cleavage by Trypsin: cuts C-term side of KR unless next residue is P
Sequence Coverage: **43%**

Matched peptides shown in **Bold Red**

```
     1 MSWSLQPPSF LLCCLLLLFS PTGLAYVATR DNCCILDERF GSFCPTTCGI
    51 ADFLSSYQTD VDNDLRTLED ILFRAENRTT EAKELIKAIQ VYYNPDQPPK
   101 PGMIDSATQK SKKMVEEIVK YEALLLTHET SIRYLQEIYN SNNQKITNLK
   151 QKVAQLEAQC QEPCKDSVQI HDTTGKDCQE IANKGAKESG LYFIRPLKAK
   201 QQFLVYCEID GSGNGWTVLQ KRIDGSLDFK KNWIQYKEGF GHLSPTGTTE
   251 FWLGNEKIHL ISMQSTIPYA LRIQLKDWNG RTSTADYAMF RVGPESDKYR
   301 LTYAYFIGGD AGDAFDGYDF GDDPSDKFFT SHNGMQFSTW DNDNDKFEGN
   351 CAEQDGSGWW MNKCHAGHLN GVYHQGGTYS KSSTTNGFDD GIIWATWKSR
   401 WYSMKETTMK IIPFNRLSIG EGQQHHMGGS KQAGDV
```

Start - End	Observed	Mr(expt)	Mr(calc)	Delta	Miss	Sequence
31 - 39	597.7900	1193.5654	1193.4805	0.0849	0	R.DNCCILDER.F (Ions score 55)
67 - 74	503.9700	1005.9254	1005.5495	0.3760	0	R.TLEDILFR.A (Ions score 51)
88 - 110	860.0500	2577.1282	2576.2581	0.8701	0	K.AIQVYYNPDQPPKPGMIDSATQK.S Oxidation (M) (Ions score 24)
114 - 120	432.3800	862.7454	862.4470	0.2985	0	K.MVEEIVK.Y Oxidation (M) (Ions score 18)

121 - 133 773.4600 1544.9054 1544.8198 0.0856 0 K.YEALLLTHETSIR.Y (Ions score 48)
134 - 145 757.4600 1512.9054 1512.7208 0.1846 0 R.YLQEIYNSNNQK.I (Ions score 40)
146 - 150 294.8500 587.6854 587.3642 0.3212 0 K.ITNLK.Q (Ions score 18)
188 - 198 661.8900 1321.7654 1321.7394 0.0261 0 K.ESGLYFIRPLK.A (Ions score 19)
188 - 198 661.9500 1321.8854 1321.7394 0.1461 0 K.ESGLYFIRPLK.A (Ions score 32)
188 - 198 441.8800 1322.6182 1321.7394 0.8788 0 K.ESGLYFIRPLK.A (Ions score 28)
223 - 230 447.9400 893.8654 893.4494 0.4160 0 R.IDGSLDFK.K (Ions score 38)
238 - 257 736.7300 2207.1682 2206.0331 1.1351 0 K.EGFGHLSPTGTTEFWLGNEK.I (Ions score 36)
258 - 272 581.7000 1742.0782 1741.9549 0.1233 0 K.IHLISMQSTIPYALR.I (Ions score 12)
258 - 272 581.7400 1742.1982 1741.9549 0.2433 0 K.IHLISMQSTIPYALR.I (Ions score 8)
258 - 272 587.3700 1759.0882 1757.9498 1.1384 0 K.IHLISMQSTIPYALR.I Oxidation (M) (Ions score 23)
282 - 291 581.8300 1161.6454 1161.5125 0.1330 0 R.TSTADYAMFR.V (Ions score 44)
282 - 291 581.8300 1161.6454 1161.5125 0.1330 0 R.TSTADYAMFR.V (Ions score 42)
282 - 291 589.8400 1177.6654 1177.5074 0.1581 0 R.TSTADYAMFR.V Oxidation (M) (Ions score 40)
292 - 300 525.8800 1049.7454 1049.5142 0.2313 1 R.VGPESDKYR.L (Ions score 71)
382 - 398 633.3400 1896.9982 1897.8847 -0.8865 0 K.SSTTNGFDDGIIWATWK.S (Ions score 13)
399 - 405 479.1800 956.3454 956.4538 -0.1083 1 K.SRWYSMK.E (Ions score 17)
417 - 431 791.4400 1580.8654 1580.7365 0.1289 0 R.LSIGEGQQHHMGGSK.Q Oxidation (M) (Ions score 10)
417 - 431 528.0800 1581.2182 1580.7365 0.4816 0 R.LSIGEGQQHHMGGSK.Q Oxidation (M) (Ions score 26)

C.15 Baboon IgG

User : Deepa Patel
Email : d.patel@auckland.ac.nz
Search title :
MS data file : P:\mass spec\250708\DP250708\exported compounds\250708 15.mgf
Database : SwissProt 56.0 (392667 sequences; 141217034 residues)
Taxonomy : Primates (26514 sequences)
Timestamp : 28 Jul 2008 at 23:51:51 GMT
Protein hits : IGHG2_HUMAN Ig gamma-2 chain C region OS=Homo sapiens GN=IGHG2 AN PE=1 SV=1
IGHG1_HUMAN Ig gamma-1 chain C region OS=Homo sapiens GN=IGHG1 AN PE=1 SV=1

Probability Based Mowse Score

Ions score is -10*Log(P), where P is the probability that the observed match is a random event. Individual ions scores > 37 indicate identity or extensive homology (p<0.05). Protein scores are derived from ions scores as a non-probabilistic basis for ranking protein hits.

Match to: **IGHG2_HUMAN** Score: **66**
Ig gamma-2 chain C region OS=Homo sapiens GN=IGHG2 PE=1 SV=1
Found in search of P:\mass spec\250708\DP250708\exported compounds\250708 15.mgf

Nominal mass (M_r): **36489**; Calculated pI value: **7.66**
NCBI BLAST search of IGHG2_HUMAN against nr
Unformatted sequence string for pasting into other applications

Taxonomy: Homo sapiens

Fixed modifications: Carbamidomethyl (C)
Variable modifications: Oxidation (M)
Cleavage by Trypsin: cuts C-term side of KR unless next residue is P
Sequence Coverage: **12%**

Matched peptides shown in **Bold Red**

```
     1 ASTKGPSVFP LAPCSRSTSE STAALGCLVK DYFPEPVTVS WNSGALTSGV
    51 HTFPAVLQSS GLYSLSSVVT VPSSNFGTQT YTCNVDHKPS NTKVDKTVER
   101 KCCVECPPCP APPVAGPSVF LFPPKPKDTL MISRTPEVTC VVVDVSHEDP
   151 EVQFNWYVDG VEVHNAKTKP REEQFNSTFR VVSVLTVVHQ DWLNGKEYKC
   201 KVSNKGLPAP IEKTISKTKG QPREPQVYTL PPSREEMTKN QVSLTCLVKG
   251 FYPSDIAVEW ESNGQPENNY KTTPPMLDSD GSFFLYSKLT VDKSRWQQGN
   301 VFSCSVMHEA LHNHYTQKSL SLSPGK
```

Start - End	Observed	Mr(expt)	Mr(calc)	Delta	Miss	Sequence
17 - 30 (Ions score 56)	712.4400	1422.8654	1422.7024	0.1630	0	R.STSESTAALGCLVK.D
17 - 30 (Ions score 18)	475.4800	1423.4182	1422.7024	0.7157	0	R.STSESTAALGCLVK.D

128 - 134 418.3600 834.7054 834.4269 0.2785 0 K.DTLMISR.T (Ions score 35)
128 - 134 426.4100 850.8054 850.4218 0.3836 0 K.DTLMISR.T Oxidation (M) (Ions score 35)
224 - 234 643.9300 1285.8454 1285.6666 0.1788 0 R.EPQVYTLPPSR.E (Ions score 23)
224 - 234 643.9400 1285.8654 1285.6666 0.1988 0 R.EPQVYTLPPSR.E (Ions score 18)
224 - 234 429.7100 1286.1082 1285.6666 0.4415 0 R.EPQVYTLPPSR.E (Ions score 12)
240 - 249 581.4000 1160.7854 1160.6223 0.1631 0 K.NQVSLTCLVK.G (Ions score 40)

Match to: **IGHG1_HUMAN** Score: **51**
Ig gamma-1 chain C region OS=Homo sapiens GN=IGHG1 PE=1 SV=1
Found in search of P:\mass spec\250708\DP250708\exported compounds\250708 15.mgf

Nominal mass (M_r): **36596**; Calculated pI value: **8.46**
NCBI BLAST search of IGHG1_HUMAN against nr
Unformatted sequence string for pasting into other applications

Taxonomy: Homo sapiens

Fixed modifications: Carbamidomethyl (C)
Variable modifications: Oxidation (M)
Cleavage by Trypsin: cuts C-term side of KR unless next residue is P
Sequence Coverage: **13%**

Matched peptides shown in **Bold Red**

```
   1 ASTKGPSVFP LAPSSKSTSG GTAALGCLVK DYFPEPVTVS WNSGALTSGV
  51 HTFPAVLQSS GLYSLSSVVT VPSSSLGTQT YICNVNHKPS NTKVDKKVEP
 101 KSCDKTHTCP PCPAPELLGG PSVFLFPPKP KDTLMISRTP EVTCVVVDVS
 151 HEDPEVKFNW YVDGVEVHNA KTKPREEQYN STYRVVSVLT VLHQDWLNGK
 201 EYKCKVSNKA LPAPIEKTIS KAKGQPREPQ VYTLPPSRDE LTKNQVSLTC
 251 LVKGFYPSDI AVEWESNGQP ENNYKTTPPV LDSDGSFFLY SKLTVDKSRW
 301 QQGNVFSCSV MHEALHNHYT QKSLSLSPGK
```

Start - End	Observed	Mr(expt)	Mr(calc)	Delta	Miss	Sequence
132 - 138	418.3600	834.7054	834.4269	0.2785	0	K.DTLMISR.T (Ions score 35)
132 - 138	426.4100	850.8054	850.4218	0.3836	0	K.DTLMISR.T Oxidation (M) (Ions score 35)
158 - 175	721.0200	2160.0382	2159.0912	0.9470	1	K.FNWYVDGVEVHNAKTKPR.E (Ions score 40)
228 - 238	643.9300	1285.8454	1285.6666	0.1788	0	R.EPQVYTLPPSR.D (Ions score 23)
228 - 238	643.9400	1285.8654	1285.6666	0.1988	0	R.EPQVYTLPPSR.D (Ions score 18)
228 - 238	429.7100	1286.1082	1285.6666	0.4415	0	R.EPQVYTLPPSR.D (Ions score 12)
244 - 253	581.4000	1160.7854	1160.6223	0.1631	0	K.NQVSLTCLVK.G (Ions score 40)

C.16 Chimpanzee IgG

User : Deepa Patel
Email : d.patel@auckland.ac.nz
Search title :
MS data file : P:\mass spec\250708\DP250708\exported compounds\250708 14.mgf
Database : SwissProt 56.0 (392667 sequences; 141217034 residues)
Taxonomy : Primates (26514 sequences)
Timestamp : 28 Jul 2008 at 23:57:49 GMT
Protein hits : IGHG1_HUMAN Ig gamma-1 chain C region OS=Homo sapiens GN=IGHG1 AN PE=1 SV=1
IGHG3_HUMAN Ig gamma-3 chain C region OS=Homo sapiens GN=IGHG3 AN PE=1 SV=2

Probability Based Mowse Score

Ions score is -10*Log(P), where P is the probability that the observed match is a random event.

Individual ions scores **> 37 indicate identity or extensive homology** (p<0.05).

Protein scores are derived from ions scores as a non-probabilistic basis for ranking protein hits.

Match to: **IGHG1_HUMAN** Score: **204**
Ig gamma-1 chain C region OS=Homo sapiens GN=IGHG1 PE=1 SV=1
Found in search of P:\mass spec\250708\DP250708\exported compounds\250708 14.mgf

Nominal mass (M_r): **36596**; Calculated pI value: **8.46**
NCBI BLAST search of IGHG1_HUMAN against nr
Unformatted sequence string for pasting into other applications

Taxonomy: Homo sapiens

Fixed modifications: Carbamidomethyl (C)
Variable modifications: Oxidation (M)
Cleavage by Trypsin: cuts C-term side of KR unless next residue is P
Sequence Coverage: **37%**

Matched peptides shown in **Bold Red**

```
     1 ASTKGPSVFP LAPSSKSTSG GTAALGCLVK DYFPEPVTVS WNSGALTSGV
    51 HTFPAVLQSS GLYSLSSVVT VPSSSLGTQT YICNVNHKPS NTKVDKKVEP
   101 KSCDKTHTCP PCPAPELLGG PSVFLFPPKP KDTLMISRTP EVTCVVVDVS
   151 HEDPEVKFNW YVDGVEVHNA KTKPREEQYN STYRVVSVLT VLHQDWLNGK
   201 EYKCKVSNKA LPAPIEKTIS KAKGQPREPQ VYTLPPSRDE LTKNQVSLTC
   251 LVKGFYPSDI AVEWESNGQP ENNYKTTPPV LDSDGSFFLY SKLTVDKSRW
   301 QQGNVFSCSV MHEALHNHYT QKSLSLSPGK
```

Start - End	Observed	Mr(expt)	Mr(calc)	Delta	Miss	Sequence
5 - 16 (Ions score 48)	593.9100	1185.8054	1185.6394	0.1661	0	K.GPSVFPLAPSSK.S
5 - 16 (Ions score 39)	594.0200	1186.0254	1185.6394	0.3861	0	K.GPSVFPLAPSSK.S
5 - 16 (Ions score 48)	594.0700	1186.1254	1185.6394	0.4861	0	K.GPSVFPLAPSSK.S

17 - 30	661.4000	1320.7854	1320.6708	0.1147	0	K.STSGGTAALGCLVK.D (Ions score 60)
132 - 138	418.3500	834.6854	834.4269	0.2585	0	K.DTLMISR.T (Ions score 26)
132 - 138	426.3800	850.7454	850.4218	0.3236	0	K.DTLMISR.T Oxidation (M) (Ions score 35)
139 - 157	713.9700	2138.8882	2138.0202	0.8680	0	R.TPEVTCVVVDVSHEDPEVK.F (Ions score 30)
158 - 171	839.4400	1676.8654	1676.7947	0.0707	0	K.FNWYVDGVEVHNAK.T (Ions score 23)
158 - 171	839.4700	1676.9254	1676.7947	0.1307	0	K.FNWYVDGVEVHNAK.T (Ions score 74)
158 - 171	560.1600	1677.4582	1676.7947	0.6635	0	K.FNWYVDGVEVHNAK.T (Ions score 24)
158 - 171	560.2900	1677.8482	1676.7947	1.0535	0	K.FNWYVDGVEVHNAK.T (Ions score 46)
185 - 200	603.4000	1807.1782	1806.9992	0.1789	0	R.VVSVLTVLHQDWLNGK.E (Ions score 8)
185 - 200	904.6300	1807.2454	1806.9992	0.2462	0	R.VVSVLTVLHQDWLNGK.E (Ions score 19)
185 - 200	603.7400	1808.1982	1806.9992	1.1989	0	R.VVSVLTVLHQDWLNGK.E (Ions score 10)
228 - 238	643.8500	1285.6854	1285.6666	0.0188	0	R.EPQVYTLPPSR.D (Ions score 12)
228 - 238	644.0100	1286.0054	1285.6666	0.3388	0	R.EPQVYTLPPSR.D (Ions score 11)
228 - 243	936.9900	1871.9654	1871.9629	0.0026	1	R.EPQVYTLPPSRDELTK.N (Ions score 13)
228 - 243	625.0800	1872.2182	1871.9629	0.2553	1	R.EPQVYTLPPSRDELTK.N (Ions score 10)
228 - 243	625.0900	1872.2482	1871.9629	0.2853	1	R.EPQVYTLPPSRDELTK.N (Ions score 16)
228 - 243	625.3800	1873.1182	1871.9629	1.1553	1	R.EPQVYTLPPSRDELTK.N (Ions score 15)
244 - 253	581.4300	1160.8454	1160.6223	0.2231	0	K.NQVSLTCLVK.G (Ions score 49)
276 - 292	937.5700	1873.1254	1872.9146	0.2109	0	K.TTPPVLDSDGSFFLYSK.L (Ions score 21)
276 - 292	625.5100	1873.5082	1872.9146	0.5936	0	K.TTPPVLDSDGSFFLYSK.L (Ions score 37)

Match to: **IGHG3_HUMAN** Score: **87**
Ig gamma-3 chain C region OS=Homo sapiens GN=IGHG3 PE=1 SV=2
Found in search of P:\mass spec\250708\DP250708\exported compounds\250708 14.mgf

Nominal mass (M_r): **42287**; Calculated pI value: **8.23**
NCBI BLAST search of IGHG3_HUMAN against nr
Unformatted sequence string for pasting into other applications

Taxonomy: Homo sapiens

Fixed modifications: Carbamidomethyl (C)
Variable modifications: Oxidation (M)
Cleavage by Trypsin: cuts C-term side of KR unless next residue is P
Sequence Coverage: **18%**

Matched peptides shown in **Bold Red**

```
   1 ASTKGPSVFP LAPCSRSTSG GTAALGCLVK DYFPEPVTVS WNSGALTSGV
  51 HTFPAVLQSS GLYSLSSVVT VPSSSLGTQT YTCNVNHKPS NTKVDKRVEL
 101 KTPLGDTTHT CPRCPEPKSC DTPPPCPRCP EPKSCDTPPP CPRCPEPKSC
 151 DTPPPCPRCP APELLGGPSV FLFPPKPKDT LMISRTPEVT CVVVDVSHED
 201 PEVQFKWYVD GVEVHNAKTK PREEQYNSTF RVVSVLTVLH QDWLNGKEYK
 251 CKVSNKALPA PIEKTISKTK GQPREPQVYT LPPSREEMTK NQVSLTCLVK
 301 GFYPSDIAVE WESSGQPENN YNTTPPMLDS DGSFFLYSKL TVDKSRWQQG
 351 NIFSCSVMHE ALHNRFTQKS LSLSPGK
```

Start - End	Observed	Mr(expt)	Mr(calc)	Delta	Miss	Sequence
5 - 16	644.3200	1286.6254	1286.6442	-0.0187	0	K.GPSVFPLAPCSR.S (Ions score 32)
17 - 30	661.4000	1320.7854	1320.6708	0.1147	0	R.STSGGTAALGCLVK.D (Ions score 60)
179 - 185	418.3500	834.6854	834.4269	0.2585	0	K.DTLMISR.T (Ions score 26)
179 - 185	426.3800	850.7454	850.4218	0.3236	0	K.DTLMISR.T Oxidation (M) (Ions score 35)
232 - 247	603.4000	1807.1782	1806.9992	0.1789	0	R.VVSVLTVLHQDWLNGK.E (Ions score 8)
232 - 247	904.6300	1807.2454	1806.9992	0.2462	0	R.VVSVLTVLHQDWLNGK.E (Ions score 19)
232 - 247	603.7400	1808.1982	1806.9992	1.1989	0	R.VVSVLTVLHQDWLNGK.E (Ions score 10)
275 - 285	643.8500	1285.6854	1285.6666	0.0188	0	R.EPQVYTLPPSR.E (Ions score 12)
275 - 285	644.0100	1286.0054	1285.6666	0.3388	0	R.EPQVYTLPPSR.E (Ions score 11)
291 - 300	581.4300	1160.8454	1160.6223	0.2231	0	K.NQVSLTCLVK.G (Ions score 49)

C.17 BaCl-precipitated Prothrombin

Match to: **THRB_HUMAN** Score: **789**
Prothrombin OS=Homo sapiens GN=F2 PE=1 SV=2
Found in search of P:\mass spec\160409\mass spec 16apr09\6.mgf

Nominal mass (M_r): **71475**; Calculated pI value: **5.64**
NCBI BLAST search of THRB_HUMAN against nr
Unformatted sequence string for pasting into other applications

Taxonomy: Homo sapiens

Fixed modifications: Carbamidomethyl (C)
Variable modifications: Oxidation (M)
Cleavage by Trypsin: cuts C-term side of KR unless next residue is P
Sequence Coverage: **55%**

Matched peptides shown in **Bold Red**

```
    1 MAHVRGLQLP GCLALAALCS LVHSQHVFLA PQQARSLLQR VRRANTFLEE
   51 VRKGNLEREC VEETCSYEEA FEALESSTAT DVFWAKYTAC ETARTPRDKL
  101 AACLEGNCAE GLGTNYRGHV NITRSGIECQ LWRSRYPHKP EINSTTHPGA
  151 DLQENFCRNP DSSTTGPWCY TTDPTVRRQE CSIPVCGQDQ VTVAMTPRSE
  201 GSSVNLSPPL EQCVPDRGQQ YQGRLAVTTH GLPCLAWASA QAKALSKHQD
  251 FNSAVQLVEN FCRNPDGDEE GVWCYVAGKP GDFGYCDLNY CEEAVEEETG
  301 DGLDEDSDRA IEGRTATSEY QTFFNPRTFG SGEADCGLRP LFEKKSLEDK
  351 TERELLESYI DGRIVEGSDA EIGMSPWQVM LFRKSPQELL CGASLISDRW
  401 VLTAAHCLLY PPWDKNFTEN DLLVRIGKHS RTRYERNIEK ISMLEKIYIH
  451 PRYNWRENLD RDIALMKLKK PVAFSDYIHP VCLPDRETAA SLLQAGYKGR
  501 VTGWGNLKET WTANVGKGQP SVLQVVNLPI VERPVCKDST RIRITDNMFC
  551 AGYKPDEGKR GDACEGDSGG PFVMKSPFNN RWYQMGIVSW GEGCDRDGKY
  601 GFYTHVFRLK KWIQKVIDQF GE
```

Start - End	Observed	Mr(expt)	Mr(calc)	Delta	Miss	Sequence
87 - 94	486.3100	970.6054	970.4178	0.1876	0	K.YTACETAR.T (Ions score 35)
98 - 117	738.3800	2212.1182	2211.0048	1.1134	1	R.DKLAACLEGNCAEGLGTNYR.G (Ions score 22)
100 - 117	657.1100	1968.3082	1967.8829	0.4253	0	K.LAACLEGNCAEGLGTNYR.G (Ions score 49)
125 - 133	574.9100	1147.8054	1147.5444	0.2610	0	R.SGIECQLWR.S (Ions score 36)
125 - 133	574.9500	1147.8854	1147.5444	0.3410	0	R.SGIECQLWR.S (Ions score 43)
159 - 177	719.3500	2155.0282	2153.9324	1.0957	0	R.NPDSSTTGPWCYTTDPTVR.R (Ions score 23)
178 - 198	816.7900	2447.3482	2447.1356	0.2126	1	R.RQECSIPVCGQDQVTVAMTPR.S Oxidation (M) (Ions score 12)
199 - 217	1036.0000	2069.9854	2069.9688	0.0167	0	R.SEGSSVNLSPPLEQCVPDR.G (Ions score 15)
199 - 217	691.3000	2070.8782	2069.9688	0.9094	0	R.SEGSSVNLSPPLEQCVPDR.G (Ions score 43)
199 - 217	691.3600	2071.0582	2069.9688	1.0894	0	R.SEGSSVNLSPPLEQCVPDR.G (Ions score 20)
225 - 243	665.8300	1994.4682	1994.0408	0.4274	0	R.LAVTTHGLPCLAWASAQAK.A (Ions score 44)
225 - 243	665.9500	1994.8282	1994.0408	0.7874	0	R.LAVTTHGLPCLAWASAQAK.A (Ions score 38)
225 - 243	666.0400	1995.0982	1994.0408	1.0574	0	R.LAVTTHGLPCLAWASAQAK.A (Ions score 45)
248 - 263	655.3600	1963.0582	1962.9007	0.1575	0	K.HQDFNSAVQLVENFCR.N (Ions score 37)
248 - 263	655.3900	1963.1482	1962.9007	0.2475	0	K.HQDFNSAVQLVENFCR.N (Ions score 36)
248 - 263	655.4200	1963.2382	1962.9007	0.3375	0	K.HQDFNSAVQLVENFCR.N (Ions score 43)

248 - 263	655.6300	1963.8682	1962.9007	0.9675	0	K.HQDFNSAVQLVENFCR.N (Ions score 51)
248 - 263	655.6400	1963.8982	1962.9007	0.9975	0	K.HQDFNSAVQLVENFCR.N (Ions score 43)
248 - 263	655.6500	1963.9282	1962.9007	1.0275	0	K.HQDFNSAVQLVENFCR.N (Ions score 33)
310 - 314	273.2300	544.4454	544.2969	0.1486	0	R.AIEGR.T (Ions score 20)
315 - 327	781.3800	1560.7454	1560.7209	0.0246	0	R.TATSEYQTFFNPR.T (Ions score 33)
315 - 327	781.4300	1560.8454	1560.7209	0.1246	0	R.TATSEYQTFFNPR.T (Ions score 56)
315 - 327	521.4800	1561.4182	1560.7209	0.6973	0	R.TATSEYQTFFNPR.T (Ions score 28)
328 - 344	628.6300	1882.8682	1882.8884	-0.0202	0	R.TFGSGEADCGLRPLFEK.K (Ions score 4)
328 - 344	942.5700	1883.1254	1882.8884	0.2371	0	R.TFGSGEADCGLRPLFEK.K (Ions score 24)
328 - 344	628.7700	1883.2882	1882.8884	0.3998	0	R.TFGSGEADCGLRPLFEK.K (Ions score 27)
328 - 344	628.9200	1883.7382	1882.8884	0.8498	0	R.TFGSGEADCGLRPLFEK.K (Ions score 24)
346 - 353	489.3000	976.5854	976.4825	0.1029	1	K.SLEDKTER.E (Ions score 31)
354 - 363	597.8600	1193.7054	1193.5928	0.1127	0	R.ELLESYIDGR.I (Ions score 56)
354 - 363	597.8700	1193.7254	1193.5928	0.1327	0	R.ELLESYIDGR.I (Ions score 46)
354 - 363	597.9800	1193.9454	1193.5928	0.3527	0	R.ELLESYIDGR.I (Ions score 59)
364 - 383	756.0100	2265.0082	2264.0970	0.9112	0	R.IVEGSDAEIGMSPWQVMLFR.K (Ions score 39)
364 - 383	756.0400	2265.0982	2264.0970	1.0012	0	R.IVEGSDAEIGMSPWQVMLFR.K (Ions score 56)
364 - 383	761.1900	2280.5482	2280.0919	0.4563	0	R.IVEGSDAEIGMSPWQVMLFR.K Oxidation (M) (Ions score 61)
364 - 383	761.2000	2280.5782	2280.0919	0.4863	0	R.IVEGSDAEIGMSPWQVMLFR.K Oxidation (M) (Ions score 49)
364 - 383	766.3100	2295.9082	2296.0868	-0.1786	0	R.IVEGSDAEIGMSPWQVMLFR.K 2 Oxidation (M) (Ions score 38)
364 - 383	766.6300	2296.8682	2296.0868	0.7814	0	R.IVEGSDAEIGMSPWQVMLFR.K 2 Oxidation (M) (Ions score 53)
384 - 399	592.1600	1773.4582	1772.9091	0.5491	1	R.KSPQELLCGASLISDR.W (Ions score 36)
384 - 399	592.2100	1773.6082	1772.9091	0.6991	1	R.KSPQELLCGASLISDR.W (Ions score 29)
384 - 399	592.3700	1774.0882	1772.9091	1.1791	1	R.KSPQELLCGASLISDR.W (Ions score 24)
385 - 399	823.9300	1645.8454	1644.8141	1.0313	0	K.SPQELLCGASLISDR.W (Ions score 65)
441 - 446	360.8600	719.7054	719.3887	0.3167	0	K.ISMLEK.I (Ions score 18)
441 - 446	368.8100	735.6054	735.3837	0.2218	0	K.ISMLEK.I Oxidation (M) (Ions score 24)
447 - 452	399.8300	797.6454	797.4548	0.1907	0	K.IYIHPR.Y (Ions score 30)
457 - 467	659.3800	1316.7454	1316.6758	0.0697	1	R.ENLDRDIALMK.L (Ions score 23)
457 - 467	440.0500	1317.1282	1316.6758	0.4524	1	R.ENLDRDIALMK.L (Ions score 5)
462 - 467	353.8200	705.6254	705.3731	0.2524	0	R.DIALMK.L Oxidation (M) (Ions score 19)
487 - 498	626.3900	1250.7654	1250.6506	0.1148	0	R.ETAASLLQAGYK.G (Ions score 85)
487 - 498	626.4400	1250.8654	1250.6506	0.2148	0	R.ETAASLLQAGYK.G (Ions score 67)
501 - 508	437.9000	873.7854	873.4709	0.3146	0	R.VTGWGNLK.E (Ions score 15)
509 - 517	503.3300	1004.6454	1004.4927	0.1527	0	K.ETWTANVGK.G (Ions score 29)
509 - 517	503.3500	1004.6854	1004.4927	0.1927	0	K.ETWTANVGK.G (Ions score 41)
509 - 517	503.4200	1004.8254	1004.4927	0.3327	0	K.ETWTANVGK.G (Ions score 47)
518 - 537	745.0100	2232.0082	2231.2460	0.7622	0	K.GQPSVLQVVNLPIVERPVCK.D (Ions score 21)
518 - 537	745.0200	2232.0382	2231.2460	0.7922	0	K.GQPSVLQVVNLPIVERPVCK.D (Ions score 34)
518 - 537	745.1400	2232.3982	2231.2460	1.1522	0	K.GQPSVLQVVNLPIVERPVCK.D (Ions score 18)
544 - 559	616.0900	1845.2482	1844.8073	0.4409	0	R.ITDNMFCAGYKPDEGK.R (Ions score 36)

544 - 559	**616.1500**	**1845.4282**	**1844.8073**	**0.6209**	**0**	**R.ITDNMFCAGYKPDEGK.R** (Ions score 33)
544 - 559	**621.5900**	**1861.7482**	**1860.8022**	**0.9459**	**0**	**R.ITDNMFCAGYKPDEGK.R** Oxidation (M) (Ions score 20)
544 - 560	**668.2600**	**2001.7582**	**2000.9084**	**0.8498**	**1**	**R.ITDNMFCAGYKPDEGKR.G** (Ions score 21)
561 - 575	**763.8500**	**1525.6854**	**1525.6178**	**0.0677**	**0**	**R.GDACEGDSGGPFVMK.S** (Ions score 62)
561 - 575	**771.8600**	**1541.7054**	**1541.6127**	**0.0928**	**0**	**R.GDACEGDSGGPFVMK.S** Oxidation (M) (Ions score 68)
561 - 575	**515.0500**	**1542.1282**	**1541.6127**	**0.5155**	**0**	**R.GDACEGDSGGPFVMK.S** Oxidation (M) (Ions score 30)
576 - 581	**367.8200**	**733.6254**	**733.3507**	**0.2747**	**0**	**K.SPFNNR.W** (Ions score 32)
576 - 581	**367.8300**	**733.6454**	**733.3507**	**0.2947**	**0**	**K.SPFNNR.W** (Ions score 20)
600 - 608	**595.3800**	**1188.7454**	**1188.5716**	**0.1738**	**0**	**K.YGFYTHVFR.L** (Ions score 25)
600 - 608	**595.4200**	**1188.8254**	**1188.5716**	**0.2538**	**0**	**K.YGFYTHVFR.L** (Ions score 50)
600 - 608	**595.4200**	**1188.8254**	**1188.5716**	**0.2538**	**0**	**K.YGFYTHVFR.L** (Ions score 59)
600 - 608	**397.3300**	**1188.9682**	**1188.5716**	**0.3965**	**0**	**K.YGFYTHVFR.L** (Ions score 41)
600 - 608	**397.3400**	**1188.9982**	**1188.5716**	**0.4265**	**0**	**K.YGFYTHVFR.L** (Ions score 46)
600 - 608	**397.5000**	**1189.4782**	**1188.5716**	**0.9065**	**0**	**K.YGFYTHVFR.L** (Ions score 38)
616 - 622	**404.2700**	**806.5254**	**806.3810**	**0.1444**	**0**	**K.VIDQFGE.-** (Ions score 30)
616 - 622	**404.4000**	**806.7854**	**806.3810**	**0.4044**	**0**	**K.VIDQFGE.-** (Ions score 32)

Appendix D
Seroconversion against $SSL10_{95-197}$

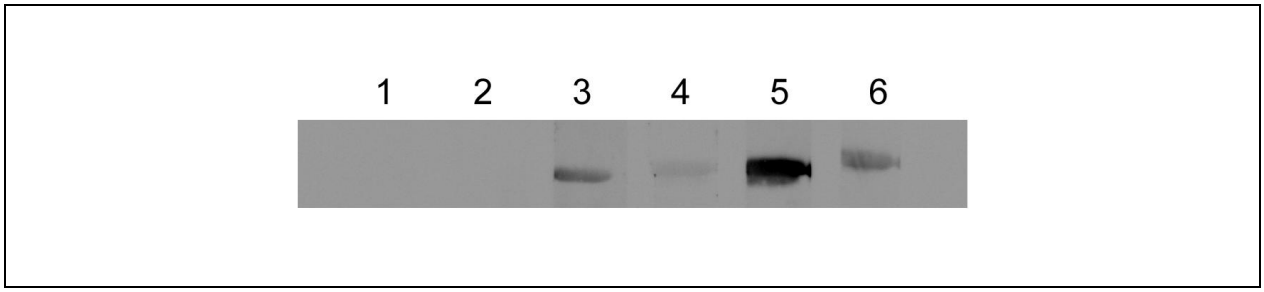

Appendix D: Seroconversion against $SSL10_{95-197}$

Western blot of $SSL10_{95-197}$ separated by reducing SDS-PAGE gel (2-6) and incubated with diluted sera (1:500) from patients with *S.aureus* infection (3-6). Bound antibodies were detected using goat anti-IgG coupled to HRP. Control lane without (1) and with (2) $SSL10_{95-197}$ probed with secondary antibody alone were also included. Patient sera was used with formal consent.

Appendix E
SSL7 and Complement C5

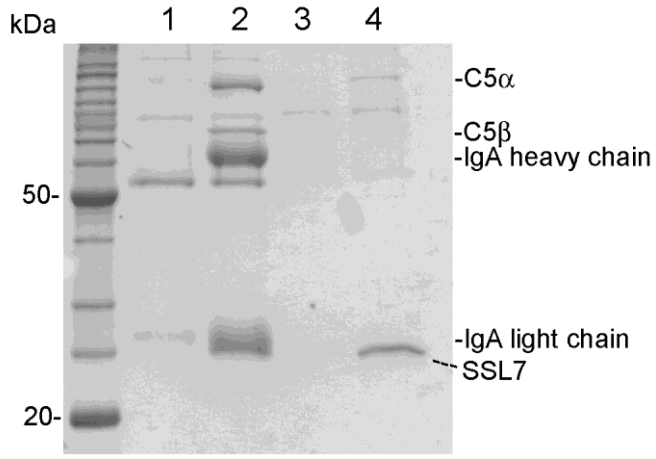

Appendix E: Affinity purification of serum protein by SSL7 Sepharose

Human serum (1,2) or guinea pig serum (3,4) (10%) was incubated with Sepharose (1,3) or SSL7 Sepharose (2,4) at 4 °C for 1 h. The Sepharose beads were extensively washed and bound proteins were eluted and separated by 12 % reducing SDS-PAGE gel. SSL7 bound to C5α and C5β chains from human sera but displayed lower affinity from guinea pig sera.

Bibliography

Adams, P. D., Grosse-Kunstleve, R. W., Hung, L. W., Ioerger, T. R., McCoy, A. J., Moriarty, N. W., et al. (2002). PHENIX: building new software for automated crystallographic structural determination. *Acta Crystallographica Biological Crystallography, D58*(11), 1948-1954.

Ades, E. W., Phillips, D. J., Shore, S. L., Gordon, D. S., Lavia, M. F., Black, C. M., et al. (1976). Analysis of mononuclear cell surfaces with fluoresceinated staphylococcal Protein A complexed with IgG antibody or heat-aggregated γ-globulin. *The Journal of Immunology, 117*(6), 2119-2123.

Aguiar-Alves, F., Mederios, F., Fernandes, O., Pereira, R. M. G., Perdreau-Remington, F., & Riley, L. W. (2006). New *Staphylococcus aureus* genotypig method based on exotoxin (set) genes. *Journal of Clinical Microbiology, 44*(8), 2728-2732.

Ahmed, A., Gogal, R. M., & Walsh, J. E. (1994). A new rapid and simple non-radioactive assay to monitor and determine the proliferation of lymphocytes: an alternative to [3H] thymidine incorporation assay. *Journal of Immunological Methods, 170*(2), 211-224.

Ahsen, N. v., Lewczuk, P., Schutz, E., Oellerich, M., & Ehrenreich, H. (2000). Prothrombin activity and concentration in healthy subjects with and without prothrombin G20210A mutation. *Thrombosis Research, 99*(6), 549-556.

Akerstrom, B., & Bjorck, L. (1986). A physiochemical study of Protein G, a molecule with unique immunoglobulin G binding properties. *The Journal of Biological Chemistry, 261*(22), 10240-10247.

Al-Shangiti, A. M., Naylor, C. E., Nair, S. P., Briggs, D. C., Hederson, B., & Chain, B. M. (2004). Structural relationship and cellular tropism of staphylococcal superantigen-like proteins. *Infection and Immunity, 72*(7), 4261-4270.

Anderson, A. L., Sporici, R., Lambris, J., LaRosa, D., & Levinson, A. I. (2006). Pathogenesis of B-cell superantigen-induced immune complex mediated inflammation. *Infection and Immunity, 74*(2), 1196-1203.

Andrews, S. C., Robinson, A. K., & Rodriguez-Quinones, F. (2003). Bacterial iron homeostasis. *FEMS Microbioloy Reviews 27*(2-3), 215-237.

Arcus, V. (2002). OB fold domains: a snapshot of the evolution of sequence, structure and function. *Current Opinion in Structural Biology, 12*(6), 794-801.

Arcus, V. L., Langley, R., Proft, T., Fraser, J. D., & Baker, E. N. (2002). The three-dimensional structure of a superantigen-like protein, SET3, from a pathogenicity island of the *Staphylococcus aureus* genome. *The Journal of Biological Chemistry, 277*(35), 32274-32281.

Arnold, K., Bordoli, L., Kopp, J., & Schwede, T. (2006). The SWISS-MODEL workspace: a web-based environment for protein structure homology modelling. *Bioinformatics, 22*(2), 195-201.

Atkins, K. L., Burman, J. D., Chamberelain, E. S., Cooer, J. E., Poutrel, B., Bagby, S., et al. (2008). *S.aureus* IgG-binding proteins SpA and Sbi: Host specificity and mechansims of immune complex formation. *Molecular Immunology, 45*(6), 1600-1611.

Attia, A. S., Benson, M. A., Stauff, D. L., & Skaar, V. J. T. E. P. (2010). Membrane damage elicits an immunomodulatory program in *Staphylococcus aureus*. *PloS Pathogens, 6*(3), e1000802.

Avirutnan, P., Fuchs, A., Hauhart, R. E., Somnuke, P., Youn, S., Diamond, M. S., et al. (2010). Antagonism of the complement component C4 by flavivirus nonstructural protein NS1. *Journal of Experimental Medicine, 207*(4), 793-806.

Baba, T., Bae, T., Schneewind, O., Takeuchi, F., & Hiramatsu, K. (2008). Genome sequencing of *Staphylococcus aureus* strain Newman and comparitive analysis of staphylococcal genomes: polymorphism and evolution of two major pathogenicity islands. *Journal of Bacteriology, 190*(1), 300-310.

Baba, T., Takeuchi, F., Kuroda, M., Yuzawa, H., Aoki, K.-i., Oguchi, A., et al. (2002). Genome and virulence determinants of high virulence community acquired MRSA *Lancet, 359*(9320), 1819-1827.

Baker, H. M., Basu, I., Chung, M. C., Caradoc-Davies, T., Fraser, J. D., & Baker, E. N. (2007). Crystal structure of the staphylococcal toxin SSL5 in complex with sialyl lewis X reveal a conserved binding site that shares common features with viral and bacterial sialic acid binding proteins. *Journal of Molecular Biology, 374*(5), 1298-1308.

Banner, D., Darcy, A., Chene, C., Winkler, F., Guha, A., Konigsberg, W., et al. (1996). The crystal structure of the complex of blood coagulation factor VIIa with soluble tissue factor. *Nature, 380*(6569), 41-46.

Barrett, D. J., & Ayoub, E. M. (1986). IgG2 subclass restriction of antibody to pneumococcal polysaccharides. *Clinical and Experimental Immunology, 63*(1), 127-134.

Bera, A., Herbert, S., Jakob, A., Vollmer, W., & Gotz, F. (2005). Why are pathogenic staphylococci so lysosyme resistance? The petidoglycan O-acetyltransferase OatA is the major determinant for lysozyme resistance of *Staphylococcus aureus*. *Molecular Microbiology, 55*(3), 778-787.

Bernal, A., Proft, T., Fraser, J. D., & Posnett, D. N. (1999). Superantigens in human disease. *Journal of Clinical Immunology, 19*(3), 149-157.

Bhardwaj, N., Friedman, S. M., Cole, B. C., & Nisanian, A. J. (1992). Dendritic cells are potent antigen-presenting cells for microbial superantigens. *Journal of Experimental Medicine, 175*(1), 267-273.

Bindon, C. I., Hale, G., Bruggemann, M., & Waldmann, H. (1988). Human monoclonal IgG isotype differ in complement activating function at the level of C4 as well as C1q. *Journal of Experimental Medicine, 168*(1), 127-143.

Bjerknes, R., & Bassoe, C. (1984). Phagocyte C3-mediated attachment and internalisation: flow cytometric studies using a fluorescence quenching technique. *Blut, 49*(4), 315-323.

Blanc, E., Roversi, P., Vonrhein, C., Flensburg, C., Lea, S. M., & Bricogne, G. (2004). Refinement of severely incomplete structures with maximum likelihood in BUSTER-TNT. *Acta Crystallographica, D60*(12-1), 2210-2221.

Blom, A. M., Kask, L., Ramesh, B., & Hillarp, A. (2003). Effects of zinc on factor I cofactor activity of C4b-binding protein and factor H. *Archives of Biochemistry and Biophysics, 418*(2), 108-118.

Blom, A. M., Rytkonin, A., Vasquez, P., Lindahl, G., Dahlback, B., & Jonsson, A. (2001). Pili of Neisseria gonorrhoeae and the human complement regulator C4b-binding protein. *The Journal of Immunolgy, 166*(11), 6764-6770.

Bloom, A., Webb, J., Villoutreix, B. O., & Dalback, B. (1999). A cluster of positively charged amino acids in the C4BP α-chain is cruical for C4b-binding and Factor I cofactor function. *The Journal of Biological Chemistry, 274*(27), 19237-19245.

Boden, M., & Flock, J.-I. (1992). Evidence for three different fibrinogen-binding proteins with unique properties from *Staphylococcus aureus* strain Newman. *Microbial Pathogenesis, 12*(4), 289-298.

Bruggemann, M., Williams, G. T., Bindon, C. I., Clark, M. R., Walker, M. R., Jefferis, R., et al. (1987). Comparison of the effector functions of human immunoglobulins using a matched set of chimeric antibodies. *Journal of Experimental Medicine, 166*(5), 1351-1361.

Budayova-Spano, M., Lacroix, M., Thielens, N. M., Arlaud, G. J., Fontecilla-Camps, J. C., & Gaboriaud, C. (2002). The crystal structure of the zymogen catalytic domain of complelment protease C1r reveals that a disruptive mechanical stress is required to trigger activation of the C1 complex. *The EMBO Journal, 21*(3), 231-239.

Bugg, T. D. H., Dutka-Malen, S., Arthur, M., Courvalin, P., & Walsh, C. T. (1991). Identification of vancomycin resistance protein VanA as a D-alanine:D-alanine ligase of altered substrate specificity. *Biochemistry, 30*(8), 2017-2021.

Bullen, J. J. (1981). The significance of iron in infection. *Reviews of Infectious Disease, 3*(6), 1127-1138.

Burman, J. D., Leung, E., Atkins, K. L., O'Seaghdah, M. S. N., Lango, L., Bernado, P., et al. (2008). Interaction of human complement with Sbi, a staphylococcal immunoglobulin binding protein: indications of a novel mechanism fo compelment evasion by *Staphylococus aureus*. *Journal of Biological Chemistry, 283*(25), 17579-17593.

Burmeister, W. P., Huber, A. H., & Bojorkman, P. J. (1994). Crystal structure of the complex of rat neonatal Fc receptor with Fc. *Nature, 372*(6504), 379-383.

Campbell, R. D., Dodds, A. W., & Porter, R. R. (1980). The binding of human complement component C4 to antibody-antigen aggregates. *Biochemical Journal, 189*(1), 67-80.

Canfield, S. M., & Morrison, S. L. (1991). The binding affinity of human IgG for its high affinity Fc receptor is determined by multiple amino acids in the CH2 domain and is modulated by the hinge region. *Journal of Experimental Medicine, 173*(6), 1483-1491.

Carroll, M. C., Tathallah, D. M., Bergamaschini, L., Alicot, E. M., & Isenman, D. E. (1990). Substitution of a single amino acid (aspartic acid for histidine) converts the functional activity of human complement C4B to C4A. *Proceedings of National Academy of Science, 87*(17), 6868-6872.

Cedergren, L., Andersson, R., Jansson, B., Uhlen, M., & Nilsson, B. (1993). Mutational analysis of the interaction between staphylococcal protein A and human IgG1. *Protein Engineering, 6*(44), 441-448.

Chang, M. W., Toghrol, F., & Bentley, W. E. (2007). Toxicogenomic response to chlorination includes induction of major virulence genes in *Staphylococcus aureus*. *Environmental Science and Technology, 41*(21), 7570-7575.

Chang, S., Sievert, D. M., Hageman, J. C., Boulton, M. L., Tenover, F. C., Downes, F. P., et al. (2003). Infection with vancomycin-resistant *Staphylococcus aureus* containing the *vanA* resistance gene. *The New England Journal of Medicine, 348*(14), 1342-1347.

Chavakis, T., Hussain, M., Kanse, S. M., Peters, G., Bretzel, R. G., Flock, J.-I., et al. (2002). *Staphylococcus aureus* extracellular adherence protein serves an anti-inflammatory factor by inhibiting the recruitment of host leukocytes. *Nature Medicine, 8*(7), 687-693.

Chavakis, T., Preissner, K. T., & Herrmann, M. (2007). The anti-inflammatory activities of *Staphylococcus aureus*. *Trends in Immunology, 28*(9), 408-416.

Chen, J., & Novick, R. P. (2009). Phage-mediated intergeneric transfer of toxin genes. *Science, 323*(5910), 139-142.

Cheung, A. L., Bayer, A. S., Zhang, G., Gresham, H., & Xiong, Y.-Q. (2004). Regulation of virulence determinants *in vitro* and *in vivo* in *Staphylococcus aureus*. *FEMS Immunology and Medical Microbiology, 40*(1), 1-9.

Cheung, A. L., & Zhang, G. (2002). Global regulation of virulence determinants in Staphylococcus aureus by the SarA protein familly. *Frontiers in Bioscience, 7*, 1825-1842.

Chung, M. C., Wines, B. D., Baker, H., Langley, R. J., Baker, E. N., & Fraser, J. D. (2007). The crystal structure of staphylococcal superantigen like protein 11 in complex with sialyl Lewis X reveals the mechanism for cell binding and immune inhibition. *Molecular Microbiology, 66*(6), 1342-1355.

Clarke, S. R., Harris, L. G., Richards, G., & Foster, S. J. (2002). Analysis of Ebh, a 1.1 megadalton cell wall-associated fibronectin binding protein of *Staphylococcus aureus*. *Infection and immunity, 70*(12), 6680-6687.

Clements, M. O., Watson, S. P., & Foster, S. J. (1999). Characterisation of the major superoxide dismutase of Staphylococcus aureus and its role in starvation survival, stress resistance, and pathogenicity. *Journal of Bacteriology, 181*(13), 3898-3903.

Collins, L., Kristian, S. A., Weldenmaier, C., Faigle, M., van Kessel, K. P. M., van Strijp, J. A. G., et al. (2002). *Staphylococcus aureus* strains lacking D-Alanine modification of teichoic acids are highly susceptible to human neutrophil killing and are virulence attentuated in mice. *The Journal of Infectious Diseases, 186*(2), 214-219.

Corbin, B. D., Seeley, E. H., Raab, A., Feldmann, J., Miller, M. R., Torres, J. J., et al. (2008). Metal chelation and inhibition of bacterial growth in tissue abscesses. *Science, 319*(5865), 962-965.

Cui, L., Ma, X., Sato, K., Okuma, K., Tenover, F. C., Mamizuka, E. M., et al. (2003). Cell wall thickening is a common feature of vancomycin resistance in *Staphylococcus aureus*. *Journal of Clinical Microbiology, 41*(1), 5-14.

Dahlback, B. (1983). Purification of human C4b-binding protein and formation of its complex with vitamin K-dependent protein S. *Biochemical Journal, 209*(3), 847-856.

Davis, I. W., Leaver-Fay, A., Chen, V. B., Block, J. N., Kapral, G. J., Wang, X., et al. (2007). MolProbity: all atom contacts and structure validation for proteins and nucleic acids. *Nucleic Acids Research, 35*, W375-W383.

Dawson, K. M., Cook, A., Devine, J. M., Edwards, M., Hunter, M. G., Raper, R. H., et al. (1994). Plasminogen mutants activated by thrombin. *The Journal of Biological Chemistry, 269*(23), 15989-15992.

Deisenhofer, J. (1981). Crystallographic refinement and atomic models of a human Fc fragment and its complex with fragment B of protein A from *Staphylococcus aureus* at 2.9 and 2.8 A resolution. *Biochemistry, 20*(9), 2361-2370.

Deutsch, D. G., & Mertz, E. T. (1970). Plasminogen: purification from plasma by affinity chromatography. *Science, 170*(962), 1095-1096.

Dmitriev, B., Toukach, F., & Ehlers, S. (2005). Towards a comprehensive view of the bacterial cell wall. *Trends in Microbiology, 12*(12), 569-574.

Dodds, A. W. (2002). Which came first, the lectin/classical pathway or the alternative pathway of complement? *Immunobiology, 205*(4-5), 340-354.

Domiati-Saad, R., Attrep, J. F., Brezinschek, H. P., Cherrie, A. H., Karp, D. R., & Lipsky, P. E. (1996). Staphylococcal enterotoxin D functions as a human B cell superantigen by rescuing VH4 expressing B cells from apoptosis. *The Journal of Immunolgy, 156*(10), 3608-3620.

Drake, T., Morrissey, J., & Edgington, T. (1989). Selective cellular expression of tissue factor in human tissues. *American Journal of Pathology, 134*(5), 1087-1097.

Drewinko, B., Mars, W., Minowada, J., Burk, K. H., & Trujillo, J. M. (1984). ARH-77 an established human IgG-producing myeloma cell line. *Cancer, 54*(9), 1883-1892.

Dryla, A., Prustomersky, S., Gelbmann, D., Hanner, M., Bettinger, E., Kocsis, B., et al. (2005). Comparison of antibody repertoires against *Staphylococcus aureus* in healthy individuals and in acutely infected patients. *Clinical and Diagnostic Laboratory Immunology, 12*(3), 387-398.

Dunman, P. M., Murphy, E., Haney, S., Palacios, D., Tucker-kellogg, G., Wu, S., et al. (2001). Transcription profiling-based identification of *Staphylococcus aureus* genes regulated by the *arg* and/or *sarA* loci. *Journal of Bacteriology, 183*(24), 7341-7353.

Dziewanowska, K., Patti, J. M., Deobald, C. F., Bayles, K. W., Trumble, W. R., & Bohach, G. A. (1999). Fibronectin binding protein and host cell tyrosine kinase are required for internalisation of *Staphylococcus aureus* by epithelial cells. *Infection and Immunity, 67*(9), 4673-4678.

Eidhin, D. N., Perkins, S., Francois, P., Vaudaux, P., Hook, M., & Foster, T. J. (1998). Clumping factor B (ClfB), a new surface-located fibrinogen-binding adhesin of *Staphylococcus aureus*. *Molecular Microbiology, 30*(2), 245-257.

Emsley, P., & Cowtan, K. (2004). Coot: model-building tools for molecular graphics. *Acta Crystallographica, 60*(12), 2126-2132.

Esmon, C. T. (2004). Interactions between the innate immune and blood coagulation systems *Trends in Immunology, 25*(10), 537-542.

Espersen, F., Clemmensen, I., & Barkholt, V. (1985). Isolation of *Staphylococcus aureus* clumping factor. *Infection and Immunity, 49*(3), 700-708.

Evans, P. (2006). Scaling and assessment of data quality. *Acta Crystallographica Biological Crystallography, D62*(1), 72-82.

Fallman, M., Andersson, R., & Andersson, T. (1993). Signaling properties of CR3 (CD11b/CD18) and CR1 (CD35) in relation to phagocytosis of complement opsonised particles. *The Journal of Immunology, 151*(1), 330-338.

Feinstein, A., Richardson, N., & Taussig, M. I. (1986). Immunoglobulin flexibility in complement activation. *Immunology Today, 7*(6), 169-174.

Feng, Y., Chen, C., Su, L., Hu, S., Yu, J., & Chiu, C. (2008). Evolution and pathogeneisis of *Staphylococcus aureus*: lessons learned from genotyping and comparative genomics. *FEMS Microbiology Review, 32*(1), 23-37.

Fine, D. P., Marney, S. R., Colley, D. G., Sergent, J. S., & Des Prez, R. M. (1972). C3 shunt activation in human serum chelated with EGTA. *The Journal of Immunology, 109*(4), 807-809.

Fischer, A., & Lisowska-Grospierre, B. (1988). Leukocyte adhesion deficiency: molecular basis and functional consequences. *Immunodeficiency Reviews, 1*(1), 39-54.

Fischer, M. B., Ma, M., Goerg, S., Zhou, X., Xia, J., Finco, O., et al. (1996). Regulation of the B cell response to T-dependent antigens by classical pathway complement. *The Journal of Immunology, 157*(2), 549-556.

Fishelson, Z., Pangburn, M. K., & Muller-Eberhard, H. J. (1983). C3 convertase of the alternative complement pathway. *The Journal of Biological Chemistry, 258*(12), 7411-7415.

Fitzgerald, J. R., Foster, T. J., & Cox, D. (2006). The interaction of bacterial pathogens with platelets. *Nature Reviews Microbiology, 4*(6), 445-457.

Fitzgerald, J. R., Loughman, A., Keane, F., Brennan, M., Knobel, M., Higginss, J., et al. (2006). Fibronectin-binding proteins of *Staphylococcus aureus* medaite activation of human platelets via fibrinogen and fibronectin bridges to integrin GPIIb/IIIa and IgG binding to FcγRIIa receptor. *Molecular Microbiology, 59*(1), 212-230.

Fitzgerald, J. R., Reid, S. D., Ruotsalainen, E., Tripp, T. J., Liu, M., Cole, R., et al. (2003). Genome diversification in *Staphylococcus aureus*: molecular evolution of a highly

variable chromosomal region encoding the staphylococcal exotoxin like family of proteins. *Infection and Immunity, 71*(5), 2827-2838.

Foster, T. J. (2005). Immune evasion by staphylococci. *Nature Reviews Microbiology, 3*(12), 948-958.

Foster, T. J., & Hook, M. (1998). Surface protein adhesins of *Staphylococcus aureus*. *Trends in Microbiology, 6*(12), 484-488.

Fournier, B., & Philpott, D. J. (2005). Recognition of *Staphylococcus aureus* by the innate immune system. *Clinical Microbiology Reviews, 18*(3), 521-540.

Fraser, J., Arcus, V., Kong, P., Baker, E., & Proft, T. (2000). Superantigens-powerful modifiers of the immune system. *Molecular Medicine Today, 6*(3), 125-132.

Friedrich, C. L., Moyles, D., Beveridge, T. J., & Hancock, R. E. W. (2000). Antibacterial action of structurally diverse cationic peptides on gram positive bacteria. *Antimicrobial Agents and Chemotheraphy, 44*(8), 2086-2092.

Gaboriaud, C., Juanhuix, J., Gruez, A., Lacroix, M., Darnault, C., Pignol, D., et al. (2003). The crystal structure of the globular head of complement protein C1q provides a basis for its versatile recognition properties. *Journal of Biological Chemistry, 278*(47), 46974-46982.

Gaboriaud, C., Thielens, N. M., Gregory, L. A., Rossi, V., Fontecilla-Camps, J. C., & Arlaud, G. J. (2004). Structure and activation of the C1 complex of complement: unravelling the puzzle. *Trends in Immunology, 25*(7), 368-373.

Gak-Mor, O., & Finlay, B. B. (2006). Pathogenicity islands: a molecular toolbox for bacterial virulence. *Cellular Microbiology, 8*(11), 1707-1719.

Ganz, T., Seisted, M. E., Szkiarek, D., Harwig, S. S. L., Daher, K., Bainton, D. F., et al. (1985). Defensins-natural peptide antibiotics of human neutrophils. *Journal of Clinical Investigation, 76*(4), 1427-1435.

Garzoni, C., Francois, P., Huyghe, A., Couzinet, S., Tapparel, C., Charbonnier, Y., et al. (2007). A global view of *Staphylococcus aureus* whole genome expression upon internalization in human epithelial cells. *BMC genomics, 8*, 171.

Gattiker, E. G. C. H. A., Duvaud, S., Wilkins, M., Appel, R., & Bairoch, A. (2005). *Protein identification and analysis tools on the ExPASy server*: Humana Press.

Genovese, A., Borgia, G., Bjorck, L., Petraroli, A., dePaulis, A., Piazza, M., et al. (2003). Immunoglobulin superantigen protein L induces IL-4 and IL-13 secretion from human FcεRI cells through interaction with the κ light chain of IgE. *The Journal of Immunolgy, 170*(4), 1854-1861.

Gessner, J. E., Heiken, H., Tamm, A., & Schmidt, R. E. (1998). The IgG Fc receptor family. *Annual of Hematology, 76*(6), 231-248.

Gigli, I., von Zabern, I., & Porter, R. R. (1977). The isolation and structure of C4, the fourth component of human complement. *Biochemical Journal, 165*(3), 439-446.

Gill, S. R., Fouts, D. E., Archer, G. L., Mongodin, E. F., DeBoy, R. T., Ravel, J., et al. (2005). Insights on evolution of virulence and resistance from the complete genome analysis of an early methicillin-resistant *Staphylococcus aureus* strain and a biofilm-producing methicillin-resistant *Staphylococcus epidermidis* strain. *Journal of Bacteriology, 187*(7), 2426-2438.

Goldschmidt, L., Cooper, D., Derewenda, Z., & Eisenberg, D. (2007). Toward rational protein crystallisation: a web server for the design of crystallisable protein variants. *Protein Science, 16*(8), 1569-1576.

Gouaux, E. (1998). α-hemolysin from *Staphylococcus aureus*: an archetype of β-barrel, channel forming toxins. *Journal of Structural Biology, 121*(2), 110-122.

Griffin, J. H. (1978). Role of surface in surface-dependent activation of Hageman factor (blood coagulation factor XII). *Proceedings of National Academy of Science, 75*(4), 1998-2002.

Gu, B. J., Saunders, B. M., Jursik, C., & Wiley, J. S. (2010). The P2X7-non muscle myosin membrane complex regulates phagocytosis of non-opsonised particles and bacteria by a pathway attenuated by extracellular ATP. *Blood, 115*(8), 1621-1631.

Haas, P.-J., de Haas, C. J. C., Poppelier, M. J. J. C., van Kessel, K. P. M., van Strijp, J. A. G., Dijkstra, K., et al. (2005). The structure of the C5a receptor-blocking domain of chemotaxis inhibitory protein of *Staphylococcus aureus* is related to a group of immune evasive molecules. *Journal of Molecular Biology, 353*(4), 859-872.

Hamilton, K. K., Hattori, R., Esmon, C. T., & Sims, P. J. (1990). Complement proteins C5b-9 induce vesiculation of the endothelial plasma membrane and expose catalytic surface for assembly of the prothrombinase enzyme complex. *The Journal of Biological Chemistry, 265*(7), 3809-3814.

Hammel, M., Sfyroera, G., Ricklin, D., Magotti, P., Lambris, J. D., & Geisbrecht, B. V. (2007a). A structural basis for complement inhibition by *Staphylococcus aureus*. *Nature Immunology, 8*(4), 430-437.

Hammel, M., Sfyroera, G., Ricklin, D., Magotti, P., Lambris, J. D., & Geisbrecht, B. V. (2007b). A structural basis for complement inhibition by *Staphylococcus aureus*. *Nature immunology*.

Hanssen, A.-M., & Sollid, J. U. E. (2006). SCCmec in staphylococci: genes on the move. *FEMS Immunology and Medical Microbiology, 46*(1), 8-20.

Harlow, E., & Lane, D. (1988). *Antibodies- a lab manual*: Cold Spring Harbor Laboratory Press.

Harmat, V., Gal, P., Kardos, J., Szilagyi, K., Ambrus, G., Vegh, B., et al. (2004). The structure of MBL-associated serine protease-2 reveals that identical substrate specificities of C1s and MASP-2 are realised through different sets of enzyme-substrate interactions. *Journal of Molecular Biology, 342*(5), 1533-1546.

Haupt, K., Reuter, M., van den Elsen, J., Burman, J., Halbich, S., Richter, J., et al. (2008). The *Staphylococcus aureus* protein Sbi acts as a complement inhibitor and forms a tripartite complex with host complement factor H and C3b. *PloS Pathogens, 4*(12), 1-11.

Hendrix, H., Lindhout, T., Mertens, K., Engels, W., & Hemker, H. (1983). Activation of human prothrombin by stoichiometric levels of staphylocoagulase. *The Journal of Biological Chemistry, 258*(6), 3637-3644.

Herron-Olson, L., Fitzgerald, J. R., Musser, J. M., & Kapur, V. (2007). Molecular correlates of host specialisation in *Staphylococcus aureus*. *PLoS ONE, e1120*(10), 1-13.

Hessell, A. J., Hangartner, L., Hunter, M., Havenith, C. E. G., Beurskens, F. J., Bakker, J. M., et al. (2007). Fc receptor but not complement binding is important in antibody protection against HIV. *Nature, 449*(7158), 101-104.

Highlander, S. H., Hulten, K. G., Qin, X., Jiang, H., Yerrapragda, S., Mason, E. O., et al. (2007). Subtle genetic changes enchance virulence of methicillin resitant and sensitive *Staphylococcus aureus BMC Microbiology, 7*(99).

Ho, S. N., Hunt, H. D., Horton, R. M., Pullen, J. K., & Pease, L. R. (1989). Site-directed mutageneis by overlap extension using the polymerase chain reaction. *Gene, 77*(1), 51-59.

Holden, M. T. G., Feil, E. J., Lindsay, J. A., Peacock, S. J., Day, N. P. J., Enright, M. C., et al. (2004). Complete genome of two clinical *Staphylococcus aureus* strains: evidence for the rapid evolution of virulence and drug resistance. *Proceedings of National Academy of Science, 101*(26), 9786-9791.

Holden, M. T. G., Lindsay, J. A., Corton, C., Quail, M. A., Cockfield, J. D., Pathak, S., et al. (2010). Genome sequence of a recently emerged, highly transmissible multi-antibiotic and antiseptic-resistant variant of methicillin resistant *Staphylococcus aureus*, sequence type 239, (TW). *Journal of Bacteriology, 192*(3), 888-892.

Holtfreter, S., Nguyen, T. T. H., Wertheim, H., Steil, L., Kusch, H., Truong, Q. P., et al. (2009). Human immune proteome in experimental colonisation with *Staphylococcus aureus*. *Clinical and Vaccine Immunology, 16*(11), 1607-1614.

Hornef, M. W., Wick, M. J., Rhen, M., & Normark, S. (2002). Bacterial strategies for overcoming host innate and adaptive immune responses. *Nature Immunology, 3*(11), 1033-1040.

Huber-Lang, M., Sarma, V., Zetoune, F. S., Rittirsch, D., Neff, T. A., McGuire, S. R., et al. (2006). Gereration of C5a in the absence of C3: a new complement activation pathway. *Nature Medicine, 12*(6), 682-687.

Hughes-Jones, N. C. (1977). Functional affinity constants of the reaction between 125I-labelled C1q and C1q binders and their use in the measurement of plasma C1q concentrations. *Immunology, 32*(2), 191-198.

Huseby, M., Shi, K., Brown, K., Digre, J., Mengistu, F., Seo, K. S., et al. (2007). Structure and biological activities of beta toxin from *Staphylococcus aureus*. *Journal of Bacteriology, 189*(23), 8719-8726.

Iandolo, J., Worrell, V., Groicher, K. H., Qian, Y., Tian, R., Kenton, S., et al. (2002). Comparative analysis of the genome of the temperate bacteriophages phi11, phi12, phi 12 of staphylococcus aureus 8325. *Gene, 289*(1-2), 109-118.

Idusogie, E. E., Presta, L. G., Gazzano-Santoro, H., Totpal, K., Wong, P., Ultsch, M., et al. (2000). Mapping of the C1q binding site on rituxan, a chimeric antibody with a human IgG1 Fc. *The Journal of Immunology, 164*(8), 4178-4184.

Inal, J. M., Hui, K.-M., Miot, S., Lange, S., Ramirez, M. I., Schneider, B., et al. (2005). Complement C2 receptor inhibitor trispanning: a novel human complement inhibitory receptor. *The Journal of Immunolgy, 174*(1), 356-366.

Ingham, K. C., Brew, S., Vaz, D., Sauder, D. N., & McGavin, M. J. (2004). Interaction of *Staphylococcus aureus* fibronectin binding protein with fibronectin. *The Journal of Biological Chemistry, 279*(41), 42945-42953.

Itoh, S., Hamada, E., Kamoshida, G., Yokoyama, R., Takii, T., Onozaki, K., et al. (2010). Staphylococcal superantigen-like protein 10 (SSL10) binds to human immunoglobulin G (IgG) and inhibits complement activation via the classical pathway. *Molecular Immunology, 47*(4), 932-938.

Janssen, B. J. C., Christodoulidou, A., McCarthy, A., Lambris, J. D., & Gros, P. (2006). Structure of C3b reveals conformational changes that underlie complement activity. *Nature, 444*(7116), 213-216.

Janssen, B. J. C., Huizinga, E. G., Raaijmakers, H. C. A., Roos, A., Daha, M. R., Nilsson-Ekdahl, K., et al. (2005). Structure of complement components C3 provide insights into the function and evolution of immunity. *Nature, 437*(7058), 505-511.

Jefferis, R., & Kumararatne, D. S. (1990). Selective IgG subclass deficiency: quantificaiton and clinical relevance. *Clinical and Experimental Immunology, 81*(3), 357-367.

Jefferis, R., & Lund, J. (2002). Interaction sites on human IgG-Fc for FcγR: current models. *Immunology Letters, 82*(1-2), 57-65.

Jefferis, R., Lund, J., & Pound, J. D. (1998). IgG-Fc mediated effector functions: molecular definition of interaction sites for effector ligands and the role of glycosylation. *Immunological Reviews, 163*, 59-76.

Jendeberg, L., Persson, B., Andersson, R., Karlsson, R., Uhlen, M., & Nilsson, B. (1995). Kinetic analysis of the interaction between Protein A domain variants and the human Fc using plasmon resonance detection. *Journal of Molecular Recognition, 8*(4), 270-278.

Jin, T., Bokarewa, M., Foster, T. J., Mitchell, J., Higgins, J., & Tarkowski, A. (2004). *Staphylococcus aureus* resists human defensins by production of Staphylokinase, a novel bacterial evasion mechanism. *The Journal of Immunology, 172*(2), 1169-1176.

Jongerius, I., Kohl, J., Pandey, M. K., Ruyken, M., van Kessel, K. P. M., van Srijp, J. A. G., et al. (2007). Staphylococcal complement evasion by various convertase blocking molecules. *Journal of Experimental Medicine, 204*(10), 2461-2471.

Jongerius, I., Puister, M., Wu, J., Ruyken, M., van Strijp, J. A. G., & Rooijakkers, S. H. M. (2010). Staphylococcal complement inhibitor modulates phagocyte responses by dimerization of convertases. *The Journal of Immunolgy, 184*(1), 420-425.

Kahn, M. L., Zheng, Y.-W., Huang, W., Biogmai, V., Zeng, D., Moff, S., et al. (1998). A dual thrombin receptor system for platelet activation. *Nature, 394*(6694), 690-694.

Kardos, J., Gal, P., Szilagyi, L., Thielens, N. M., Szilagyi, K., Lorincz, Z., et al. (2001). The role of the individual domains in the structure and function of the catalytic region of a modular serine protease C1r. *The Journal of Immunolgy, 167*(9), 5202-5208.

Karray, S., & Zouali, M. (1997). Identification of the B cell superantigen-binding site of HIV-1 gp120. *Proceedings of National Academy of Science, 94*(4), 1356-1360.

Kishore, U., Leigh, L. E. A., Eggleton, P., Strong, P., Perdikouliis, M. V., Willis, A. C., et al. (1998). Functional characterisation of a recombinant form of the C-terminal globular head region of the B-chain of human serum complement protein, C1q. *Biochemical Journal, 333*(Pt 1), 27-32.

Kishore, U., & Reid, K. B. M. (2000). C1q: structure, function and receptors. *Immunopharmacology, 49*, 159-170.

Klickstein, L. B., Barbashov, S. F., Liu, T., Jack, R. M., & Nicholson-Weller, A. (1997). Complement receptor type 1 (CR1, CD35) is a receptor for C1q. *Immunity, 7*(3), 345-355.

Kock, M. A., Hew, B. E., Bammert, H., Fritzinger, D. C., & Vogel, C.-W. (2004). Structure and function of recombinant cobra venom factor. *The Journal of Biological Chemistry, 279*(29), 30836-30843.

Kojouharova, M., Reid, K., & Gadjeva, M. (2010). New insights into the molecular mechanisms of classical complement activation. *Molecular Immunology, 47*(13), 2154-2160.

Kolb, W. P., & Muller-Eberhard, H. J. (1975). Neoantigens of the membrane attack complex of human complement. *Proceedings of National Academy of Science, 72*(5), 1687-1689.

Krapp, S., Mimura, Y., Jefferis, R., Huber, R., & Sondermann, P. (2003). Structural analysis of human IgG-Fc glycoforms reveals a correlation between glycosylation and structural integrity. *Journal of Molecular Biology, 325*(5), 979-989.

Kreikemeyer, B., McDevitt, D., & Podbielski, A. (2002). The role of Map protein in *Staphylococcus aureus* matrix protein and eukayotic cell adherence. *International Journal of Medical Microbiology, 292*(3-4), 283-295.

Krishanswamy, S. (1990). Prothrombinase complex assembly. *The Journal of Biological Chemistry, 265*(7), 3708-3718.

Kuroda, M., Ohta, T., Uchiyama, I., Baba, T., Yuzawa, H., Kobayashi, I., et al. (2001). Whole genome sequencing of methicilin resistant *Staphylococcus aureus*. *The Lancet, 357*(9264), 1225-1240.

Lambris, J. D., Ricklin, D., & Geibrecht, B. V. (2008). Complement evasion by human pathogens. *Nature Microbiology, 6*(2), 132-142.

Langley, R., Wines, B., Willoughby, N., Basu, I., Proft, T., & Fraser, J. D. (2005). The staphylococcal superantigen-like protein 7 binds IgA and complement C5 and inhibits IgA-FcaRI binding and serum killing of bacteria. *The Journal of Immunology, 174*(5), 2926-2933.

Laughton, J. M., Devillard, E., Heinrichs, D. E., Reid, G., & McCormick, J. K. (2006). Inhibition of expression of a staphyloccal superantigen-like protein by a soluble factor from Lactobacillus reuteri. *Microbiology, 152*(Pt 4), 1155-1167.

Laursen, N. S., Gordon, N., Hermans, S., Lorenz, N., Jackson, N., Wines, B., et al. (2010). Structural basis for inhibition of complement C5 by the SSL7 protein from *Staphylococcus aureus*. *Proceedings of National Academy of Science, 107*(8), 3681-3686.

Law, A., & Dodds, A. W. (1997). The internal thioester and the covalent binding properties of the complement proteins C3 and C4. *Protein Science, 6*(2), 263-274.

Law, S. K. A., Dodds, A. W., & Porter, R. R. (1984). A comparison of the properties of two classes, C4A and C4B of human complement component C4. *The EMBO Journal, 3*(8), 1819-1823.

Lee, B., Sharron, M., Montaner, L. J., Weissman, D., & Doms, R. W. (1999). Quantification of CD4, CCR5 and CXCR4 levels on lymphocyte subsets, dendritic cells and differentially conditioned monocyte-derived macrophages. *Proceedings of National Academy of Science, 96*(9), 5215-5220.

Lee, L., Hook, M., Havilan, D., Wesel, R. A., Yonter, E. O., Syribeys, P., et al. (2004). Inhibition of complement activation by a secreted *Staphylococcus aureus* protein. *The Journal of Infectious Diseases, 190*(3), 571-579.

Leslie, A. G. W. (1992). Recent changes to MOSFLM package for processing film and image plate data. *Joint CCP4+ ESF-EAMCB Newsletter on Protein Crystallography, 26*.

Lewis, M. J., Meehan, M., Owen, P., & Woof, J. M. (2008). A common theme in interaction of bacterial immunoglobluin binding proteins with immunoglobulins illustrated in the equine system. *The Journal of Biological Chemistry, 283*(25), 17615-17623.

Lindsay, J. A., & Holden, M. T. G. (2004). Staphylococcal aureus: superbug, supergenome? *Trends in Microbiology, 12*(8), 378-385.

Liu, C., Liu, G. Y., Song, Y., Yin, F., Hensler, M. E., Jeng, W.-Y., et al. (2008). A cholesterol biosynthesis inhibitor blocks *Staphylococcus aureus* virulence. *Science, 319*(5868), 1391-1394.

Liu, C., Shih, M.-H., & Tsai, P.-J. (2005). $ClfA_{221-550}$, a fibrinogen-binding segment of *Staphylococcus aureus* clumping factor A disrupts fibrinogen function. *Thrombosis Haemostasis, 94*(2), 286-294.

Liu, G. Y., Essex, A., Buchanan, J. T., Datta, V., Hoffman, H. M., Bastian, J. F., et al. (2005). *Staphylococcus aureus* golden pigment impairs neutrophil killing and promotes virulence through its antioxidant activity. *Journal of Experimental Medicine, 202*(2), 209-215.

Loughman, A., Fitzgerald, J. R., Brennan, M. R., Higgins, J., Downer, R., Cox, D., et al. (2005). Role of fibrinogen, immunoglobulin and complement in platelet activation promoted by *Staphylococcus aureus* clumping factor A. *Molecular microbiology, 57*(3), 804-818.

Lowy, F. D. (1998). *Staphylococcus aureus* infections. *The New England Journal of Medicine, 399*(8), 520-532.

Lu, J., Teh, B. K., Wang, L., Wang, L., Tan, Y. S., Lai, M. C., et al. (2008). The classical and regulatory functions of C1q in immunity and autoimmunity. *Cellular and Molecular Immunology, 5*(1), 9-21.

Lu, J., Wu, X., & Teh, B. K. (2007). The regulatory roles of C1q. *Immunobiology, 212*(4-5), 245-252.

Lucas, M. A., Fretto, L. J., & McKee, P. A. (1983). The binding of human plasminogen to fibrin and fibrinogen. *The Journal of Biological Chemistry, 258*(7), 4249-4256.

Luong, T. T., Dunman, P. M., Murphy, E., Projan, S. J., & Lee, C. Y. (2006). Transcription profiling of the *mgrA* regulon in *Staphylococcus aureus*. *Journal of Bacteriology, 188*(5), 1899-1910.

Maenaka, K., van der Merwe, A., Stuart, D. I., Jones, Y., & Sondermann, P. (2001). The human low affinity Fcγ receptors IIa, IIb and III bind IgG with fast kinetics and distinct thermodynamic properties. *The Journal of Biological Chemistry, 276*(48), 44898-448904.

Markiewski, M. M., Nilsson, B., Ekdahl, K. N., Mollnes, T. E., & Lambris, J. D. (2007). Complement and coagulation: strangers or partners in crime? *Trends in Immunology, 28*(4), 184-192.

Mazmanian, S. K., Liu, G., Ton-That, H., & Schneewind, O. (1999). *Staphylococcus aureus* sortase, an enzyme that anchors surface proteins to the cell wall. *Science, 285*(5428), 760-763.

McCoy, A. J., Grosse-Kunstleve, R. W., Storoni, L. C., & Read, R. J. (2005). Likelihood-enhanced fast translation functions. *Acta Crystallographica Biological Crystallography, D61*(4), 458-464.

Mendina, E. (2009). Neutrophil extracellular traps: a strategic tactic to defeat pathogens with potential consequences for the host. *Journal of Innate Immunity, 1*(3), 176-180.

Moon, K. E., Gorski, J. P., & Hughli, T. E. (1981). Complete primary structure of human C4a anaphylatoxin. *The Journal of Biological Chemistry, 256*(16), 8685-8692.

Moreland, N., Ashton, R., Baker, H. M., Ivanovic, I., Patterson, S., Arcus, V. L., et al. (2005). A flexible and economical medium-throughput strategy for protein production and crystallisation. *Acta Crystallographica Biological Crystallography, D61*(Pt 10), 1378-1385.

Morgan, A., Jones, N. D., Nesbitt, A. M., Chaplin, L., Bodmer, M. W., & Emtage, J. S. (1995). The N-terminal end of the CH2 domain of chimeric human IgG1 and anti-HLA-DR is necessary for C1q, FcγRI and FcγRIII binding. *Immunology, 86*(2), 319-324.

Morgan, P., & Walport, M. J. (1991). Complement deficiency and disease. *Immunology Today, 12*(9), 301-306.

Morse, S. I. (1962). Studies on the chemistry and immunochemistry of cell walls of *Staphylococcus aureus*. *Journal of Experimental Medicine, 116*(2), 229-245.

Mosher, D. F. (1975). Crosslinking of cold insoluble globulin by fibrin-stabilizing factor. *Journal of Biological Chemistry, 250*, 6614-6621.

Moza, B., Varma, A. K., Buonpane, R. A., Zhu, P., Herfst, C. A., Nicholson, M. J., et al. (2007). Structural basis of T-cell specificity and activation by the bacterial superantigen TSST-1. *The EMBO Journal, 26*(4), 1187-1197.

Murshudov, G. N., Vagin, A. A., & Dodson, E. J. (1997). Refinement of macromolecular structures by the maximum-likelihood method. *Acta Crystallographica, D53*(Pt 3), 240-255.

Mwangi, M. M., Wu, S. W., Zhou, Y., Sieradzki, K., de Lencastre, H., Richardson, P., et al. (2007). Tracking the *in vivo* evolution of multidrug resistance in *Staphylococcus aureus* by whole-genome sequencing. *Proceedings of National Academy of Science, 104*(22), 9451-9456.

Navarre, W. W., & Schneewind, O. (1999). Surface proteins of gram-positive bacteria and mechanisms of their targetting to the cell wall envelope. *Microbiology and Molecular Biology Reviews, 63*(1), 174-229.

Neoh, H.-m., Cui, L., Yuzawa, H., Takeuchi, F., Matsuo, M., & Hiramatsu, K. (2008). Mutated response regulator *graR* is responsible for phenotypic conversion of *Staphylococcus aureus* from heterogenous vancomycin-intermediate resistance to vancomycin-intermediate resistance. *Antimicrobial Agents and Chemotheraphy, 52*(1), 45-53.

Nielsen, H., Engelbrecht, J., Brunak, S., & Heijne, G. v. (1997). Identification of prokaryotic and eukaryotic signal peptides and prediction of their cleavage sites. *Protein Engineering, 10*(1), 1-6.

Nimmerjahn, F., & Ravetch, J. V. (2006). Fcγ receptors: old friends and new family members. *Immunity, 24*(1), 19-28.

Novick, R. P. (2003). Mobile genetic elements and bacterial toxinoses: the superantigen-encoding pathogenicity islands of *Staphylococcus aureus*. *Plasmid, 49*(2), 93-105.

Novick, R. P., Schlievert, P., & Ruzin, A. (2001). Pathogenicity and resistance islands of staphylococci. *Microbes and Infection, 3*(4), 585-594.

Nubel, U., Dordel, J., Kurt, K., Strommenger, B., Weslt, H., Skukla, S. K., et al. (2010). A timescale for evolution, population, expansion, and spatial spread of an emerging clone of methicillin-resistant *Staphylococcus aureus*. *PloS pathogens, 6*(4), e1000855.

Oganesyan, V., Gao, C., Shirinian, L., Wu, H., & Dall'Acqua, W. F. (2008). Structural characterization of a human Fc fragment engineered for lack of effector functions. *Acta Crystallographica, 64*(Pt 6), 700-704.

Palazzolo-Ballance, a. M., Reniere, M. L., Braughton, K. R., Sturdevant, D. E., Otto, M., Kreiswirth, B. N., et al. (2008). Neutrophil microbicides induce a pathogen survival response in community associated methicillin-resistant *Staphylococcus aureus*. *The Journal of Immunology, 180*(1), 500-509.

Palma, M., Wade, D., Flock, M., & Flock, J.-I. (1998). Multiple binding sites in the interaction between an extracellular fibrinogen-binding protein from *Staphylococcus aureus* and fibrinogen. *Journal of Biological Chemistry, 273*(21), 13177-13181.

Patel, A. H., Nowlan, P., Weavers, E. D., & Foster, T. (1987). Virulence of Protein A-deficient and alpha toxin-deficient mutants of *Staphylococcus aureus* isolated by allele replacement. *Infection and Immunity, 55*(12), 3103-3110.

Patel, L., Charlton, S. J., Chambers, J. K., & Macphee, C. H. (2001). Expression and functional analysis of chemokine receptors in human peripheral blood leukocyte population. *Cytokine, 14*(1), 27-36.

Peacock, S. J., de Silva, I., & Lowry, F. D. (2001). What determines nasal carriage of *Staphylococcus aureus*. *Trends in Microbiology, 9*(12), 605-610.

Pedelacq, J.-D., Maveyraud, L., Prevost, G., Baba-Moussa, L., Gonzalez, A., Courcelle, E., et al. (1999). The structure of a *Staphylococcus aureus* leucocidin component (LukF-PV) reveals the fold of the water-soluble species of a family of transmembrane pore-forming toxins. *Structure, 7*(3), 277-287.

Perrakis, A., Harkiolaki, M., Willson, K. S., & Lamzin, V. S. (2001). ARP/wARP and molecular replacement. *Acta Crystallographica Biological Crystallography, D57*(Pt 10), 1445-1450.

Peschel, A., Jack, R. W., Otto, M., Collins, L., Staubitz, P., Nicholson, G., et al. (2001). *Staphylococcus aureus* resistance to human defensins and evasion of neutrophil killing via the novel virulence factor MprF is based on modification of membrane lipids with L-lysine. *Journal of Experimental Medicine, 193*(9), 1067-1076.

Petersen, S. V., Thiel, S., & Jensenius, J. C. (2001). The mannan-binding lectin pathway of complement activation: biology and disease association. *Molecular Immunology, 38*(2-3), 133-149.

Peterson, P. K., Verhoef, J., Sabath, L. D., & Quie, P. G. (1977). Effect of Protein A on staphylococcal opsonisation. *Infection and Immunity, 15*(3), 760-764.

Pickering, M. C., Cook, T., Warren, J., Bygrave, A. E., Moss, J., Walport, M. J., et al. (2002). Uncontrolled C3 activation causes membranoproliferative glomerulonephritis in mice deficient in complement factor H. *Nature Genetics, 31*(4), 424-428.

Postma, B., Kleibeuker, W., Poppelier, M. J. J. G., Boonstra, M., van Kessel, K. P. M., van Strijp, J. A. G., et al. (2005). Residues 10 -18 within the C5a receptor N-terminus compose a binding domain for chemotaxis inhibitory protein of *Staphylococcus aureus*. *The Journal of Biological Chemistry, 280*(3), 2020-2027.

Prabakaran, P., Vu, B. K., Gan, J., Feng, Y., Dimitrov, D. S., & Ji, X. (2008). Structure of an isolated unglycoslyated antibody C(H)2 antibody. *Acta Crystallographica Biological Crystallography, 64*(Pt 10), 1062-1067.

Prat, C., Bestebroer, J., de Haas, C. J. C., van Strijp, J. A. G., & van Kessel, K. P. M. (2006). A new staphylococcal anti-inflammatory protein that antagonises the formyl peptide receptor-like 1. *The Journal of Immunology, 177*(11), 8017-8026.

Prat, C., Haas, P.-J., Bestebroer, J., de Haas, C., van Srijp, J. A. G., & van Kessel, K. (2009). A homolog of formyl peptide receptor-like 1 (FPRL1) inhibitor from Staphylococcus aureus (FPRL1 inhibitory protein) that inhibits FPRL1 and FPR. *The Journal of Immunolgy, 183*(10), 6569-6578.

Prevost, G., Cribier, C., Couppie, P., Petiau, P., Supersac, G., Finck-Barbancon, V., et al. (1995). Panton-valentine leucocidin and gamma-hemolysin from *Staphylococcus aureus* ATCC49775 are encoded by distinct genetic loci and have different biological activities. *Infection and Immunity, 63*(10), 4121-4129.

Prodeus, A. P., Goerg, S., Shen, L.-M., Pozdnyakova, O. O., Chu, L., Alicot, E. A., et al. (1998). A critical role for complement in maintenance of self tolerance. *Immunity, 9*(5), 721-731.

Proft, T., & Fraser, J. D. (2003). Bacterial superantigens. *Clincal and Experimental Immunology, 133*(3), 299-306.

Quie, P. G., White, J. G., Holmes, B., & Good, R. A. (1967). *In vitro* bactericidal capacity of human polymorphonuclear leukocytes: diminished activity in chronic granulomatosus disease of childhood. *Journal of Clinical Investigation, 46*(4), 668-679.

Rabijns, A., De Bondt, H. L., & De Ranter, C. (1997). Three-dimensional structure of staphylokinase, a plasminogen activator with therapeutic potential. *Nature Structural Biology, 4*(5), 357-360.

Ramsland, P. A., Willoughby, N., Trist, H. M., Farrugia, W., Hogarth, M., & Fraser, J. D. (2007). Structural basis for evasion of IgA immunity by *Staphylococcus aureus* revealed in the complex of SSL7 with Fc of human IgA1. *Proceedings of National Academy of Science, 104*(38), 15051-15056.

Ramu, P., Tanskanen, R., Holmberg, M., Lahteenmaki, K., Korhonen, T., & Meri, S. (2007). The surface protease PgtE of Salmonella enterica affects complement activity by proteolytically cleaving C3b, C4b and C5. *FEBS Letters, 581*(9), 1716-1720.

Randall, T. D., King, L. B., & Corley, R. B. (1990). The biological effects of IgM hexamer formation. *European Journal of Immunology, 20*(9), 1971-1979.

Reilly, B. D. (1999). Analysis of human C4A and C4B binding to an immune complex in serum. *Clinical and Experimental Immunology, 117*(1), 12-18.

Reilly, B. D., & Mold, C. (1997). Quantitative analysis of C4Ab and C4Bb binding to the C3b/C4b receptor (CRI, CD35). *Clinical and Experimental Immunology, 110*(2), 310-316.

Ritchie, G. E., Moffatt, B. E., Sim, R. B., Morgan, P., Dwek, R. A., & Rudd, P. M. (2002). Glycosylation and the complement system. *Chemical Reviews, 102*(2), 305-319.

Rooijakkers, S. H., Wu, J., Ruyken, M., van Domselaar, R., Planken, K. L., Tzekou, A., et al. (2009). Structural and functional implications of the alternative complement pathway C3 convertase stabilised by a staphylococcal inhibitor. *Nature Immunology, 10*(7), 920-927.

Rooijakkers, S. H. M., Ruyken, M., Roos, A., Daha, M. R., Presanis, J. S., Sim, R. B., et al. (2005). Immune evasion by a staphylococcal complement inhibitor that acts on C3 convertases. *Nature Immunology, 6*(9), 920-927.

Rooijakkers, S. H. M., Ruyken, M., van Roon, J., van Kessel, K. P. M., van Strijp, J. A. G., & van Warnel, W. J. B. (2006). Early expression of SCIN and CHIPS drives instant immune evasion by *Staphylococcus aureus*. *Cellular Microbiology, 8*(8), 1282-1293.

Rooijakkers, S. H. M., van Kessel, K. P. M., & van Strijp, J. A. G. (2005). Staphylococcal innate immune evasion. *Trends in Microbiology, 13*(12), 596-601.

Rooijakkers, S. H. M., & van Strijp, J. A. G. (2007). Bacterial complement evasion. *Molecular Immunology, 44*(1-3), 23-32.

Rooijakkers, S. H. M., van Wamel, W. J. B., Ruyken, M., van Kessel, K. P. M., & Van Srijp, J. A. G. (2005). Anti-opsonic properties of staphylokinase. *Microbes and Infection, 7*(3), 476-484.

Root, R. K., Rosenthal, A. S., & Balestra, D. J. (1972). Abnormal bactericidal, metabolic, and lysosomal functions of Chediak-Higashi syndrome leukocytes. *The Journal of Clinical Investigation, 51*(3), 649-665.

Rosenstein, R., Nerz, C., Biswas, L., Resch, A., Raddatz, G., Shuster, S. C., et al. (2009). Genome analysis of the meat starter culture bacterium *Staphylcoccus carnosus* TM300. *Applied and Environmental Microbiology, 75*(3), 811-822.

Rutkowski, M. J., Sughrue, M. E., Kane, A. J., Mills, S. A., Fang, S., & Parsa, A. T. (2010). Complement and the central nervous system: emerging roles in development, protection and regeneration. *Immunology and Cell Biology, 88*(8), 781-786.

Sakiniene, E., Bremell, T., & Tarkowski, A. (1999). Compelment depletion aggravates *Staphylococcus aureus* speticaemia and septic arthritis. *Clinical and Experimental Immunology, 115*(1), 95-102.

Sambrano, G. R., Weiss, E. J., Zheng, Y.-W., Huang, W., & Coughlin, S. R. (2001). Role of thrombin signalling in platelets in haemostasis and thrombosis. *Nature, 413*(6851), 74-78.

Sauer-Eriksson, E., Kleywegt, G. J., Uhlen, M., & Jones, T. A. (1995). Crystal structure of the C2 fragment of streptococcal Protein G in complex with the Fc domain of human IgG. *Structure, 3*(3), 265-278.

Seelen, M. A., Roos, A., Wieslander, J., Mollnes, T. E., Sjoholm, A. G., Wurzner, R., et al. (2005). Functional analysis of the classical, alternative, and MBL pathways of the complement system: standardization and validation of a simple ELISA. *Journal of Immunological Methods, 296*(1-2), 187-198.

Shevchenko, A., Wilm, M., Vrm, O., & Mann, M. (1996). Mass spectrometric sequencing of proteins from silver stained polyacylamide gels. *Analytical chemistry, 68*(5), 850-858.

Shibata, H., Ngaoka, M., Sakai, M., Sawada, H., Watanabe, T., & Yokokura, T. (1994). Kinetic studies on the plasminogen activation by the staphylokinase-plasmin complex. *Journal of Biochemistry, 115*(4), 738-742.

Shields, R. L., Namenuk, A. K., Hong, K., Meng, Y. G., Rae, J., Briggs, J., et al. (2001). High resolution mapping of the binding site on human IgG1 for FcγRI, FcγRII, FcγRIII and FcRn and design of IgG1 variants with improved binding to the FcγR. *The Journal of Biological Chemistry, 276*(9), 6591-6604.

Sibbald, M. J. J. B., Ziebandt, A. K., Engelman, S., Heker, M., de Jong, A., Harmsen, H. J., et al. (2006). Mapping the pathways of staphylococcal pathogenesis by comparative secretomics. *Microbiology and Molecular Biology Reviews, 70*(3), 755-788.

Sieprawska-Lupa, M., Mydel, P., Krawczyk, K., Wojcik, K., Puklo, M., Lupa, B., et al. (2004). Degradation of human antimicrobial peptides LL-37 by *Staphylococcus aureus*-derived proteinase. *Antimicrobial Agents and Chemotheraphy, 48*(12), 4673-4679.

Sieradzki, K., Roberts, R. B., Haber, S. W., & Tomasz, A. (1999). The development of vancomycin resistance in a patient with methicillin-resistant *Staphylococcus aureus* infection. *The New England Journal of Medicine, 340*(7), 517-523.

Silverman, G. J., & Goodyear, C. S. (2006). Confounding B-cell defences:lessons from a staphylococcal superantigen. *Nature Reviews Immunology, 6*(6), 465-475.

Silverman, G. J., Pires, R., & Bouvet, J. P. (1996). An endogenous sialoprotein and a bacterial B cell superantigen compete in their VH family-specific binding interaction with Igs. *Journal of Immunology, 157*(10), 4496-4502.

Sims, P. J., & Wiedmer, T. (1991). The response of human platelets to activated components of the complement system. *Immunology Today, 12*(9), 338-342.

Sivaraman, K., Venkataraman, N., Tsai, J., Dewell, S., & Cole, A. M. (2008). Genome sequencing and analysis reveals possible determinants of *Staphylococcus aureus* nasal carriage. *BMC Genomics, 9*, 433.

Smyth, D. S., Meaney, W. J., Hartigan, P. J., & Smyth, C. J. (2007). Occurence of ssl genes in isolates of *Staphylococcus aureus* from animal infection. *Journal of Medical Microbiology, 56*(Pt 3), 418-425.

Sondermann, P., Huber, R., Ooshuizen, V., & Jacob, U. (2000). The 3.2A crystal stucture of the human IgG1 Fc fragment-FcγIII complex. *Nature, 406*(6793), 267-273.

Starovasnik, M. A., O'Connell, M. P., Fairbrother, W. J., & Kelly, R. F. (1999). Antibody variable region binding by staphylococcal protein A: thermodynamic analysis and location of the Fv binding site on E-domain. *Protein Science, 8*(7), 1423-1431.

Stauff, D. L., Bagaley, D., Torres, V. J., Joyce, R., Andersn, K. L., Kuechenmeister, L., et al. (2008). *Staphylococcus aureus* HrtA is an ATPase required for protection against heme toxicity and prevention of a transcriptional heme stress response. *Journal of Bacteriology, 190*(10), 3588-3596.

Strey, C. W., Markiewski, M., Mastellos, D., Tudoran, R., Spruce, L. A., Greenbaum, L. E., et al. (2003). The proinflammatory mediators C3a and C5a are essential for liver regeneration. *Journal of Experimental Medicine, 198*(6), 913-923.

Takei, S., Arora, Y. K., & Walker, S. M. (1993). Intravenous immunoglobulin contains specific antibodies inhibitory to activation of T cells by Staphylococcal toxin superantigens. *Journal of Clinical Investigation, 91*(2), 602-607.

Tan, L. K., Shopes, R. J., Oi, V. T., & Morrison, S. L. (1990). Influence of the hinge region on complement activation, C1q binding, and segmental flexibility in chimeric human immunoglobulin. *Proceedings of National Academy of Science, 87*(1), 162-166.

Tedesco, F., Pausa, M., Nardon, E., Introna, M., Mantovani, A., & Dobrina, A. (1997). The cytolytically inactive terminal complement complex activates endothelial cells to express adhesion molecules and tissue factor procoagulant activity. *Journal of Experimental Medicine, 185*(9), 1619-1627.

Theil, S., Peteren, S. V., Vorup-Jensen, T., Matsushita, M., Fujita, T., Stover, C. M., et al. (2000). Interaction of C1q and mannan-binding lectin (MBL) with C1r, C1s, MBL-associated serine proteases 1 and 2, and the MBL-associated protein MAp19. *The Journal of Immunology, 165*(2), 878-887.

Thern, A., Stenberg, L., Dahlback, B., & Lindahl, G. (1995). Ig-binding surface proteins of *Streptococcus pyogenes* also bind human C4b-binding protein (C4BP), a regulatory component of the complement system. *The Journal of Immunolgy, 154*(1), 375-386.

Thiel, S., Vorup-Jensen, T., Stover, C. M., Schwaeble, W., Laursen, S. B., Poulsen, K., et al. (1997). A second serine protease associated with mannan-binding lectin that activates complement. *Nature, 386*(6624), 506-510.

Thommesen, J. E., Michaelsen, T. E., Loset, G. A., Sandlie, I., & Brekke, O. H. (2000). Lysine 322 in human IgG3 CH2 domain is crucial for antibody dependent complement activation. *Molecular Immunology, 37*(16), 995-1004.

Thompson, J. D., Higgins, D. G., & Gibson, T. J. (1994). CLUSTALW: improving the sensitivity of progressive multiple sequence alignment through sequence weighting, position-specific gap penalties and weight matrix choice. *Nucleic Acids Research, 22*(22), 4673-4680.

Torres, V. J., Stauff, D. L., Pishchany, G., Bezbradica, J. S., Gordy, L. E., Iturrengui, J., et al. (2007). A *Staphylococcus aureus* regulatory system that responds to host heme and modulates virulence. *Cell Host Microbe, 1*(2), 109-119.

Travis, S. M., Anderson, N. N., Forsyth, W. R., Espiritu, C., Conway, B. D., Greenberg, E. P., et al. (2000). Bactericidal activitiy of mammalian cathelicidin-derived peptides. *Infection and Immunity, 68*(5), 2748-2755.

Ubukata, K., Nonoguchi, R., Matsuhashi, M., & Konno, M. (1989). Expression and inducibility in *Staphylococcus aureus* of the *mecA* gene, which encodes a methicillin-resistant *S.aureus*-specific penicillin-binding protein. *Journal of Bacteriology, 171*(5), 2882-2885.

Ulrich, R. G. (2000). Evolving superantigens of *Staphylococcus aureus*. *FEMS Immunology and Medical Microbiology, 27*(1), 1-7.

Upadhyay, A., Burman, J. D., Clark, E. A., Leung, E., Isenman, D. E., van den Elsen, J. M. H., et al. (2008). Structure-function analysis of the C3 binding region of *Staphylococcus aureus* immue subversion protein Sbi. *The Journal of Biological Chemistry, 283*(32), 22113-22120.

Valet, G., & Cooper, N. R. (1974). Isolation and characterisation of the proenzyme form of the C1s subunit of the first complement component. *The Journal of Immunology, 112*(1), 339-350.

van den Elsen, J. M. H., Martin, A., Wong, V., Clemenza, L., Rose, D. R., & Isenman, D. E. (2002). X-ray crystal structure of the C4d fragment of human complement component C4. *Journal of Molecular Biology, 322*(5), 1103-1115.

Verburgh, H. A., Peterson, P. K., Nguyen, B. T., Sisson, S. P., & Kim, Y. (1982). Opsonisation of encapsulated *Staphylococcus aureus*: the role of specific antibody and complement. *The Journal of Immunology, 129*(4), 1681-1687.

Vojtov, N., Ross, H. F., & Novick, R. P. (2002). Global repression of exotoxin synthesis by staphylococcal superantigens. *Proceedings of National Academy of Science, 99*(15), 10102-10107.

von Eiff, C., Becker, K., Machka, K., Stammer, H., & Peters, G. (2001). Nasal carriage as a source of *Staphylococcus aureus* bacteremia. *New England Journal of Medicine, 344*(1), 11-16.

Voyich, J. M., Sturdevant, K. R. B. D. E., Whitney, A. R., Said-Salim, B., Porcella, S. F., Long, D., et al. (2005). Insights into mechanisms used by Staphylococcus aureus to avoid destruction by human neutrophils. *The Journal of Immunology, 175*(6), 3907-3919.

Walenkap, A. M. E., Boer, I. G. J., Bestebroer, J., Rozeveld, D., Timmer-Bosscha, H., Hemrika, W., et al. (2009). Staphylococcal superantigen-like 10 inhibits CXCL12-induced human tumor cell migration. *Neoplasia, 11*(4), 333-344.

Walker, P. A., Leong, L. E. C., Ng, P. W. P., Tan, S. H., Waller, S., Murphy, D., et al. (1994). Efficient and rapid affinity purification of proteins using recombinant fusion proteases. *Nature Biotechnology, 12*(6), 601-605.

Wallis, R., Dodds, A. W., Mitchell, D. A., Sim, R. B., Reid, K. B. M., & Schewaeble, W. J. (2007). Molecular interactions between MASP-2, C4 and C2 and their activation fragments leading to complement activation via the lectin pathway. *The Journal of Biological Chemistry, 282*(11), 7844-7851.

Walport, M. J. (2001). Complement. *New England Journal of Medicine, 344*(14), 1058-1066.

Walter, T. S., Meier, C., Assenberg, R., Au, K.-F., Ren, J., Verma, A., et al. (2006). Lysine methylation as a routine ways and means rescue strategy for protein crystallizaiton. *Structure, 14*(11), 1617-1622.

Wang, A. C., & Wang, I. Y. (1977). Cleavage sites of human IgG1 immunoglobulin by papain. *Immunochemistry, 14*(3), 197-200.

Warn-Cramer, B. J., & Bajaj, P. (1986). Intrinsic versus extrinsic coagulation. *Biochemical Journal, 239*(3), 757-762.

Williams, R. J., Ward, H. M., Henderson, B., Poole, S., O'hara, B. P., Wilson, M., et al. (2000). Identification of a novel gene cluster encoding staphylococcal exotoxin-like proteins: characterisation of the prototypic gene and its protein product, SET1. *Infection and Immunity, 68*(6), 4407-4415.

Wines, B., Powell, M. S., Parren, P. W. H. I., Barnes, N., & Hogarth, P. M. (2000). The IgG Fc contains distinct FcR binding sites: the leukocyte receptors FcγRI and FcγRIIa bind to a region in the Fc distinct from that recognised by neonatal FcR and Protein A. *The Journal of Immunology, 164*(10), 5313-5318.

Wines, B. D., Willoughby, N., Fraser, J. D., & Hogarth, P. M. (2006). A competitive mechanism for staphylococcal toxin SSL7 inhibiting the leukocyte IgA receptor, FcαRI, is revealed by SSL7 binding at the Cα2/Cα3 interface of IgA. *The Journal of Biological Chemistry, 281*(3), 1389-1393.

Wright, A. J., Higginbottom, A., Philipee, D., Upadhyay, A., Bagby, S., Read, R. C., et al. (2007). Characterisation of receptor binding by the chemotaxis inhibitory protein of *Staphylococcus aureus* and the effects of the host immune response. *Molecular Immunology, 44*(10), 2507-2517.

Wuhrer, M., Stam, J. C., van de Geijn, F. E., Koeleman, C. A. M., Verrips, T., Dolhain, R. J. E. M., et al. (2007). Glycosylation profiling of immunoglobulin G (IgG) subclasses from human serum. *Proteomics, 7*(22), 4070-4081.

Yamaguchi, Y., Nishimura, M., Nagano, M., Yagi, H., Sasakawa, H., Uchida, K., et al. (2006). Glycoform-dependent conformational alteration of the Fc region of human immunoglobulin G1 as revealed by NMR spectroscopy. *Biochimica et Biophysica Acta - General Subjects, 1760*(4), 693-700.

Yasui, K., & Baba, A. (2006). Therapeutic potential of superoxide dismutase (SOD) for resolution of inflammation. *Inflammation Research, 55*(9), 359-363.

Zakour, N. L. B., Guinane, C. M., & Fitzgerald, J. R. (2008). Pathogenomics of the staphylococci: insights into niche adaptation and the emergence of new virulent strains. *Federation of European Microbiological Societies, 289*(1), 1-12.

Zipfel, P. F., & Reuter, M. (2009). Complement activation products C3a and C4a as endogenous antimicrobial peptides. *International Journal of Peptide Research and Therapeutics, 15*(2), 87-95.

Zipfel, P. F., Wurzner, R., & Skerka, C. (2007). Complement evasion of pathogens: common strategies are shard by diverse organisms. *Molecular Immunology, 44*(16), 3850-3857.